THE INFLUENCE OF SHAPE ON THE STRENGTH OF TABLETS

A THESIS BY

PETER NEIL DAVIES

FOR THE DEGREE OF DOCTOR OF PHILOSOPHY

THE SCHOOL OF PHARMACY, LONDON UNIVERSITY,

29 - 39 BRUNSWICK SQUARE,

LONDON WC1N 1AX

ProQuest LLC.
789 East Eisenhower Parkway
P.O. Box 1346
Ann Arbor, MI 48106 – 1346

ABSTRACT

The effect of the compact perimeter shape on the compressional properties of pharmaceutical excipients has been examined. Compacts of a deforming material, Avicel PH-102 and a fragmenting material, Emcompress were prepared. The compacts were prepared on single punch and rotary machines using flat faced circular, hexagonal and square tooling.

The mechanical strengths of the compacts were determined using the diametral compression test and an axial compression test. The validity of using the diametral compression test for shaped compacts was assessed using shaped casts of gypsum. It was shown that with the appropriate selection of platens the test could reliably induce tensile failure in square and hexagonal specimens as well as in conventional circular specimens.

The diametral compression test did not reveal any differences in the tensile strengths of different shaped compacts prepared with the same compaction pressure. Visual inspection of Emcompress compacts did reveal flaws present on the lower surface of square compacts produced on the single punch machine that were not evident on circular compacts. Further evidence of such structural differences was seen when comparing the axial compression test results for square and circular compacts of Emcompress. The differences are due to poor force transmission at the corners of the squares and may be prevented by improving lubrication. No such differences are seen between square and circular compacts of Avicel.

Large differences were detected in the compaction pressure/ tensile strength profiles of Avicel compacts produced on different tablet machines. The compacts prepared using the rotary machine had lower tensile

strengths and exhibited a lower capping pressure. The pressure at which capping commenced was greater for the square compacts than the circles.The differences are attributed to the material being compressed between two moving punches on the rotary machine as opposed to one moving punch on the single punch machine.

ACKNOWLEDGEMENTS

I would like to thank my employers, Roche Products Ltd, for giving me the opportunity to undertake the investigation and preparation of this thesis.

In particular I am grateful to Dr. Harry Worthington who was responsible for initiating the project and who, through his support and encouragement, has also been instrumental in seeing the project through to completion. I am especially grateful for his many hours spent checking this thesis.

I would like to thank all my other colleagues at Roche Products who have helped with practical assistance and advice. I am especially indebted to Dr. Peter Williams for his advice on statistical techniques.

Finally, I would like to express my gratitude to Professor Mike Newton at the School of Pharmacy for his guidance and encouragement.

CONTENTS

	Page
Abstract	2
Acknowledgements	4
Contents	5
List of tables	11
List of figures	18
Glossary	31
Chapter 1 - Introduction	35
1.1 Studies of powder compaction	38
1.1.1 Mechanisms of powder compaction	38
1.1.2 The compression process	42
1.1.3 Pressure-volume relationships	46
1.1.3.1 Particle re-arrangement	46
1.1.3.2 Formation of supporting structures	46
1.1.3.3 Deformation and recombination of particles	47
1.1.4 Relationship of compact strength to applied pressure and porosity	51
1.1.5 Pressure transmission through powders	54
1.2 Determination of the mechanical strength of pharmaceutical compacts	62
1.2.1 Direct tensile testing	62
1.2.2 Flexural tests	64
1.2.3 The diametral compression test	69

1.2.3.1 Analytical solution 69

1.2.4.2 The effect of loading conditions on the diametral compression test 73

1.2.4.3 The effect of loading rate on the diametral compression test 77

1.2.4.4 Tensile strength testing of non plane-faced circular compacts 78

1.2.5 Line loading of rectangles 79

1.2.6 Line loading of ellipses 83

1.2.7 Statistical treatment of tensile strength determinations 83

1.2.8 Mechanical properties related to stiffness 85

1.2.8.1 Determination of Young's modulus 85

1.2.8.2 Work of failure 87

1.2.8.3 Brittle Fracture Index 88

1.2.9 Indentation hardness 89

1.3 Aims of this work 93

Chapter 2 - Evaluation of the diametral compression test using shaped gypsum casts 95

2.1 Introduction 96

2.2 Materials and methods 98

2.2.1 Physical and chemical properties of gypsum 98

2.2.2 Characterisation of the casting process 99

2.2.3 Storage conditions 100

2.2.4 Preparation of casts 104

2.2.5 Testing the casts 104

2.3 Results and discussion 106

2.3.1 Determination of the tensile strength of gypsum discs 106

2.3.2 Effect of sample shape on the load required to produce tensile failure 115

2.4 Conclusions 123

Chapter 3 - Compaction studies using the single punch tablet machine 126

3.1 Introduction 127

3.2 Materials and methods 128

3.2.1 Materials selection 128

3.2.2 Preparation of mixes 130

3.2.3 Tooling 131

3.2.4 Compression force monitoring 131

3.2.5 Preparation of compacts 136

3.2.6 Compact storage 138

3.2.7 Testing of the compacts 140

3.2.7.1 Diametral compression test 140

3.2.7.2 Axial compression test 142

3.2.7.3 Transverse compression test 142

3.2.7.4 Ball bearing diametral compression test 142

3.2.7.5 Three point bending test 145

3.2.7.6 Varying the platen positions used in the test configurations 145

3.2.8 Statistical treatment of results 147

3.2.8.1 Linear regression 147

3.2.8.2 Comparison of lines 147

3.3 Results and discussion 148

3.3.1 Effect of platen shape on the diametral compression test results 148

3.3.2 Characterisation of the compaction properties of circular compacts 162

3.3.2.1 Diametral compression test data 162

3.3.2.2 Effect of porosity on the mechanical properties of compacts 181

3.3.3 Comparison of the compaction properties of circular and shaped compacts 190

3.3.3.1 Compact appearance 190

3.3.3.2 Diametral compression 190

3.3.3.3 Axial compression 214

3.3.3.4 Transverse compression 214

3.3.3.5 Three point bending test 221

3.3.3.6 Effect of varying platen position on the tensile strength 224

3.3.3.7 Effectiveness of magnesium stearate as a die wall lubricant 225

3.4 Conclusions 240

Chapter 4 - Compaction studies using the rotary tablet machine 242

4.1 Introduction 243

4.2 Materials and methods 243

4.2.1 Materials 243

4.2.2 Tooling 243

4.2.3 Force monitoring 244

4.2.4 Preparation of compacts 250

4.2.5 Compact storage 252

4.2.6 Testing the compacts 252

4.2.6.1 Diametral compression test 252

4.2.6.2 Axial compression test 252

4.3 Results and discussion 253

4.3.1 Compact appearance 253

4.3.2 Diametral compression 256

4.3.3 Axial compression 273

4.4 Conclusions 273

Chapter 5 - Comparison of the single punch and rotary tablet machine results 286

5.1 Introduction 287

5.2 The eccentric single punch tablet press 287

5.3 The rotary tablet press 292

5.4 Effect of machine type on compaction properties 300

5.4.1 Effect of machine type on the compaction properties of Avicel PH-102 300

5.4.2 Effect of machine type on the compaction properties of Emcompress 310

5.5 Conclusions 323

Chapter 6 - The influence of shape on the strength of compacts prepared from granulated formulations 325

6.1 Introduction 326

6.2 Materials and methods 328

6.2.1 Materials 328

6.2.2 Experimental design 328

6.2.3 Preparation of tablet mixes 330

6.2.4 Preparation of compacts 333

6.2.5 Testing of the compacts 335

6.2.6 Data analysis 335

6.3 Results and discussion 337

6.3.1 Effect of machine type on the relationship between Avicel PH-102 and magnesium stearate levels and tensile strength 354

6.3.1.1 Diametral compression 354

6.3.1.2 Axial compression test 356

6.3.2 Effect of compact shape on the tensile strength 357

6.4 Conclusions 358

Chapter 7 - Conclusions 360

7.1 Conclusions 361

7.2 Suggestions for further work 363

Chapter 8 - References 366

Appendix 1 375

LIST OF TABLES

Page

Chapter 1 - Introduction

1.1 Approximate values of P_{max} and γ observed in plastic and brittle materials. 53

Chapter 2 - Evaluation of the diametral compression test using shaped gypsum casts

2.1 Tensile strength of 20mm diameter circular gypsum casts prepared by manual spatulation and tested with flat platens. 102

2.2 ANOVA table for 20mm diameter circular gypsum casts prepared by manual spatulation and tested with flat platens. 102

2.3 Tensile strength of 20mm circular gypsum casts prepared using the Waring Blender and tested with flat platens. 103

2.4 ANOVA table for 20mm circular gypsum casts prepared using the Waring Blender and tested with flat platens. 103

2.5 Effect of storage on the tensile strength of gypsum discs. 103

2.6 Moulds used in the preparation of gypsum casts. 105

2.7 Tensile strength values of individual batches of 20mm diameter circular casts produced using the Waring Blender. 108

2.8	Tensile strength values of individual batches of 10mm circular gypsum casts produced using the Waring Blender.	109
2.9	Pooled tensile strength results for circular gypsum discs prepared using the Waring Blender.	111
2.10	Predicted mean tensile strength values of circular gypsum casts tested by diametral compression using flat platens.	114
2.11	Predicted mean tensile strength values of circular gypsum casts tested by diametral compression using semicircular platens.	114
2.12	Tensile strength values of individual batches of 20mm shaped gypsum casts.	116
2.13	Tensile strength values of individual batches of 10mm shaped gypsum casts.	117
2.14	Pooled tensile strength results for shaped gypsum casts.	118
2.15	Tensile strength results obtained when preparing all four 20mm shapes from a single batch of slurry tested using semicircular platens.	120
2.16	Tensile strength results obtained when preparing all four 20mm shapes from a single batch of slurry tested using pointed platens.	121
2.17	Tensile strength values for 20mm casts where two shapes were produced from one batch of slurry.	122

Chapter 3 - Compaction studies using the single punch tablet machine.

3.1	Punch shapes and sizes used in compaction studies on the Manesty F3 single punch machine.	132
3.2	True density values of excipients used.	132
3.3	Compression weights of excipients used in single punch studies.	139
3.4	Effect of storage time on the tensile strength of 20mm diameter circular compacts with 2.8mm zero porosity thickness.	141
3.5	Contact widths between circular compacts and platens determined by cathetometry.	158
3.6	Contact widths between compacts and platens determined using self-carboned copy paper.	159
3.7	Comparison of actual tensile strength values with predicted values from the relative contact widths of circular compacts tested with flat and semicircular platens.	161
3.8	Comparison of contact widths for 20mm square and circular compacts tested with semicircular platens.	161
3.9	Diametral compression data for Emcompress circular compacts tested using semicircular platens.	163
3.10	Diametral compression data for Avicel circular compacts tested using semicircular platens.	164

3.11 Diametral compression data for Lactose DMV 100 circular compacts tested using semicircular platens. 165

3.12 Diametral compression data for Anhydrous Lactose DCL 21 circular compacts tested using semicircular platens. 165

3.13 Linear regression data for circular compacts tested by diametral compression using semicircular platens. 173

3.14 Axial compression data for Avicel circular compacts tested using semicircular platens. 174

3.15 Axial compression data for Emcompress circular compacts tested using semicircular platens. 175

3.16 Diametral compression results for shaped Avicel compacts tested using notched platens. 210

3.17 Diametral compression datafor Emcompress compacts tested using notched platens. 210

3.18 Comparison of the R-values obtained for square and circular compacts. 219

Chapter 4 - Compaction studies using the rotary tablet machine

4.1 Compression weights of excipients used in rotary machine studies. 251

4.2 Summary of diametral compression data for Emcompress compacts prepared on the Manesty D3B rotary tablet machine. 257

4.3 Summary of diametral compression data for Avicel compacts prepared on the Manesty D3B rotary tablet machine. 258

4.4 Weighted linear regression data for compacts prepared on the Manesty D3B rotary tablet machine and tested by diametral compression. 259

4.5 Summary of axial compression data for Emcompress circular compacts prepared on the Manesty D3B rotary tablet press. 274

4.6 Summary of axial compression data for square Emcompress compacts prepared on the Manesty D3B rotary tablet machine. 275

4.7 Summary of axial compression data for Avicel PH-102 compacts prepared on the Manesty D3B rotary tablet machine. 276

4.8 Linear regression data for compacts prepared on the Manesty D3B rotary tablet machine and tested by axial compression. 277

Chapter 5 - Comparison of the single punch and rotary tablet machine results

5.1 Maximum punch velocities for Avicel and Emcompress circular compacts prepared on a single punch machine. 290

5.2 Initial punch velocities for Avicel and Emcompress circular compacts prepared on the rotary tablet press. 296

Chapter 6 - The influence of shape on the strength of compacts prepared from granulated formulations.

6.1	Tablet formulations prepared in optimisation study.	331
6.2	Particle size data of granulates	334
6.3	Regression data describing the tensile strength of circular compacts prepared on the single punch machine and tested by diametral compression.	338
6.4	Regression data describing the tensile strength of circular compacts prepared on the single punch machine and tested by axial compression.	340
6.5	Regression data describing the tensile strength of circular compacts prepared on the rotary machine and tested by diametral compression.	342
6.6	Regression data describing the tensile strength of circular compacts prepared on the rotary machine and tested by axial compression.	344
6.7	Regression data describing the tensile strength of square compacts prepared on the single punch machine and tested by diametral compression.	346
6.8	Regression data describing the tensile strength of square compacts prepared on the single punch machine and tested by axial compression.	348
6.9	Regression data describing the tensile strength of square compacts prepared on the rotary machine and tested by diametral compression.	350

6.10 Regression data describing the tensile strength of square compacts prepared on the rotary machine and tested by axial compression. 352

Appendix

A1 Analysis of variance table for regression equation containing 9 independent variables. 375

A2 Analysis of variance table for regression equation containing all independent variables except Avicel. 376

A3 Contribution of Avicel to the sum of squares. 377

A4 Significance of the contribution of independent variables to the regression equation. 379

A5 Significance of the contribution of independent variables to the regression equation. 380

LIST OF FIGURES

		Page
Chapter 1 - Introduction		
1.1a	Relationship between compaction pressure and specific surface area.	41
1.1b	Relationship between specific surface area and compact porosity.	41
1.2	Relationship between compaction pressure and relative volume of a compact.	45
1.3	Forces operating on a powder under compression.	55
1.4	Relationship between observed pressure distribution and density distribution within compacts.	58
1.5	Development of the pressure pattern within a compact.	59
1.6	Diagrammatic representation of the stresses induced by beam bending tests.	65
1.7	Loading configurations for beam bending tests.	66
1.8	Diagram of stress distribution across loaded diameter for a cylinder compressed between two line loads.	71
1.9a	Diagram of stress distribution across loaded diameter for a cylinder compressed between two line loads.	74
1.9b	Diagram of stress distribution across loaded diameter for a cylinder compressed between two platens with uniform contact pressures.	74
1.10	Types of failure induced by the diametral compression test.	75

1.11a Diagram of stress distribution across loaded line for a rectangle (A/B = 0.4) compressed between two line loads. 81

1.11b Diagram of stress distribution across loaded line for a square (A/B = 1) compressed between two platens (a_i/A = 0.1). 81

1.12 Diagram of the indentation hardness test. 91

Chapter 2 - Evaluation of the diametral compression test using shaped gypsum casts

2.1 Effect of storage on the properties of 20mm gypsum discs. 101

2.2 Loading configurations used to test gypsum casts diametrally. 107

Chapter 3 - Compaction studies using the single punch tablet machine.

3.1 Schematic representation of the force monitoring instrumentation on the single punch tablet machine. 134

3.2 Typical force/time compression cycle on the single punch tablet machine. 135

3.3 Axial compression test. 143

3.4 Transverse compression test. 144

3.5 Ball bearing diametral compression test. 144

3.6 Three point bending test. 146

3.7 Effect of platen shape on the compaction pressure/ tensile strength profile of Lactose DMV 100 circular 149

compacts.

3.8 Effect of platen shape on the compaction pressure/ tensile strength profile of Avicel 10mm circular compacts. 150

3.9 Effect of platen shape on the compaction pressure/ tensile strength profile of Avicel 20mm circular compacts. 151

3.10 Effect of platen shape on the compaction pressure/ tensile strength profile of Anhydrous Lactose DCL 21 10mm circular compacts. 152

3.11 Effect of platen shape on the compaction pressure/ tensile strength profile of Anhydrous Lactose DCL 21 20mm circular compacts. 153

3.12 Effect of platen shape on the compaction pressure/ tensile strength profile of Emcompress 10mm circular compacts. 154

3.13 Effect of platen shape on the compaction pressure/ tensile strength profile of Emcompress 20mm circular compacts. 155

3.14 Effect of diameter on the compaction pressure/tensile strength profile of Avicel circular compacts. 167

3.15 Effect of diameter on the compaction pressure/tensile strength profile of Emcompress circular compacts. 168

3.16	Effect of diameter on the compaction pressure/tensile strength profile of Anhydrous Lactose DCL 21 circular compacts.	169
3.17	Effect of diameter on the compaction pressure/tensile strength profile of Lactose DMV 100 compacts.	170
3.18	Effect of compact thickness on the compaction pressure/tensile strength profile of Emcompress circular compacts.	171
3.19	Effect of compact thickness on the compaction pressure/tensile strength profile of Avicel circular compacts.	172
3.20	Effect of compact thickness on the compaction pressure/tensile strength profile of Avicel circular compacts.	177
3.21	Effect of compact thickness on the compaction pressure/tensile strength profile of Emcompress circular compacts.	178
3.22	Axial compression/diametral compression tensile strength ratios for Avicel 10mm circular compacts.	179
3.23	Axial compression/diametral compression tensile strength ratios for Emcompress 10mm circular compacts.	180
3.24	Plot of tensile strength versus porosity for circular Avicel compacts.	182
3.25	Plot of tensile strength versus porosity for circular Emcompress compacts.	183

3.26	Plot of tensile strength versus porosity for circular Avicel compacts.	184
3.27	Plot of tensile strength versus porosity for circular Emcompress compacts.	185
3.28	Heckel plot for Avicel 10mm diameter circular compacts.	188
3.29	Heckel plot for Emcompress 10mm diameter circular compacts.	189
3.30	Appearance of square compacts of Emcompress with theoretical zero porosity of 4mm prepared on the single punch machine.	191
3.31	Effect of shape on the compaction pressure/tensile strength profile of Emcompress 20mm compacts.	192
3.32	Effect of shape on the compaction pressure/tensile strength profile of Emcompress 10mm compacts.	193
3.33	Effect of shape on the compaction pressure/tensile strength profile of Emcompress 10mm compacts.	194
3.34	Effect of shape on the compaction pressure/tensile strength profile of Avicel 20mm compacts.	195
3.35	Effect of shape on the compaction pressure/tensile strength profile of Avicel 10mm compacts.	196
3.36	Effect of shape on the compaction pressure/tensile strength profile of Avicel 10mm compacts.	197
3.37	Effect of shape on the compaction pressure/tensile strength profile of Avicel 10mm compacts.	198

3.38	Effect of shape on the compaction pressure/tensile strength profile of Anhydrous Lactose DCL 21 20mm compacts.	199
3.39	Effect of shape on the compaction pressure/tensile strength profile of Anhydrous Lactose DCL 21 10mm compacts.	200
3.40	Effect of shape on the compaction pressure/tensile strength profile of Lactose DMV 100 20mm compacts.	201
3.41	Effect of shape on the compaction pressure/tensile strength profile of Lactose DMV 100 10mm compacts.	202
3.42	Plot of tensile strength versus porosity for 10mm Avicel compacts.	203
3.43	Plot of tensile strength versus porosity for 10mm Emcompress compacts.	204
3.44	Plot of tensile strength versus porosity for 10mm Anhydrous Lactose DCL 21 compacts.	205
3.45	Plot of tensile strength versus porosity for 10mm Lactose DMV 100 compacts.	206
3.46	Heckel plots for 10mm Avicel shaped compacts.	207
3.47	Heckel plots for 10mm Emcompress shaped compacts.	208
3.48	Effect of platen shape and test configuration on the compaction pressure/tensile strength profile of Avicel 10mm square compacts tested by diametral compression.	211

3.49	Effect of platen shape and test configuration on the compaction pressure/tensile strength profile of Avicel 10mm square compacts tested by diametral compression.	212
3.50	Effect of platen shape and test configuration on the compaction pressure/tensile strength profile of hexagonal shaped compacts.	213
3.51	Effect of compact shape on the compaction pressure/ tensile strength profiles of Avicel 10mm compacts.	215
3.52	Effect of compact shape on the compaction pressure/ tensile strength profiles of Avicel 10mm compacts.	216
3.53	Effect of compact shape on the compaction pressure/ tensile strength profiles of Emcompress 10mm compacts.	217
3.54	Effect of compact shape on the compaction pressure/ tensile strength profiles of Emcompress 10mm compacts.	218
3.55	Effect of compact shape on the compaction pressure/ tensile strength profiles of Emcompress 10mm compacts.	222
3.56	Effect of test method on the value of tensile strength obtained for 10mm diameter circular Emcompress compacts.	223
3.57	Effect of platen position on the value of tensile strength obtained for 10mm square Emcompress compacts.	226

3.58 Effect of platen position on the value of tensile strength obtained for 10mm square Emcompress compacts. 227

3.59 Effect of shape and thickness on the R-value of Avicel 10mm compacts. 229

3.60 Effect of shape and thickness on the R-value of 10mm Emcompress compacts. 230

3.61 Effect of shape on the force loss/die area for Emcompress compacts. 231

3.62 Effect of diminishing die wall lubricant levels on the tensile strength of Emcompress 10mm square compacts. 233

3.63 Effect of diminishing die wall lubricant levels on the R-values obtained when preparing 10mm Emcompress compacts. 235

3.64 The development of density patterns within compacts. 237

Chapter 4 - Compaction studies using the rotary tablet machine.

4.1 Diagram illustrating the location of the piezoelectric load cell for monitoring compaction forces on a Manesty D3B rotary tablet machine. 246

4.2 Diagram of the ejection ramp modifications enabling the insertion of 3 piezoelectric load cells. 249

4.3 Effect of shape on the compaction pressure/tensile strength profile of Avicel compacts produced on a rotary tablet machine. 261

4.4 Effect of shape on the compaction pressure/tensile 262

strength profile of Avicel compacts produced on a rotary tablet machine.

4.5 Effect of shape on the compaction pressure/tensile strength profile of Avicel compacts produced on a rotary tablet machine. 263

4.6 Effect of Magnesium Stearate on the compaction pressure/tensile strength profile of Avicel circular compacts produced on a rotary tablet machine. 264

4.7 Effect of shape on the compaction pressure/tensile strength profile of Emcompress compacts produced on a rotary tablet machine. 266

4.8 Effect of shape on the compaction pressure/tensile strength profile of Emcompress compacts produced on a rotary tablet machine. 267

4.9 Plot of tensile strength versus porosity for Emcompress compacts produced on a rotary tablet machine. 268

4.10 Effect of thickness on the compaction pressure/tensile strength of circular Emcompress compacts produced on a rotary tablet machine. 269

4.11 Effect of thickness on the compaction pressure/tensile strength of square Emcompress compacts produced on a rotary tablet machine. 270

4.12 Effect of thickness on the compaction pressure/tensile strength profile of Avicel compacts produced on a rotary tablet machine. 271

4.13 Effect of thickness on the compaction pressure/tensile strength of square Avicel compacts produced on a rotary tablet machine. 272

4.14 Effect of shape on the compaction pressure/tensile strength profile of Avicel compacts produced on a rotary tablet machine. 278

4.15 Effect of shape on the compaction pressure/tensile strength profile of Avicel compacts produced on a rotary tablet machine. 279

4.16 Effect of shape on the compaction pressure/tensile strength profile of Avicel compacts produced on a rotary tablet machine. 280

4.17 Effect of shape on the compaction pressure/tensile strength profile of Emcompress compacts produced on a rotary tablet machine. 281

4.18 Effect of shape on the compaction pressure/tensile strength profile of Emcompress compacts produced on a rotary tablet machine. 282

4.19 Plot of tensile strength versus porosity for Emcompress compacts produced on a rotary tablet machine. 283

4.20 Plot of tensile strength versus porosity for Emcompress compacts produced on a rotary tablet machine. 284

Chapter 5 - Comparison of the single punch and rotary tablet machine results

5.1 Schematic representation of the upper punch 288

	mechanism on a single punch machine.	
5.2	Geometry of a punch passing over the roller of a rotary tablet machine.	293
5.3a	Punch position on roller at start of dwell time.	295
5.3b	Punch position on roller at end of dwell time.	295
5.4	Plot of punch velocity versus time for an Avicel circular compact compressed at 64MPa.	298
5.5	Plot of punch separation versus time for an Avicel circular compact compressed at 64MPa.	299
5.6	Comparison of the force/time profiles obtained on the single punch and rotary tablet machines when compressing 10mm circular compacts of Avicel at approximately 95MPa (7.5kN).	301
5.7	Effect of machine type on the compaction pressure/ tensile strength profile of Avicel circular compacts.	302
5.8	Effect of machine type on the compaction pressure/ tensile strength profile of circular Avicel compacts.	303
5.9	Effect of machine type on the compaction pressure/ tensile strength profile of square Avicel compacts.	304
5.10	Effect of machine type on the compaction pressure/ tensile strength profile of square Avicel compacts.	305
5.11	Effect of machine type on the compaction pressure/ tensile strength profile of square Avicel compacts.	306
5.12	Effect of machine speed on the compaction pressure/ tensile strength profiles of Avicel circular compacts.	309

5.13	Diagrammatic representation of powder movement during the early stages of compression.	311
5.14	Effect of die wall friction on powder movement on a rotary tablet machine.	311
5.15	Effect of machine type on the compaction pressure/ tensile strength profile of circular Emcompress compacts.	313
5.16	Effect of machine type on the compaction pressure/ tensile strength profile of circular Emcompress compacts.	314
5.17	Effect of machine type on the compaction pressure/ tensile strength profile of square Emcompress compacts.	315
5.18	Effect of machine type on the compaction pressure/ tensile strength profile of square Emcompress compacts.	316
5.19	Effect of machine type on the compaction pressure/ tensile strength profile of circular Emcompress compacts.	317
5.20	Effect of machine type on the plot of tensile strength versus porosity for circular Emcompress compacts.	318
5.21	Effect of machine type on the plot of tensile strength versus porosity for square Emcompress compacts.	319
5.22	Effect of machine type on the plot of tensile strength versus porosity for circular Emcompress compacts.	320
5.23	Effect of machine type on the plot of tensile strength versus porosity for circular Emcompress compacts.	321
5.24	Effect of machine type on the plot of tensile strength versus porosity for square Emcompress compacts.	322

Chapter 6 - The influence of shape on the strength of compacts prepared from granulated formulations

6.1	Schematic representation of the Box-Benkhen experimental design.	332
6.2	Contour plots for circular compacts prepared on the single punch machine and tested by diametral compression.	339
6.3	Contour plots for circular compacts prepared on the rotary tablet machine and tested by diametral compression.	341
6.4	Contour plots for square compacts prepared on the single punch machine and tested by diametral compression.	343
6.5	Contour plots for square compacts prepared on the rotary tablet machine and tested by diametral compression.	345
6.6	Contour plots for circular compacts prepared on the single punch machine and tested by axial compression.	347
6.7	Contour plots for circular compacts prepared on the rotary tablet machine and tested by axial compression.	349
6.8	Contour plots for square compacts prepared on the single punch machine and tested by axial compression.	351
6.9	Contour plots for square compacts prepared on the rotary tablet machine and tested by axial compression.	353

GLOSSARY

a	Horizontal distance between upper and lower loading points in 4 point bending test.
a_i	Platen width.
A	Width of rectangle.
A_c	Area of the curved segment of a capsule shaped compact.
A_H	Hamaker constant.
b	Width of beam.
B	Length of the line of loading.
BFI	Brittle Fracture Index
BHN	Brinell Hardness Number.
c	Constant
C	Capping Index.
C_L	Cylinder length.
C_P	Applied pressure.
d	Depth of rectangular beam.
d_c	Contact width.
d_i	Indentation diameter.
d_m	Mean particle diameter.
d_0	Distance of separation of particles.
D	Diameter.
D_i	Indentor diameter.
D_r	Relative density.
E	Young's Modulus.
f	Frequency of rotation of rotary tablet machine.

F	Van der Waal's force.
F_A	Externally applied force.
F_D	Die reaction.
F_I	Force absorbed overcoming interparticle friction.
F_L	Force transmitted to lower punch.
F_R	Radial force.
G	Strain Energy Release.
h_c	Height of the curved segment of a capsule shaped specimen.
H	Diametral crushing strength.
H	Height of lower roller above the cam track on a rotary tablet machine.
I	Second moment of bending.
K	Stress Intensity Factor
K_H	Heckel constant.
L	Distance between lower supports in the 3 point bending test.
m	Weibull Modulus
M	Bending moment.
NWF	Normalised Work of Failure.
p	Porosity.
P	Applied load.
P_f	Probability of failure.
P_s	Punch separation.
Q	Deformation hardness.

r	Correlation coefficient.
R_p	Radius of circle through which punches travel.
R_r	Radius of roller.
R-value	Ratio of upper and lower punch forces on a single punch machine.
t	Thickness.
t_c	Contact time between punch and powder.
V	Volume.
V_i	Initial powder volume.
V_t	True powder volume.
V	Velocity.
V_P	Upper punch velocity on a single punch machine.
V_V	Vertical punch velocity on a rotary tablet machine.
W	Applied load.
W_f	Work of Failure.
Wt.	Weight.
γ	Compression susceptibility parameter.
δ	Vertical displacement of the mid-point of beam during beam bending tests.
ΔF	Van der Waal's Energy.
ε	Strain.
μ_I	Coefficient of interparticle friction.
μ_W	Coefficient of die wall friction.
σ_f	Tensile failure stress.
σ_x	Tensile stress.

σ_y	Compressive stress.
ϕ	Angle between cam track and position of punch on roller.
ρ_i	Poured bulk density.
ρ_n	Tapped bulk density.
ρ_t	True density
$\tau_{x,y}$	Shear stress.
υ	Poisson's Ratio.
ω	Angular velocity.

CHAPTER 1

INTRODUCTION

1. Introduction

Tablets are the most popular method of administering drug substances, accounting for about 70% of all ethical pharmaceutical preparations produced. Tablets are produced by compressing a medicinal substance, usually with a number of inactive materials, in a die between two punches. The earliest reference to a dosage form resembling the tablet is to be found in arabic medical literature, in which drug particles were compressed between the ends of engraved ebony rods, force being applied by means of a hammer. In December 1843 a patent was granted for a machine to compress powders to form compacts. The invention was first used to produce compacts of potassium bicarbonate. Later, Wellcome in Britain was the first company to use the term tablet to describe this compressed dosage form.

There are several reasons for the continued popularity of the tablet as a dosage form. It enables an accurate dosage of medicament to be administered simply. It is easy to transport in bulk and carry by the patient. The tablet is a uniform final product as regards weight and appearance. As solid formulations, tablets are usually more stable than liquid formulations. Tablets can be produced simply at a greater rate than other dosage forms and the resultant manufacturing costs are very much lower.

Early tablets were produced in cylindrical dies with flat faced, flat bevel edged or concave punches. While the majority of tablets produced are still circular, over the last 20 years there has been an increasing shift away from circular to shaped tablets for new products. The tablet identification

section of the Chemist and Druggist Directory (1992) describes 370 non-circular tablet products that are on the market in Britain while the Physicians Desk Reference (1991) contains illustrations of 428 non-circular tablets that are available in the U.S.A.

After round tablets the most common presentation is the capsule shaped tablet, sometimes referred to as a caplet. This shape is particularly popular for high dose products where the compression weight is necessarily high as the elongated shape makes the tablets easier to swallow than round tablets of equal weight.

Rheumatic patients often have impaired manual dexterity and experience difficulty handling small tablets. Shaped tablets have been used to ease these problems (Tovey 1987). A range of tablet designs containing central projections have been described in design patents and registrations. The purpose of the domes is to tilt the tablets so that they are easier to pick up.

A survey performed on the reaction of patients to the appearance of tablets has indicated that the tablet shape can influence patients' expectations of a medicine in terms of its potency, side effects and suitability for a particular ailment (Anon 1989). The studies found that tablets with highly angular appearances were universally disliked on the basis that they would be hard to swallow. Less predictable was the finding that other elements of tablet design such as the number and depth of scorelines, the degree of rounding on the corners and the hardness of the finish, indicated by surface shine, appeared to play a role in determining how easy or hard to swallow a tablet might be.

One effect of moving away from a circular shape is that the surface area to volume ratio will increase. The effect of altering the shape on the dissolution of sulfadiazine has been investigated (Zein 1989). The rate of release of the drug was found to be related to the surface area of the tablet. Hogan (1989) studied the relationship between tablet shape and the drug release rate from hydroxypropylmethylcellulose matrices.

The recent proliferation of novel shaped tablets has been driven by marketing needs, particularly in the U.S.A. In the U.S.A., where generic substitution by pharmacists is permitted, novel shapes are seen as a method of increasing patient loyalty to the branded product. Furthermore, the registration of novel designs offers the manufacturers protection from imitation by generic companies. While such regulations exist the number of novel shaped tablets will inevitably increase.

The production of shaped tablets is generally perceived as being more difficult than producing round tablets, however, there is little evidence in the literature to support or refute this belief. The aim of the work described in this thesis was to determine whether there are difficulties associated with the production of shaped compacts. The densification of powders is an operation of interest to a wide variety of industries such as ceramics, fertilisers, foodstuffs, metallurgy and nuclear fuels. The understanding of the compression/compaction processes has evolved through research in all of these fields. This research has been performed almost exclusively on circular samples using single ended compression. Section 1.1 of the introduction reviews this literature.

Many of the test methods used to determine the strength of

pharmaceutical compacts have been developed from tests used in the concrete, coal and ceramic industries. While little work has been reported on the strength of shaped pharmaceutical specimens there are a number of examples of tests that have been used on shaped specimens in other fields. A review of methods used to characterise the strength of pharmaceutical compacts is given in Section 1.2.

1.1 Studies of powder compaction

Powder materials are often characterised in terms of their compression or compaction properties. The term "compressibility" is defined as the ability of the powdered material to decrease in volume under pressure, and the term "compactability" is defined as the ability of the powdered material to be compressed into a compact of specified strength (Leuenberger and Rohera 1986).

1.1.1 Mechanisms of compaction

The process of producing strong coherent compacts from free flowing powders has been extensively studied and a variety of mechanisms proposed for the development of compact strength. It is almost universally accepted that compacts are formed due to interparticulate bonding that occurs on the molecular scale and that a prerequisite of such bonding is intimate contact between particles.

The magnitude of Van der Waals forces between two flat surfaces can be expressed by;

$$\Delta F = \frac{A_H}{12 \pi d_0^2} \qquad (1.1)$$

where A_H is the Hamaker constant, d_0 is the distance of separation and ΔF is the Van der Waals energy. The Hamaker constant can be obtained by surface free energy measurements. If the separation of surfaces takes place in liquids rather than air the Hamaker constant will be related to the interfacial forces of the liquid. Luangtana-Anan and Fell (1990) determined the tensile strength of compacts, saturated in a range of solvents, by diametral compression. The relationship between the tensile strength of a compact and the dielectric constant of the saturating solvent was mirrored by the relationship between the Hamaker constant and the dielectric constant, suggesting that Van der Waals forces contribute significantly to the tensile strength of compacts.

Jones (1937) described the formation of interparticulate bonding as "cold welding". For Van der Waals forces to operate particle separations of less than 50 nanometres have to be achieved between clean crystal faces. It was suggested that these conditions were achieved by shearing forces developed during compaction. Interparticulate bonding was weaker than internal bonding because the contact surfaces were not flat but composed of random asperities so the effective contact area was only a fraction of the true surface area.

Higuchi et al (1954) showed that plots of specific surface against applied pressure and porosity exhibited maxima, suggesting that a cold-welding mechanism was operating (Figure 1.1). At low pressures there was an increase in specific surface corresponding to the formation of new surfaces by fragmentation, indicating the predominance of a breaking mechanism. As the pressure increased, the surface area increased to a maximum before

Figure 1.1a
Relationship between compaction pressure and specific surface area (after Higuchi et al 1954)

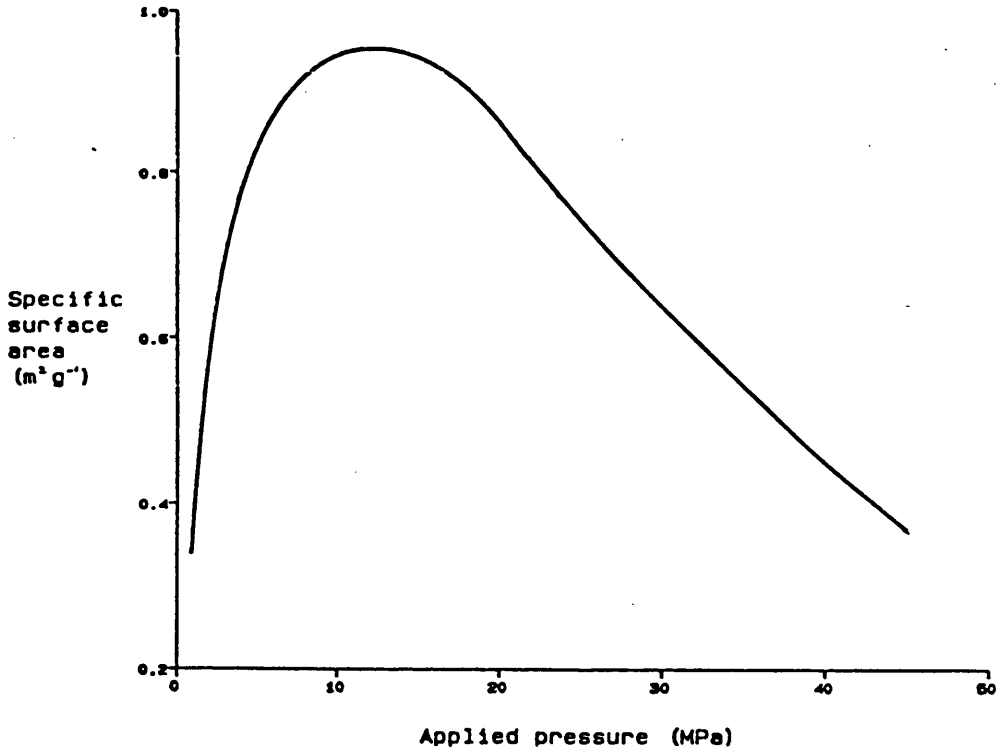

Figure 1.1b
Relationship between specific surface area and compact porosity (after Higuchi et al 1954)

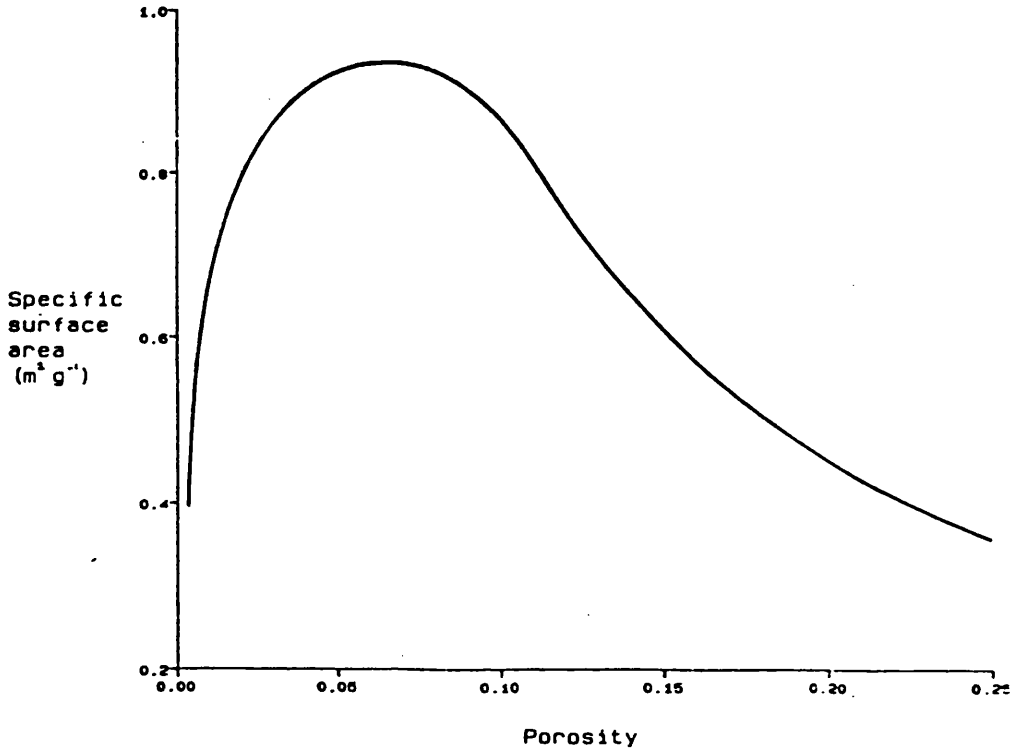

decreasing as the fresh surfaces were brought together and a cold-welding mechanism predominated.

Hardy (1939) used the model of low effective contact area (Jones 1937) to support a theory of localised fusion due to stress concentrations at surface asperities. It was postulated that the strength of metal compacts arose from the formation of necks and bridges at these points. Bonding by fusion at asperities is an unlikely process in view of the alternative methods of stress relief in materials. In hard, brittle materials the yield stress is greater than the breaking stress and a fracture mechanism is likely. For soft, yielding materials, the yield strength is lower than the breaking strength and plastic flow will predominate. For either process the energy requirement to disrupt structural bonds on a slip plane or fracture plane is much less than that required to produce fusion.

1.1.2 The compression process

When a powder is poured into a container the volume that it occupies depends on a number of factors such as particle size, particle shape and surface properties. If the powder bed is subjected to vibration or pressure, the particles move relative to each other to improve their packing arrangement. Ultimately, a condition is reached where further densification is not possible without particle deformation. This is termed the tapped density of a powder. In practise it is generally unrealistic to attain the theoretical tapped density and a lower value obtained under specified conditions is used for powder characterisation.

When a powder bed at tapped density is subjected to further compression the particles will deform elastically to accommodate induced stresses and

the density of the bed will increase with increasing pressure at a characteristic rate. When the elastic limit is exceeded there is a change in the rate of reduction in the bed volume as plastic deformation or brittle fracture of particles begins. Brittle materials will undergo fragmentation and the fine particles formed will percolate through the bed to give secondary packing. Plastically deforming materials will distort to fill voids and may also exhibit void filling by percolation when the limit of plastic deformation is reached and fracture occurs. Either mechanism, therefore, consists of at least two sub mechanisms and the processes could be repeated on the secondary particles produced by fracture until the porosity is at a minimum and the internal crystalline structure supports the compressional stress.

The concept of a sequential consolidation process was deduced by Seelig and Wulff (1946) from observations of pressure-volume relationships in metal powders. A 3 stage process was postulated:

1. Interparticle movement to give an improved packing arrangement, leading to the formation of temporary arches and struts capable of supporting the applied pressure.
2. Elastic or plastic deformation of individual particles depending on material properties.
3. Fracture and recombination of particles until voidage was at a minimum and the material itself was being compressed.

It is important to note that the process is sequential only for small elements of powder within a compact because of non-uniform pressure and density distribution. Externally determined pressure-volume values should

not be expected to give indication of distinct stages in the compression process when appreciable density gradients are present in the compact (Train 1956). This problem was demonstrated in the results presented by Shotton and Ganderton (1960) . Train (1956) examined the compression process of Magnesium Carbonate compacts and defined four distinct stages (Figure 1.2):

1. Interparticle slippage leading to closer packing.
2. The formation of arches and vaults protecting small voids and supporting the imposed loads.
3. A multi-stage process of deformation and cold-welding with fracture mechanisms predominating at low pressures and recombination processes at higher pressures.
4. A structure formed, strong enough to support the applied load, so that further densification would involve compression of the solid itself.

This sequential process was confirmed by Marshall (1963) who measured the electrical resistance of Sodium Chloride compacts containing 8% by weight of graphite. The second stage, involving vault and arch formation, was dependent on the particle size of the Sodium Chloride.

It is evident that there is general agreement on the sequence of the compression process. As there are a number of different stages in the process, some of them overlapping, it is unlikely that a single mathematical expression can describe the entire process. A large number of mathematical equations have been proposed to describe the relationship between compression pressure and compact volume, some of which are described in Section 1.1.3.

Figure 1.2
Relationship between compaction pressure and relative volume of a compact (after Train 1956)

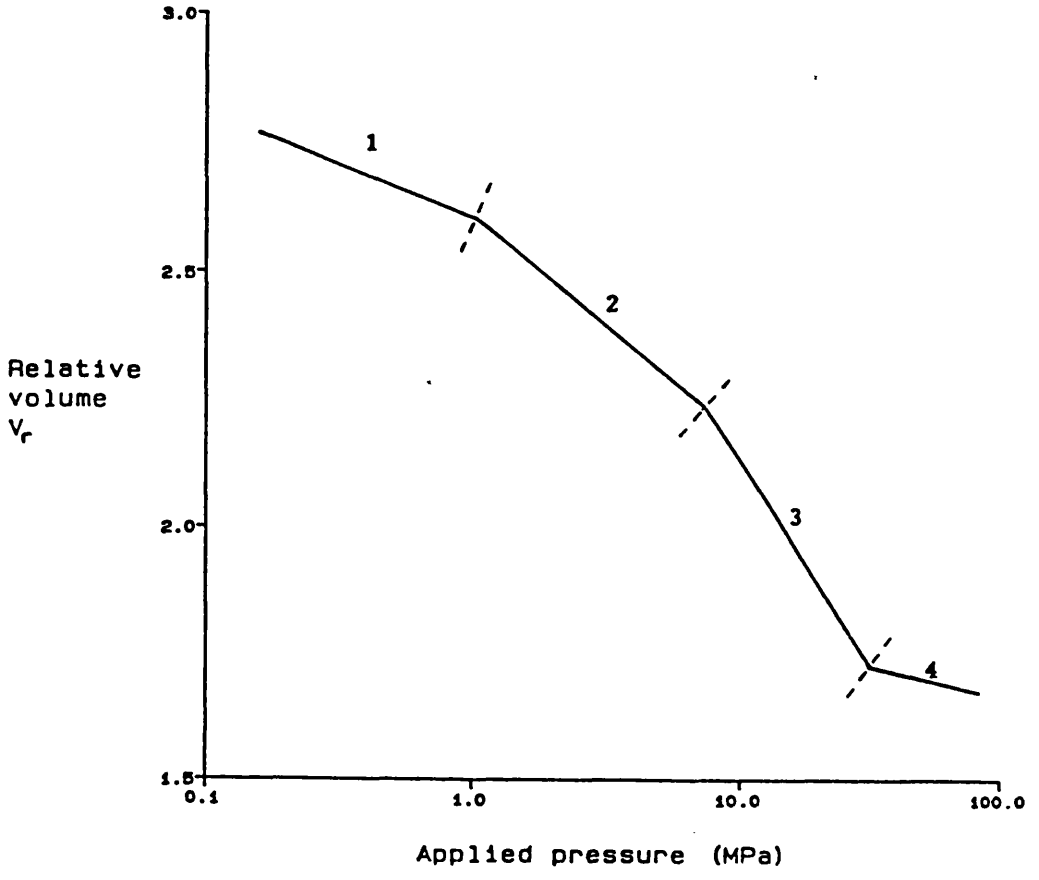

1.1.3 Pressure-volume relationships

1.1.3.1 Particle re-arrangement

The initial packing behaviour of a powder is one of the most difficult aspects of the consolidation process to classify and control because of its sensitivity to changes in packing conditions and material properties.

Hausner (1967) investigated the effects of interparticle friction on packing behaviour and used the ratio of tapped density (ρ_n) over poured density (ρ_l), termed the Friction Ratio, to define material packing. The Friction Ratio has been used to classify the flowability of powders, a ratio of less than 1.25 indicates good flow, greater than 1.5 poor flow (Wells 1988).

The mechanism of densification at bulk densities between poured density, ρ_l, and tapped density, ρ_n, will reflect the physical properties of the feed and will depend largely on interparticulate frictional forces. These mechanisms will vary from extensive re-arrangement of particles in the case of hard/rigid particles to deformation and limited slippage by soft/plastic particles.

1.1.3.2 Formation of supporting structures

This stage of the consolidation process is characterised by a reduction in the rate of reduction of volume with pressure as the particles lock together and resist the applied load. Such a decrease in volume reduction was clearly demonstrated by Marshall (1963) who also indicated the effect of particle size on this process.

While Train (1956) reported the presence of the strut and arch formation process, the plot of relative volume against pressure does not show a reduction in the rate of densification. A possible explanation is that the

incremental method of load application employed masked this pressure sensitive process.

1.1.3.3 Deformation and recombination of particles

This is the major densification stage of the compression process and its nature and extent is dependent on the physical properties of the material being densified. Ductile powders will deform plastically to occupy voids, while a brittle material will fragment and occupy voids by re-arrangement and percolation of fines. Most pharmaceutical materials exhibit a combination of these deformation behaviours.

The compression behaviours of four materials with differing mechanical properties have been examined (Lawrence 1970). It was concluded that a combination of elastic, plastic and fracture deformation mechanisms occurred simultaneously in each. The materials were classified as either hard-brittle or soft-yielding. Hard-brittle materials are generally considered more difficult to densify than soft-yielding materials. A possible explanation is that the filling of voids by a fragmentation-percolation mechanism is a much less efficient process than filling by plastic deformation.

Hardman and Lilley (1973) examined the change in specific surface, pore volume and bulk volume, with increasing applied pressure, of sodium chloride, sucrose and coal powders. A different deformation mechanism was found to predominate for each material. Sodium chloride densified by the plastic deformation of particles, the process becoming progressively more difficult as work hardening of the particles increased. For sucrose a fragmentation mechanism predominated with pore filling by percolation of

fine fragments an important secondary process. Coal densified by a fracture mechanism, like sucrose, but the fragments produced tended to form bridges and maintain an open pore structure.

A large number of equations have been proposed to describe the densification process. Many of these have an empirical basis and may relate to a particular material or range of pressures, while others attempt to define the complete process of densification.

The equation that has been most widely used to describe the densification of pharmaceutical powders is the Heckel equation (Heckel 1961);

$$\ln \frac{1}{1 - D_r} = K_H C_p + c \qquad (1.2)$$

where D_r = Relative density = Bulk density/True density

C_p = Applied pressure

K_H and c are constants

This equation, originally used to describe the densification of ceramics, is essentially a curve-fitting equation that provides reasonable correlation with the observed facts over a wide range of pressures (Sheikh-Salem and Fell 1981). Heckel (1961) considered that the constant, K_H, representing the slope of the function, could be correlated with the yield strength of the material being compressed.

Many authors have used the equation to describe the compression behaviour of their materials. Rue and Rees (1978) found that Sodium Chloride gave non-linear plots up to an applied pressure of 50MPa, while Microcrystalline Cellulose (Elcema) gave non-linear plots at all pressures.

Increasing the contact times produced increased consolidation of plastically deforming materials but had little effect on brittle or fragmenting materials. It was suggested that it might be useful to measure the areas under Heckel plots made at different contact times, in order to quantify the amount of plastic deformation.

York (1979) showed that the Heckel plot could be affected by a large number of factors including the history of the powder, the mode of die filling, the rate of compression, the contact time, the state and type of lubrication, the dimensions of the die and the technique used to determine the dimensions of the compact. The values obtained are likely to apply only to the set of experimental conditions chosen.

Roberts and Rowe (1985) produced Heckel plots for a number of materials using punch velocities over the range $0.033mms^{-1}$ to $400mms^{-1}$. The change in the yield strength with punch velocity, termed the Strain Rate Sensitivity, was used as an indication of the plasticity of a material.

The Heckel plot provides a useful measure of the way in which the density of a compact increases with applied force, however, it may not fit the observed facts at low pressures. Care is required when comparing values produced by different workers due to the sensitivity of the method to machine variables.

Cooper and Eaton (1962) proposed an equation containing two independent processes to describe the densification process. In the first stage of compaction large voids of dimensions corresponding to the powder particle size were filled by particle re-arrangement. In the second stage, occurring at higher applied pressures, small pores were filled by fragmentation and

percolation or by plastic deformation of the powder particles. The probability of hole filling was related to applied pressure by the equation;

$$\frac{V_i - V}{V_i - V_t} = c_1 e^{-c_2 C_p} + c_3 e^{-c_4 C_p} \qquad (1.3)$$

where V_i = initial powder volume

V_t = true material volume

V = compact volume at pressure C_P

c_1, c_2, c_3 and c_4 are constants for the material being examined. This equation has been used by Hunter (1985) to assess the compressibilty of pharmaceutical materials. Kawakita and Lüdde (1970) evaluated a number of equations used to describe the densification process. Re-arranging the equations so that the porosity was expressed in terms of relative volume and applied pressure they tested the equations by examining the effect on porosity as applied pressure tended to zero and infinity. On the basis that as C_p tends to zero, the compact density should tend to the initial density, and as C_p tends to infinity the compact density should tend to the true density of the material, they concluded that a number of equations were invalid. It is difficult to see the justification of judging the validity of the equations on the basis of 2 limiting results in view of the non-uniform relationship between pressure and volume within the 2 extremes. Many of the equations simply define the slope of stage 3 of the consolidation process and it is obvious by inspection that they cannot apply to the extremes of the process. Deviations from these equations will invariably occur at low applied pressures when stages 1 and 2 of the

process are still incomplete.

1.1.4 Relationship of compact strength to applied pressure and porosity

A large number of equations have been derived to describe the volume reductions that occur when a compressive force is applied. Despite the fact that, in the pharmaceutical industry, it is more important to be able to obtain a tablet of adequate strength than to obtain a specific volume reduction, only a few equations predicting the strength of a compact have been published.

Ryshekewitch (1953) and Duckworth (1953) found that the following equation held for ceramic materials;

$$H = H_0 e^{-c \cdot p} \qquad (1.4)$$

where; H = Diametral crushing strength

H_0= Diametral crushing strength at zero porosity

p = Porosity

c = Constant

Shotton and Ganderton (1960) demonstrated that the equation could be applied to the compaction properties of sucrose granules.

Higuchi et al (1954) found a linear relationship between the diametral crushing strength (H) and the logarithm of the maximum compressional force (P_{max});

$$H = c_1 . \ln P_{max} + c_2 \qquad (1.5)$$

where c_1 and c_2 are constants. Deviations were only found to occur at high

compressional forces.

Shotton and Ganderton (1961) examined the relationship between the crushing force (H) and the mean particle size (d_m) of Hexamine and Aspirin compacts, employing the following equations:

$$H = \frac{c}{\sqrt{d_m}} \qquad (1.6)$$

$$H = H_1 + \frac{c}{\sqrt{d_m}} \qquad (1.7)$$

where H_1 and c are material constants.

The equations are only applicable to situations where the interparticulate bonds are strong and failure occurs across particles rather than around particles. In such instances Equation 1.6 was found to be applicable to both Hexamine and Aspirin.

Leuenberger (1982) developed an equation relating the deformation hardness of a compact to the applied compressive stress;

$$Q = Q_{max}[1 - \exp(-\gamma\ C_p\ D_r)] \qquad (1.8)$$

where Q is the deformation (Brinell) hardness, Q_{max} is the magnitude of Q as the compression stress $C_p \rightarrow \infty$ and the relative density, $D_r \rightarrow 1$. γ is the compression susceptibility.

The equation contains 2 material constants; Q_{max} and γ. Q_{max} describes the compactability of the material. A low value for Q_{max} shows a relatively poor

compactability, for even with a high compression stress this figure cannot be exceeded. The parameter γ, termed the compression susceptibility, specifies the rate at which the compact hardness, Q, builds up with an increase in the compression stress, C_p. A high value of the compression susceptibility parameter indicates that the limiting hardness may be attained with relatively low compression stress. This results in a sharp decrease in compact porosity being attained with a relatively low compression stress.

For brittle materials, such as sucrose and lactose, the tensile strength determined using the diametral compression test could be used in place of the deformation hardness.

Jetzer et al (1983) presented a classification of the deformation behaviour of materials based on the values of Q_{max} and γ

Table 1.1

Approximate values of Q_{max} and γ observed in plastic and brittle materials

Parameter	Type of deformation under stress	
	Plastic	Brittle
Compactability	Small	Large
Q_{max} (MPa)	0 - 10^2	10^2 - 10^3
Compressibility	Large	Small
γ (MPa^{-1})	10^{-2}	10^{-3}

1.1.5 Pressure transmission through powders

When an axial force is applied to a cylindrical column of powder the pressures developed within the powder vary with depth. This phenomenon is attributed to the development of friction between the powder and the walls of the container.

As a result of an externally applied force, F_A, several reaction forces are induced in a powder mass confined in a die. Figure 1.3 shows schematically these forces in a cylindrical compact being compressed from one end. The external axial force, F_A, is balanced by 3 induced forces:

1. F_L, the force transmitted through the compact to the lower punch.
2. F_D, the die reaction or force absorbed by die-wall friction.
3. F_I, the force absorbed in overcoming interparticle friction.

The relationship may be written as;

$$F_A = F_L + F_D + F_I \qquad (1.9)$$

Die wall friction is dependent on the radial force, F_R, produced in the compact by induced shear stresses. Therefore;

$$F_D = \mu_W . F_R \qquad (1.10)$$

where μ_W is the coefficient of die wall friction. Similarly the force absorbed by interparticle friction may be expressed as;

$$F_I = \mu_I . F_R \qquad (1.11)$$

Figure 1.3
Forces operating on a powder under compression

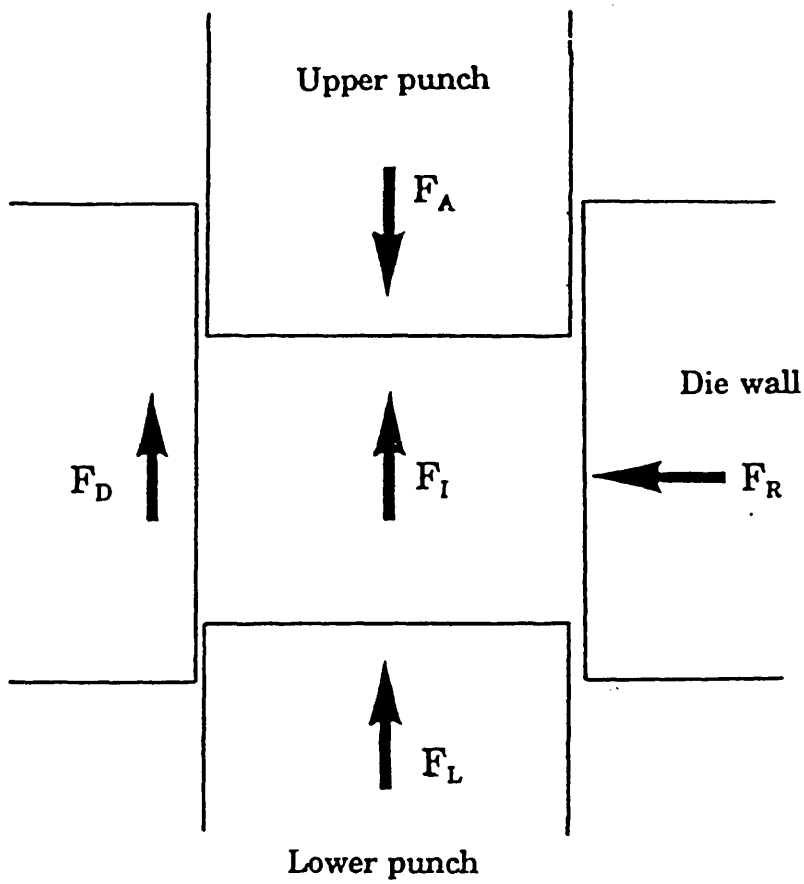

Combining the 3 equations;

$$F_A = F_L + F_R(\mu_W + \mu_I) \qquad (1.12)$$

The value of μ_I is much smaller than μ_W except at low values of F_A so that in practise the effect of interparticle friction is swamped by the effect of die-wall friction.

The die wall friction, therefore, produces pressure gradients within a powder during the compression process which in turn produces density variation within the final compact. The nature of such variations has been the subject of a number of investigations.

The distribution of pressure within a compact has been examined by inserting a lead grid into a powder in a die before compaction and examining the deformation of the grid after successive pressure increments using a radiographic technique (Seelig and Wulff 1946) and (Kamm et al 1949). Grid deformation was related to stress distributions within the compact. It was shown that, for single ended compaction, the density was at a maximum at the outer circumference of the compact adjacent to the moving punch and at a minimum at the outer circumference adjacent to the stationary punch. While the mean density decreased with increasing distance from the moving punch, a dense core of material existed on the compact axis near the stationary punch. This variation in density increased as the applied load increased. The effect was attributed to die-wall friction and it was demonstrated that lubrication of the die wall was effective in reducing the variation.

Train (1957) examined the distribution of pressure within a compact by

placing manganin wire resistance gauges at uniformly spaced stations in the compact. Pressure levels were measured under a range of applied forces and an isobaric chart of the compact obtained at each force interval. The results confirmed the existence of a region of high pressure remote from the moving punch (Figure 1.4). Density determinations on accurate volumes of material, produced a density pattern which corresponded closely to the pressure distribution measurements. Train (1957) supported the suggestion that die wall friction was the cause of non-uniform density distribution and also suggested that capping and lamination faults in compacts were attributable to this effect. An explanation for the observed patterns of density distribution, based on the development of high density wedges of material owing to high shearing forces at the die wall adjacent to the moving punch. Figure 1.5 represents the forces developed in the compact. At equilibrium the axial force is supported by the punch in direction a and by the powder in direction b. The radial component is supported by the die wall in direction c and by the powder bed in direction d. The resultant force acting on the mass is denoted by k and, because of the axial symmetry in the compact, the pressure front may be considered as a conical surface with focal point, B. Area B will show enhanced pressure and density values compared to its surroundings because of effective pressure concentration. The wedge-shaped area adjacent to the moving punch, bounded by dotted lines, will be subject to high shearing forces and will be highly densified. The central area A on the axis will be subjected to negligible shearing forces and will be protected from normal axial pressures by the vaulting effect of the high density wedges. Area C

Figure 1.4
Relationship between observed pressure distribution and density distribution within compacts (after Train 1957)

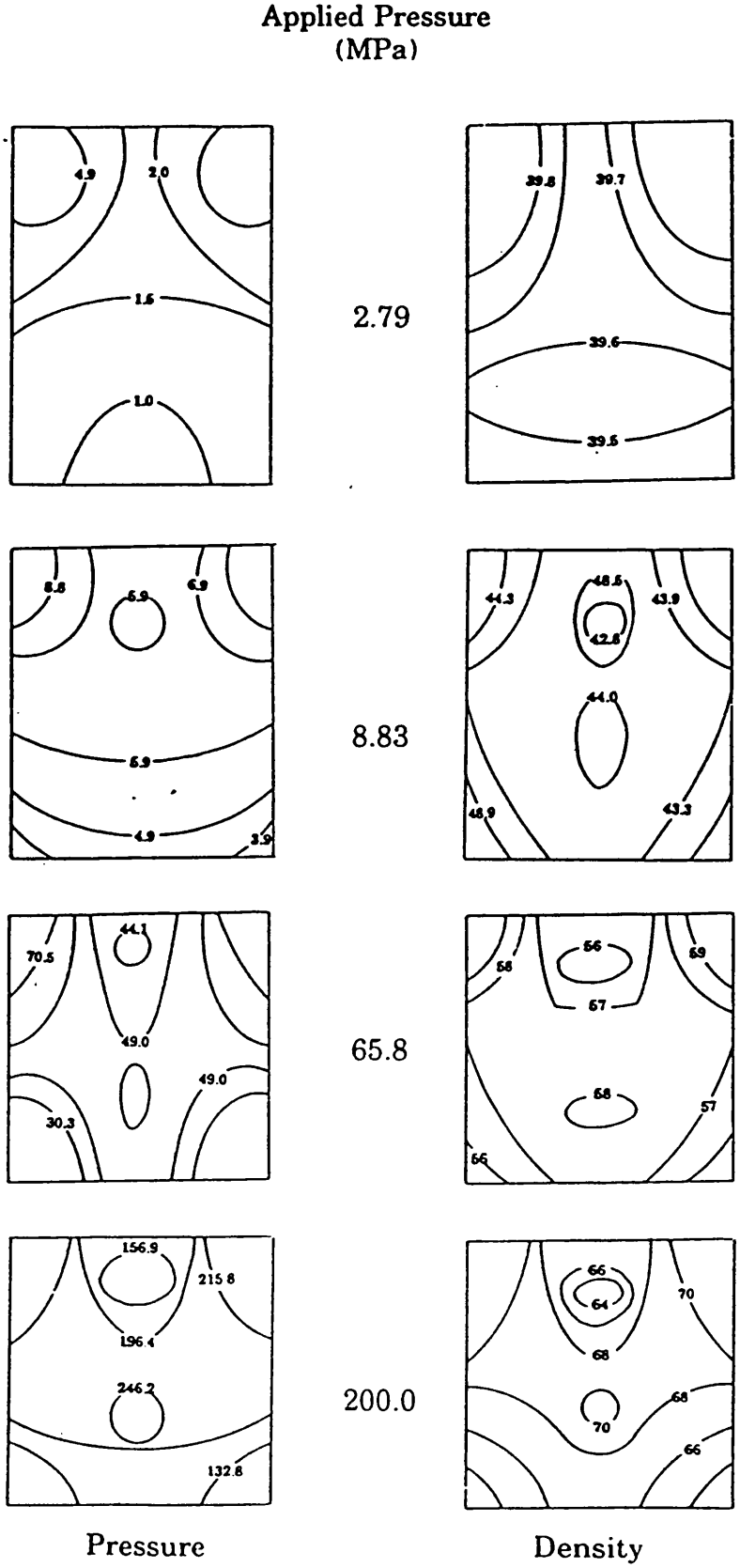

Figure 1.5
Development of the pressure pattern within a compact
(after Train 1957)

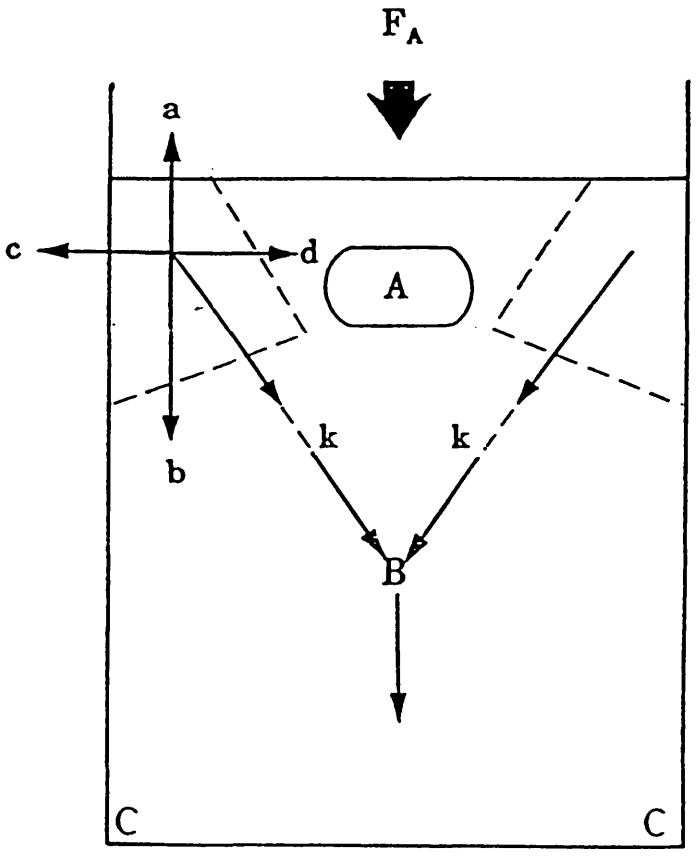

adjacent to the stationary punch will undergo no movement relative to the die wall, so that shearing forces will be absent. Density will be low since consolidation will depend on transmitted axial forces only.

The density distributions within compacts of uranium dioxide have been measured using autoradiography (Macleod 1974). Again similar results to those of Train (1956) and Kamm et al (1949) were obtained with an area of high density being produced near to the stationary punch. The results of Macleod (1974) differed from earlier studies by the appearance of a second area of high density positioned between the moving punch and the first area of high density. The development of this secondary area was attributed to a mechanism similar to that causing the formation of the primary high density area. The outward material movement and consequent densification is initiated when the axial reaction from the area of primary high density exceeds the radial pressure at any point between it and the moving punch.

The appearance of this secondary area in uranium dioxide compacts was attributed to higher frictional forces being present during their formation than those experienced by Train (1956) when preparing Magnesium Carbonate compacts.

Density distributions within circular compacts of Ammonium Sulphate were investigated by Charlton and Newton (1985) using a gamma ray attenuation technique. A beam of gamma-radiation was passed through compacts at points across the diameter. Layers of set thickness were removed and the measurements repeated. Comparison of the two sets of results enables the density of the material in the removed layer to be

calculated. The density distributions measured showed similar features to those reported by Train (1957), high density regions at the perimeter of the compact near the moving punch and low density regions near the stationary punch. The compacts examined had diameters of 5cm, which is larger than pharmaceutical compacts, because the resolution of the technique was limited by the diameter of the radiation beam used.

Most studies on particle movement and the resultant density distributions within compacts have used flat faced cylinders. Sixsmith and McCluskey (1981) assessed the effect of punch curvature on the movement of powders within a die using alternate layers of coloured and uncoloured powders. Increasing punch curvature resulted in an increase in axial powder movement adjacent to the die and a decrease in the centre of a compact. Horizontal movement of the powder within the die increased as the punch curvature increased. Mechtersheimer and Sucker (1986) measured the compression and ejection forces produced when pressing tablet formulations using flat faced and curved face punches on a rotary machine. Die wall pressures were greater when curved punches were used, again suggesting increased horizontal movement.

The value of much of the work reported in the literature is limited because of the artificial experimental conditions employed. The external measurement of the applied pressure gives average values with respect to the compact, since the compaction processes are not sequential. The results of internal measurements obtained by the introduction of measuring devices into the powder before compaction must be influenced to some extent by their presence. There remains a need for a technique that will

enable measurement of the density and/or pressures within compacts under conditions relevant to production processes.

1.2 Determination of the mechanical strength of pharmaceutical compacts

The determination of the mechanical strength of pharmaceutical compacts is carried out for several reasons;

1. As an in-process control to ensure that tablets are sufficiently strong to withstand handling yet remain bioavailable.
2. To assist in obtaining a fundamental understanding of compaction mechanisms.
3. To aid in the characterisation of the mechanical properties of the compacted material.

For many years the strength of pharmaceutical compacts has been determined in terms of the force required to fracture a specimen across its diameter. Such a test does not take into account the mode of failure or the dimensions of the tablet i.e. the result is not a fundamental property of the compact. An ideal test would allow comparison to be made between samples of different shapes or sizes. An essential feature of such a test is that the geometry of the specimens and the loading must be such that a calculable stress state prevails at the section where fracture occurs so that the fracture stress can be readily calculated from the fracture load.

1.2.1 Direct tensile testing

Pharmaceutical powder compacts tend to be brittle, that is fracture is not preceded by significant permanent deformation. For this reason the simple tensile specimen is not ideal for these materials and is rarely used.

Tensile tests have been performed on brittle materials, such as gypsum, by preparing dumb-bell shaped specimens. The enlarged ends are held in special grips and an axial tensile load applied. The results of such uniaxial tests are open to question. Photoelastic studies show large stress concentrations in the gripped portions of the specimen which can cause fracture elsewhere than in the central cross-section. In tests with concrete conglomerates, the fracture usually occurs at the weakest point between the grips and the central cross-section (Mitchell 1961). Strength calculations using this testing procedure neglect these stress concentrations. Also, small misalignments in the grips can add a bending component to the applied tensile stress. Ductile materials would correct this problem by plastic flow, without significantly affecting the results. Brittle materials have little or no capacity to flow plastically and the bending stress can seriously lower the measured strength (Rudnick et al). In the case of gypsum the material can be introduced into the mould while in a fluid state before it hardens making the preparation of samples relatively simple. The preparation of compacted powder specimens would be problematic, making the method unsuitable for the testing of pharmaceutical compacts.

An axial tensile strength test has been used to determine the tensile strength of round plane-faced tablets (Nyström et al 1977). The tablets were fixed to a pair of platens by a cyanoacrylate adhesive and strained in tension until fracture occurred. No analysis of the stress state induced by this method is reported.

1.2.2 Flexural tests

In the flexural test or bending test a specimen in the form of a parallel beam is subjected to 3 or 4 point bending and the maximum tensile stress estimated from the load at fracture. A feature of such a test is that under the correct conditions of loading the specimen will be subjected to a pure longitudinal tensile stress along a line on the opposite surface to that on which the load is applied.

In general for a beam subjected to bending the tensile fracture stress, σ_f, can be calculated from the following expressions (Stanley 1985);

$$\sigma_f = \frac{M\, y_{max}}{I} \qquad (1.13)$$

where M is the bending moment at fracture, y_{max} is the transverse coordinate measure in the plane of bending (Figure 1.6) and I is the second moment of bending. For a beam of rectangular cross section, width b and depth d;

$$I = \frac{b\, d^3}{12} \qquad (1.14)$$

and

$$y_{max} = \frac{d}{2} \qquad (1.15)$$

The maximum bending moment, M, is dependent on the loading configuration used. In practise, one of two loading models is used; 3 point

Figure 1.6
Diagrammatic representation of the stresses induced by beam bending tests

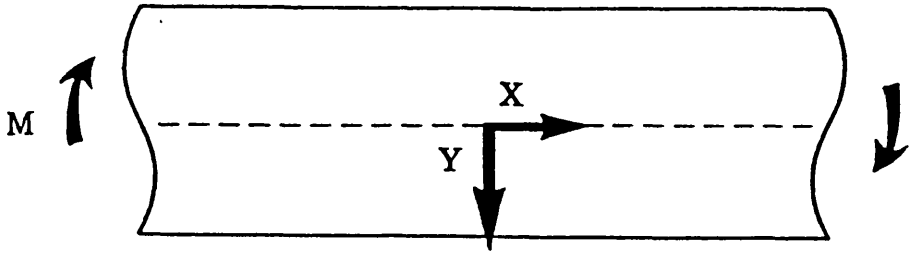

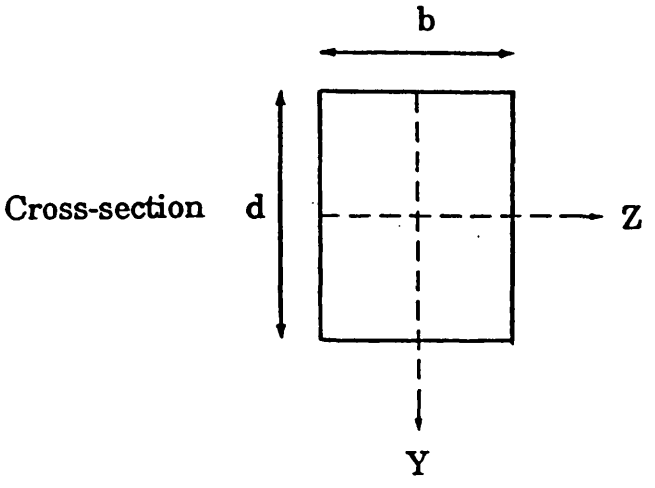

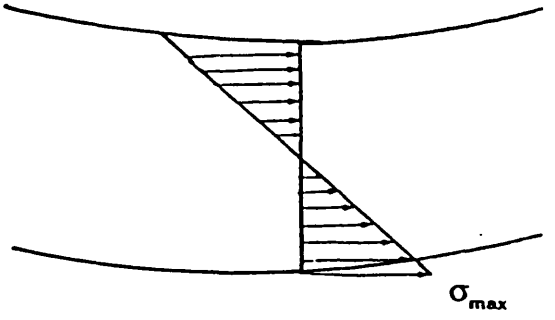

Figure 1.7
Loading configurations for beam bending tests

3 point bending

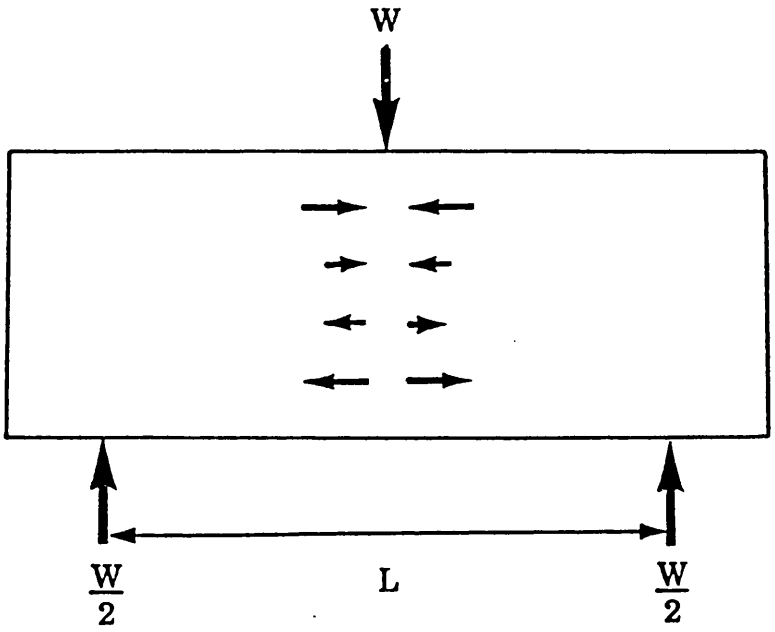

4 point bending

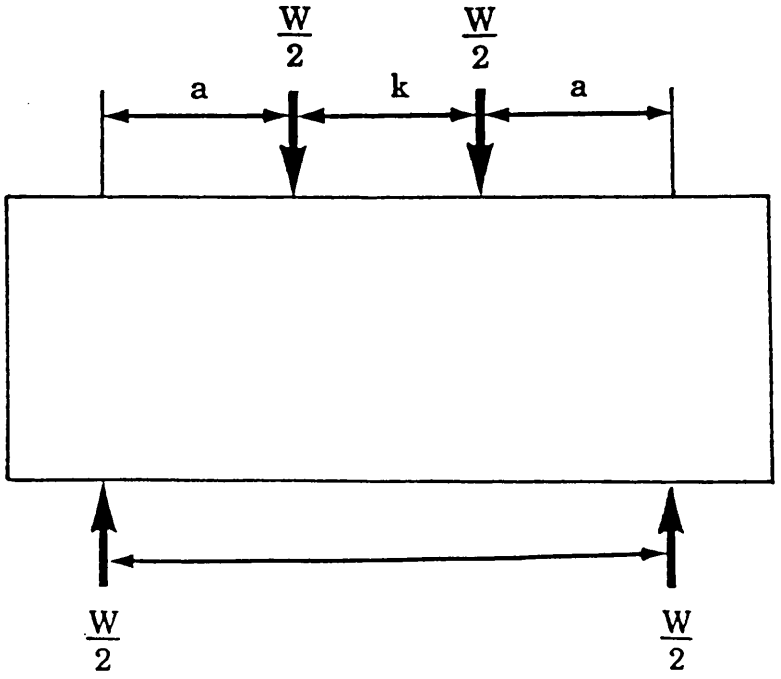

loading or 4 point loading (Figure 1.7).

For the symmetrical three point loading configuration the maximum bending moment is

$$M = \frac{W L}{4} \qquad (1.16)$$

where W is the fracture load, and L is the distance between supports. Thus at failure the tensile fracture stress is;

$$\sigma_f = \frac{W L}{4} \cdot \frac{d}{2} \cdot \frac{12}{b d^3} \qquad (1.17)$$

leading to,

$$\sigma_f = \frac{3 W L}{2 b d^2} \qquad (1.18)$$

The maximum bending moment obtained using the four point loading configuration is;

$$M = \frac{W a}{2} \qquad (1.19)$$

thus at failure;

$$\sigma_f = \frac{W a}{2} \cdot \frac{d}{2} \cdot \frac{12}{b d^3} \qquad (1.20)$$

leading to,

$$\sigma_f = \frac{3 W a}{b d^2} \qquad (1.21)$$

Modifications for asymmetric cross sections can be readily introduced.

Four point loading is usually considered to be preferable since a region of constant bending moment is obtained between the two inner loading points. The stress distribution in the specimen is non-uniform, varying from zero at the neutral axis to a maximum at the outer edge surface. This accentuates the effects of surface conditions on the measured strength and results obtained using this test are considerably higher than the true tensile strength (Berenbaum and Brodie 1959). Beams of rectangular cross-section prepared from pharmaceutical materials have been tested using this method to characterise the material properties of compacted powders (Church and Kennerley 1984) and (Mashadi and Newton 1987). Rectangular beams are not a conventional tablet shape and the density distributions developed during beam formation are unlikely to be the same as those produced in a right circular cylinder (Charlton and Newton 1985).

The three point flexure test has been applied to plane-faced round tablets (Endicott et al 1961). This was a manually operated test which meant the application of stress was variable and operator dependent. While the design of the test produced a bending moment there was also likely to be a large contribution of shear stresses at failure.

David and Augsburger (1974) also used the three point flexure to measure the tensile strength of round tablets. One problem with such an approach is that the dimensions of the tablets are unsuitable, generally being too stubby to allow a valid application of the equations derived from classical theories of bending; shear stresses would be important in such specimens. It is unlikely that the tensile fracture stresses obtained by diametral

compression and flexure will be equal (Wright 1955). It is, therefore, surprising that David and Augsburger (1974) found results that correlated very well. This could be explained by the fact that the mathematical analysis was incomplete. Stanley and Newton (1980) stated that some of the mathematical analysis was based on incorrect assumptions.

Capsule shaped tablets have been tested using a 3 point flexure test (Gold et al 1980). The breaking load was used to express the strength of the compacts and no attempt was made to calculate the tensile stresses. Stanley and Newton (1980) calculated the theoretical tensile stresses induced by the three point flexure tests on capsule shaped specimens. It was concluded that a reasonable approximation of the tensile stresses could be obtained using the equation;

$$\sigma_x = \frac{3WI}{2d^2}\left[\frac{6 + 2h_c}{6A_c + bd}\right] \qquad (1.22)$$

where A_c is the area of the curved segment of the capsule and h_c the height of that segment.

The flexure test has been used to characterise the strength of compacts prepared from pharmaceutical materials. The test does not, however, lend itself to the testing of circular compacts or thin square compacts where the shear stresses may significantly affect the results obtained.

1.2.3 The diametral compression test

1.2.3.1 Analytical solution

A method of testing brittle materials that does not suffer from the previous disadvantages is the diametral compression test. This consists of a simple flat faced disc specimen which is subjected to two diametrically opposed

point loads. The diametral compression test was developed independently at the same time by Carneiro and Barcellos (1953) in Brazil and by Akazawa (1953) in Japan and is referred to as the "Brazilian disc" or indirect tensile test, the indirect referring to the fact that a tensile fracture is obtained from compressive loading.

The test has been used to measure the tensile strength of concrete (Wright 1955), coal (Berenbaum and Brodie 1959), gypsum (Earnshaw and Smith 1966) and pharmaceutical compacts (Fell and Newton 1970). A complete analytical solution exists for the stress state induced by this loading configuration.

Assuming plane stress and considering a circular disc with concentrated loads on the diameter, three general equations can be used to express the stress conditions at all points within the disc (Figure 1.8)(Den Hartog 1952):

$$\sigma_x = \frac{-2P}{\pi t}\left(\frac{(R-y)x^2}{r_1^4} + \frac{(R+y)x^2}{r_2^4} - \frac{1}{D}\right) \qquad (1.23)$$

$$\sigma_y = \frac{-2P}{\pi t}\left(\frac{(R-y)^3}{r_1^4} + \frac{(R+y)^3}{r_2^4} - \frac{1}{D}\right) \qquad (1.24)$$

$$\tau_{xy} = \frac{2P}{\pi t}\left(\frac{(R-y)^2x}{r_1^4} - \frac{(R+y)^2x}{r_2^4}\right) \qquad (1.25)$$

Considering points between OC on the horizontal X axis where y = 0;

Figure 1.8
Diagram of stress distribution across loaded diameter for a cylinder compressed between two line loads

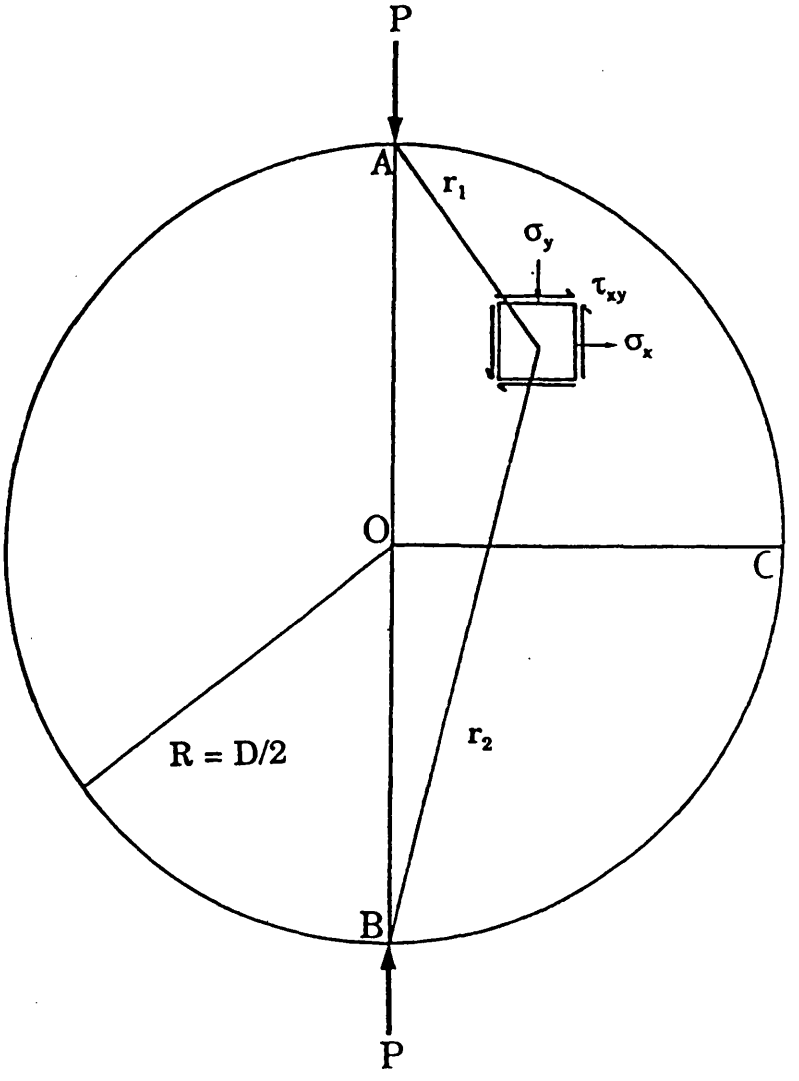

$$r_1 = r_2 = \sqrt{x^2 + R^2} \qquad (1.26)$$

Both stresses vanish at the circumference and reach maximum values at the centre. The stresses at the centre are;

$$\sigma_x = \frac{2P}{\pi tD} \qquad (1.27)$$

$$\sigma_y = \frac{-6P}{\pi tD} \qquad (1.28)$$

Therefore, the compressive strength needs to be at least three times the tensile strength to ensure a tensile failure.

Along the Y-axis AB where x = 0;

$$r_1 = R - y \qquad (1.29)$$

$$r_2 = R + y \qquad (1.30)$$

$$\tau_{xy} = 0 \qquad (1.31)$$

$$\sigma_x = \frac{2P}{\pi tD} \qquad (1.32)$$

This indicates that tensile failure of the specimen could start at any point

$$\sigma_y = \frac{-2P}{\pi t}\left(\frac{2}{D-2y} + \frac{2}{D+2Y} - \frac{1}{D}\right) \qquad (1.33)$$

along the vertical AB axis due to the even distribution of tensile stresses. The compressive stress on this axis increases from $\sigma_y = -6P/\pi Dt$ at the centre to $\sigma_y = \infty$ at the loading points. With a concentrated load, the specimen will fail at the loading points due to the compressive stresses and not in the central part of the specimen due to the tensile stress.

1.2.4.2 The effect of loading conditions on the diametral compression test

In practise, the theoretical condition of lines of contact between specimen and platens cannot be achieved; instead the load is distributed over areas of contact. Comparison of Figures 1.9a and 1.9b shows that provided the area of contact is small in relation to the diameter of the disc this only affects the stress distribution near the ends of the loaded diameter and the tensile stress is $2P/\pi Dt$ over a large fraction of the loaded diameter (Rudnick et al 1963).

It has been shown that tensile stresses can be held uniform across a reasonable proportion of the loaded diameter if the width of the contact area does not exceed one tenth of the specimen diameter (Peltier 1954).

The solution for the tensile stresses can only be used to calculate the tensile strength of a specimen provided it fails in tension. This is characterised by failure along the loaded diameter (Figure 1.10). The fracture does not always extend right to the ends of the diameter. A second fracture pattern, the triple cleft failure has also been identified as being failure in tension (Rudnick et al 1954). Compressive failure occurs at the specimen surface immediately beneath the loads where the compressive

Figure 1.9a
Diagram of stress distribution across loaded diameter for a cylinder compressed between two line loads

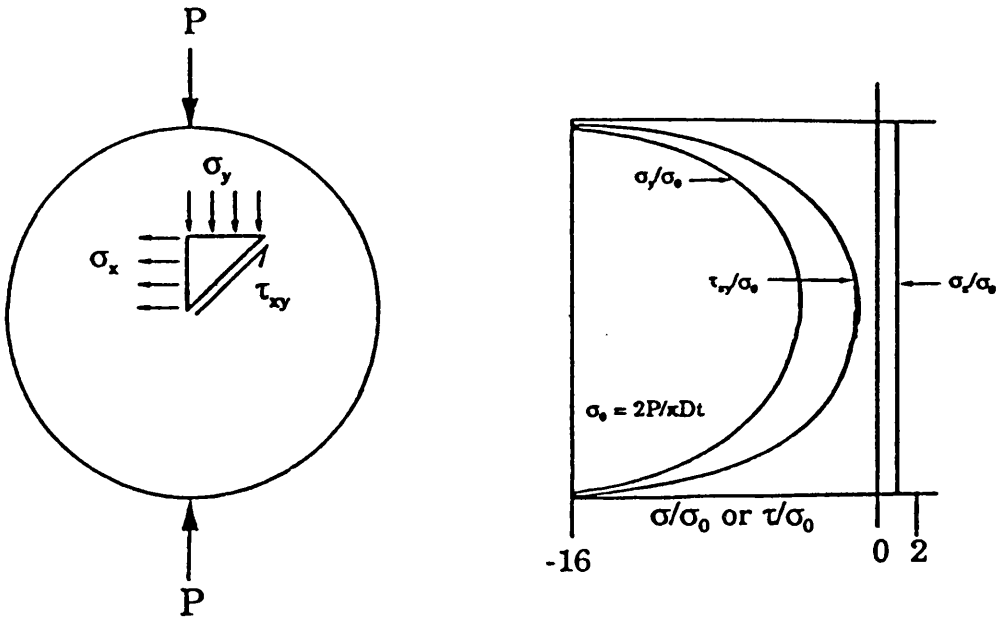

Figure 1.9b
Diagram of stress distribution across loaded diameter for a cylinder compressed between two platens with uniform contact pressures

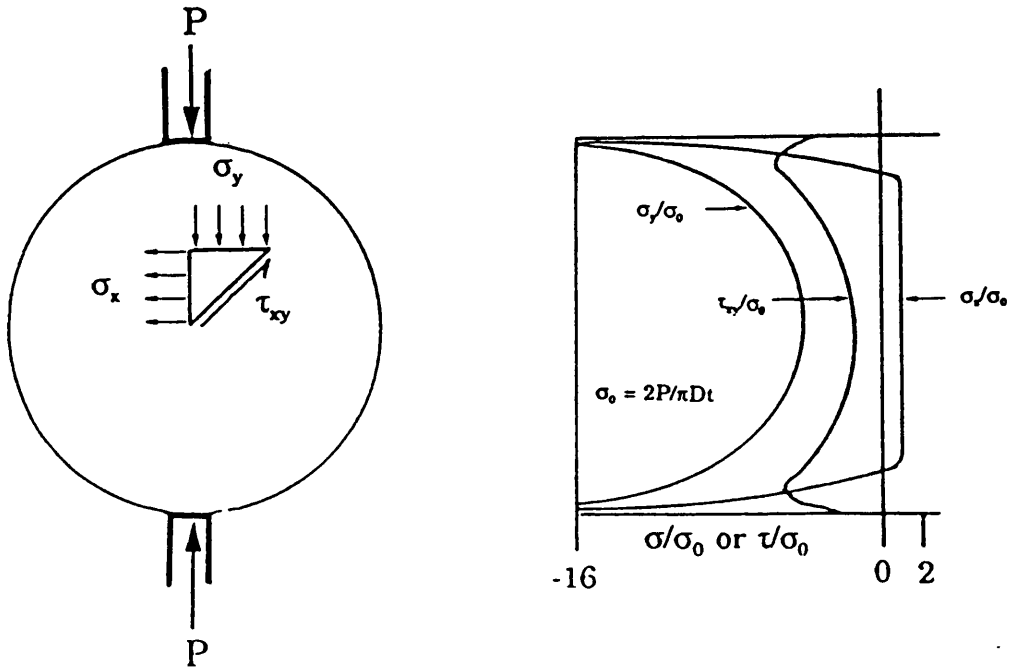

Figure 1.10
Types of failure induced by the diametral compression test

Simple tensile failure

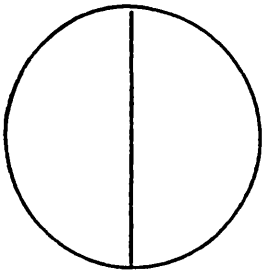

Triple cleft failure
(tensile failure)

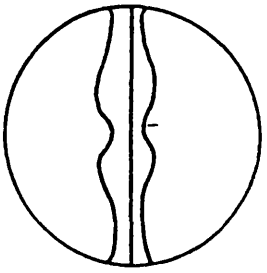

Failure due to shear
at platen edges

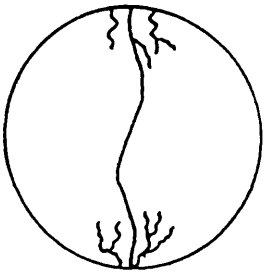

stresses are at a maximum and appears as local crushing. If this crushing is not extensive it may only result in an increase in the area over which the load is applied so that ultimate failure may be in shear or tension.

As shown in Figure 1.9b the maximum shear stresses occur beneath the surface. The exact location and magnitude of these stresses depend on the distribution of applied loads. Shear failures start at an angle to the loaded diameter and are followed by secondary failures causing an irregular fracture pattern. Thus, the validity of using the diametral compression test under a given set of conditions to determine a tensile strength from a fracture load , can be easily assessed by examining the specimen fragments after failure (Addinall and Hackett 1964).

The mode of failure is affected by the width of the contact area. Some materials such as concrete (Mitchell 1961) and ceramics (Rudnick et al 1955) require relatively soft packing pieces to be placed between the platens and specimens to ensure adequate load distribution and therefore failure in tension. Other specimens such as autoclaved plaster deform sufficiently at the points contact to ensure that failure occurs in tension (Earnshaw and Smith 1966). The failure is also influenced by the type and extent of padding. The effect of padding can be predicted by mathematical study although experimental evidence indicates that such predictions are only general at best (Mitchell 1961).

The material properties of the platen will modify the stress distribution within the disc. Photoelastic studies using epoxy resin discs showed that platens made of different materials such as steel, rubber and cardboard produced different stress patterns (Addinall and Hackett 1964).

Experimentally determined fracture strengths indicated that the lower the elastic moduli of the platens or padding the higher was the apparent tensile strength of the disc and the greater the variance of the results. This may be explained by the increased contact area causing a reduction in the volume of material subjected to the maximum tensile stress. Such effects appear to be material and condition dependent as Wright (1955) and Fell and Newton (1970) reported a decrease of variability with an increase in padding material.

The shape of the platens is also of importance in determining the outcome of the diametral compression test. Concave semicircular platens have been used to induce tensile failure in graphite specimens where formerly only compressive failure occurred. A modified solution for the stresses produced by the platens is required in this case (Awaji and Sato 1979).

1.2.4.3 The effect of loading rate on the diametral compression test

The rate at which the load is applied to specimens can affect the results obtained. Increasing the rate of loading of concrete cylinders resulted in higher observed tensile strengths (Mitchell 1961). Tablets containing lactose and microcrystalline cellulose were tested at loading rates corresponding to cross-head movements of 0.05 to 5cm min^{-1} (Rees et al 1970). An increase in the loading rate produced a significant increase in the breaking strength although the standard deviation of replicate values was apparently unaffected. It was also concluded that discrepancies in tensile strength values obtained by different testing instruments may be partially attributed to differences in rates of loading.

The effect of the loading rate on the value of tensile strength obtained for

compacts of acetylsalicylic acid and ammonium sulphate has been investigated (Newton et al 1986). Increasing the loading rate produced a decrease in the tensile strength obtained for compacts of both materials. For ammonium sulphate, the change in strength with strain rate was a linear function of the log of the strain rate.

The response of a material to loading rate changes appears to be dependent on the mechanism of failure. Variations in strain rate can lead to changes in the failure mode. At low strain rates some materials may fail in a ductile manner. The faster the strain rate the more likely the failure is to be brittle in nature.

1.2.4.4 Tensile strength testing of non plane-faced circular compacts

The diametral compression test has also been used to measure the tensile strength of round convex-faced compacts. The loads required to produce tensile failure of flat-faced and deep convex tablets were compared to produce an empirical equation for tensile strength (Newton et al 1972). The method requires that a linear relation exists between the breaking load and the compaction pressure for the convex tablets and does not allow the isolated determination of the tensile strength of convex-faced tablets. An equation for the tensile strength of convex-faced tablets was calculated utilising the central thickness of the tablet (Esezbo and Pilpel 1976). The equation was a correction for the difference in the cross sectional area between a convex-faced and plane-faced specimen which has no theoretical basis in relation to elastic theory.

The stresses induced in convex-faced specimens by the diametral compression test have been examined photoelastically (Pitt et al 1989).

Formulae were derived that enable the tensile strength of a convex-faced specimen to be determined from a knowledge of the fracture load and the specimen dimensions. The formulae were verified by comparing the loads required to produce tensile failure of flat-faced and convex-faced gypsum specimens (Pitt et al 1988). The tensile strength of a convex specimen may be determined from the fracture load by the equation;

$$\sigma_f = \frac{10P}{\pi D^2}\left(2.84\frac{t}{D} - 0.126\frac{t}{C_L} + 3.15\frac{C_L}{D} + 0.01\right)^{-1} \quad (1.34)$$

where P is the fracture load of the convex-faced disc, D the diameter, C_L the cylinder length and t the overall thickness of the disc.

The diametral loading of flat faced discs with a groove across the diameter of one face has been examined photoelastically (Newton et al 1977). The tensile stress distribution was affected by the depth of the groove and also the orientation of the groove with respect to the loaded diameter.

1.2.5 Line loading of rectangles

An analysis of the line loading of rectangles was performed using both point loading and loading with indentors of different widths (Goodier 1932)(Figure 1.11). The analysis showed that in general the average tension along the loaded line was given by;

$$\sigma_x = \frac{2P}{\pi B t} \quad (1.35)$$

where B is the length of the line of loading. This expression is independent of the proportions of the rectangle, with the middle portion of the loaded line subjected to approximately uniform normal stress.

The maximum tensile stress is the important quantity in determining failure; for point loading this tensile stress was calculated to rise to a peak value near to the loading platens, before becoming compressive in the immediate vicinity of the indentor (Figure 1.11a). However, for broad indentors ($a_i/B = 0.1$, where a_i = width of indentor), there was little if any rise in the tensile stress along the loaded line (Figure 1.11b). The stress remained uniform for a considerable portion of the section before becoming compressive in the loading zone. Hence, for the latter condition, the tensile strength would be given by;

$$\sigma_f = \frac{2\,P}{\pi\,B\,t} \qquad (1.36)$$

The tensile strength of concrete cubes was assessed experimentally by using an indentor method (Nillson 1961). The indentors were used with padding and, under these conditions, good correlation was found between the determined tensile strength of the cubes using Equation 1.36 and the determined tensile strength of cylinders using Equation 1.26. Subsequently, a finite element method was used (Davies and Bose 1968) to assess the indentor method. Equation 1.36 was shown to be a good approximation of the tensile strength of the material.

The indentor test was examined by photoelasticity for squares (Berenbaum and Brodie 1959). The width of the indentor, a_i, was varied and the resulting stress state calculated. As the indentor width was increased (from $a_i/B = 0.1$ to $a_i/B = 0.75$) with the load kept constant, the tensile stress along the loaded line decreased. However, when the applied stress

Figure 1.11a
Diagram of stress distribution across loaded line for a rectangle (A/B = 0.4) compressed between two line loads

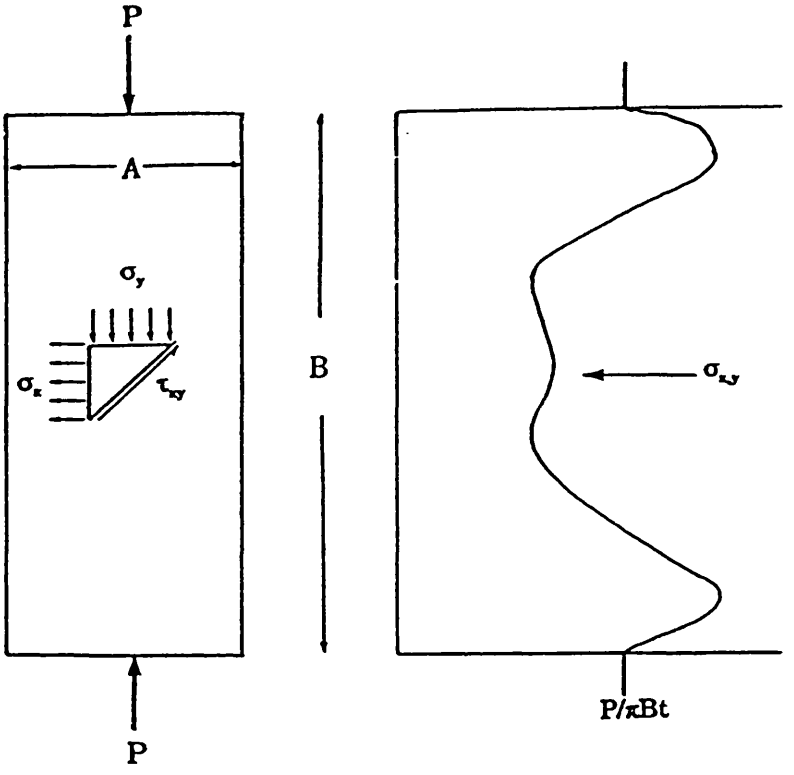

Figure 1.11b
Diagram of stress distribution across loaded line for a square (A/B = 1) compressed between platens (a_i/A = 0.1)

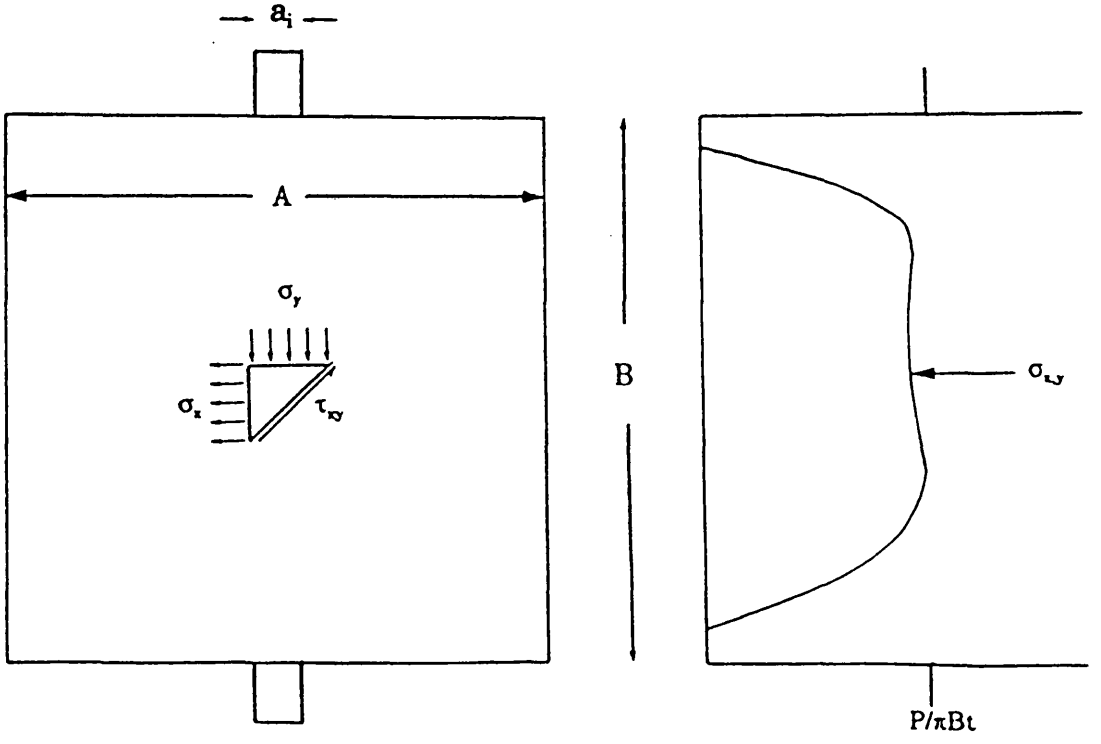

was kept constant the maximum tensile stress reached its greatest value at $a_i/B = 0.4$.

A theoretical solution for indentor loading was attempted by Jordan and Evans (1962). Four approximate solutions for the elastic stresses in a square were obtained. These solutions were compared with the photoelastic analysis of Berenbaum and Brodie (1959). Only one solution was found to be in approximately good agreement with the experimental results; the other theoretical results were markedly different. The inadequacies of the theoretical solutions can be attributed to the differences in approximating the boundary conditions.

A different theoretical solution for the indentation test on squares was attempted by Sundara and Chandrashekhara (1962). The stresses along the central loaded axis were evaluated by considering the shape of the pressure distribution under the indentor. Again difficulties were found in the theoretical modelling of the stress distribution.

The photoelastic results of Berenbaum and Brodie (1959) are used in preference to the theoretical results above when a reliable value for a tensile strength is required (Hiestand et al 1974). However, the experimental results of Berenbaum and Brodie (1959) and the theoretical solution of Goodier (1932) give approximately the same tensile strengths for indentor widths in the region $a_i/b = 0.1$ to 0.2. Therefore, when these particular indentor widths are used, Equation 1.36 can be used to determine the tensile strength.

Cube shaped specimens have also been tested by loading across a diagonal i.e applying the load to opposite edges rather than faces. Analysis of this

test configuration by the finite element method indicated that the maximum tensile stress along the loaded axis is approximately 0.77 of that predicted by Equation 1.22 (Davies and Bose 1968)

1.2.6 Line loading of ellipses

A theoretical analysis for the stress distribution in an elliptical disc due to concentrated axial loading showed that the tensile stresses were a function of the width to length ratio and were at a maximum for a circular disc (Brisbane 1963). The tensile stress along the loaded axis, σ_x, was calculated to be uniform for the majority of the central portion, but rises to a maximum value at the edge of ellipse at the loading point. The stress, σ_x, was not calculated to become compressive under the loading zone, this being in contrast to the experimentally determined stress distribution of Frocht (1948), indicating a limitation of the analysis of Brisbane (1963).

A finite element method was used (Appl 1972) to predict the stress distribution when ellipses and rectangles were loaded along their central axis. Photoelastic results of Phillips and Mantei (1969), and the theoretical results of Brisbane (1963) and of Goodier (1932), were used to demonstrate the validity of the solutions obtained.

The analyses showed that any elliptical disc with a width to length ratio of 0.9 to 1.1 would have the entire Y-axis loaded to 95% or more of the maximum tensile stress. This was because of the non-uniform stresses produced along the Y-axis, particularly once the shape of the ellipse departed significantly from that of a circle.

1.2.7 Statistical treatment of tensile strength determinations

The stress solutions presented for all the aforementioned tensile strength

determinations assume the specimen is isotropic. Such an assumption is unlikely to be true for any pharmaceutical compact as studies have shown that there are distinct density distributions within a compact (Train 1956). Furthermore, within a brittle material there are structural and material defects in the form of interstitial cavities, fractured particles and inter-particular boundaries. Since these defects are randomly distributed throughout the material and are of random severity, there is an inherent variability in the strength of nominally identical brittle specimens. This variability requires that tensile strength test results for brittle materials are treated statistically. The Weibull probability distribution is often used for this purpose (Weibull 1951). An important attribute of the Weibull hypothesis is that the mean fracture stress of a batch of nominally identical compacts is a characteristic of the specimen and not of the material itself and it is size dependent. The larger the specimen the more likely it is that it will contain a flaw of a given severity and consequently the smaller will be the mean fracture stress of a batch of such specimens. The predicted relationship between the mean fracture stresses and volumes of two batches A and B is;

$$\frac{\sigma_{f_A}}{\sigma_{f_B}} = \left(\frac{V_B}{V_a}\right)^{\frac{1}{m}} \qquad (1.37)$$

where V is the specimen volume and m is the Weibull modulus. This equation assumes that the materials of the different batches are physically identical, which is unlikely to be the case for two batches of tablets. Stanley and Newton (1978) prepared six different sizes of lactose compacts

and compared the experimental mean fracture stresses obtained with those predicted by the Weibull distribution function. For each batch the strength variability was satisfactorily represented by the Weibull distribution although the effect of size could not be predicted by Equation 1.37. A similar conclusion was obtained when comparing two sizes of sodium chloride tablets (Kennerley et al 1977)

1.2.8 Mechanical properties related to stiffness

1.2.8.1 Determination of Young's Modulus

The tensile strength has been the most common expression used to describe the strength of compacts, but tensile strength values alone are not sufficient to fully characterise a material's mechanical properties. The stress-strain behaviour of a material has been used to measure the toughness and stiffness of materials.

Young's Modulus, E, defined as the ratio of stress, σ, to strain, ε, describes the stiffness of a material. The Young's Modulus of Avicel PH-101 has been determined using the four point flexure test (Church and Kennerley 1982). In such an arrangement the tensile stress and the associated strain are given by ;

$$\sigma = \frac{3\,W\,a}{2\,b\,d^2} \qquad (1.38)$$

$$\epsilon = \frac{4\,\delta\,d}{k^2} \qquad (1.39)$$

where δ is the vertical displacement of the mid-point of the beam and k is

the distance between the loading points on the upper surface of the beam. It was demonstrated that the Young's Modulus increases as the porosity decreases. Determination of the Young's Moduli for a range of pharmaceutical excipients demonstrated that there is no relationship between the Young's Modulus and the tensile strength of a material (Church and Kennerley 1984). To enable comparison of Young's Modulus values for porous materials the Sprigg's equation has been used to determine empirically the Young's Modulus at zero porosity (Kerridge and Newton 1986);

$$E_s = E_0 \exp(-cp) \qquad (1.40)$$

where E_0 is the Young's Modulus at zero porosity, E_s is the specimen's Young's Modulus value at porosity p and c is a material constant.

The four point bending test has been used to characterise the fracture toughness of Avicel PH-101 (Mashadi and Newton 1987). For a crack to grow under static loading the stress must be high enough to initiate fracture and the energy released must be at least as much as that required to form the new surfaces. The stress field near the crack tip will be proportional to the general stress in the material and the square root of the crack length and is called the stress intensity factor (K). This is related to the rate of strain-energy release, G, with crack growth by the elastic modulus of the material;

$$K^2 = EG \qquad (1.41)$$

The crack will grow when the stress has been raised sufficiently for K and G to reach their critical values K_{IC} and G_{IC}. K_{IC} can be determined by carrying out four point bending tests on beam shaped specimens in which a notch has been made in the surface at the point of maximum tension. The value can be calculated from the dimensions of the beam, the maximum load and the notch depth when this load is reached.

Similar studies have been performed by York et al (1990) who obtained lower values of K_{IC} for Avicel PH-101 to those reported by Mashadi and Newton (1987). The differences were attributed to Avicel PH-101 being a material with a rising crack growth resistance curve. For such materials the method of crack induction and notch geometry become critical.

Roberts and Rowe (1989) described a method of determining the critical stress intensity factor using circular compacts into which a radial crack was cut. Values for K_{IC} were obtained by two methods; edge opening in which the cracked compacts were gripped in the jaws of a tensometer and pulled apart and a diametral compression test performed with the crack positioned along the line of loading. Of the two techniques the edge opening was preferred since it gave the most stable crack propagation.

1.2.8.2 Work of failure

The diametral compression test has also been used to measure the "toughness" of compacts (Rees and Rue 1978). In this case the change in length of the loaded diameter was monitored throughout testing. Values were recorded of force and corresponding change in diameter. The product of these values, the area under a force/displacement curve, was called the work of failure, W_f ;

$$W_f = \int P.dx \qquad (1.42)$$

Tablets with a high work of failure were considered to deform plastically under compressive loading thus requiring a relatively large platen displacement to produce failure while brittle materials require only a small displacement to produce failure.

Since most specimens fail in tension during the diametral compression test a further expression, the normalised work of failure, (NWF), was introduced to convert the applied load, P to a tensile stress (Rees et al 1977);

$$NWF = \frac{2}{\pi Dt}\int P.dx \qquad (1.43)$$

As the specimen fails in tension it might be argued that the increase in the transverse diameter would be a more appropriate measurement to determine the work done. This technique is significant because it demonstrates that materials do behave differently under load, exhibiting different degrees of deformability. This may be due, in part, to the hardness of the material rather than the inherent strength of the compact. Work of failure measurements have been extended to the flexure test (Moschos and Rees 1986) and axial tensile strength tests (Jarosz and Parrott 1982).

1.2.8.3 Brittle Fracture Index

The work of failure test has been used to distinguish between ductile and brittle materials. A further method used to measure the brittleness of

materials is the Brittle Fracture Index (BFI) (Hiestand and Smith 1984). Two sets of square compacts are prepared, one set containing a small circular hole along the axis. The compacts are tested by an indentor test with a platen to compact width ratio of 0.4, (see Section 1.2.5), and the tensile strengths of the compacts with and without the central hole compared. Under the conditions of the test the hole acts as a stress concentrator. Elasticity theory predicts that the stress concentration factor is approximately 3.2 for a hole in an isotropic solid. However for most pharmaceutical materials the ratio of the tensile strengths of the two types of compact is less than 3. This is believed to be because of the relief of the highly localised stresses by plastic deformation i.e the material is not completely brittle. Thus, the ratio of the tensile strength of a compact without a hole, σ_f, to the tensile strength with a hole, σ_{f_0}, may indicate its ability to relieve stress by plastic deformation. Based on this the brittle fracture index has been defined;

$$BFI = 0.5\left(\frac{\sigma_f}{\sigma_{f_0}} - 1\right) \qquad (1.44)$$

Roberts and Rowe (1986) have used the BFI to measure the brittleness of circular compacts using the diametral compression test and have obtained values in good agreement with those of Hiestand and Smith (1984).

1.2.9 Indentation hardness

While tensile strength measurements describe the global strength of a specimen, indentation hardness describes the "local" plasticity of a material. Hardness may be defined as the resistance of a solid to local

permanent deformation, and is usually measured by a non destructive indentation or scratch test.

The most widely used methods in determining hardness are static indentation methods. These involve the formation of a permanent indentation on the surface of the material to be examined. Normally the diameter of the impression is determined and, from it, the hardness is calculated by means of the formula.

$$BHN\ (Q) = \frac{2W}{\pi D_i (D_i - \sqrt{D_i^2 - d_i^2})} \qquad (1.45)$$

where W is the applied load, D_i is the diameter of the spherical indentor and d_i the diameter of the indentation (Figure 1.12). The Brinell hardness number (BHN) is not a constant for a material but depends on the load and diameter of the indentor (Leuenberger and Rohera 1986). The method has been used to determine the hardness at various points across the diameter of Aspirin compacts (Ridgway et al 1970) and direct compression excipients (Aulton et al 1974). Studies on the surface hardness distribution over tablet faces with different face curvatures indicated that as the degree of curvature increased the hardness of the outer portions of the compact increased relative to the centre of the compacts (Aulton and Tebby 1975). Hardness tests have been used to measure the elastic recovery. Under load the indentor, radius of curvature r_1, penetrates to a depth h_1 giving an impression of diameter d_i. When the load is removed , elastic recovery occurs and the radius of curvature of the impression increases to r_2, its depth decreasing to h_2. The change, $h_1 - h_2 = h$, is a measure of the

Figure 1.12
Diagram of the indentation hardness test

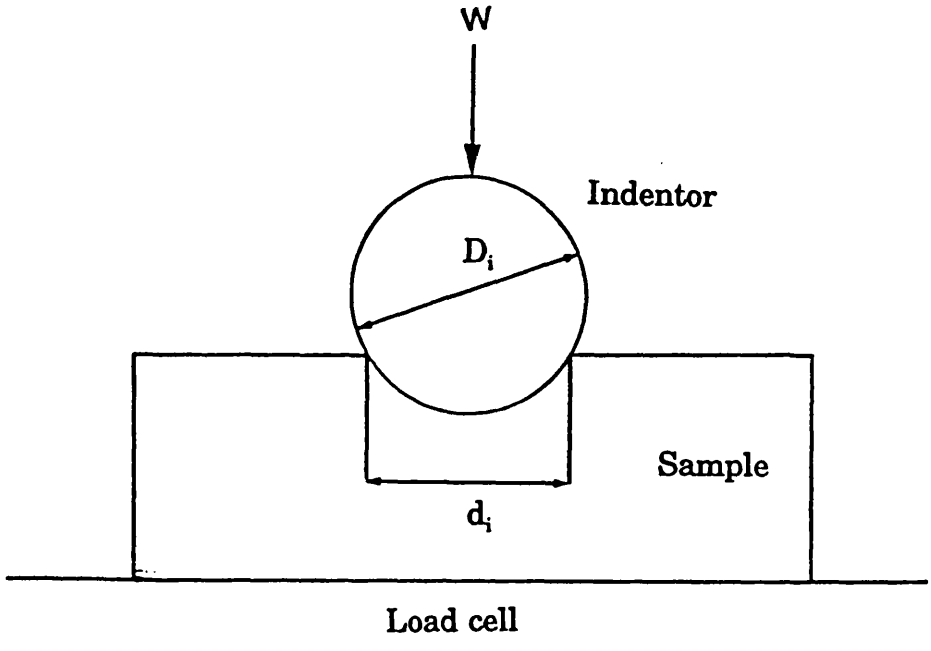

elasticity. Using this method it is possible to derive a value for the elastic modulus of elasticity (Ridgway et al 1970).

Hardness values of tablets have also been determined using dynamic tests. In dynamic methods, either a pendulum is allowed to strike from a known distance or an indentor is allowed to fall under gravity onto the surface of the test material. The hardness is determined from the rebound height of the pendulum or the volume of the resulting indentation.

The volume of the indentation is directly proportional to the kinetic energy of the indentor. It therefore implies that the material offers an average pressure of resistance to the indentor equal to the ratio:

Energy of impact/Volume of indentation

This ratio has the dimensions of pressure and is sometimes referred to as the dynamic hardness number. Hiestand et al (1977) have used the dynamic method to characterise a range of pharmaceutical materials. The indentation hardness, Q, was divided by the tensile strength of the tablet to form a bonding index;

Bonding Index = Indentation hardness/Tensile strength

The objective of the bonding index is to estimate the survival, during decompression of areas of true contact that were established at maximum compression stress.

There are several disadvantages associated with the measurement of the indentation hardness of a specimen. Pharmaceutical compacts consist of particles compacted with voids between them . It is very difficult to decide whether an indentation has been made into a particle, a void or a combination of the two, raising doubts as to what the indentation figure

is describing. Furthermore, if the elastic recovery is time dependent it is difficult to assess when the recovery measurement should be made.

1.3 Aims of this work

There is an increasing move in the pharmaceutical industry towards the use of shaped tablets. A perception exists that shaped tablets may be more problematic to produce than circular tablets although there is little evidence in the literature to support this. Density distributions observed within circular compacts have been attributed principally to the effects of die wall friction. It is likely, therefore, that altering the die wall geometry will affect the die wall friction which in turn may affect the way in which the applied pressure is transmitted through the material being compressed.

Manufacturers of tablets are concerned less with their density variations than their strengths. However, a possible consequence of altering the density distribution within a compacted material is that the mechanical strength will also change. The aim of this study is to determine whether changing the shape of flat faced compacts of pharmaceutical materials influences their tensile strength.

Assessment of the effect of shape on the strength of compacted materials requires a method of determining strength that does not depend on specimen shape. The diametral compression test, or indentor test as it has been referred to for the testing of square and rectangular specimens, is selected as the most appropriate method. Stress analysis solutions exist for circular and square specimens and indicate that similar tensile stresses

are induced in both shapes. However, the results obtained by this test depend greatly on the loading conditions used and studies have not been performed to show that square and circular specimens of the same material tested under the same conditions yield similar values of tensile strength. The inital part of the study was to develop a test method that would produce tensile strength values that were independent of the shapes being tested, namely circles, squares and hexagons.

Having developed such a test it was used to determine whether the die shape affects the strength of compacts prepared using pharmaceutical excipients. The aim was to prepare the compacts using conditions that were representative of those used in commercial tablet production. Compacts were prepared on a single punch eccentric press that is used extensively in product development and also a rotary tablet machine. A range of pharmaceutical excipients, that are known to compress to differing degrees by plastic deformation and brittle fracture, were used.

The final part of the study examines the properties of square and circular compacts prepared from granulated formulations.

CHAPTER 2

EVALUATION OF THE DIAMETRAL COMPRESSION TEST USING SHAPED GYPSUM CASTS

2.1 Introduction

The purpose of the work described in this chapter was to determine whether the diametral compression test could be used to compare the tensile strengths of circular and shaped compacts. The test is to be used to assess whether shape influences the structure of such compacts. Davies and Bose (1968) investigated the potential for using the diametral compression test to determine the tensile strengths of concrete cubes and beams by the finite element method of analysis. It was concluded that the stresses along the loaded axis of cubes being compressed across two faces were similar to the corresponding stresses for a cylinder except for discrepancies adjacent to the loading points. The equation;

$$\sigma_x = \frac{2P}{\pi Dt} \qquad (2.1)$$

was considered a good estimate of the maximum tensile stress, σ_x, where P is the load applied and D and t are the diameter and thickness of the cylinder respectively. The discrepancies adjacent to the loading points could result in differences in the tensile strength values obtained (Peltier 1954). An important part of this study, therefore, was to find a method of inducing tensile failure, as indicated by a break across the loading points, for all shapes tested by varying the shape of the platens used to apply the loads. Prior to comparing compacts in this manner it is necessary to eliminate, if possible, the variable of the material. Therefore to investigate the relationship between fracture load and specimen shape and dimension it was necessary to test specimens of a material of a uniform structure giving constant tensile strength results. Methods available to produce such homogeneous specimens

include machining from a block or casting into a mould of the required dimensions. The test specimens need to have the following characteristics :

1. Homogeneity. The homogeneity of a specimen will depend on the scale of scrutiny. The material may be non-uniform in nature but it must have a flaw distribution which is statistically uniform i.e. there must be a fixed probability of finding a flaw of a given severity within a small volume of the sample irrespective of the position of that volume. This is in contrast to a compacted material where there are density variations and hence the most severe flaws are located in specific areas of the compact (Train 1957).

2. The material should fail in tension under diametral loading i.e at right angles to the point of loading. There should not be significant plastic or elastic deformation prior to loading.

3. There should be no contraction or expansion of the specimen after formation.

4. The specimens should be easy to manufacture.

5. The specimens should be physically and chemically stable.

6. The material should be cheap and readily available.

Pitt (1986) investigated a number of such materials when studying the relationship between the fracture loads and tensile strength of circular convex faced specimens. The materials examined were polymethylmethacrylate, polyethylene glycols, epoxy resins, zinc phosphate cement and gypsum. Of these gypsum, formed in situ from dental stone, was found to be the most suitable and was therefore selected for this study.

2.2 Materials and methods

2.2.1 Physical and chemical properties of gypsum

Dental plaster, calcium sulphate hemihydrate , is produced by the calcining of gypsum;

$$2\ CaSO_4.2H_2O \xrightarrow{110\text{-}130^{\circ}C} (CaSO_4)_2.H_2O + 3H_2O \qquad (2.2)$$

Gypsum — Plaster or stone (Calcium sulphate hemihydrate)

Depending on the method of calcination two different forms of the hemihydrate can be obtained. Heating in a kettle, vat or rotary kiln open to the air results in the formation of the beta-hemihydrate or Plaster of Paris, characterised by irregularly shaped crystals. The alpha-hemihydrate or dental stone can be prepared by three different procedures; it may be calcined under steam pressure in an autoclave at a temperature of 120-130°C, dehydrated in an autoclave in the presence of sodium succinate or dehydrated in a boiling solution of 30% calcium chloride in a kettle. The alpha-hemihydrate crystals are more dense and have a prismatic shape. When water is added to stone or plaster the above reaction can be reversed.

$$(CaSO_4)_2.H_2O + 3H_2O \longrightarrow 2CaSO_4.2H_2O + Heat \qquad (2.3)$$

Plaster — Gypsum

From Equation 2.3 it can be calculated that 18.6g of water would be required to fully react with 100g of plaster. In practise much larger amounts of water are required to produce a mass that can be stirred and formed into casts. The tensile strength of the gypsum is affected by the initial powder to water ratio, the greater the excess water, the lower the tensile strength. The irregular shape and porous nature of the beta hemihydrate particles require

more water to produce a suitable slurry resulting in a weaker product than that from the alpha-hemihydrate. The alpha-hemihydrate results in a denser, more uniform product crystal structure (Coombe 1977) and is readily mixed to produce a reproducible material. A commercial grade of the alpha-hemihydrate, Kaffir D (British Gypsum Co) was selected for study.

2.2.2 Characterisation of the casting process

Dental stone (Kaffir D, British Gypsum Co) was sieved and the 150-600 micrometre fraction retained for use.

Initial trial castings were prepared using open perspex moulds. A powder to water ratio of 2.5:1 was used throughout the investigation. Distilled water was added to the weighed powder in a petri dish, mixed by gentle spatulation for one minute to form a smooth, air free mix and transferred into moulds 20mm in diameter and 4mm thick previously lubricated with Silicone Grease Spray (SG-4, Holt Lloyd Ltd). The casts were allowed to set for 30 minutes then excess material was removed by scalpel before removal from the moulds. They were then stored for a further 28 days before testing.

The casts were weighed, their thicknesses measured and tested by diametral compression using a CT40 mechanical tester (Engineering Systems, Nottingham). Samples were positioned vertically between two platens, the lower one being attached to a 250kg load cell. The test involves the upper platen moving downwards at a constant velocity until the force on the load cell falls below 90% of the maximum reading. The CT40 displays the maximum force attained on the load cell. Prior to use the machine was calibrated using 0.5kg and 10kg weights. The casts were loaded between flat faced silver steel platens at a crosshead speed of 1mm per minute. The

majority of casts failed diametrically in tension. The fracture load of those discs which did not fracture in tension were excluded from the analysis.

Table 2.1 presents the results for six batches of casts. It can be seen that there is considerable variation both within and between batches. One way analysis of variance (Table 2.2) indicates that the difference between batches is significant ($p > 0.05$) so the pooling of the results would not be appropriate.

To reduce the variation a more standardised method of preparation was introduced. Thirty five grammes of Kaffir D was weighed into a 200ml vessel of a Waring Blender (Model 91-358, Waring Products). Fourteen grammes of distilled water was added and allowed to stand for 30 seconds prior to mixing at the low speed setting for 30 seconds. The slurry was then transferred to the lubricated moulds and allowed to set as before. The results of three batches of casts prepared in this manner are presented in Table 2.3. They indicate that the standardised method of mixing results in an increase in the tensile strength but a reduction in both the inter and intra batch variation. In this instance the one way analysis of variance indicates that the inter batch variation is not significant (Table 2.4). The increase in cast strength may be due to the mixing process altering the rate of crystal formation and producing a change in the crystal structure.

2.2.3 Storage conditions

Storage conditions will markedly affect the tensile strength of the gypsum (Phillips 1982). The effect of ageing on the setting process is evident from Figure 2.1. Gypsum discs were stored at ambient temperature and humidity in open glass jars. The casts were weighed and tested by diametral compression at regular intervals over a six week period. Increasing the

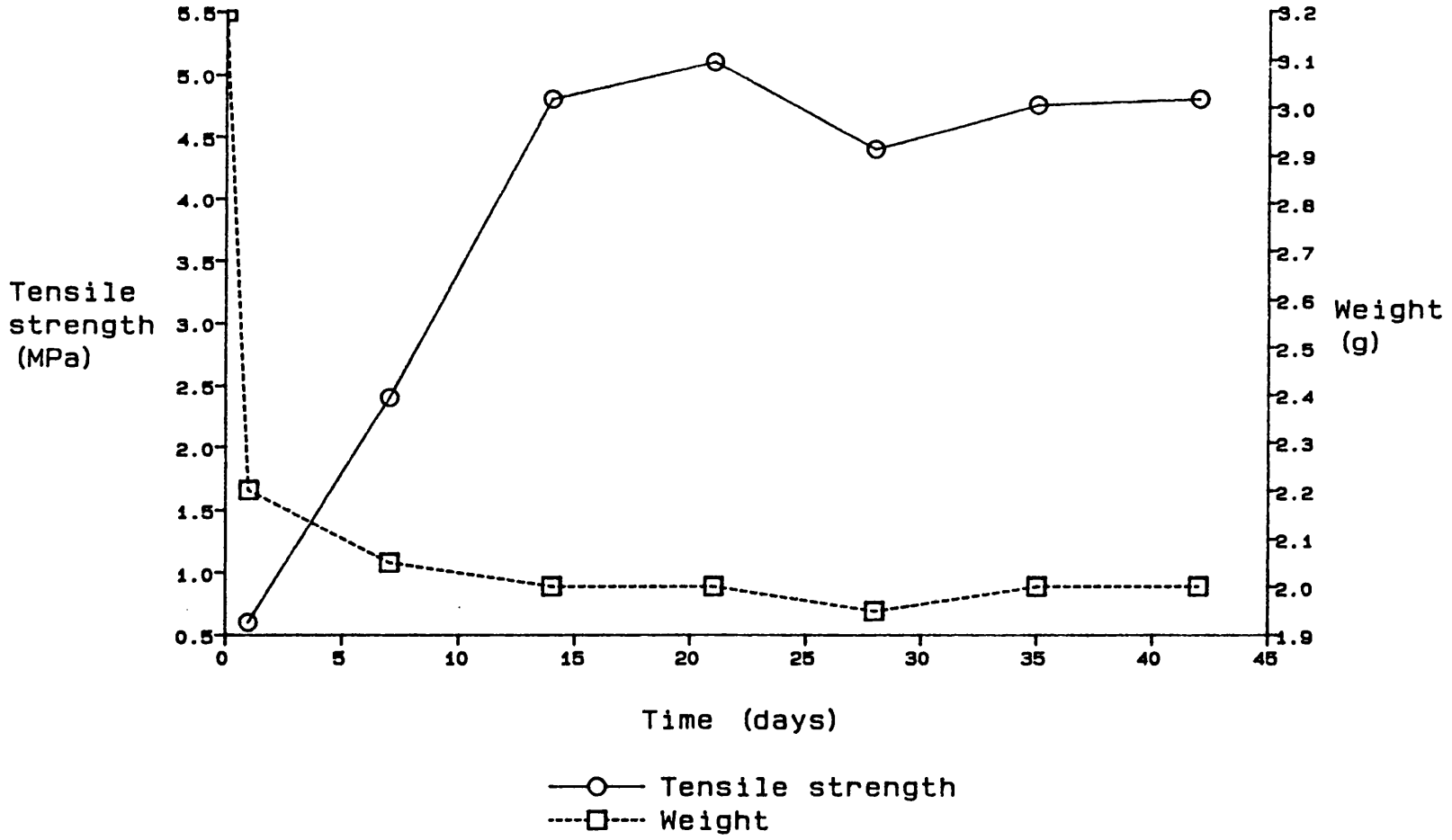

Figure 2.1 Effect of storage on the properties of 20mm gypsum discs

Table 2.1

Tensile strength of 20mm diameter circular gypsum casts prepared by manual spatulation and tested with flat platens

Tensile strength		Number of samples
Mean (MPa)	Coefficient of variation (%)	
3.95	12.7	5
4.75	14.1	10
4.99	11.2	10
4.25	16.0	9
4.31	9.7	11
4.13	12.4	12

Table 2.2

ANOVA table for 20mm diameter circular gypsum casts prepared by manual spatulation and tested with flat platens

	Sum of squares	Degrees of freedom	Mean Square	F-value
Total	23.098	55		
Between batches	6.876	5	1.375	4.239
Residual	16.222	50	0.324	

Table 2.3

Tensile strength of 20mm circular gypsum casts prepared using the Waring Blender and tested with flat platens

Tensile strength		Number of samples
Mean (MPa)	Coefficient of variation (%)	
5.00	6.8	9
4.83	8.5	11
4.72	7.8	10
4.99	7.6	9

Table 2.4

ANOVA table for 20mm circular gypsum casts prepared using the Waring Blender and tested with flat platens

	Sum of squares	Degrees of freedom	Mean Square	F-value
Total	7.380	38		
Between batches	0.516	3	0.172	0.878
Residual	6.864	35	0.196	

Table 2.5

Effect of storage conditions on the tensile strength of gypsum discs

Storage condition	Mean weight (g)	Coefficient of variation (%)	Number of samples	Mean tensile strength (MPa)	Coefficient of variation (%)
Closed jars	2.256	3.6	12	2.12	32.5
Open jars	1.934	1.7	12	4.73	10.8

20mm diameter, 4mm thick gypsum discs tested using flat platens

storage time leads to an increase in the tensile strength of the casts together with a reduction in the weight. The results indicate that the drying and ageing processes are essentially complete after 35 days.

Table 2.5 illustrates the effect of storing the casts in sealed and open glass containers. Both sets of samples were stored for 35 days at ambient temperature and humidity. There is a significant difference ($p > 0.05$) between the two samples due to incomplete drying of the samples in the closed containers, a conclusion supported by the weight differences between the two sets of samples. On the basis of these results the remaining casts were stored for a minimum of 35 days in open glass jars at ambient temperature before performing diametral compression studies.

2.2.4 Preparation of casts

The casts were prepared using a series of open faced aluminium and perspex moulds. The slurry was mixed using the Waring Blender by the method described in section 2.2.3 and used to fill one plate of 12 moulds. The casts prepared are described in Table 2.6. In order to reduce the effects of inter-batch variation when comparing different shaped casts, a number of larger batches of slurry were prepared and used to form casts of all three shapes. One hundred and forty grammes of dental stone was weighed into the 500ml vessel of the Waring Blender. Fifty six grammes of distilled water was added, allowed to stand for 30 seconds, then mixed for 30 seconds at the low speed setting. The slurry was then transferred to the lubricated moulds as before.

2.2.5 Testing the casts

The strength of the casts was determined by the diametral compression test using a CT40 Mechanical Strength Tester. The samples were positioned

Table 2.6

Moulds used in the preparation of gypsum casts.

Shape	Diameter(mm)*	Thickness(mm)
Circle	20	2
Circle	20	4
Circle	20	6**
Circle	10	2
Circle	10	3
Square	20	2
Square	20	4
Square	10	2
Hexagon	20	2
Hexagon	20	4
Hexagon	10	2
Octagon	20	2
Octagon	20	4
Octagon	10	2

* For squares, hexagons and circles the diameter refers to that of an inscribed circle.

**Prepared by using the 2mm and 4mm plates together.

vertically between two silver steel platens and compressed by the vertical movement of the top platen at a rate of 1mm per minute until failure occurred. Each shape was tested by a number of platen/position configurations, illustrated diagramatically in Figure 2.2.

1.Fifteen millimetre diameter flat faced platens. Used to test circles diametrally. Squares, hexagons and octagons were compressed between diagonally opposite points.

2. Semicircular platens. Semicircular convex platens, with a radius of curvature of 3mm, were used to test circles diametrally. Square, hexagonal and octagonal casts were tested by loading across the mid points of two opposite faces.

3. Pointed platens. Platens with two faces coming together to form a 90° point were used to test circles diametrally. Square, hexagonal and octagonal casts were tested by loading across the mid points of two opposite faces.

4. Eight millimetre flat platens. Eight millimetre wide flat platens were used to test the square, hexagonal and octagonal casts by loading across the mid points of two opposite faces.

2.3 Results and discussion

2.3.1 Determination of the tensile strength of gypsum discs

The results for the testing of circular casts are presented in Tables 2.7, 2.8 and 2.9. Tables 2.7 and 2.8 list the results of the individual batches of casts. One way analysis of variance indicates that for a given cast diameter and platen configuration the variation between batches is not significant. As a consequence the results for each platen/diameter configuration were pooled

Figure 2.2
Loading configurations used to test gypsum casts diametrally

1. Flat faced platens

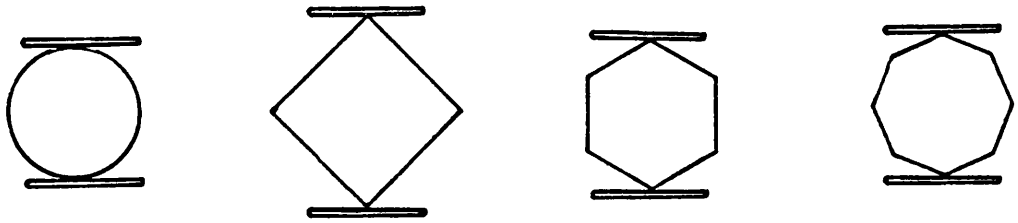

2. Semicircular platens

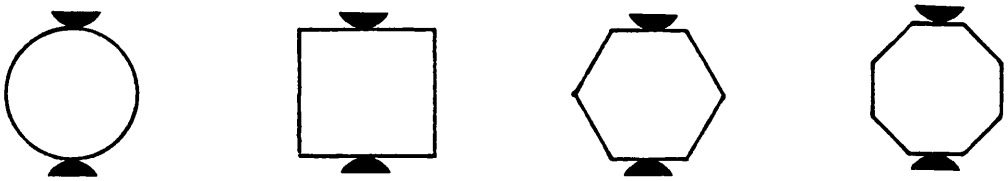

3. Pointed platens

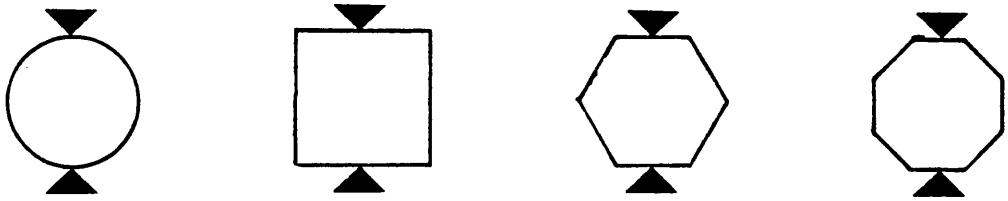

4. 8mm wide flat platens (for 20mm shapes only)

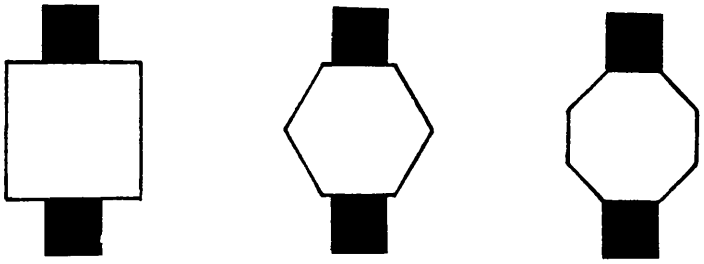

Table 2.7

Tensile strength values of individual batches of 20mm diameter circular casts produced using the Waring blender

Thickness (mm)	Platen shape	Tensile strength (MPa)	Number of samples	Coefficient of variation (%)	F-value
4	Flat	5.00	9	6.8	0.88
4	Flat	4.83	11	8.5	
4	Flat	4.72	10	7.5	
4	Flat	4.99	9	7.6	
6	Flat	4.68	7	8.8	
4	Semi-circular	2.94	10	9.5	2.28
4	Semi-circular	3.18	11	15.1	
4	Semi-circular	2.83	11	10.6	
4	Semi-circular	2.86	9	9.1	
6	Semi-circular	2.87	8	8.7	
4	Pointed	1.59	10	7.5	1.32
4	Pointed	1.50	12	9.3	
4	Pointed	1.54	11	8.0	
4	Pointed	1.62	10	11.7	

Table 2.8

Tensile strength values of individual batches of 10mm circular gypsum casts produced using the Waring Blender

Thickness (mm)	Platen shape	Tensile strength (MPa)	Number of samples	Coefficient of variation (%)	F-value
2	Flat	7.01	10	9.3	0.27
2	Flat	7.18	11	10.0	
2	Semi-circular	4.18	5	11.0	0.10
2	Semi-circular	4.09	11	16.6	
3	Semi-circular	4.40	10	10.9	
2	Pointed	2.40	10	9.2	1.63
2	Pointed	2.22	10	17.1	
3	Pointed	2.22	10	10.8	

and are displayed in Table 2.9. No results are presented for 20mm diameter, 2mm thick discs as these crumbled at the loading points and did not fail in tension. The results in Table 2.9 clearly demonstrate two findings; the derived value of tensile strength is dependent on the platen shape and the value obtained is dependent on the size of specimen tested.

The conditions of diametral loading result in a combination of tensile, compressive and shear stresses within the loaded specimen. The derivation of the tensile strength value comes from the theoretical tensile stress set up along the loaded diameter under the conditions of point loading. To obtain a given value of tensile strength it is necessary for a flaw of a given severity to be present at any point along the loaded diameter. In reality the conditions of point loading do not exist, deformation will always occur at the platen/sample contact resulting in a finite contact width. The effect of this is to reduce the portion of the loaded diameter that is exposed to the maximum tensile stress.If this portion of the diameter decreases, the probability of locating a flaw of given severity along the reduced diameter will also decrease resulting in an increase in the mean tensile strength obtained for a group of specimens.The results obtained for the gypsum discs tested with the flat platens have higher mean tensile strength than those tested with semicircular platens which in turn produce higher values than the pointed platens. The width of contact between platen and specimen is also going to be greatest for the flat platens followed by the semicircular platens. The theoretical implications of increasing the width of contact between platen and specimen were studied by Peltier (1954), who concluded that an increase in the contact width will result in an increase in the mean tensile strength and

Table 2.9

Pooled tensile strength results for circular gypsum discs prepared using the Waring Blender

		Tensile strength (MPa)								
		Flat platens			Semicircular platens			Pointed platens		
Diameter (mm)	Thickness (mm)	Mean	Coefficient of variation (%)	Number of samples	Mean	Coefficient of variation (%)	Number of samples	Mean	Coefficient of variation (%)	Number of samples
20	4	4.88	9.02	39	2.96	12.2	46	1.56	9.4	43
20	6	4.68	8.8	7	2.87	8.7	8			
10	2	7.10	10.3	21	4.13	14.1	9	2.31	13.7	20
10	3				4.40	10.9	10	2.22	10.8	10

an increase in the variance. The results obtained here confirm this conclusion. The size of a specimen will also affect the tensile strength value obtained for a material as the larger the specimen the greater is the likelihood of it possessing a flaw of given severity. If the distribution of flaws within a material is known it should be possible to allow for the effect of size when comparing two samples of that material. One method of describing the strength variability is the calculation of the Weibull modulus.

The basic two-parameter Weibull relationship between a particular value of fracture stress (σ_f) and the associated failure probability (P_f) has the form

$$P_f = 1 - \exp\left[\left(\frac{1}{m}!\right)^m \left(\frac{\sigma_{f_a}}{\sigma_{f_b}}\right)^m\right] \qquad (2.4)$$

where σ_f is the mean fracture stress of the batch, m is the Weibull modulus and (1/m!) is the factorial function of (1/m). An important attribute of the Weibull hypothesis is that the mean fracture stress of a batch is a characteristic of the specimen and not the material alone. It is a size dependent quantity. With certain conditions and assumptions (Stanley and Newton 1975), the following relationship between the mean fracture stresses (σ_{fa} and σ_{fb}) of two batches of specimens with different volumes (V_a and V_b) can be derived;

$$\frac{\overline{\sigma_{f_a}}}{\overline{\sigma_{f_b}}} = \left(\frac{V_b}{V_a}\right)^{\frac{1}{m}} \qquad (2.5)$$

The Weibull moduli of 10mm diameter, 2mm thick casts tested using semicircular platens and 20mm diameter, 4mm thick casts tested with flat platens were calculated using a computer program, Weiberg, on the ULCC

Amdahl computer. The values obtained are displayed in Tables 2.10 and 2.11 together with a value for the standard error which was calculated as:

$$\Delta m = \frac{m}{\sqrt{2n}} \qquad (2.6)$$

where n is the number of samples tested. The tables also compare the tensile strength values for different size discs as predicted by equation 2.5 with the experimentally derived values.

The results indicate that the distribution of flaws, as described by the Weibull modulus, account for most of the differences in tensile strength observed between 10mm and 20mm diameter casts. The Weibull modulus slightly underestimates the differences between the two cast sizes when tested by both the platen configurations. A possible explanation for the slight discrepancy could again be the stress distributions at the point of contact between the specimen and platen.

The Weibull modulus for this system would be expected to be a material property and not a specimen property so it is interesting that the values of m obtained with the two platen configurations differ. This is further evidence that the platens do affect the stress distributions within the test specimens. The Weibull modulus is a reciprocal measure of the variability of tensile strength around the mean, therefore the greater the value of m, the lower the variability. The value obtained using the semicircular platens is greater than for the flat platens indicating lower variability. This is to be expected if, as proposed, the contact between platen and specimen is reduced with semicircular platens, resulting in a larger portion of the specimen being

Table 2.10

Predicted mean tensile strength values of circular gypsum casts tested by diametral compression using flat platens

Diameter (mm)	Thickness (mm)	Weibull Modulus	Δm	Measured Tensile Strength (MPa)	Predicted tensile strength(MPa)		
					m = 5.63	m = 6.07	m = 6.51
20	4	6.07	0.44	4.88	-	-	-
20	6	-	-	4.68	4.50	4.56	4.59
10	2	-	-	7.11	7.06	6.87	6.72

Table 2.11

Predicted mean tensile strength values of circular gypsum casts tested by diametral compression using semicircular platens

Diameter (mm)	Thickness (mm)	Weibull modulus	Δm	Measured tensile strength (MPa)	Predicted tensile strength (MPa)		
					m=6.81	m=7.62	m=8.43
10	2	7.62	0.81	4.13	-	-	-
10	3	-	-	4.40	3.89	3.92	3.94
20	4	-	-	3.05	3.04	3.14	3.23
20	6	-	-	4.68	4.50	4.56	4.59

exposed to the maximum tensile stress.

2.3.2 Effect of sample shape on the load required to produce tensile failure

The purpose of this chapter of work was to determine whether the diametral compression test is a suitable method of calculating the tensile strength of shaped specimens. Such an assessment needs to be based on two criteria; does the test set up stresses within the specimens that will reliably produce tensile failure and how are the tensile stresses related to the breaking loads of the different shapes?

Four testing configurations were used on each shape as described in Section 2.2.4. Of these tests only those involving loading the specimens across the flat sides of the shapes with semicircular and pointed platens produced tensile failure in the majority of specimens.

The test involving loading samples across the faces between flat platens has been used to determine the tensile strength of cube specimens of coal (Berenbaum and Brodie 1958). Stress analysis of the test indicated that the ratio of tensile stress to compressive stress along the loaded diameter reached a maximum when the ratio of platen width to specimen width was 0.4, hence the use of 8mm wide platens to test the 20mm shapes. When used on the gypsum casts the test resulted predominantly in failure at the platen edges rather than along the centre of the specimen, indicative of failure due to shear and not tension.

Concrete cubes have been tested by loading across the points between flat platens (Davies and Bose 1968). Stress analysis of this test, by the finite element method, indicates that the maximum tensile stress occurs at the centre of the specimen and is 0.77 of the value calculated by equation 2.1. The

Table 2.12

Tensile strength values of individual batches of 20mm shaped gypsum casts

Shape	Diameter (mm)	Thick-ness (mm)	Platen shape	Tensile strength		Number of samples	F-value
				Mean (MPa)	Coefficient of variation (%)		
1. Square	20	4	Semi-circular	3.03	11.8	6	2.66*
2. Square	20	4	Semi-circular	3.21	10.9	9	
3. Square	20	4	Semi-circular	3.43	3.5	8	
4. Square	20	4	Semi-circular	3.07	13.7	10	
5. Square	20	4	Semi-circular	3.05	5.2	11	
6. Hexagon	20	4	Semi-circular	3.11	9.6	10	2.08
7. Hexagon	20	4	Semi-circular	3.35	16.4	10	
8. Hexagon	20	4	Semi-circular	3.26	11.1	10	
9. Octagon	20	4	Semi-circular	3.28	14.0	11	2.01
10. Octagon	20	4	Semi-circular	3.03	12.0	12	
11. Octagon	20	4	Semi-circular	2.96	11.5	10	
12. Square	20	4	Pointed	1.51	8.0	10	0.24
13. Square	20	4	Pointed	1.53	5.9	9	
14. Hexagon	20	4	Pointed	1.50	9.2	9	1.20
15. Hexagon	20	4	Pointed	1.58	11.5	12	
16. Octagon	20	4	Pointed	1.61	6.8	11	1.32
17. Octagon	20	4	Pointed	1.55	10.3	10	

*Indicates a significant difference at p=0.95

Table 2.13

Tensile strength values of individual batches of 10mm shaped gypsum casts

Shape	Diameter (mm)	Thickness (mm)	Platen shape	Tensile strength		Number of samples	F-value
				Mean (MPa)	Coefficient of variation (%)		
1. Square	10	2	Semi-circular	4.24	10.8	9	0.11
2. Square	10	2	Semi-circular	4.18	6.7	10	
3. Hexagon	10	2	Semi-circular	4.15	13.7	10	0.11
4. Hexagon	10	2	Semi-circular	4.05	18.5	10	
5. Octagon	10	2	Semi-circular	4.13	14.1	10	0.05
6. Octagon	10	2	Semi-circular	4.19	13.9	10	
7. Square	10	2	Pointed	2.43	13.2	9	0.54
8. Square	10	2	Pointed	2.52	5.3	8	
9. Hexagon	10	2	Pointed	2.27	15.9	8	0.77
10. Hexagon	10	2	Pointed	2.41	11.4	9	
11. Octagon	10	2	Pointed	2.21	14.3	7	1.15
12. Octagon	10	2	Pointed	2.38	13.7	12	

Table 2.14

Pooled tensile strength results for shaped gypsum casts

Shape	Diameter (mm)	Platen shape	Tensile strength (MPa)	Number of samples	F-value
Circle	20	Semi-circular	2.96	41	3.79
Square	20	Semi-circular	3.09	36	
Hexagon	20	Semi-circular	3.24	30	
Octagon	20	Semi-circular	3.09	33	
Circle	20	Pointed	1.56	43	0.95
Square	20	Pointed	1.52	19	
Hexagon	20	Pointed	1.55	21	
Octagon	20	Pointed	1.58	21	
Circle	10	Semi-circular	4.12	16	0.13
Square	10	Semi-circular	4.21	19	
Hexagon	10	Semi-circular	4.40	20	
Octagon	10	Semi-circular	4.16	20	
Circle	10	Pointed	2.31	20	0.92
Square	10	Pointed	2.47	19	
Hexagon	10	Pointed	2.34	16	
Octagon	10	Pointed	2.32	19	

test was of little value when testing the gypsum casts as the specimens tended to slip at the platen edges or fail due to crushing at the loading points. The results for the specimens tested by compressing across the mid points of faces using the semicircular and pointed platens are presented in Tables 2.12 and 2.13. The results for each shape and platen configuration were subjected to one way analysis of variance. The only specimen shape/platen configuration to show significant inter-batch variation was the 20mm squares tested with semicircular platens. By the least significant difference method it was established that batch 3 was the one showing a significant difference. Exclusion of this batch from the analysis of variance resulted in an F-value of 0.60 indicating that there was not a significant difference between the remaining batches.The remainder of the results were therefore pooled giving the populations listed in Table 2.14.

Different shaped specimens of the same size tested using the same platen configuration were tested for one way analysis of variation. This test showed that the tensile strength values obtained for 10mm casts tested with either platen configuration did not vary with the specimen shape. A similar conclusion was reached for 20mm casts tested with pointed platens. However, the results for the 20mm shapes tested with semicircular platens indicate that the shape does affect the value obtained. The tensile strength value for the hexagons was significantly higher than those of the circles, squares and octagons. If the hexagons were excluded from the analysis of variance an F-value of 0.95 is obtained.

To assess whether the differences seen with the hexagons were due to the specimen shape or the result of a variable that had not been controlled or

Table 2.15

Tensile strength results obtained when preparing all four 20mm shapes from a single batch of slurry tested using semicircular platens

Shape	Tensile strength		Number of samples	F-value
	Mean (MPa)	Coefficient of variation (%)		
Circle	2.96	7.1	9	3.08*
Square	3.35	8.4	11	
Hexagon	3.25	10.2	12	
Octagon	3.10	11.9	12	
Circle	3.02	8.3	12	3.64*
Square	2.79	6.8	10	
Hexagon	3.13	8.6	12	
Octagon	3.01	8.3	11	
Circle	2.90	10.0	12	2.28
Square	3.20	7.5	11	
Hexagon	3.05	10.5	11	
Octagon	3.12	9.3	11	

*Indicates a significant difference at p=0.95 level

Table 2.16

Tensile strength results obtained when preparing all four 20mm shapes from a single batch of slurry tested using pointed platens

Shape	Tensile strength		Number of samples	F-value
	Mean (MPa)	Coefficient of variation (%)		
Circle	1.59	7.5	10	1.26
Square	1.63	7.4	10	
Hexagon	1.55	10.5	7	
Octagon	1.55	8.4	12	
Circle	1.50	9.3	12	5.72*
Square	1.63	7.4	11	
Hexagon	1.62	4.3	10	
Octagon	1.46	8.9	12	

*Indicates a significant difference at p=0.95 level

Table 2.17

Tensile strength values for 20mm casts where two shapes were produced from one batch of slurry

Shape	Platens	Tensile strength		Number of samples	t-value
		Mean (MPa)	Coefficient of variation (%)		
Circle	Semi-circular	3.12	8.6	12	1.03
Square	Semi-circular	3.01	9.0	11	
Circle	Semi-circular	2.96	7.1	11	0.43
Hexagon	Semi-circular	3.06	11.8	10	
Circle	Semi-circular	3.02	9.4	10	0.20
Octagon	Semi-circular	3.15	12.3	11	
Circle	Pointed	1.65	6.1	12	0.15
Square	Pointed	1.67	5.5	11	
Circle	Pointed	1.55	5.2	12	0.33
Hexagon	Pointed	1.51	6.7	12	
Circle	Pointed	1.52	7.9	12	0.15
Octagon	Pointed	1.50	6.4	12	

identified, samples of all four shapes were produced from single batches of slurry. The results are presented in Table 2.15 and 2.16. In 3 of the 5 sets of batches prepared in this manner one way analysis of variance indicates that differences exist between the shapes. The hexagonal casts were not the cause of such differences in any case. For each series of shapes there was a correlation between the order in which the moulds were filled and the tensile strengths of the resultant casts. The shapes that were prepared initially had lower tensile strengths than the casts formed from the last moulds to be filled. By the time that the last mould was being filled the gypsum was already setting. The results suggest that the initial setting process occurring outside the mould could affect the final strength of the cast.

An alternative method of preparing two shapes from one batch of slurry was adopted. To minimise the effect of setting the two different shaped moulds were filled alternately until all 12 holes on each plate had been used. The results for these batches are listed in Table 2.17. The tensile strengths of the two shapes produced from each batch were compared using the students t-test. No significant differences were detected between any combination of shapes.

2.4 Conclusions

Gypsum has been used to assess the use of the diametral compression test to compare the tensile strengths of circular, square, hexagonal and octagonal specimens. The tensile strength of gypsum casts was found to vary according to the method of mixing of the powder with the water, the storage time and the storage conditions.

The value obtained for the tensile strength depends on the nature of the contact between the platen and the specimen. As the contact width increases the proportion of the loaded diameter exposed to the maximum tensile stress will decrease resulting in an increase in the mean failure load. The use of shaped platens to control the width of contact has been demonstrated. The contact width also depends on the nature of the platen material and test specimen as deformation will occur. If the load cannot be adequately distributed at the contact points, the compressive stresses may be sufficiently large to produce crumbling as was seen when testing the shaped specimens across their points. The gypsum results indicate that both the semicircular and pointed platens reliably produce stress conditions that lead to tensile failure of circular and shaped casts.

The size of the specimen also affects the tensile strength value obtained; the smaller the specimen the greater the tensile strength. This effect can be partially explained by the distribution of flaws within the specimens and the associated probability of a flaw of given severity being present in the test specimen.

The comparison of the effect of shape on the load required to produce tensile failure was impeded by the inter-batch variation. The results obtained when preparing two shapes from one batch of slurry suggest that there is not a significant difference between any of the shapes tested. The use of equation 2.1 to determine the tensile strength of shaped specimens would, therefore, be valid. In reaching such a conclusion the variability of the results, with the intra-batch variation in the region of 10% must be considered. If the stresses within the shaped specimens do vary the effects of such changes could be

masked by the variability of the gypsum.

On the basis of these results the diametral compression test will be used to measure the tensile strengths of circular and shaped compacts. Initially both semicircular and pointed platens will be assessed with a view to eventually selecting one configuration for routine testing. The tensile strengths of both circular and shaped compacts will be determined using equation 2.1.

CHAPTER 3

COMPACTION STUDIES USING THE SINGLE PUNCH TABLET MACHINE

3.1 Introduction

A number of studies have been reported in which the effect of altering the punch tip geometry on the compaction properties of excipients and formulations have been studied. The effect of altering the punch face curvature on powder movement during tabletting (Sixsmith and McCluskey 1981),on the surface hardness (Aulton and Tebby 1975) and on tensile strength (Pitt et al 1989a) have all been examined. The mechanical properties of non-circular compacts have been studied. Newton and Stanley (1980) proposed a theoretical equation for the determination of the tensile strength of capsule shaped compacts fractured using a 3 point bending test. Hiestand (1984) has used square compacts to measure the Brittle Fracture Index of materials. Leonard et al (1989) examined the surface hardness of tablets with a combination of different die shapes and punch curvatures. There have not, however, been reports of systematic studies in which the effect of varying the die geometry alone has been investigated.Tablets and compacts can be prepared on a variety of presses. Commercial manufacture of tablets is normally carried out using rotary presses although small scale manufacture and formulation work is often performed on single punch eccentric presses. There are considerable differences between these two machine types which may affect the properties of the compacts produced. These differences will be discussed in detail in Chapter 5. Experimental studies have been performed on hydraulic presses in which the upper punch is moved at a constant velocity. The use of such presses enables compacts to be produced under controlled conditions although the velocities are not necessarily

representative of those produced by commercial tablet presses. A modification of the hydraulic press is the compaction simulator. Compaction simulators are single punch machines in which the upper and lower punches are driven individually by hydraulic rams in such a way as to simulate the operation of commercial presses.The work described in this chapter examines the effect of varying the die shape from circular to hexagonal and square on the compaction properties of pharmaceutical excipients using a single punch eccentric tablet machine.

3.2 Materials and Methods

3.2.1 Material selection

The materials to be examined to determine the effect of shape on the strength of compacts should be simple so that any variables may be controlled or excluded. The inclusion of excipients (Shotton and Lewis 1964) and granulation (Rue et al 1979)are known to affect the mechanical properties of tablets. Hence the ability of a material to be directly compressible is an advantage. The material must also be compactable within the range of the forces that can be applied by the single punch machine (i.e. 0 to 30 kN) and preferably be comparatively free from moisture and humidity effects.

A number of materials are marketed as directly compressible excipients. Of these Avicel PH-102 (Honeywill and Stein), a grade of microcrystalline cellulose, Emcompress (Forum Ltd), a direct compression grade of dibasic calcium phosphate dihydrate, Lactose DMV 100 (PFW Ltd), a free flowing grade of α-lactose monohydrate and Lactose DCL 21 (PFW Ltd), a direct

compression grade of β-anhydrous lactose were selected for initial investigation. The initial particle size of fragmenting materials such as lactose and calcium phosphate may affect the tensile strength of compacts prepared from them (Fell and Newton 1970). For the two grades of Lactose and the Emcompress 75 micrometre to 250 micrometre fractions obtained by sieving were used in the studies. The Avicel PH-102 was used as received.

With the exception of Avicel PH-102 these materials require the addition of a lubricant if they are to be compacted on a tablet machine. The lubricant can be applied either by blending with the material to be compressed or by direct application to the surfaces of the punch faces and die wall. The latter method has the advantage that the lubricant is restricted to the edge of the compacts and will have a minimal effect on the nature of the interparticulate bonds. The disadvantage of the method is that the lubricant needs to be replaced after each compression cycle so compacts can not be produced by continuous running of the machine. The inclusion of the lubricant within the mix more closely represents the situation of a tablet formulation where the lubricant is added to a mix prior to compression and allows compacts to be produced continuously. The majority of work described in this chapter is carried out using blends of the excipients with 1% Magnesium Stearate (Durham Chemical Company) as lubricant, with the exception that some of the work described in Section 3.2.5, investigating the role of the lubricant in the compaction process, utilised the method of die wall lubrication.

With the exception of the Avicel PH-102, one batch of each material was

used in all the studies described in the thesis. The compactability of Avicel is affected by the level of moisture present (Chatrath et al 1990) so a moisture determination using a loss on drying method was performed on all new batches of Avicel received. All batches produced loss on drying values in the range 1% to 1.3%. Furthermore, the compactability of mixes of the new batches of Avicel PH-102 with Magnesium Stearate were compared with mixes from earlier batches using circular compacts prepared on the single punch machine. No significant differences were seen in the compaction pressure/tensile strength profiles of the batches tested. Loss on drying determinations were performed on all excipients at regular intervals to ensure moisture sorption was not occurring on storage.

3.2.2 Preparation of mixes

The Lactose DMV 100, Lactose DCL 21 and Emcompress were shaken on a nest of sieves consisting of a 250 micrometre aperture sieve, a 75 micrometre aperture sieve and receiver, using a Pascall tapping sieve shaker. The portion collected on the 75 micrometre sieve was retained for use in the preparation of the mixes. The Avicel PH-102 and Magnesium Stearate were passed through a 250 micrometre sieve to remove any agglomerates.

Twenty grammes of Magnesium Stearate was added to 1980 grammes of each of the excipients in a 6.4 litre capacity Y-cone mixer (Apex Construction, Type 165) and blended for 3 minutes. The resultant mixes were stored double wrapped in polythene bags with activated clay desiccant placed between the bags until time of use.

3.2.3 Tooling

The range of shapes and sizes of punches and dies used during the compaction studies on the single punch machine are listed in Table 3.1. All the punches were manufactured from the same steel (KE960) and treated to give surface hardnesses within the same range (570-620, Vickers pyramid number).

The tolerances of the punch and die tooling have been shown to affect the formation of tablets. A tightening of the punch tolerances, particularly a decrease in the gap between the upper punch and die will result in a decrease in the capping pressure (Mann et al 1981). This was attributed to air entrapment. The 10mm circular die was machined to an internal diameter of 10mm while the upper punch had a tip diameter of 9.95mm and the lower punch a tip diameter of 9.97mm. Similarly the 10mm shaped tools were also prepared to give a lower punch clearance of 0.03mm and an upper punch clearance of 0.05mm. The corners of the shaped punches and dies were machined to give a radius of curvature of 0.5mm.

3.2.4 Compression force monitoring

The compacts were prepared using a Manesty F3 reciprocating press adapted to permit the measurement of the forces experienced by the upper and lower punches. Both punch holders were modified to accommodate a piezoelectric load cell (Type 9031, Kistler Instruments Ltd). Piezoelectric load cells contain quartz crystals which, when subjected to physical pressure, develop electrical charges across opposing faces. The magnitude of the charge is accurately related to the force applied. The signals from the load cells are fed to charge amplifiers (Type 5054A, Kistler

Table 3.1
Punch shapes and sizes used in compaction studies on the Manesty F3 single punch machine

Shape	Size (mm)*
Circle	20
Circle	10
Square	20
Square	10
Hexagon	20
Hexagon	10

*Size is defined as the diameter of an inscribed circle.

Table 3.2
True density values of excipients used

Material	Measured True Density (g cm^{-3})	Literature values (g cm^{-3})
Avicel PH-102	1.56	1.52[1]
Lactose DMV 100	1.54	1.53[1]
		1.52[2]
Lactose DCL 21	1.55	1.55[3]
Emcompress	2.30	2.31[2]

1. Roberts and Rowe (1986)
2. Handbook of Pharmaceutical Excipients (1986)
3. Roberts and Rowe (1985)

Instruments) which convert the input charge (in the range of 4.27pC per Newton) to an output voltage of 0 to 10 volts. The charge amplifiers have been set up to give a 10 volt output corresponding to 40kN and 30kN for the upper and lower punches respectively. The instrumentation is represented diagrammatically in Figure 3.1. Data collection and analysis was performed using either an IBM PC XT fitted with a 12 bit analogue to digital convertor or a Digital Storage Oscilloscope (Type 1602, Gould Electronics). The PC was programmed to record 1000 data points per channel per second over an 18 second period and to calculate for each compression cycle the peak upper and lower punch forces, the peak ejection force and the mean residual force. A typical compression force cycle is presented in Figure 3.2 with these values illustrated. The residual force is the force that remains on the lower punch during the period between the removal of the upper punch and the start of the ejection cycle, i.e. the point at which the lower punch starts to rise. It has been suggested that the residual force is inversely related to the picking tendency of a formulation (Williams and Stiel 1984). The storage oscilloscope could be programmed to collect data over a period of up to 20 seconds.

The instrumentation is calibrated in two stages. The load cells and charge amplifiers are calibrated by compressing a calibrated load cell linked to a calibrated charge amplifier between flat faced upper and lower punches. The outputs from the charge amplifiers measuring the punch forces are compared to the output of the calibrated system. The oscilloscope and the computer were tested using a calibrated voltage generator.

Figure 3.1
Schematic representation of the force monitoring instrumentation on the single punch tablet machine

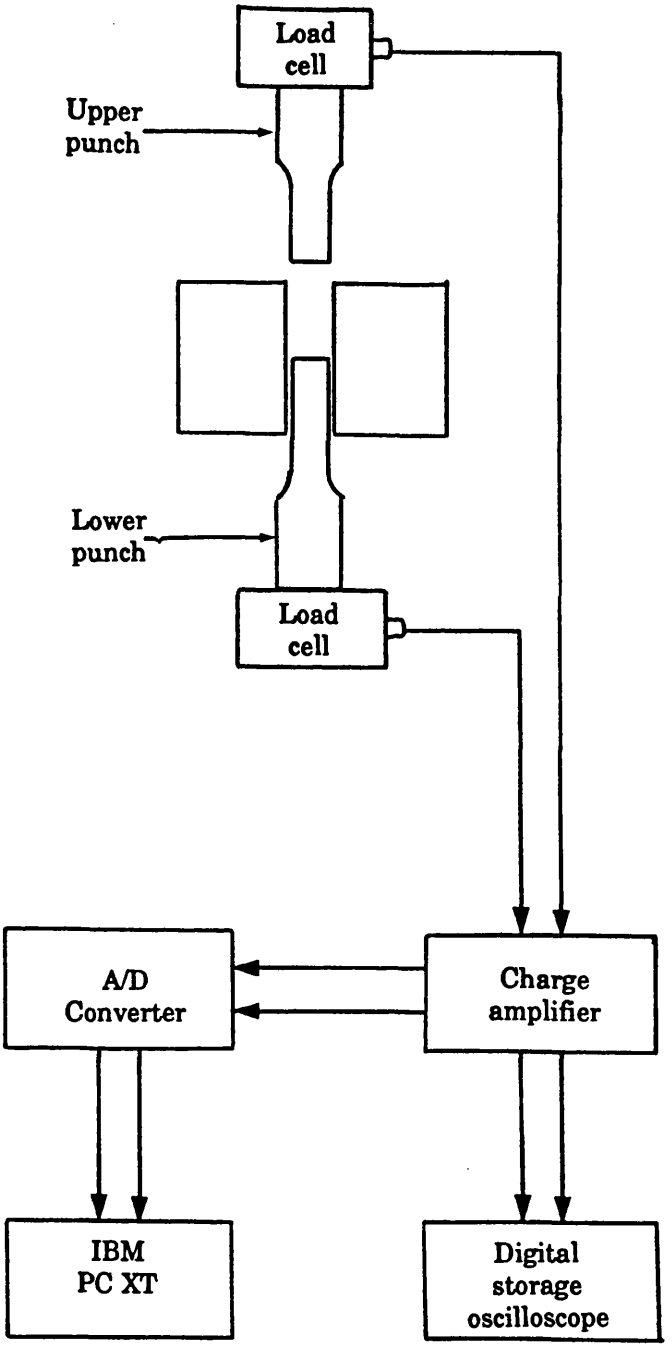

Figure 3.2
Typical force/time compression cycle obtained on the single punch tablet machine

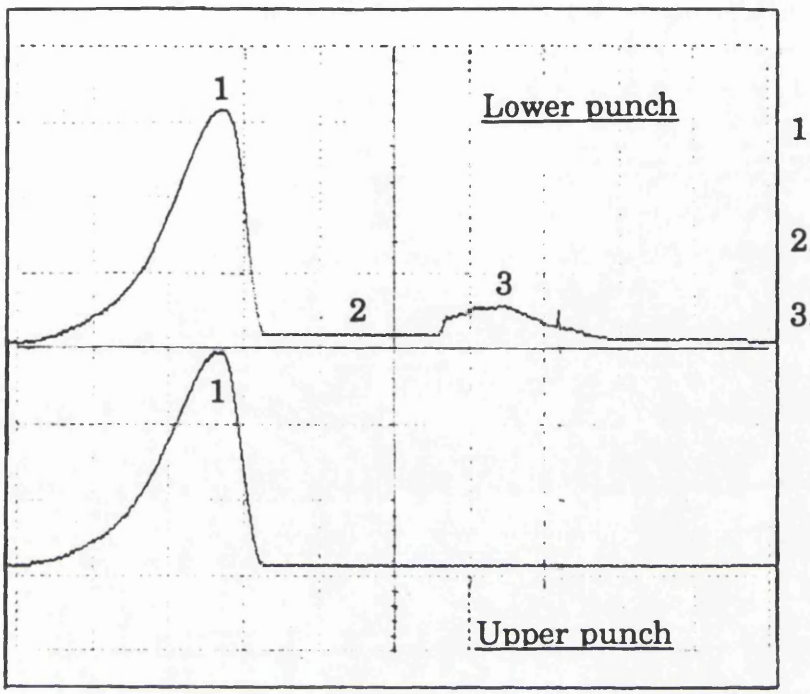

1. Peak compaction force
2. Residual force
3. Ejection force

Lower punch: 1 division = 1.5kN

Upper punch: 1 division = 2.0kN

Time scale : 1 division = 50ms

3.2.5 Preparation of compacts

The powder mixes were compacted by running the Manesty F-machine under power at a speed of one cycle per second. Using the software written for the IBM PC XT in the "set-up" mode it was possible to measure the individual peak compaction forces for the lower punch. When the force required had been obtained the "data capture" mode was initiated and 18 seconds of data was stored. During this period the compacts produced were collected in the order they were produced so they could be identified against the values of the peak compaction forces. All the compression work was performed in an environment where the temperature was controlled between 17°C and 22°C and the relative humidity was in the range of 30-45% RH.

There are a number of parameters in any tabletting investigation, such as compaction pressure, porosity, mass and thickness that can be varied. The object of the work outlined here is to assess the effect of die shape on the properties of tablets. It is desirable, therefore, to keep the dimensions of the different shaped compacts similar. One method of achieving this is to keep the weight of the powder compressed constant for each shape and compressing to a specified thickness. This means that the quantity of material available for forming bonds is constant for each shape. However, the pressure required to form compacts of a given thickness will decrease as the surface area of the punches increase. Similarly the porosity of compacts prepared with punches of greater surface area will be lower. A number of empirical equations have been proposed that relate the tensile strength to compaction pressure (Higuchi et al 1954) and (Newton and

Grant 1974) and tensile strength to porosity (Ryshkewitch 1953). It would appear more logical, therefore, to vary the amount of material compressed for each shape in such a manner that compacts of different shapes having the same thickness will also have the same porosity. This can be achieved by varying the weight of powder compressed in proportion to the punch surface area. This is the approach adopted during the work described herein. The instrumentation measures the compaction force and not the compaction pressure. The compaction pressure (Pascals) is determined by dividing the compaction force (measured in Newtons) by the punch surface area (metres^2).

The compression weights for each excipient were selected on the basis of the theoretical thickness of compacts of zero porosity. The weight of a material required to produce a compact of zero porosity is given by the equation;

$$Wt. = \rho_t V \qquad (3.1)$$

where Wt. is the weight, ρ_t is the true density of the powder and V the volume of the compact. The true densities of the materials were determined using an air pycnometer (Model 930, Beckman Instruments). Values for the true densities of the excipients studied are listed in Table 3.2. The zero porosity thickness initially selected was 2.8mm as this resulted in compacts being produced with width to thickness ratios representative of those found in pharmaceutical tablets. Later studies were performed on Emcompress compacts with zero porosity thicknesses over the range of 2mm to 6mm and Avicel compacts with zero porosity

thicknesses of 2mm to 3.8mm. The narrower range of values for Avicel is due to its low bulk density restricting the quantity of powder that can be accommodated within the die. The fill weights used for each excipient are listed in Table 3.3.

To evaluate the effect of inclusion of Magnesium Stearate in the powder mix on the compaction process, compacts were also prepared using die wall lubrication as opposed to incorporation of the lubricant within the powder mixes. To prepare such compacts the tablet machine was turned over by hand until the lower punch just reached the lowest point of its cycle. The powder shoe was removed. The die wall and punch faces were painted with a saturated solution of Magnesium Stearate in acetone, and allowed to dry. The required amount of the pre-sieved excipient was poured into the die and flattened to give a smooth upper surface. The empty powder shoe was replaced and the machine run under power for one cycle. The compression force data were captured using the digital storage oscilloscope. Unlubricated compacts of Avicel PH-102 were also compressed without the aid of die wall lubrication (Section 3.3.3.7)

3.2.6 Compact storage

After preparation all compacts were stored in tightly closed amber glass bottles. The tensile strength of tablets will change with time (Rees and Shotton, 1970) particularly during the first hour of compression. This is attributed to stress relief of the crystals and interparticulate bonding. The effect of storage time on the tensile strength of each excipient was determined by testing four 20mm circular compacts from batches compressed at a force of approximately 10kN, after 0, 1, 7 and 14 days

Table 3.3
Compression weights of excipients used in single punch studies

Material	Size (mm)	Zero porosity thickness (mm)	Compression weight (mg)		
			Circle	Hexagon	Square
Avicel PH-102	20	2.0	980	1081	1248
		2.8	1372	1513	1747
	10	2.0	245	270	312
		2.8	343	378	437
		3.2	392	432	499
		3.6	441	486	562
Emcompress	20	2.0	1445	1593	1840
		2.8	2023	2230	2576
	10	2.0	361	398	460
		2.8	505	557	644
		4.0	722	796	920
		6.0	1083	1194	1380
Lactose DCL 21	20	2.8	1363	1504	1736
	10	2.8	341	376	434
Lactose DMV 100	20	2.8	1355	1494	1725
	10	2.8	339	373	431

storage. The mean tensile strengths obtained are displayed in Table 3.4. The results indicate that any changes are complete after 14 days for all materials. A storage time of 14 days between compression and testing was adopted for all samples.

3.2.7 Testing of the compacts

3.2.7.1 Diametral compression test

Compacts prepared when using the IBM PC XT for data acquisition were produced in batches of 18. The compacts were weighed and the 10 compacts closest to the target weight selected for testing. If the coefficient of weight variation of the selected compacts exceeded 1% the batch was not used for testing. The compact thicknesses were measured using a Mercer Dial Gauge.

The strengths of the compacts were tested using the CT40 Mechanical Strength Tester by the method described in Section 2.2.5. Initially compacts of all materials were tested by diametral compression using the semicircular and pointed platens. The square and hexagonal compacts were compressed across the mid points of two opposite faces. The effect of the platen shape on the breaking load was investigated in terms of the contact width between the compact and the platen. This width was determined by two methods. The first method involved loading a compact to approximately 90% of its anticipated breaking strength and maintaining the load. Using a cathetometer (Model 2202, Precision Tool and Instrument Ltd) the width of contact could then be measured. The second method involved placing a strip of carbonless copy paper between the compact and the platens and carrying out the test as usual. After the test the paper was

Table 3.4
Effect of storage time on the tensile strength of 20mm diameter circular compacts with 2.8mm zero porosity thickness

Material	Compaction Pressure (MPa)	Tensile strength (MPa)[1]			
		Initial	1 day	7 days	14 days
Avicel PH-102	31.3	0.91	0.87	0.77	0.78
Emcompress	30.1	0.17	0.15	0.13	0.13
Lactose DMV 100	78.9[2]	0.13	0.12	0.12	0.12
Lactose DCL 21	33.4	0.24	0.24	0.23	0.24

1. Tensile strength determined by diametral compression.

2. Coherent compacts were not formed at compaction pressures of 30MPa.

removed and examined by microscopy. The width over which the ink had been released from the microcapsules in the paper was measured using a calibrated eyepiece graticule.

The testing of the Avicel and Emcompress square and hexagonal compacts was extended to include loading across 2 corners. To prevent the occurrence of sample movement at the points of loading evident when testing gypsum casts in this manner, special notched platens were used. The notches in the platens for testing hexagons had an internal angle of 60° while the platens for testing square platens had an internal angle of 90°.

3.2.7.2 Axial compression test

A further test applied to the Avicel and Emcompress compacts was an axial compression test. Using the CT 40 fitted with semicircular platens the compacts were loaded across their upper and lower faces. For circular compacts the platens were positioned along a diameter while for the square and hexagonal compacts the platens followed a line between the mid point of two opposite edges as shown in Figure 3.3.

3.2.7.3 Transverse compression test

A third test applied to compacts was a transverse compression test. The compacts were compressed between semicircular platens positioned along the middle of the compact sides parallel to the upper and lower surfaces (Figure 3.4)

3.2.7.4 Ball bearing diametral compression test

Compacts were tested by diametral compression using platens in which a 6mm diameter ball bearing had been mounted (Figure 3.5)

Figure 3.3
Axial compression test

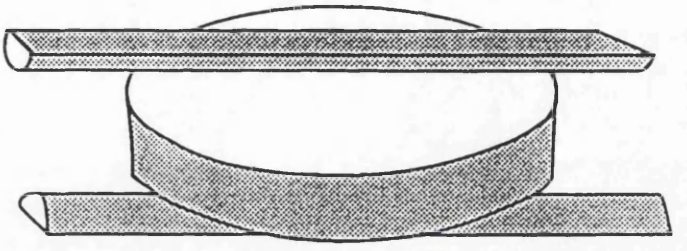

Circular compacts

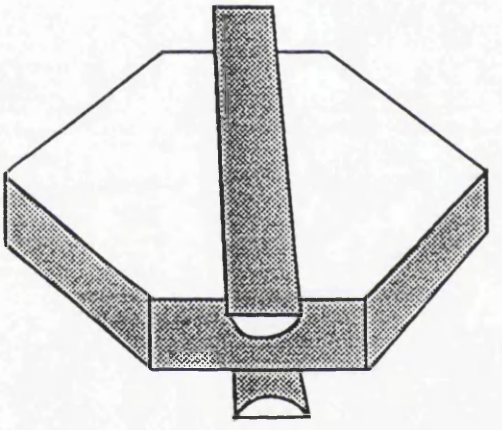

Hexagonal compacts

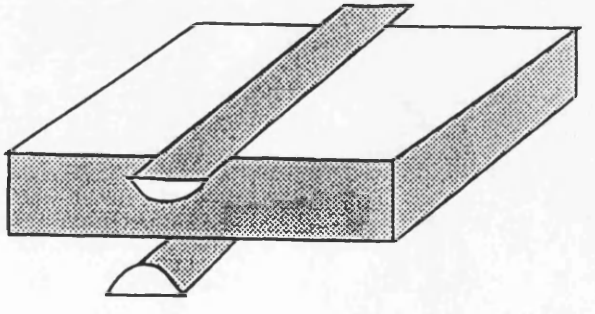

Square compacts

Figure 3.4
Transverse compression test

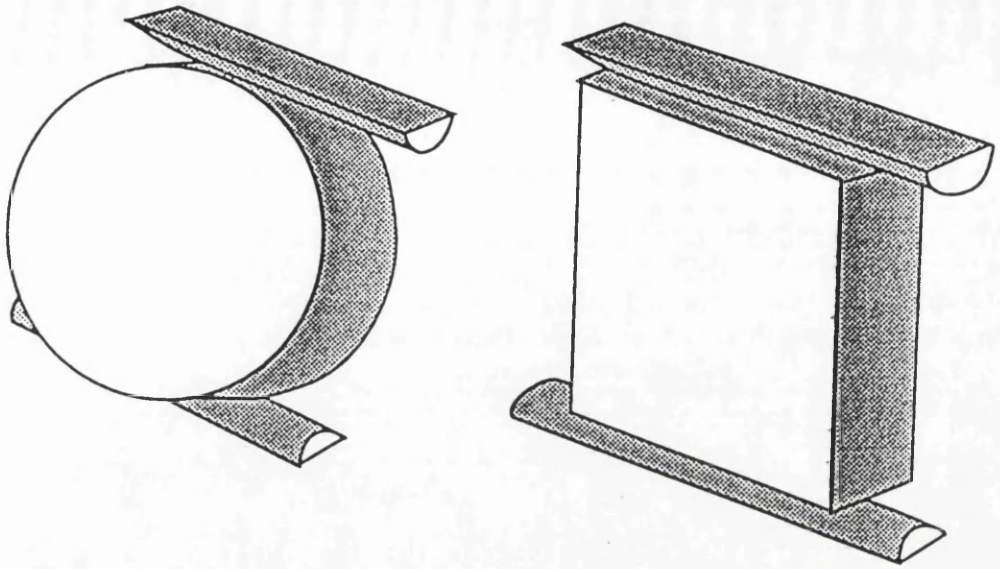

Circular compacts Square compacts

Figure 3.5
Ball Bearing Diametral Compression Test

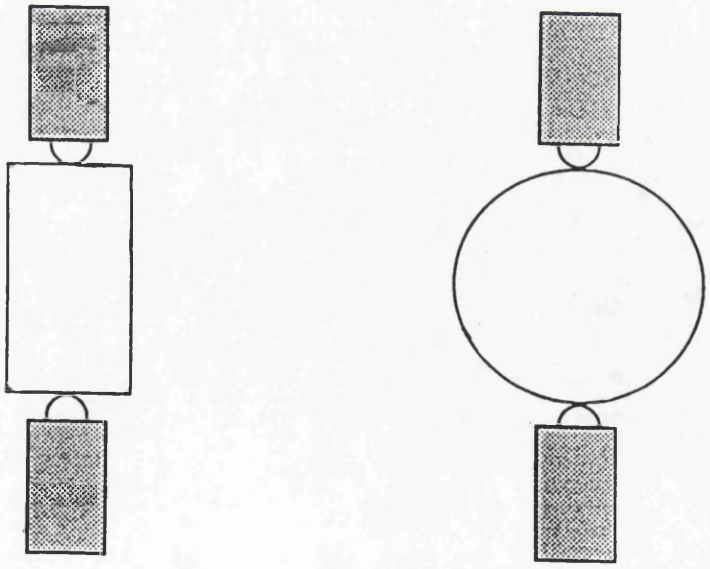

Square compacts Circular compacts

3.2.7.5. Three point bending test

Compacts were tested using a 3 point bending rig apparatus. The rig, illustrated in Figure 3.6, consists of two 3mm diameter parallel rollers, on which the test specimen is supported, that sit on the load cell of the CT 40. The distance between the two rollers can be varied. A platen with a 3mm diameter cylinder mounted horizontally is attached to the crosshead of the CT 40. The upper platen is aligned such that the cylinder is parallel to the two rollers which are equidistant from the centre of the rig. The compacts were placed on the rollers in a horizontal position. The surface of the tablet exposed to tension in the test, i.e. the surface adjacent to the lower rollers, was noted.

3.2.7.6. Varying the platen positions used in the test configurations

The tests described thus far (Sections 3.2.7.1 to 3.2.7.5) have all been performed with the platens positioned at the mid points of the faces or sides of the compacts. Tests were also performed with the platens positioned at points between the middle and edge of the compacts.

The diametral compression test was applied to squares with the platens positioned 2.5mm from the edge of the compact. The transverse compression test was carried out on square and circular compacts with the platens positioned midway between the centre of the compact and the lower and upper surfaces. The axial compression test was applied to square compacts with the platens positioned parallel to the side of the compacts, 2.5mm in from the edge. The semicircular platens would not be suitable for testing the circular compacts axially away from the centre as the decreased contact between platen and sample would be likely to affect

Figure 3.6
Three point bending test

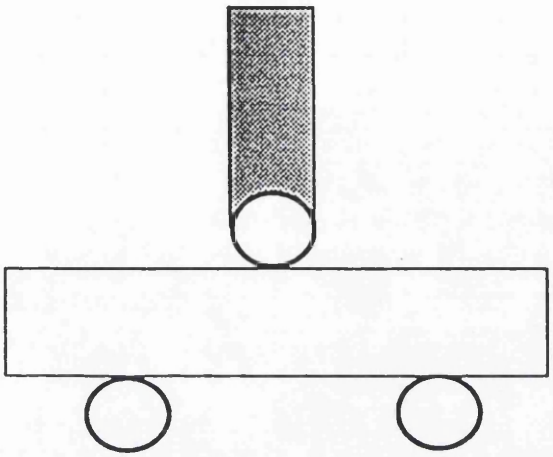

the value obtained. Instead the ball bearing platens were used to perform the axial compression test on the circular compacts. The tests were performed in the centre of the compact and also midway between the centre and edge of the compact. Square compacts were also tested axially using the ball bearing platens in a central position, midway between the centre and the middle of one of the faces and midway between the centre and a corner.

3.2.8 Statistical treatment of results

3.2.8.1 Linear regression

A feature of compaction studies is that the variance in the tensile strength values obtained tends to increase as the compaction pressure increases. This complicates the statistical handling of the data as regression and curve fitting techniques are based on the assumption that the variance about the mean values of the independent variable is constant for all values of the dependent variable. Regression analysis of the compaction data, in the untreated form, will produce a line of best fit that is unduly influenced by the tensile strength values where the variance is greatest. To overcome this problem a weighted linear regression, in which each data point is assigned a weighting, was employed. The weights are used as multipliers for each point's squared error term in determining the fit. The weighting selected was the reciprocal of the variance in the tensile strength for compacts produced with the same compaction pressure (Snedecor and Cochran 1980).

3.2.8.2 Comparison of lines

Sets of data were compared by one way analysis of covariance, a test that

combines one way analysis of variance with linear regression to determine whether two or more sets of lines are parallel. Again this test depends on the variance around the mean being equal throughout the range of values being tested. Values of both the compaction pressure and the tensile strength were divided by the standard deviation of the tensile strength values obtained for each compaction pressure. The analysis of covariance was performed on data transformed in this manner (Wetherill 1981).

3.3 Results and discussion

3.3.1 Effect of platen shape on the diametral compression test results

The compaction pressure/tensile strength profiles of Avicel PH-102, Anhydrous Lactose DCL21, Lactose DMV 100 and Emcompress circular compacts tested with flat, semicircular and pointed platens are illustrated in Figures 3.7 to 3.13. From these figures it is evident that the trend seen with the gypsum casts, where altering the platen type from pointed to semicircular to flat results in a progressive increase in the tensile strength value obtained, is also seen with compacts. A significant difference ($p < 0.05$) in tensile strength is obtained for all materials tested with flat and semicircular platens. It is postulated that the reason for the variation in tensile strength is differences in the contact widths between the platens and the compact. Berenbaum and Brodie (1959) describe a formula to determine the width of contact (d_c) between a circular test specimen and flat platens made from a harder material;

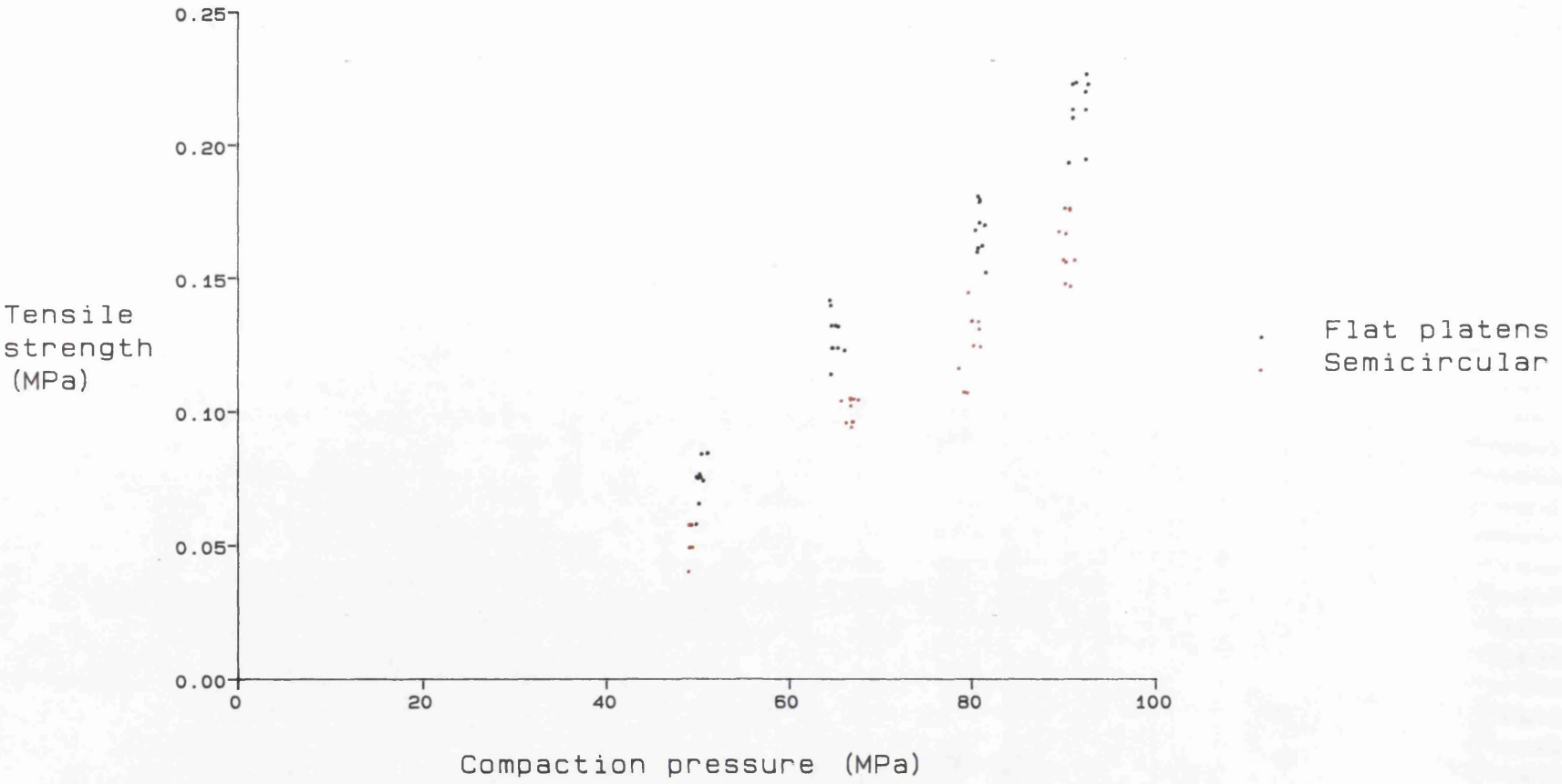

Tensile strength determined by diametral compression.

Figure 3.7 Effect of platen shape on the compaction pressure/tensile strength profile of Lactose DMV 100 circular compacts

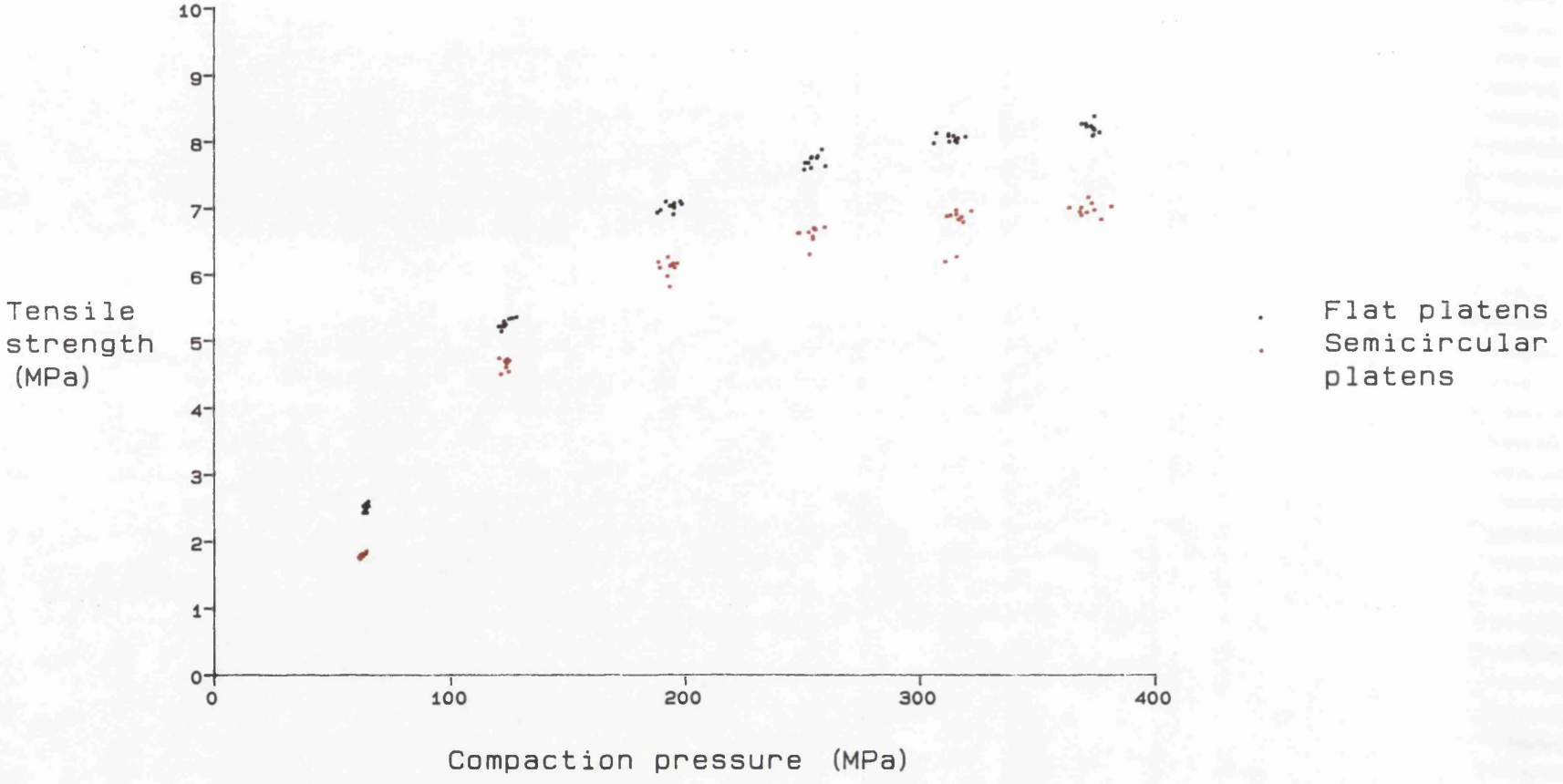

Tensile strength determined by diametral compression.

Figure 3.8 Effect of platen shape on the compaction pressure/tensile strength profile of Avicel 10mm circular compacts.

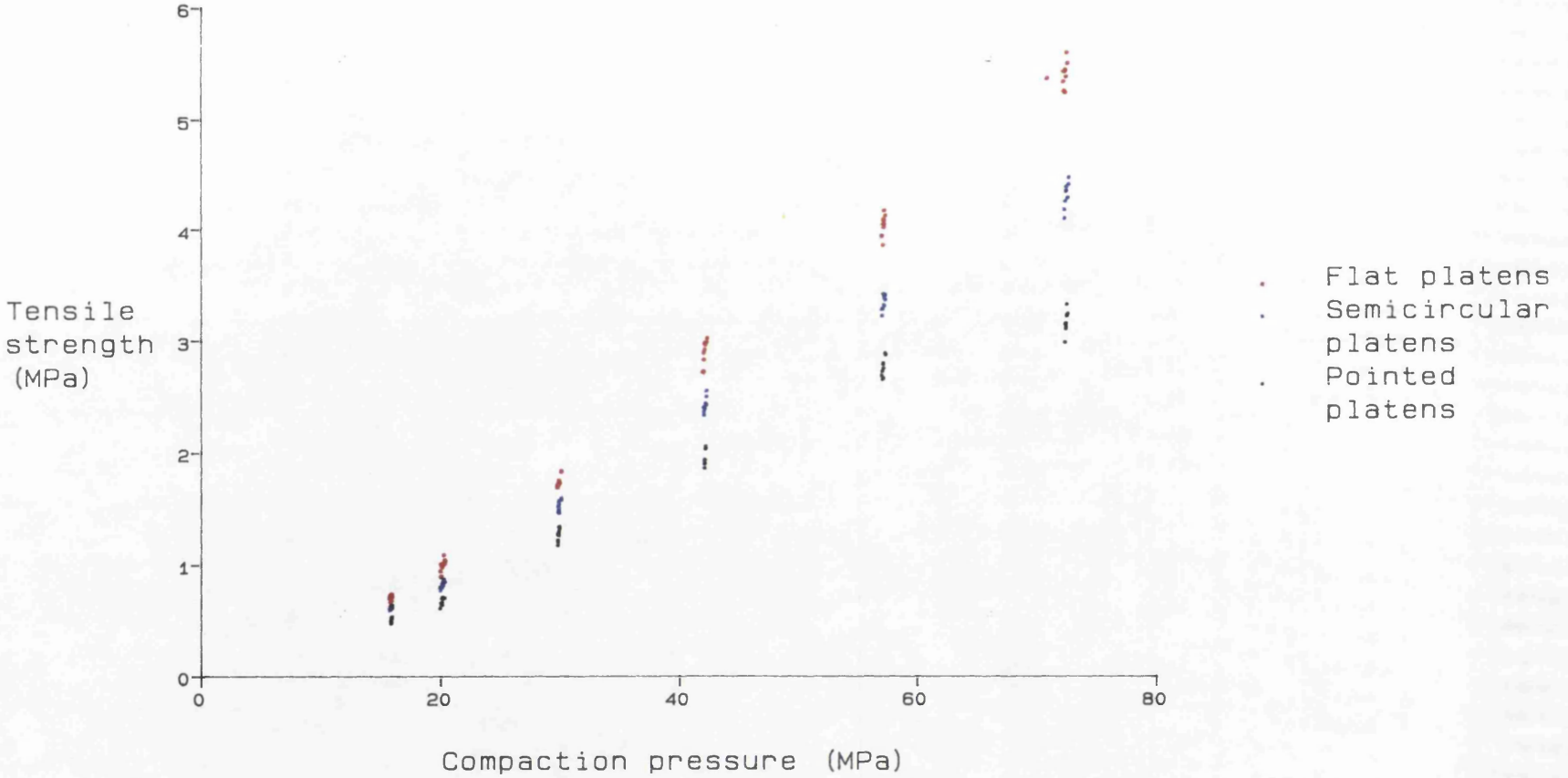

Tensile strength determined by diametral compression.

Figure 3.9 Effect of platen shape on the compaction pressure/tensile strength profile of Avicel 20mm circular compacts

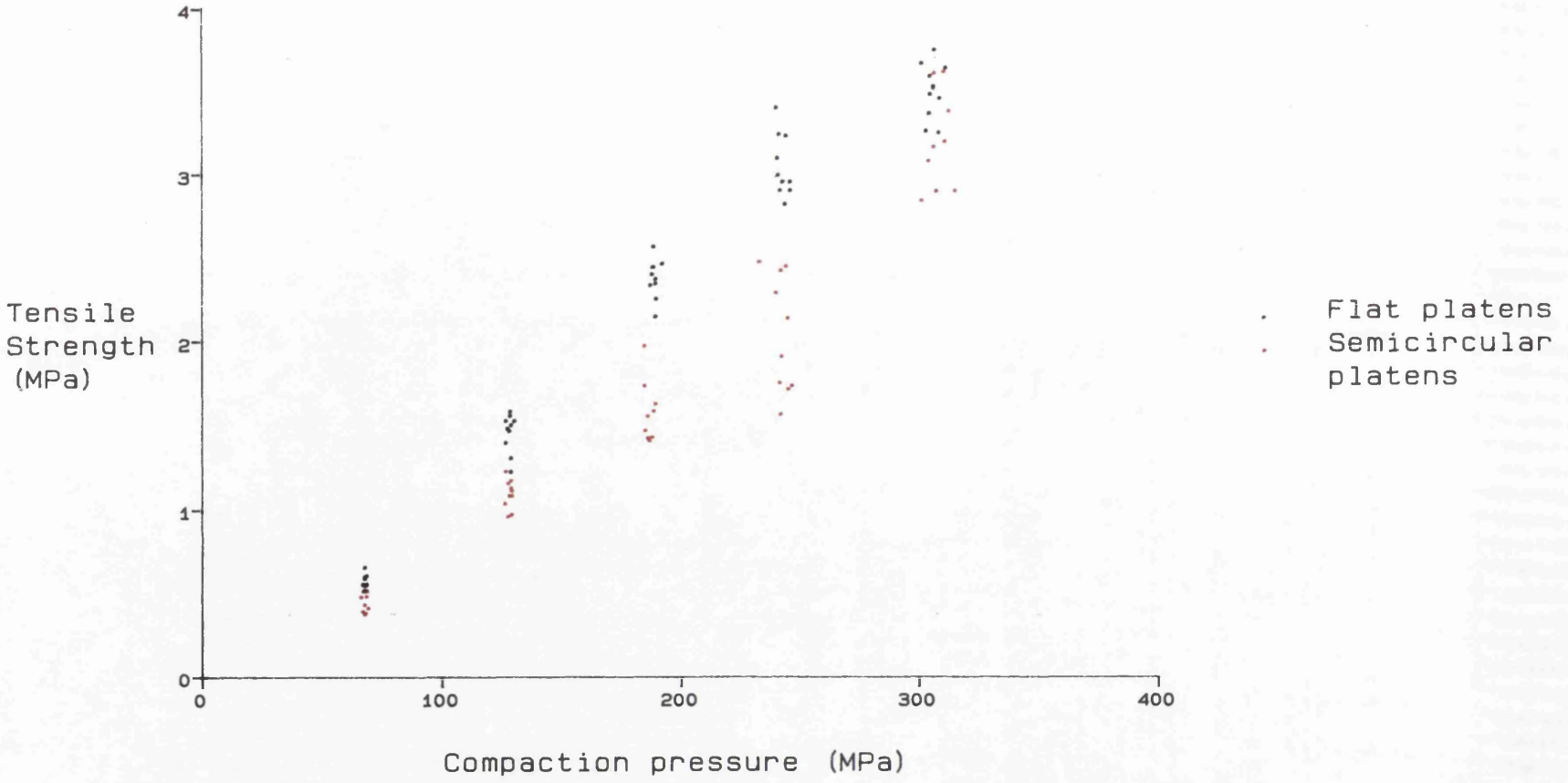

Tensile strength determined by diametral compression.

Figure 3.10 Effect of platen shape on the compaction pressure/tensile strength profile of Anhydrous Lactose DCL 21 10mm circular compacts

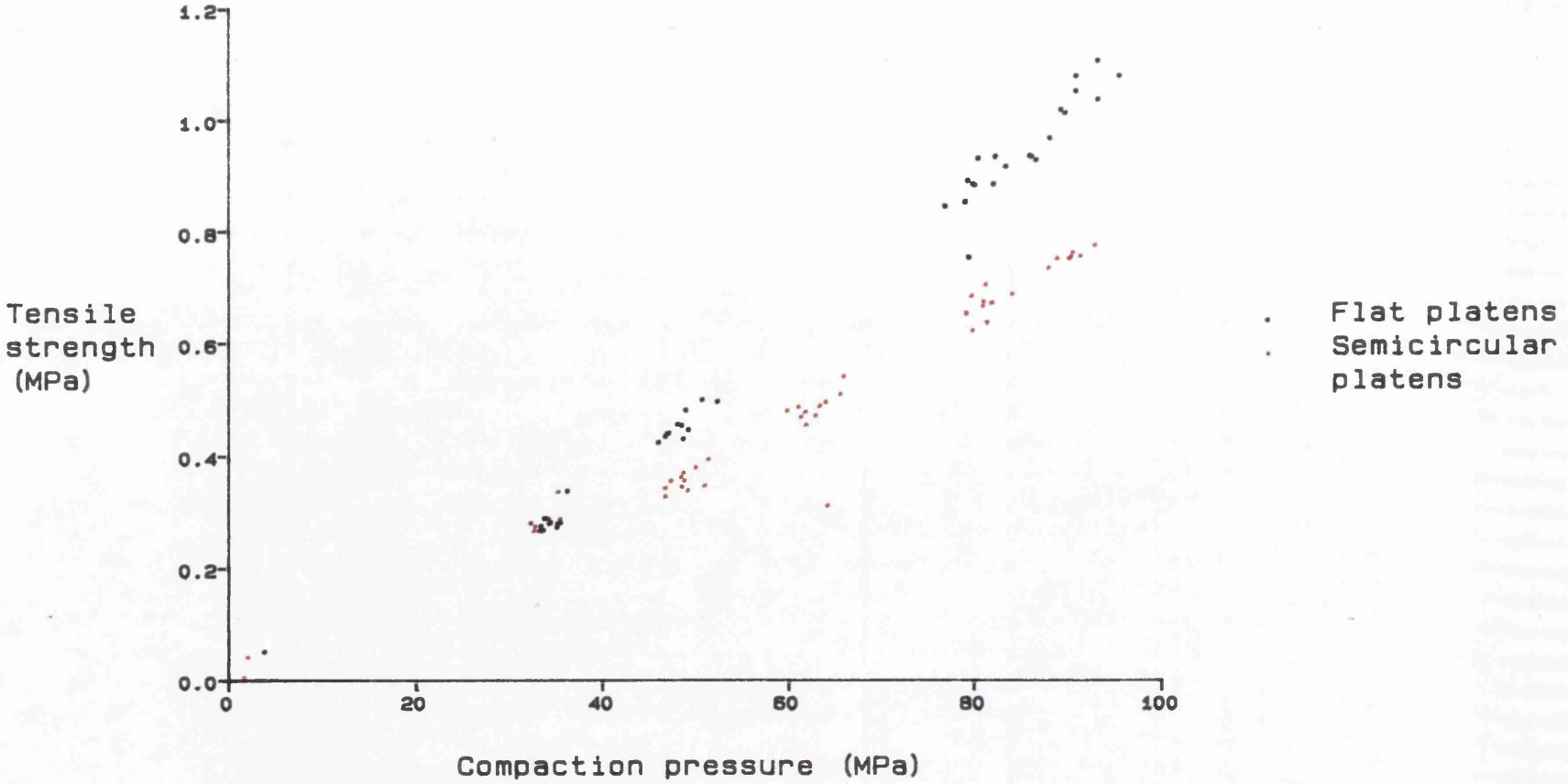

Tensile strength determined by diametral compression.

Figure 3.11 Effect of platen shape on the compaction pressure/tensile strength profile of Anhydrous Lactose DCL 21 20mm circular compacts

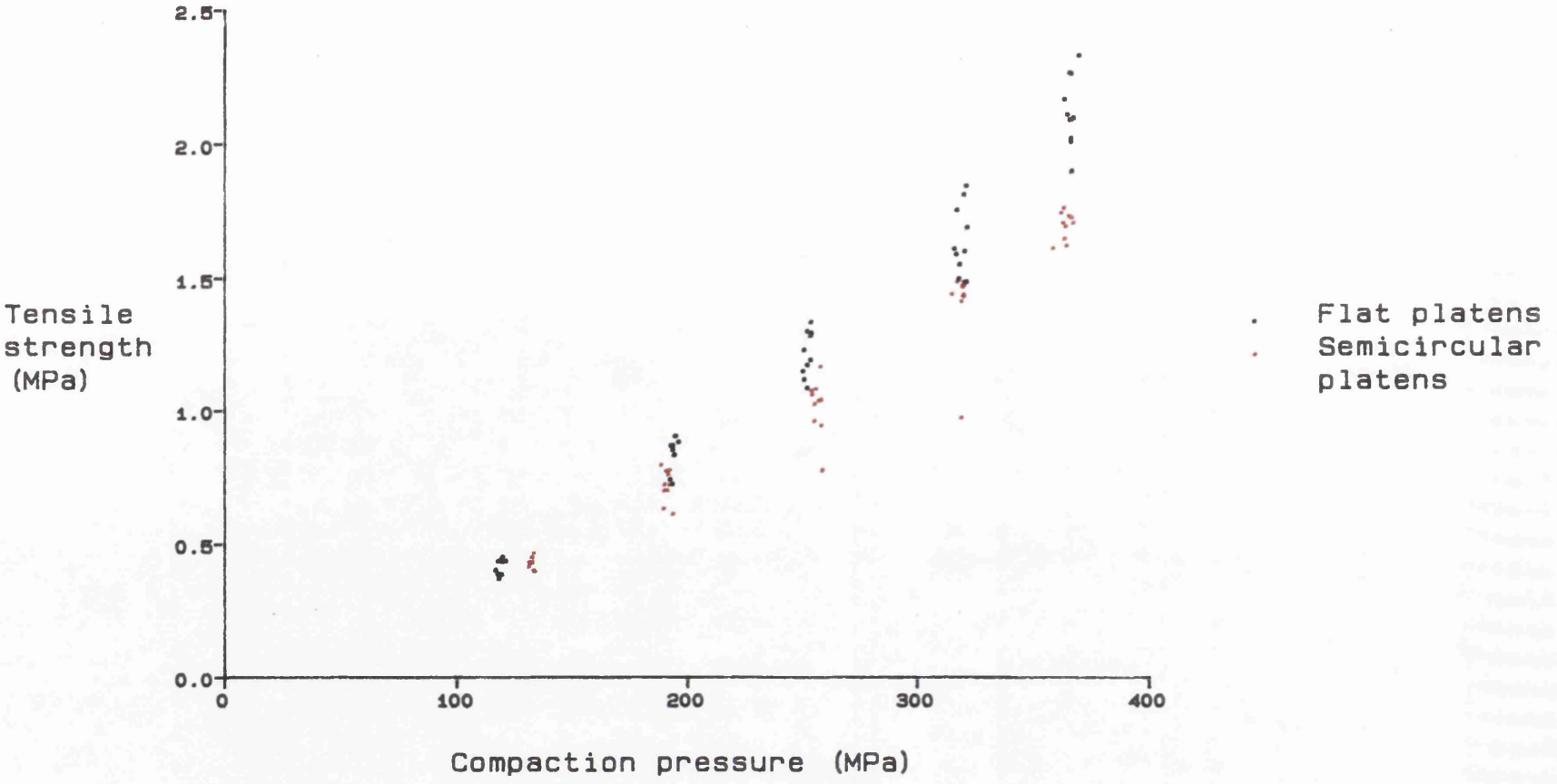

Tensile strength determined by diametral compression.

Figure 3.12 Effect of platen shape on the compaction pressure/tensile strength profile of Emcompress 10mm circular compacts

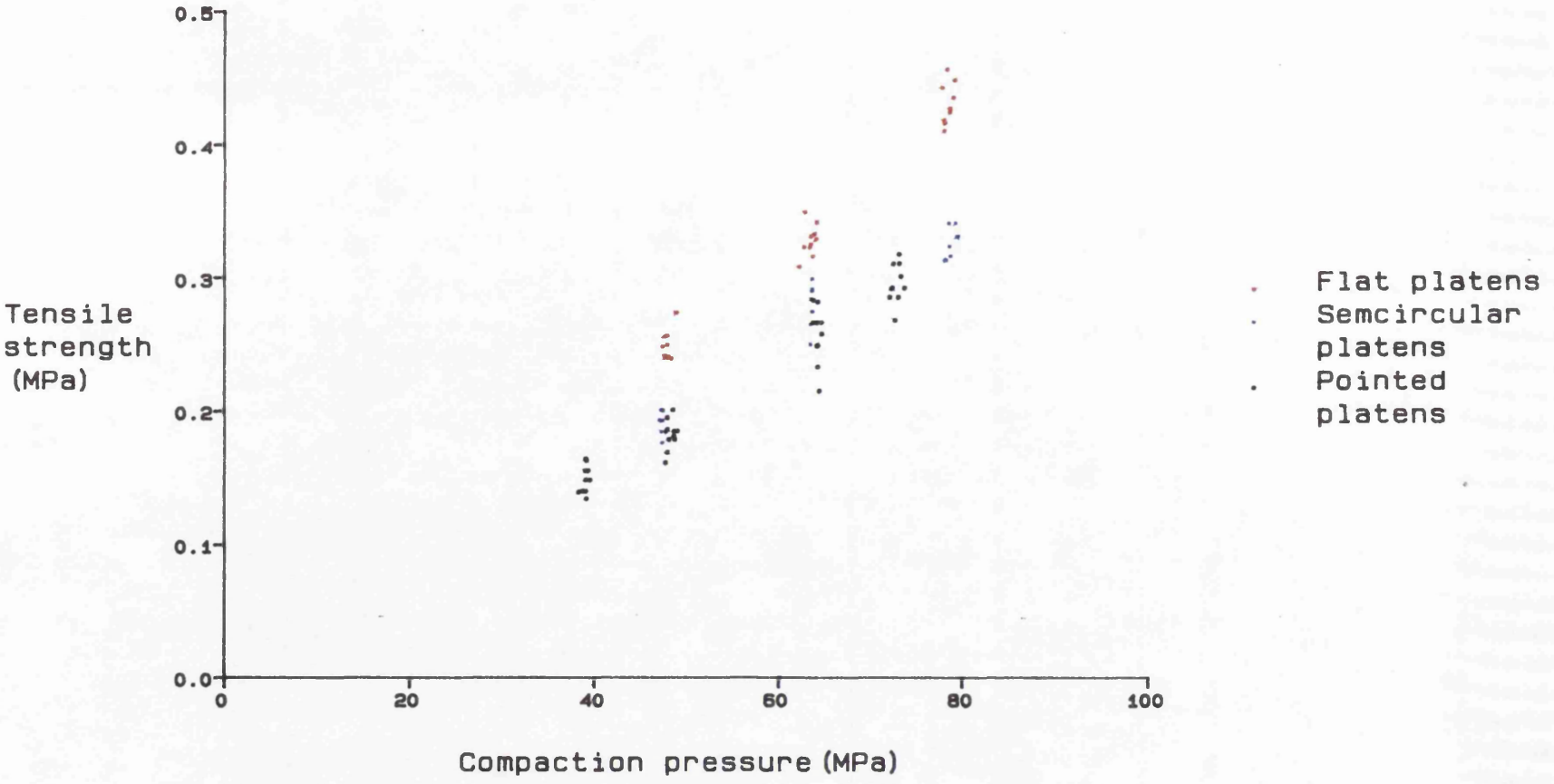

Tensile strength determined by diametral compression.

Figure 3.13 Effect of platen shape on the compaction pressure/tensile strength profile of Emcompress 20mm circular compacts

$$d_c = 1.6 \sqrt{\frac{P}{t} \times \frac{D\,(1-\nu^2)}{E}} \qquad (3.2)$$

where P = Load applied

D = Compact diameter

t = Compact thickness

E = Young's Modulus of the compacted material

υ = Poisson's Ratio of the compacted material

Using literature values for the Poisson's Ratio (Church 1983) and the compressive Young's Modulus of Avicel (Kerridge and Newton 1986) a theoretical contact width of 0.4mm was obtained for a 20mm compact prepared at 85MPa. Examination of compacts tested using flat platens showed signs of deformation at the loading points well in excess of 0.4mm. Furthermore, the formula cannot take into account changes in the platen shape so was not considered suitable for predicting the effect of such changes on contact width.

The two methods of measuring the contact widths are both open to criticism. The first method, involving holding a compact between platens at a force just below the failure load and measuring the contact by cathetometry, will result in an overestimate of the contact width if the deformation is time dependent. The second method, using carbonless copy paper, has two potential drawbacks. Firstly, the width of mark obtained on the paper will be dependent on the properties of the paper; the distribution of the ink microcapsules and the force required to induce their rupture. These factors might be expected to give a low value for the contact width. A second concern is the effect that placing the paper between the

platen and compact will have on test conditions. Paper has been used as a method of distributing the load at platen edges when testing concrete (Chapman 1968) and pharmaceutical compacts (Fell and Newton 1970). To assess whether the paper did affect the test, Avicel and Anhydrous Lactose compacts were tested with and without the paper in position. Application of the Student's t-test to the tensile strength values obtained indicated that the presence of the paper does not significantly affect the results of the test.

The contact width measurements obtained using the two methods are shown in Tables 3.5 and 3.6. Results are not presented for compacts tested with pointed platens . Although the pointed platens appeared to produce tensile failure in the compacts this failure was preceded by the platens cutting into the sides of the compacts and as such were not considered suitable for determining the tensile strength. The results indicate that the platen shape does affect the width of contact with the compacts.Both methods indicated that the mean contact width was greater with the flat platens than the semicircular platens, although the difference was only statistically significant when measured by cathetometry. It can also be seen that the contact width for Avicel compacts is related to the strength of the compact while such a trend is not evident for Anhydrous Lactose and Emcompress compacts. It is to be expected that as the strength of compacts prepared from any of the materials tested increases so will the contact width, a view supported by equation 3.2. Measuring the contact width is a method of measuring the deformation at the platen edges.

Rees and Rue (1978) examined the relationship between platen

Table 3.5
Contact widths between circular compacts and platens determined by cathetometry

Material	Diameter (mm)	Compaction Pressure (MPa)	Platen shape	Contact width (mm)	
				Mean	S.D.
Avicel PH-102	20	31.8	Flat	2.19	0.15
		47.7	Flat	2.54	0.09
		63.5	Flat	2.54	0.18
		81.2	Flat	3.32	0.15
Avicel PH-102	20	31.8	Semi-circular	1.39	0.20
		47.7	Semi-circular	1.36	0.40
		63.5	Semi-circular	1.68	0.22
		81.2	Semi-circular	1.51	0.23
Avicel PH-102	10	186	Flat	1.36	0.15
		243	Flat	1.60	0.19
		310	Flat	1.67	0.17
Avicel PH-102	10	186	Semi-circular	1.14	0.29
		243	Semi-circular	0.93	0.38
		310	Semi-circular	0.95	0.29
Anhydrous Lactose DCL 21	20	49.2	Flat	2.28	0.51
		64.3	Flat	2.05	0.41
		78.1	Flat	1.89	0.62
Anhydrous Lactose DCL 21	20	49.2	Semi-circular	1.07	0.30
		64.3	Semi-circular	1.07	0.28
		78.1	Semi-circular	0.74	0.34
Emcompress	20	48.4	Flat	1.95	0.47
		64.0	Flat	1.79	0.40
Emcompress	20	48.4	Semi-circular	1.01	0.21
		64.0	Semi-circular	1.01	0.29

Table 3.6
Contact widths between compacts and platens determined using self-carboned copy paper

Material	Diameter (mm)	Compaction pressure (MPa)	Platen shape	Contact width (mm)	
				Mean	S.D.
Anhydrous Lactose DCL 21	20	49.2	Semi-circular	0.30	0.07
		64.3	Semi-circular	0.33	0.05
		78.1	Semi-circular	0.38	0.07
Anhydrous Lactose DCL 21	20	49.2	Flat	0.40	0.02
		64.3	Flat	0.40	0.07
		78.1	Flat	0.48	0.08
Emcompress	20	48.4	Semi-circular	0.28	0.05
		64.0	Semi-circular	0.26	0.07
Emcompress	20	48.4	Flat	0.35	0.06
		64.0	Flat	0.32	0.05

displacement and load applied to compacts during the diametral compression test when developing their Work of Failure test. The results obtained support the contact width measurement results. It was reported that for Microcrystalline Cellulose the load transmitted to the lower platen increased slowly as the upper platen displacement increased, indicating that the material was deforming plastically, which would be reflected by an increase in the contact width for compacts of increasing strength. Emcompress and Anhydrous Lactose were also examined and these materials exhibited a rapid increase in load for a small increase in platen displacement suggesting minimal deformation.

The very rapid increase in force with platen displacement explains the small contact widths. While the contact width is likely to increase with increasing compact strength the methods used to determine the widths were not sensitive enough to detect the changes.

Peltier (1954) calculated the effect that varying the ratio of the contact width to the compact diameter would have on the tensile strength value derived from the diametral compression test. Using this data it is possible to estimate the effect that changing the platen shape will have on the tensile strength value obtained. Table 3.7 presents the actual tensile strength values obtained using the two platen types and compares them with the estimated values of tensile strength for compacts tested using semicircular platens based on the contact widths determined by cathetometry for the two sets of platens and the tensile strength value obtained using flat platens. The results give an accurate prediction for the semicircular platen tensile strength values. The carbonless copy paper

Table 3.7
Comparison of actual tensile strength values with predicted values from the relative contact widths of circular compacts tested with flat and semicircular platens

Material	Diameter (mm)	Compaction pressure (MPa)	Measured tensile strength (MPa)[1]		Predicted tensile strength (MPa)
			Flat platens	Semicircular platens	
Avicel PH-102	20	31.8	0.92	0.79	0.82
		47.7	1.83	1.52	1.55
		63.5	2.67	2.28	2.35
Avicel PH-102	10	186	3.16	2.81	2.91
		243	5.41	4.85	4.39
		310	6.22	5.55	5.40
Anhydrous Lactose DCL 21	20	49.2	0.78	0.52	0.63
		64.3	1.29	1.01	1.09
		78.1	1.66	1.27	1.29
Emcompress	20	48.4	0.26	0.19	0.22
		64.0	0.34	0.28	0.30

1. Tensile strength determined by diametral compression test.

Table 3.8
Comparison of contact widths for 20mm square and circular compacts tested using semicircular platens

Material	Compact shape	Compaction pressure (MPa)	Contact width (mm)	
			Mean	S.D.
Avicel PH-102	Circle	31.8	2.19	0.15
		47.7	2.54	0.09
		63.5	2.54	0.18
	Square	39.0	2.28	0.14
		50.1	2.60	0.16
		64.2	2.68	0.12
Emcompress	Circle	48.4	1.01	0.21
		64.0	1.10	0.29
	Square	49.3	1.15	0.23
		63.1	1.18	0.17

method, although giving lower mean values for the semicircular platens, did not indicate that there were significant differences between the two platens. This may indicate that the cathetometry is the more accurate method of determining the contact widths.

Table 3.8 presents values for contact widths, determined by cathetometry, of 20mm circular and square compacts of Avicel and Emcompress tested with semicircular platens. While the mean contact widths are greater for the square compacts, the large variance between measurements means the differences are not statistically significant. While the widths of contact between the platens and hexagonal compacts were not measured they are likely to be comparable to the values obtained for square compacts as the platens are in contact with flat surfaces in both instances. These results indicate that the semicircular platens are suitable for comparing circular, hexagonal and square compacts.

3.3.2 Characterisation of the compaction properties of circular compacts

3.3.2.1 Diametral compression test data

Data for compaction pressure, porosity and strength of compacts is presented here in a variety of ways to demonstrate their relationships. The results for circular compacts are used to assess which analysis gives the most logical and consistent interpretation of the compaction data, before proceeding to the analysis of data for shaped compacts.

The data for the Avicel, Emcompress, Lactose DMV100 and Anhydrous Lactose DCL 21 circular compacts are summarised in Tables 3.9 to 3.12. The results indicate that increasing the compaction pressure produces a decrease in porosity and an increase in tensile strength. The simplest

Table 3.9
Diametral compression data for Emcompress circular compacts tested using semicircular platens

Compact diameter (mm)	Zero porosity thickness (mm)	Mean compaction pressure (MPa)	Compact thickness (mm)	Mean breaking load (kg)	Mean tensile strength (MPa)	Porosity
20	2.8	47.3	3.88	2.48	0.20	0.28
20	2.8	63.5	3.75	3.42	0.28	0.25
20	2.8	78.7	3.67	3.94	0.34	0.24
10	2.0	69.1	2.70	1.69	0.39	0.24
10	2.0	142	2.47	3.38	0.85	0.19
10	2.0	195	2.40	4.67	1.21	0.17
10	2.0	272	2.33	6.50	1.74	0.14
10	2.0	328	2.28	7.44	2.04	0.12
10	2.8	86.9	3.62	3.01	0.52	0.22
10	2.8	131	3.46	4.8	0.87	0.19
10	2.8	191	3.34	6.79	1.27	0.16
10	2.8	259	3.26	8.68	1.66	0.14
10	2.8	320	3.21	10.37	2.01	0.13
10	4.0	67.2	5.28	3.47	0.41	0.24
10	4.0	132	4.93	6.82	0.86	0.19
10	4.0	198	4.74	9.67	1.27	0.16
10	4.0	256	4.64	13.41	1.80	0.14
10	4.0	327	4.56	16.28	2.23	0.12
10	6.0	68.0	7.79	5.53	0.44	0.24
10	6.0	130	7.42	10.86	0.91	0.19
10	6.0	195	7.13	15.50	1.36	0.16
10	6.0	322	6.80	23.28	2.14	0.12

Table 3.10
Diametral compression data for Avicel circular compacts tested using semicircular platens

Compact diameter (mm)	Zero porosity thickness (mm)	Mean compaction pressure (MPa)	Compact thickness (mm)	Mean breaking load (kg)	Mean tensile strength (MPa)	Porosity
20	2.8	16.5	5.53	4.97	0.28	0.50
20	2.8	29.5	4.55	11.44	0.78	0.39
20	2.8	47.0	4.03	20.15	1.56	0.30
20	2.8	62.5	3.75	27.25	2.27	0.24
10	2.0	77.7	2.58	11.92	2.88	0.23
10	2.0	135.8	2.32	17.09	4.61	0.14
10	2.0	186.3	2.23	17.96	5.02	0.11
10	2.0	226.0	2.20	19.71	5.59	0.10
10	2.8	66.0	3.72	15.05	2.52	0.25
10	2.8	121.2	3.28	23.70	4.51	0.15
10	2.8	198.2	3.10	28.72	5.79	0.11
10	2.8	265.6	3.06	29.63	6.03	0.09
10	2.8	321.4	3.01	30.64	6.34	0.08
10	3.2	51.4	4.53	14.21	1.96	0.29
10	3.2	126.7	3.74	28.16	4.70	0.15
10	3.2	199.8	3.58	33.93	5.91	0.10
10	3.2	249.8	3.52	34.85	6.18	0.09
10	3.2	319.8	3.50	35.28	6.29	0.08
10	3.8	26.8	6.51	7.28	0.70	0.41
10	3.8	35.3	6.01	10.92	1.13	0.36
10	3.8	45.8	5.57	14.63	1.64	0.31
10	3.8	57.3	5.25	18.42	2.19	0.27

Table 3.11
Diametral compression data for Lactose DMV 100 circular compacts tested using semicircular platens

Compact diameter (mm)	Zero porosity thickness (mm)	Mean compaction pressure (MPa)	Compact thickness (mm)	Mean breaking load (kg)	Mean tensile strength (MPa)	Porosity
20	2.8	49.2	3.53	0.63	0.06	0.21
20	2.8	66.7	3.46	1.16	0.10	0.19
20	2.8	79.8	3.40	1.41	0.13	0.17
20	2.8	90.3	3.30	1.76	0.17	0.16
10	2.8	129.4	3.26	1.60	0.31	0.14
10	2.8	193.0	3.16	2.85	0.56	0.11
10	2.8	258.2	3.10	3.82	0.77	0.09
10	2.8	322.6	3.05	4.55	0.93	0.08
10	2.8	363.4	3.04	5.05	1.04	0.07

Table 3.12
Diametral compression data for Anhydrous Lactose DCL 21 circular compacts tested using semicircular platens

Compact diameter (mm)	Zero porosity thickness (mm)	Mean compaction pressure (MPa)	Compact thickness (mm)	Mean breaking load (kg)	Mean tensile strength (MPa)	Porosity
20	2.8	33.7	3.82	2.94	0.24	0.26
20	2.8	48.8	3.67	4.43	0.37	0.23
20	2.8	62.9	3.56	5.83	0.59	0.20
20	2.8	80.9	3.45	7.60	0..69	0.18
20	2.8	90.3	3.37	8.37	0.77	0.17
10	2.8	67.8	3.54	2.92	0.52	0.21
10	2.8	128.0	3.28	6.08	1.16	0.14
10	2.8	186.7	3.14	8.17	1.63	0.11
10	2.8	242.1	3.05	10.32	2.11	0.08
10	2.8	308.0	2.93	15.38	3.28	0.05

method of presenting the data is a plot of tensile strength versus compaction pressure. This was used by Fell and Newton (1970) to demonstrate the linear relationship between the compaction pressure and tensile strength of Lactose compacts. Figures 3.14 to 3.17 illustrate plots of tensile strength, determined by diametral compression, versus compaction pressure for 10mm and 20mm diameter compacts with a theoretical thickness at zero porosity of 2.8mm. The effect of compact thickness on the compaction pressure/tensile strength profiles is illustrated in Figures 3.18 and 3.19. The Lactose DMV 100, Lactose DCL21 and Emcompress compacts appear to show a linear relationship between compaction pressure and tensile strength. The 20mm diameter Avicel compacts also show a linear relationship while the 10mm diameter compacts exhibit a linear response at low compaction pressures with a flattening off of the gradient at higher pressures, indicative of a second mechanism in the compaction process becoming significant.

The regression coefficients obtained using the weighted linear regression are displayed in Table 3.13. For Avicel two sets of values are presented, one for the complete set of results the second for those results in the linear portion of the data at low compaction pressures.

The tensile strength values derived from the axial compression test for 10mm circular compacts of Avicel and Emcompress are summarised in Tables 3.14 and 3.15, and plots of tensile strength versus compaction pressure are illustrated in Figures 3.20 to 3.21. The shapes of the curves are similar to those obtained by diametral compression with the tensile strength of Emcompress compacts appearing to be proportional to the

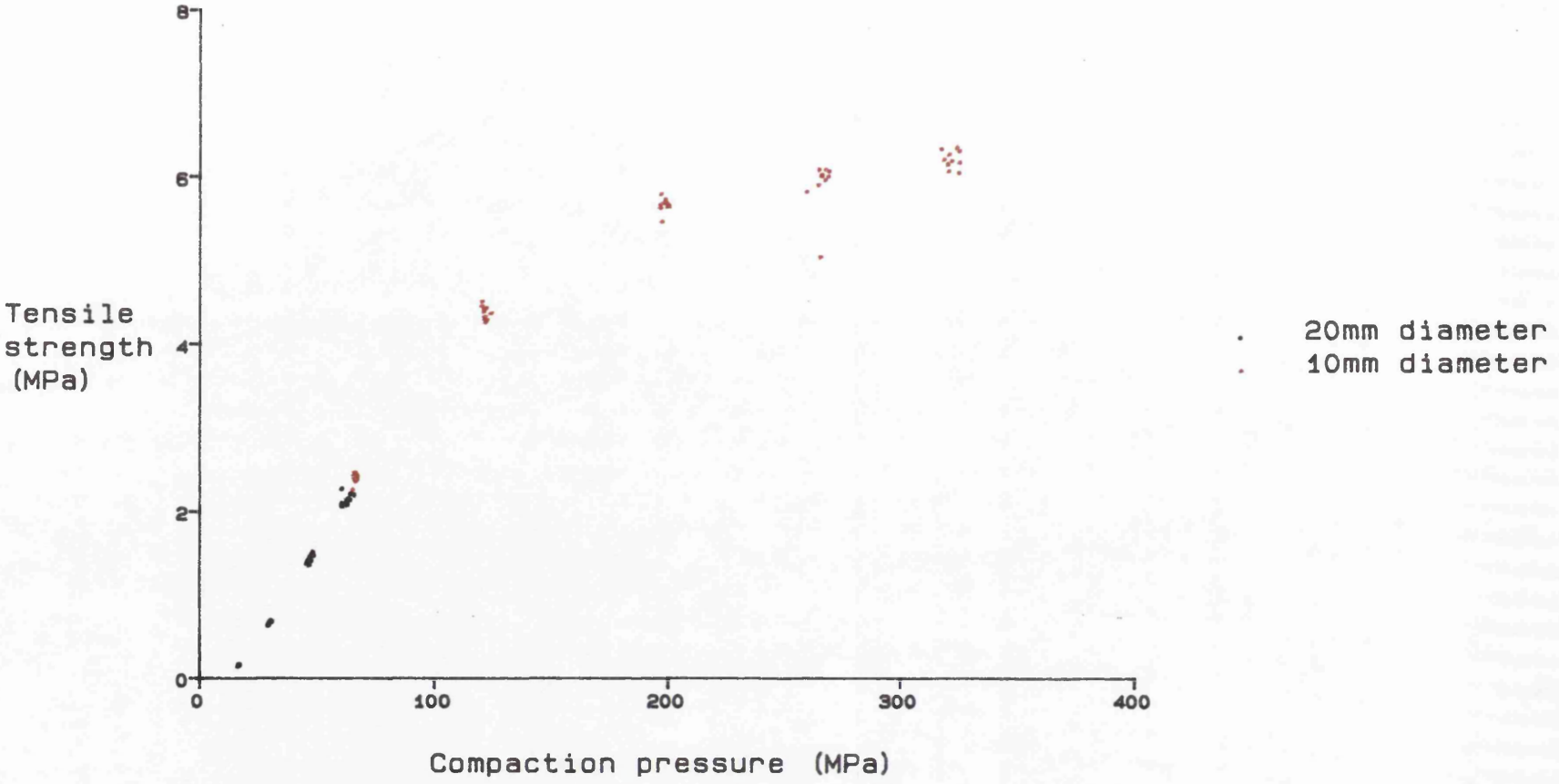

Tensile strength determined by diametral compression

Figure 3.14 Effect of diameter on the compaction pressure/tensile strength profile Avicel circular compacts

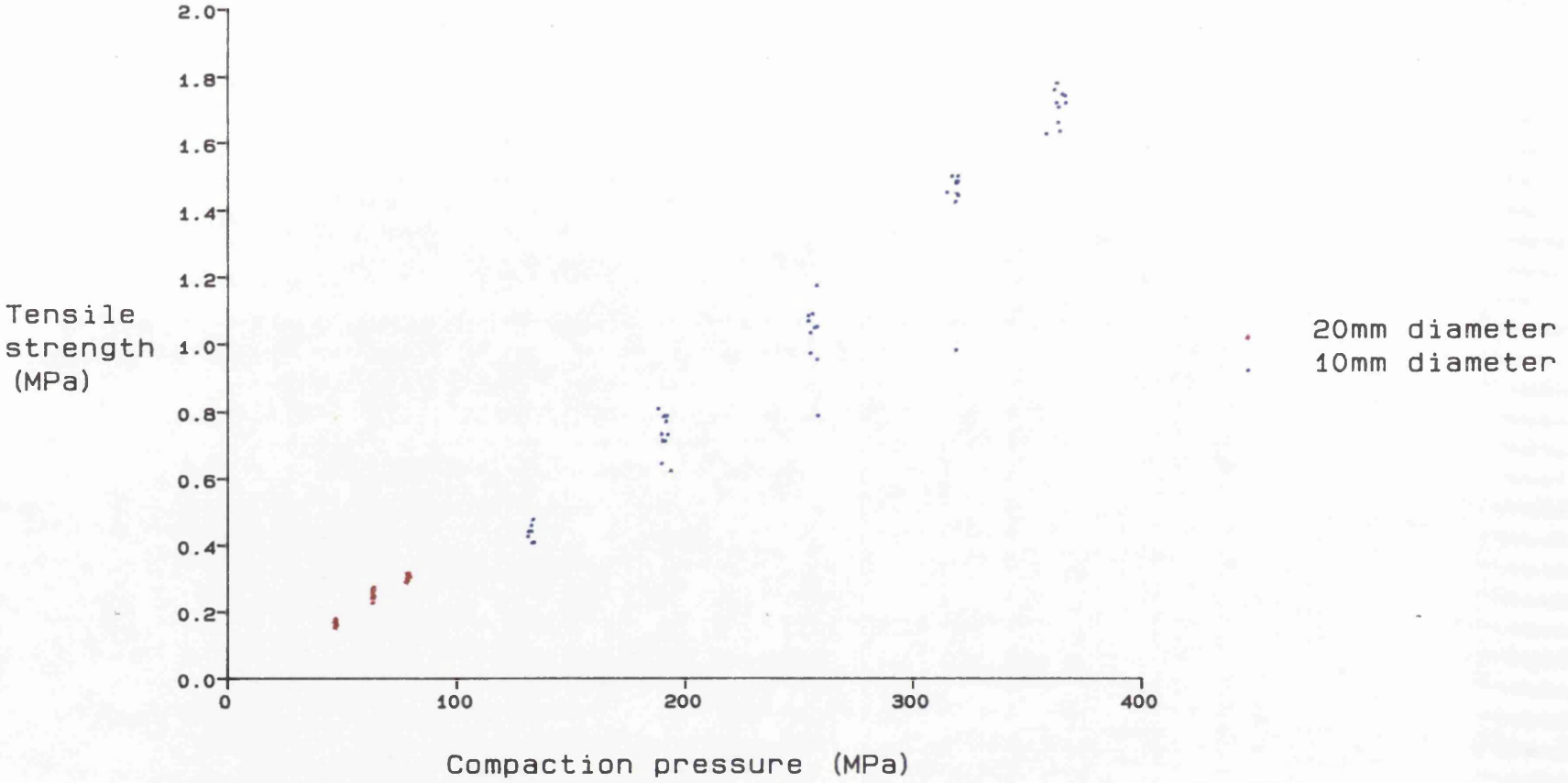

Tensile strength determined by diametral compression

Figure 3.15 Effect of diameter on the compaction pressure/tensile strength profile Emcompress circular compacts

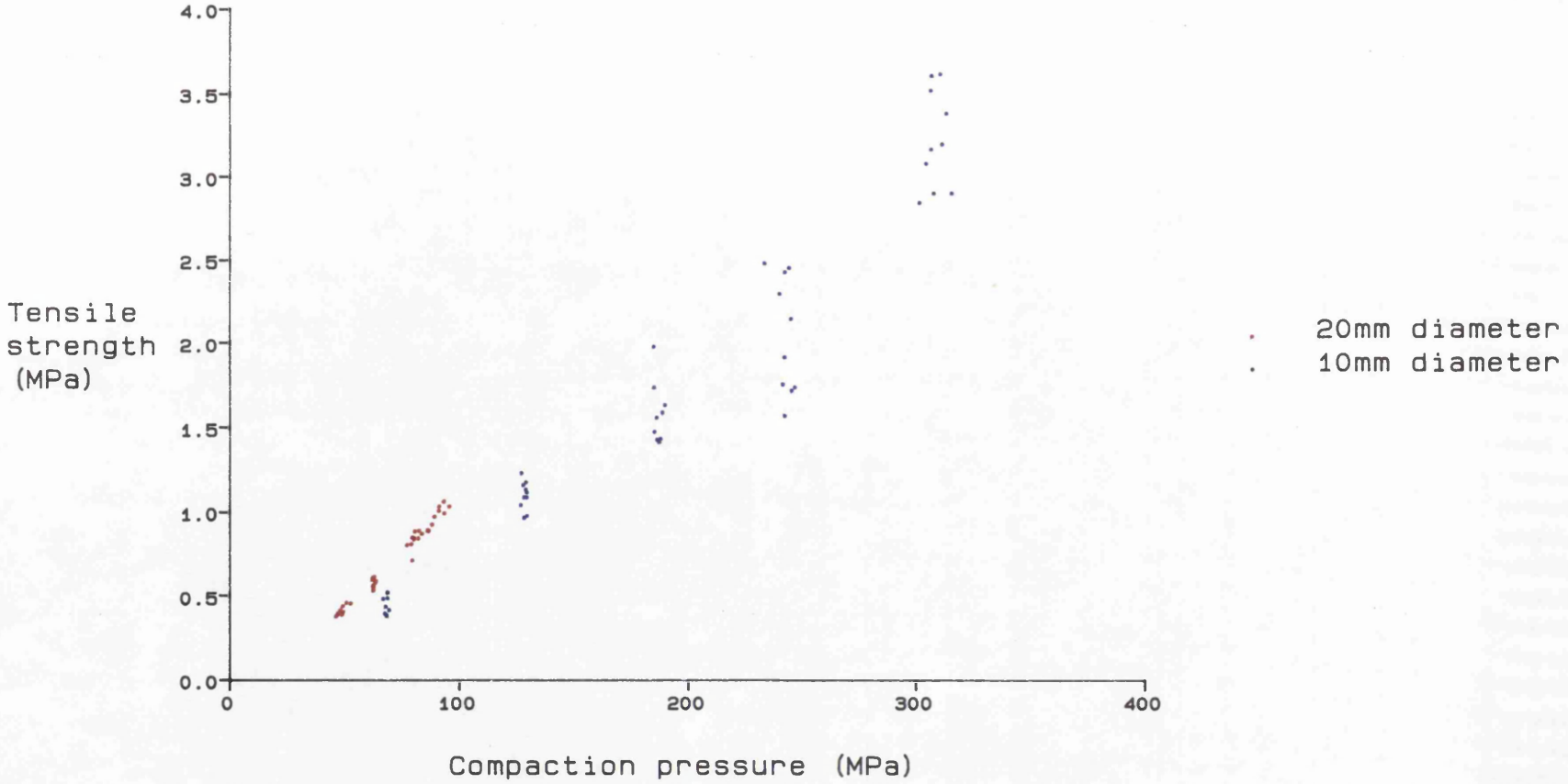

Tensile strength determined by diametral compression

Figure 3.16 Effect of diameter on the compaction pressure/tensile strength profile Anhydrous Lactose DCL21 circular compacts

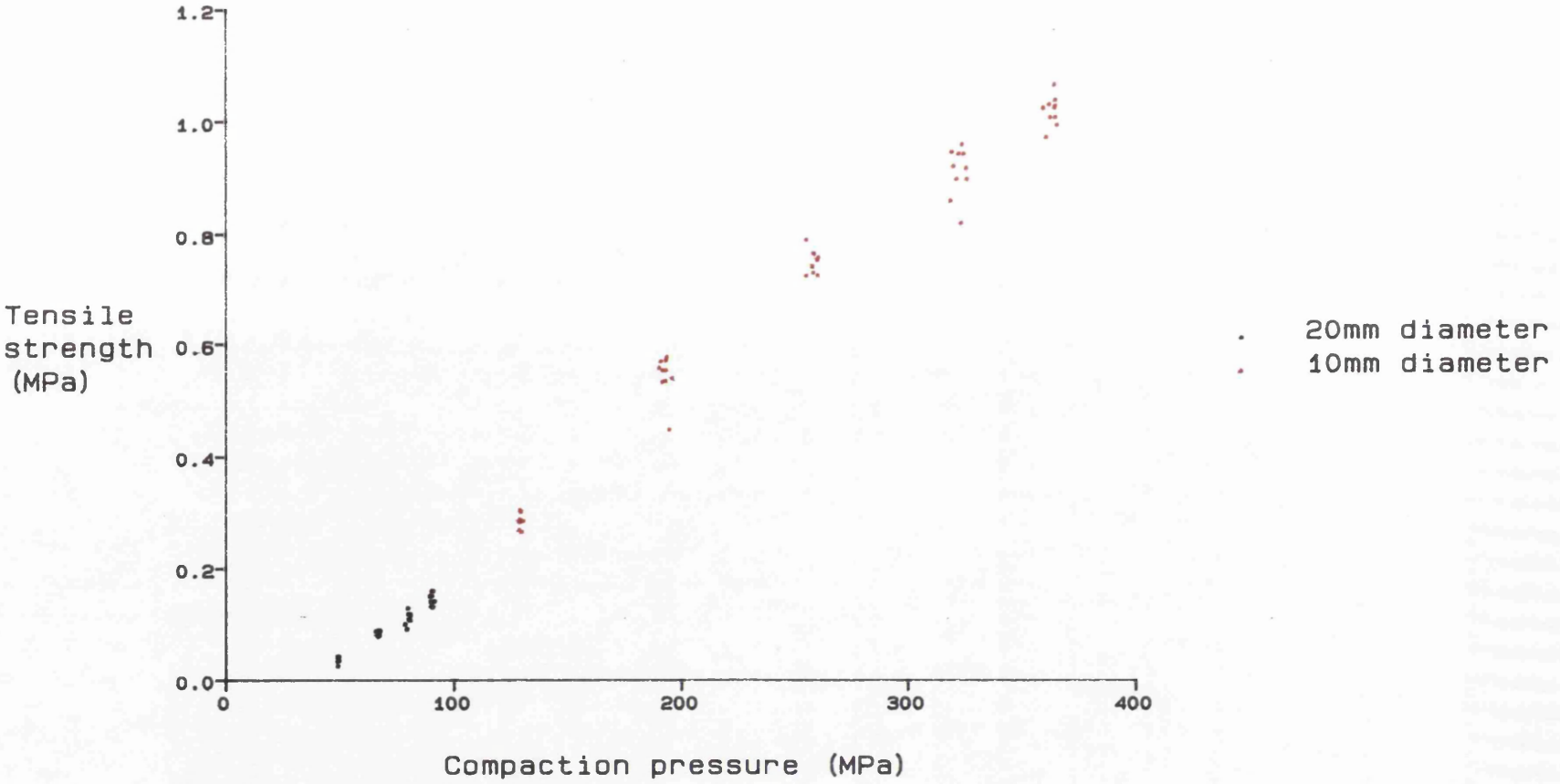

Tensile strength determined by diametral compression

Figure 3.17 Effect of diameter on the compaction pressure/tensile strength profile of Lactose DMV 100 circular compacts

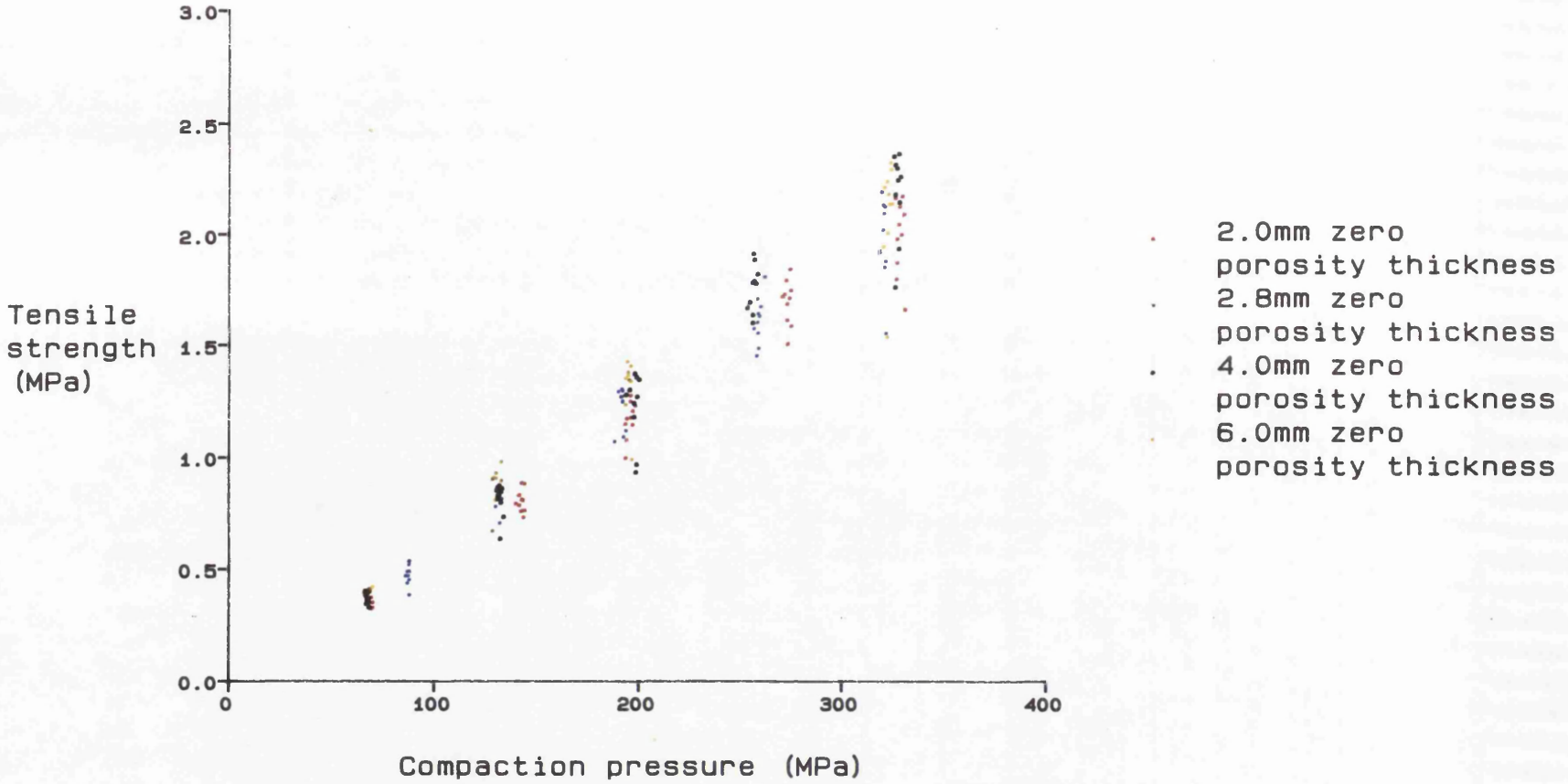

Tensile strength determined by diametral compression using semicircular platens.

Figure 3.18 Effect of compact thickness on the compaction pressure/tensile strength profile of Emcompress circular compacts

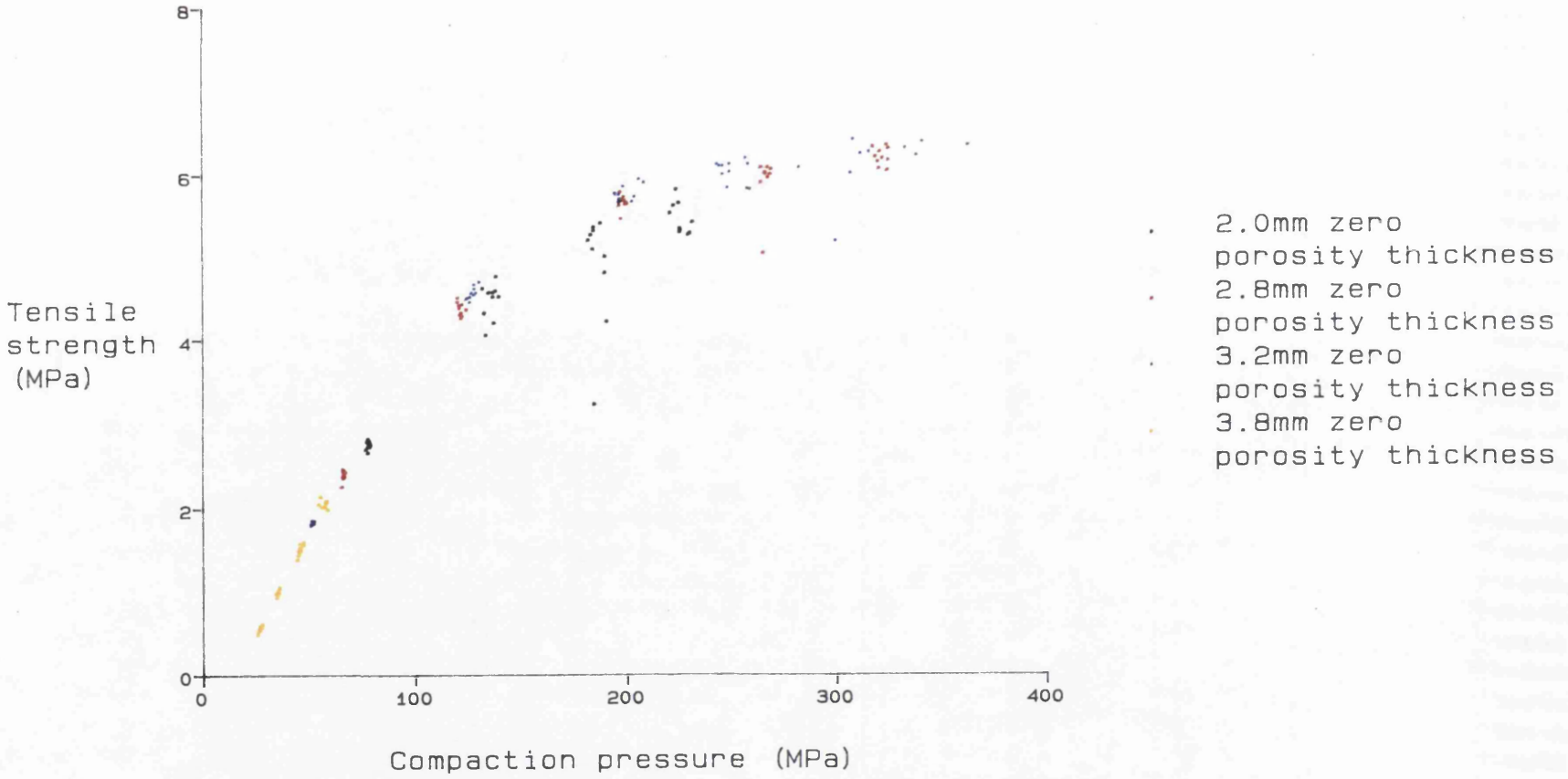

Tensile strength determined by diametral compression using semicircular platens.

Figure 3.19 Effect of compact thickness on the compaction pressure/tensile strength profile of Avicel circular compacts

Table 3.13
Linear regression data for circular compacts tested by diametral compression using semicircular platens[1]

Material	Compact diameter (mm)	Zero porosity thickness (mm)	Intercept (MPa)	Slope	Correlation coefficient
Avicel PH-102	20	2.8	-0.35	6.60×10^{-2}	0.998
	10	2.0	1.40	1.93×10^{-2}	0.974
	10	2.0	0.57[2]	2.97×10^{-2}	0.986
	10	2.8	1.92	1.63×10^{-2}	0.920
	10	2.8	0.16[3]	3.58×10^{-2}	0.997
	10	3.2	0.74	2.47×10^{-2}	0.971
	10	3.2	0.09[4]	3.64×10^{-2}	0.998
	10	3.8	0.59	4.86×10^{-2}	0.997
Emcompress	20	2.8	-6.2×10^{-4}	4.38×10^{-3}	0.983
	10	2.0	0.057	6.48×10^{-3}	0.993
	10	2.8	0.038	6.67×10^{-3}	0.985
	10	4.0	0.071	7.14×10^{-3}	0.991
	10	6.0	0.033	7.03×10^{-3}	0.986
Anhydrous Lactose DCL 21	20	2.8	-0.199	1.05×10^{-2}	0.978
	10	2.8	0.080	9.43×10^{-3}	0.995
Lactose DMV 100	20	2.8	-0.073	2.63×10^{-3}	0.978
	10	2.8	-0.102	3.23×10^{-3}	0.994

1. Linear regression was performed on plots of tensile strength versus compaction pressure.

2. Regression coefficients obtained from compacts prepared using compaction pressures below 150MPa.

3. Regression coefficients obtained from compacts prepared using compaction pressures below 140MPa.

4. Regression coefficients obtained from compacts prepared using compaction pressures below 140MPa.

Table 3.14
Axial compression data for Avicel circular compacts tested using semicircular platens

Compact Diameter (mm)	Zero porosity thickness (mm)	Mean Compaction pressure (MPa)	Compact Thickness (mm)	Mean breaking load (kg)	Mean Tensile strength (MPa)	Porosity
10	2.0	59.2	2.77	23.70	5.35	0.28
10	2.0	141.3	2.31	50.11	13.55	0.14
10	2.0	191.2	2.23	57.72	16.19	0.11
10	2.0	263.6	2.17	64.06	18.39	0.09
10	2.0	345.6	2.17	63.05	18.17	0.09
10	2.8	65.5	3.73	28.03	4.70	0.25
10	2.8	119.4	3.29	46.07	8.74	0.16
10	2.8	202.6	3.10	56.6	11.38	0.10
10	2.8	268.1	3.05	59.25	12.11	0.09
10	2.8	328.8	3.02	59.49	12.29	0.08
10	3.2	62.7	4.33	28.10	4.05	0.26
10	3.2	126.5	3.73	50.90	8.52	0.15
10	3.2	198.8	3.57	60.81	10.63	0.10
10	3.2	264.3	3.54	62.34	10.99	0.09
10	3.2	321.1	3.48	62.77	11.26	0.08
10	3.8	24.6	6.69	9.93	0.93	0.43
10	3.8	35.4	5.99	16.88	1.76	0.36
10	3.8	46.3	5.56	24.08	5.56	0.31
10	3.8	57.4	5.26	29.27	3.48	0.27

Table 3.15
Axial compression data for Emcompress circular compacts tested using semicircular platens

Compact Diameter (mm)	Zero porosity thickness (mm)	Mean Compaction pressure (MPa)	Compact Thickness (mm)	Mean breaking load (kg)	Mean Tensile strength (MPa)	Porosity
10	2.0	73.1	2.63	4.46	1.06	0.23
10	2.0	140.0	2.46	7.91	2.00	0.19
10	2.0	196.1	2.40	12.41	3.23	0.16
10	2.0	270.2	2.32	15.27	4.10	0.14
10	2.0	328.9	2.29	15.91	4.34	0.13
10	2.8	92.5	3.57	5.07	0.89	0.22
10	2.8	131.7	3.46	6.46	1.17	0.19
10	2.8	192.2	3.35	10.12	1.89	0.16
10	2.8	259.3	3.25	13.11	2.51	0.14
10	2.8	321.5	3.21	15.39	2.98	0.13
10	4.0	131.5	4.94	6.55	0.83	0.19
10	4.0	196.7	4.75	9.86	1.29	0.16
10	4.0	263.3	4.63	12.44	1.68	0.14
10	4.0	293.5	4.54	17.10	2.35	0.12
10	6.0	64.7	7.77	4.18	0.34	0.24
10	6.0	131.8	7.43	9.23	0.78	0.18
10	6.0	191.9	7.15	11.27	0.98	0.16
10	6.0	254.2	6.95	17.07	1.53	0.14
10	6.0	291.0	6.80	22.10	2.03	0.12

compaction pressure, while the Avicel compacts display a linear portion followed by a reduction of the gradient.

The axially derived data differs from the diametral compression data in two respects; the values obtained and the effects of compact thickness. Generally the axial compression test produces a larger value for the tensile strength and the variance is also greater. This can be explained by the loading conditions of the test. The test was originally envisaged as a method for testing cubic compacts to assess whether the cube was stronger in any particular dimension. With such a test specimen the loading conditions would be the same for both the diametral and axial compression test, so any differences in the tensile strength values would indicate variability in the structure of the compact. Using 10mm tooling it is not possible to prepare cubic specimens of Avicel and Emcompress on the Manesty F3 press, but it was decided to retain the axial compression test as a method of comparing circular and square compacts. If it is assumed that the contact widths between compacts and platens are similar to those in the diametral compression test a higher tensile strength value should be expected for the axial compression test because the loaded "diameter", in this case the compact thickness, is much reduced. For an isotropic material the ratio of tensile strength values obtained by the two test methods would be greatest for the thinnest compact and would approach unity as the compact thickness approached the compact diameter. Such a trend may have been seen with Avicel compacts (Figure 3.22) if compacts with a zero porosity thickness above 3.8mm could have been prepared. The Emcompress compacts demonstrate a different trend (Figure 3.23) with the

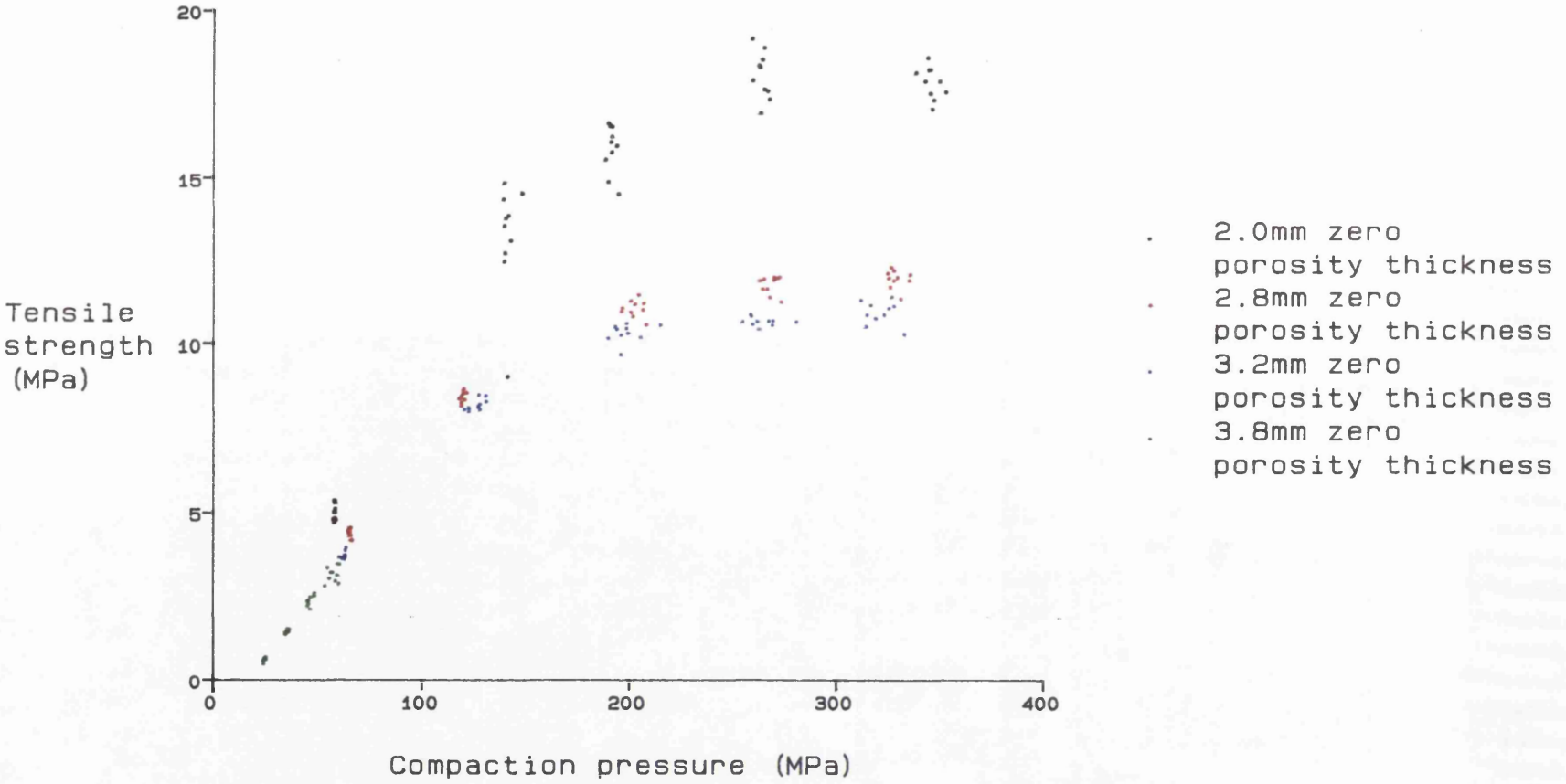

Tensile strength determined by axial compression.

Figure 3.20 Effect of compact thickness on the compaction pressure/tensile strength profile of Avicel circular compacts

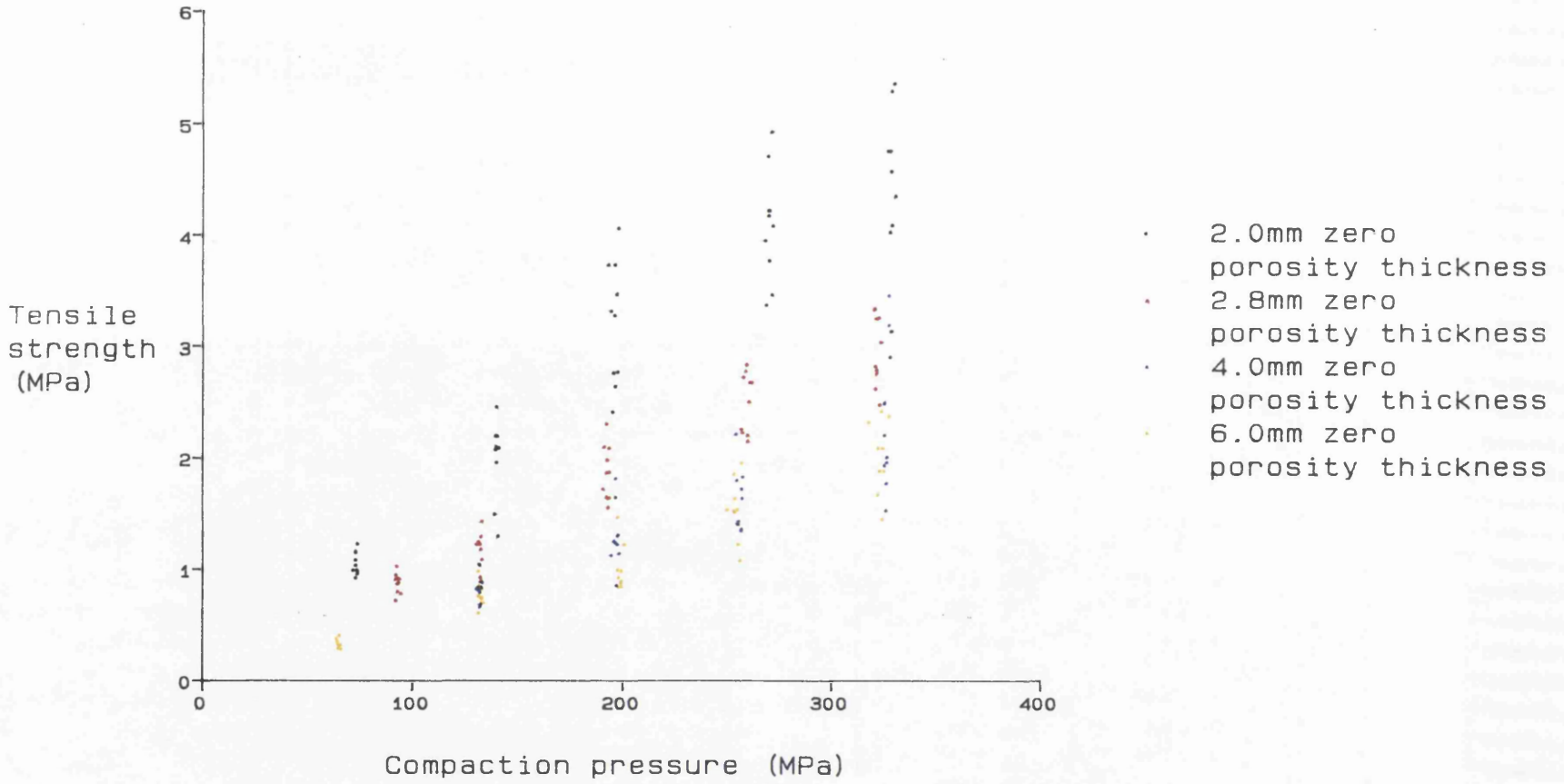

Tensile strength determined by axial compression.

Figure 3.21 Effect of compact thickness on the compaction pressure/tensile strength profile of Emcompress circular compacts

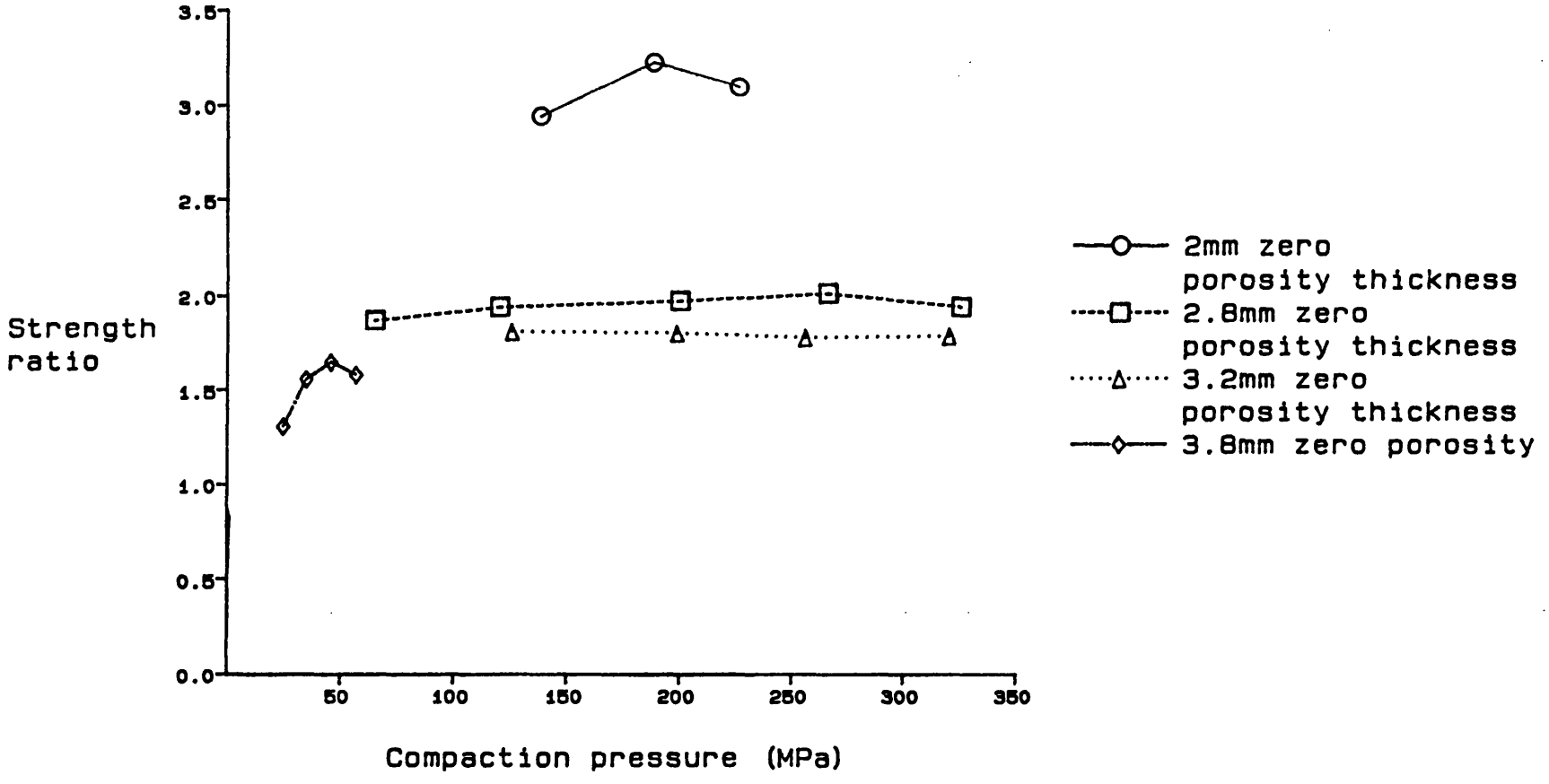

Figure 3.22 Axial compression/diametral compression tensile strength ratios for Avicel 10mm circular compacts

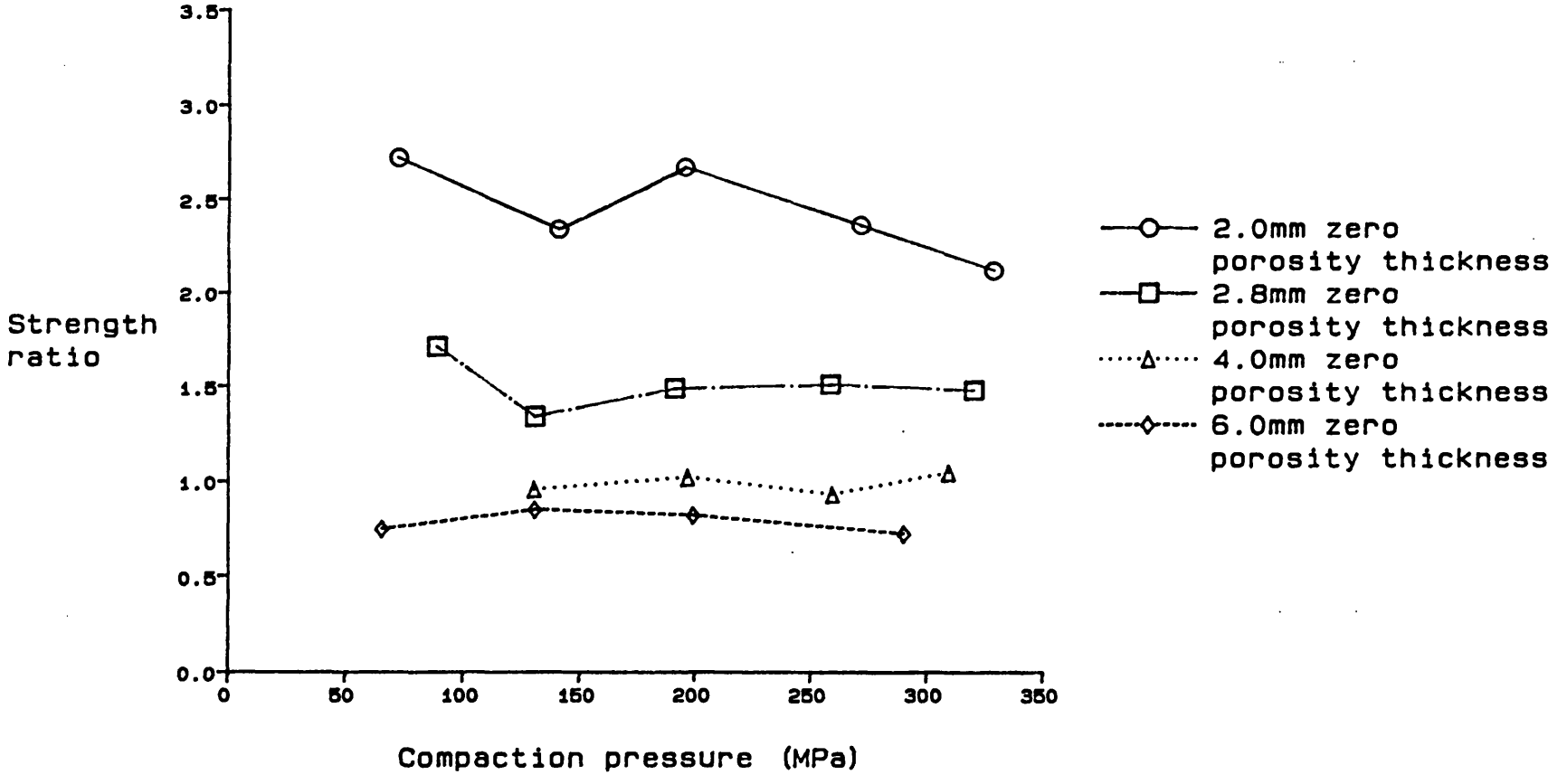

Figure 3.23 Axial compression/diametral compression tensile strength ratios for Emcompress 10mm circular compacts

axial compression values falling below the diametral compression values as the compact thickness approaches 4mm. This trend indicates variation within the Emcompress compact structure. In the axial compression test compressional stresses are applied at 90° to those applied in the diametral compression test, but fracture occurs due to tensile failure along the same plane in each test. The lower results obtained for the Emcompress compacts tested axially may be due to differences in the way the stresses are transmitted through the compact or due to crack initiation occurring at a different point along the failure plane.

3.3.2.2 Effect of porosity on the mechanical properties of compacts

The tensile strength versus compaction pressure profiles are suitable for the comparison of Emcompress compacts as a linear response is obtained. For Avicel, linear regression can only be used to describe the data at low compaction pressures. A number of other relationships were examined to provide a better model for the data. Ryshkewitch (1953) proposed an empirical relationship between tensile strength and porosity;

$$\ln \sigma_f \propto p \qquad (3.3)$$

where p = Porosity

Figures 3.24 to 3.27 illustrate plots of log tensile strength versus porosity for Avicel and Emcompress compacts. Both materials produce linear reponses at the higher porosity values. At low porosities the increase in log tensile strength ceases to be proportional to decreases in porosity. As with the compaction pressure/ tensile strength profiles, the compact thickness does not affect the relationship between porosity and log tensile strength

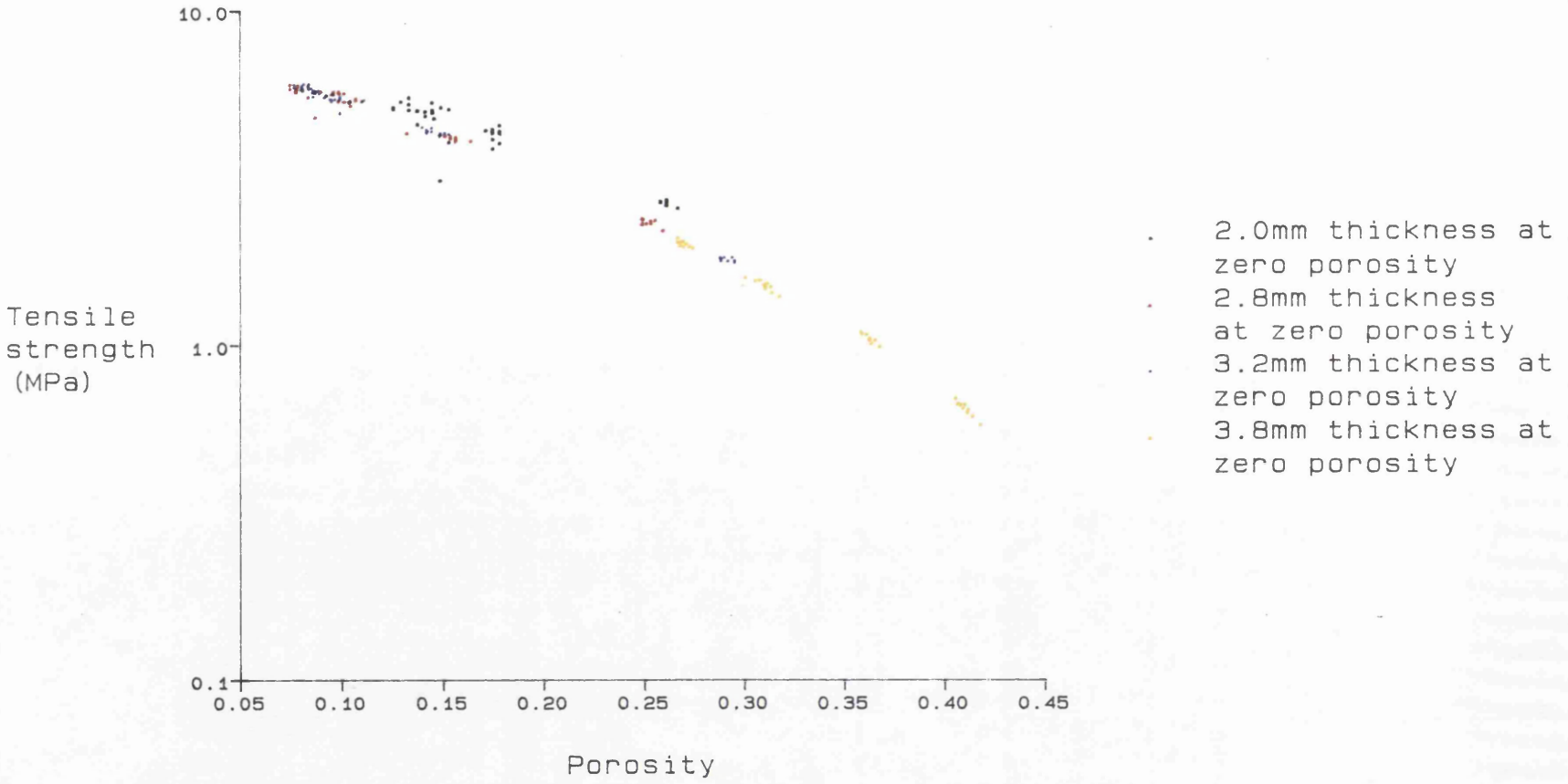

Tensile strength determined by diametral compression using semicircular platens

Figure 3.24 Plot of tensile strength versus porosity for circular Avicel compacts

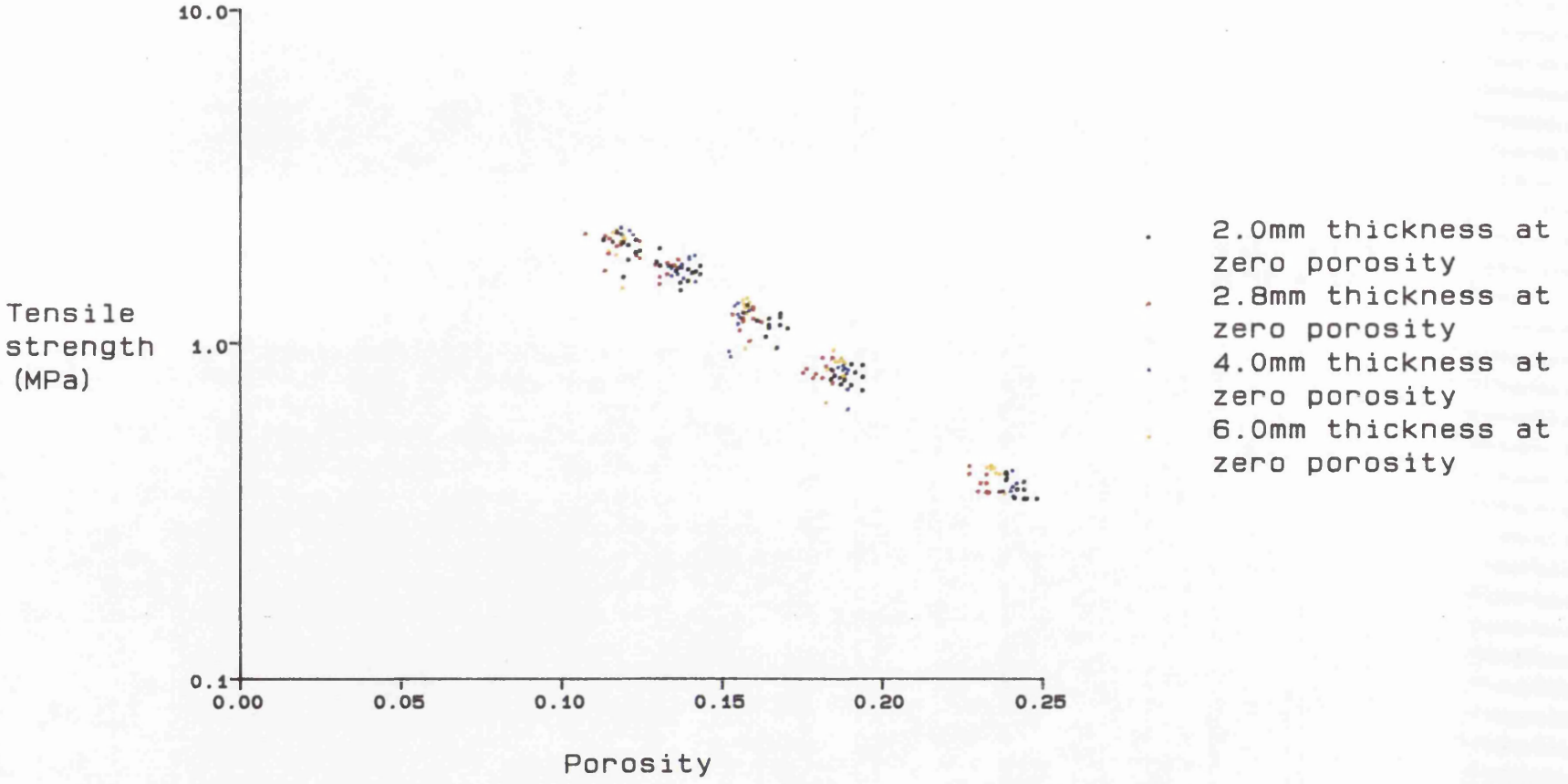

Tensile strength determined by diametral compression using semicircular platens

Figure 3.25 Plot of tensile strength versus porosity for circular Emcompress compacts

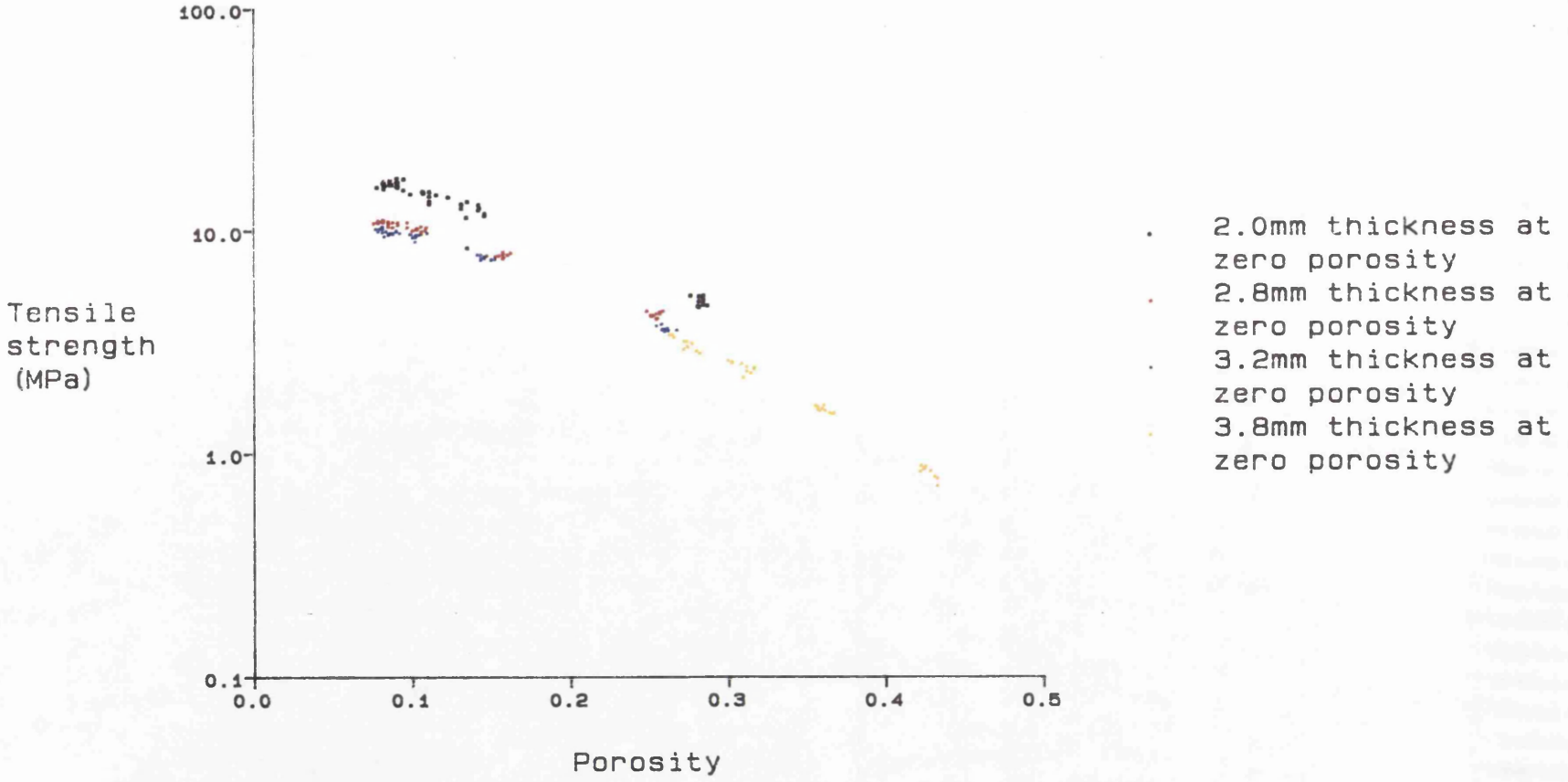

Tensile strength determined by axial compression.

Figure 3.26 Plot of tensile strength versus porosity for circular Avicel compacts

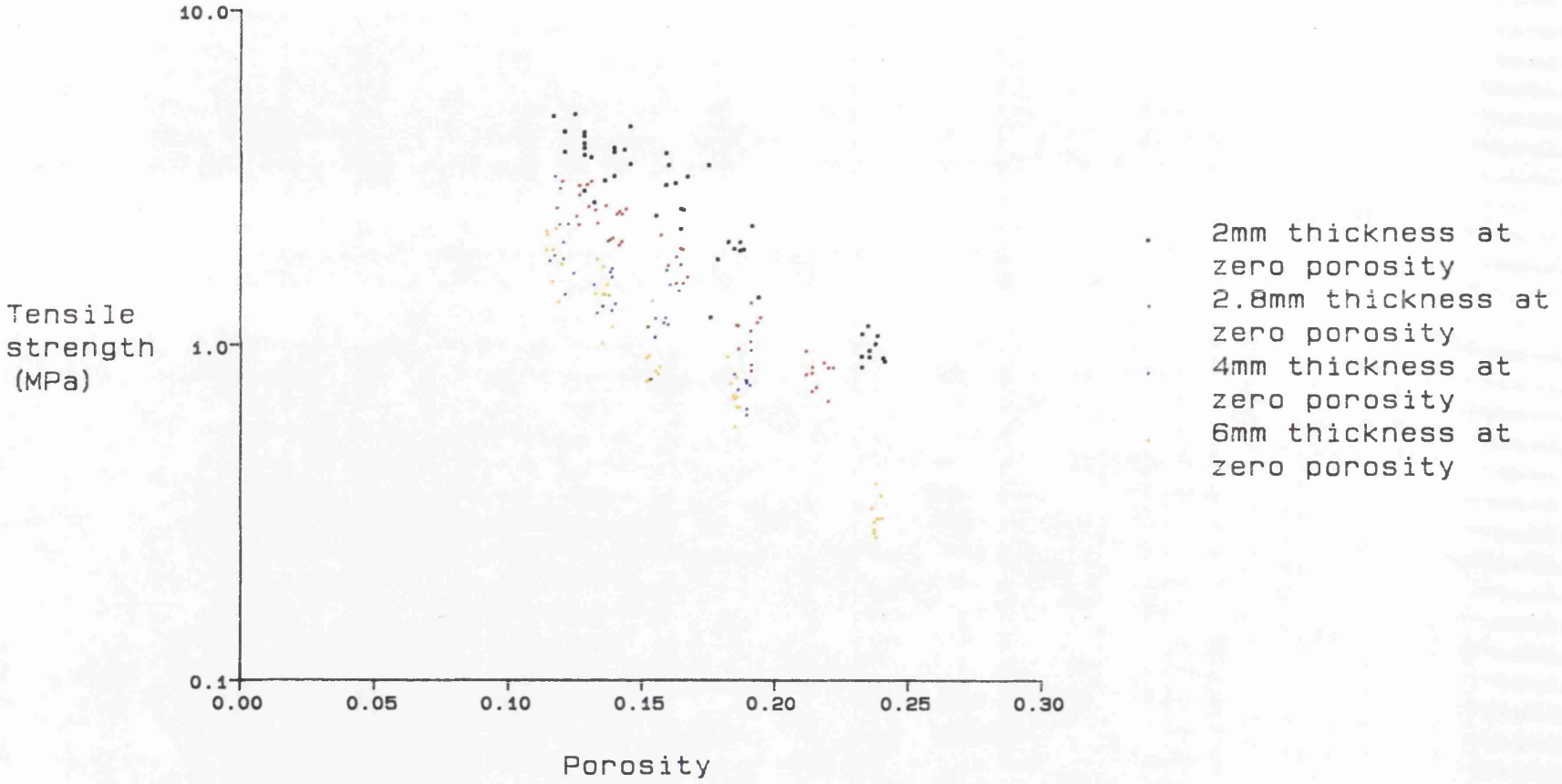

Tensile strength determined by axial compression.

Figure 3.27 Plot of tensile strength versus porosity for circular Emcompress compacts

determined by diametral compression while the axial compression test results are thickness dependent. For any given material porosity is a measure of the degree of particle contact and therefore the degree of bonding present in a compact. Therefore for a given porosity the compacts should have the same tensile strength. If one group of compacts has a lower strength than another of the same porosity this indicates the presence of a different distribution of flaws within the lower tensile strength group. Thus a comparison of the tensile strength with porosity may be of interest when comparing circular compacts with shapes.

The compact shape may also affect the densification process, which has been described by the Heckel (1961) equation:

$$\ln \frac{1}{1-D_r} = K_H C_P + c \qquad (3.4)$$

where D_r = relative density = Bulk density/True density

C_p = compaction pressure

K_H and c are constants

This equation is not derived from theoretical considerations of the compaction process, but is essentially a curve fitting equation that provides a reasonable correlation with the observed facts over a wide range of pressures (Sheikh-Salem and Fell 1981). Heckel considered that the constant, K_H, representing the slope of the function, could be correlated with the yield strength of the material being compressed. The so-called constant c is of doubtful constancy, and appears often to be a function of the pressure range used. A plot of compaction pressure versus $\ln(1 / 1 - D_r)$

should produce a linear relationship above the yield pressure.

The Heckel plot is usually calculated from the relative densities of the materials under pressure. As the single punch machine used in this study was not fitted with displacement transducers the relative densities of compacts under pressure could not be determined. Instead the relative densities were calculated from compact thicknesses measured immediately after ejection. Heckel plots of Avicel and Emcompress compacts based upon the densities of tablets after ejection from the die are shown in Figures 3.28 and 3.29.

The interpretation of the curves is restricted by the limited number of data points. The relative density changes at higher pressures are also too small to be measured accurately and this would limit the value of preparing curves with a greater number of data points. The curves do illustrate some general characteristics of the relationship between density and compaction pressure;

1. For both excipients there is a large relative density change prior to coherent compacts being formed.

2. There is little change in relative density between the pressure at which a compact can be produced and the maximum pressure attained.

3. The relative density produced by a given pressure is not dependent on the compact thickness.

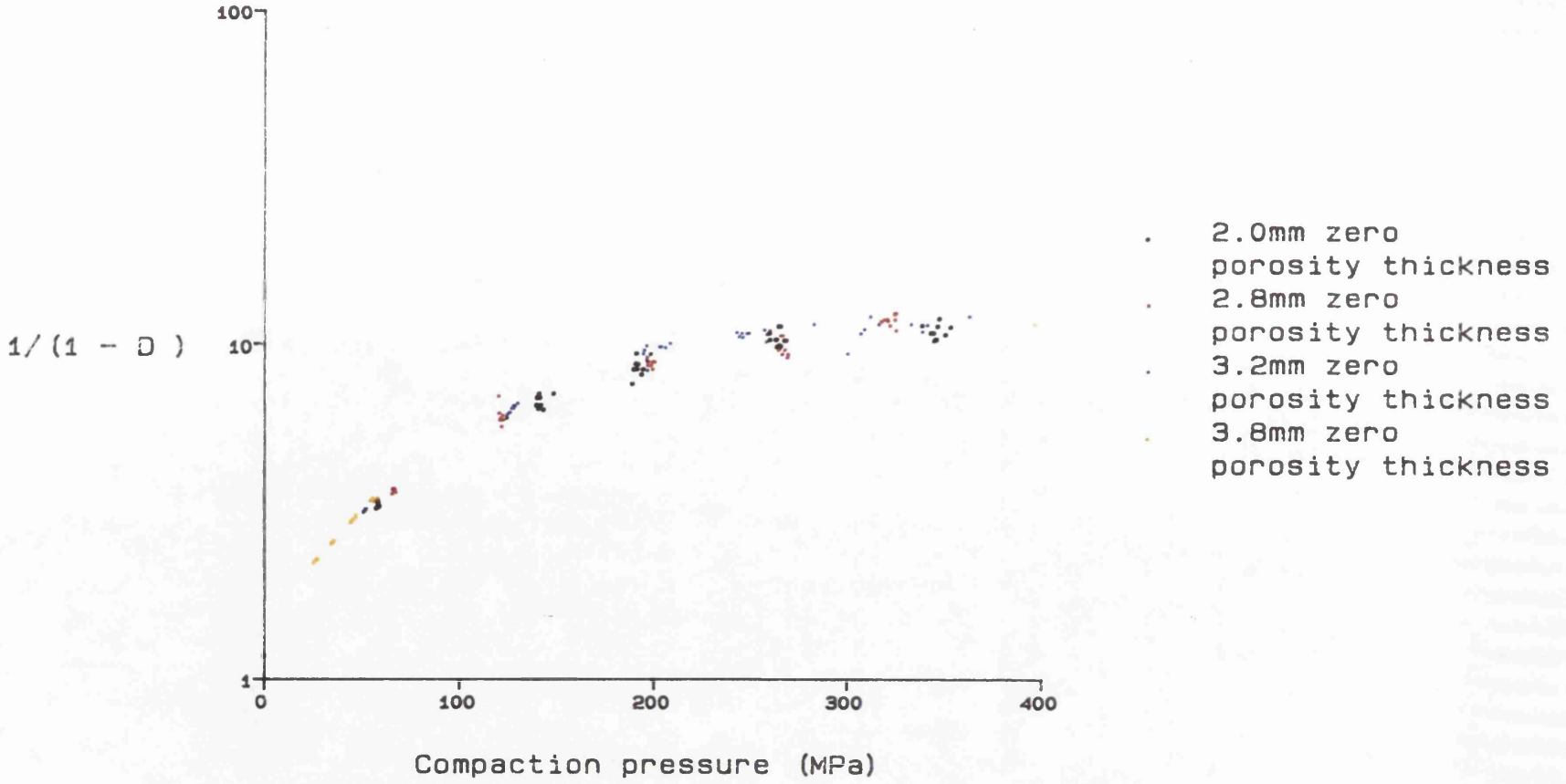

Figure 3.28 Heckel plot for Avicel 10mm diameter circular compacts

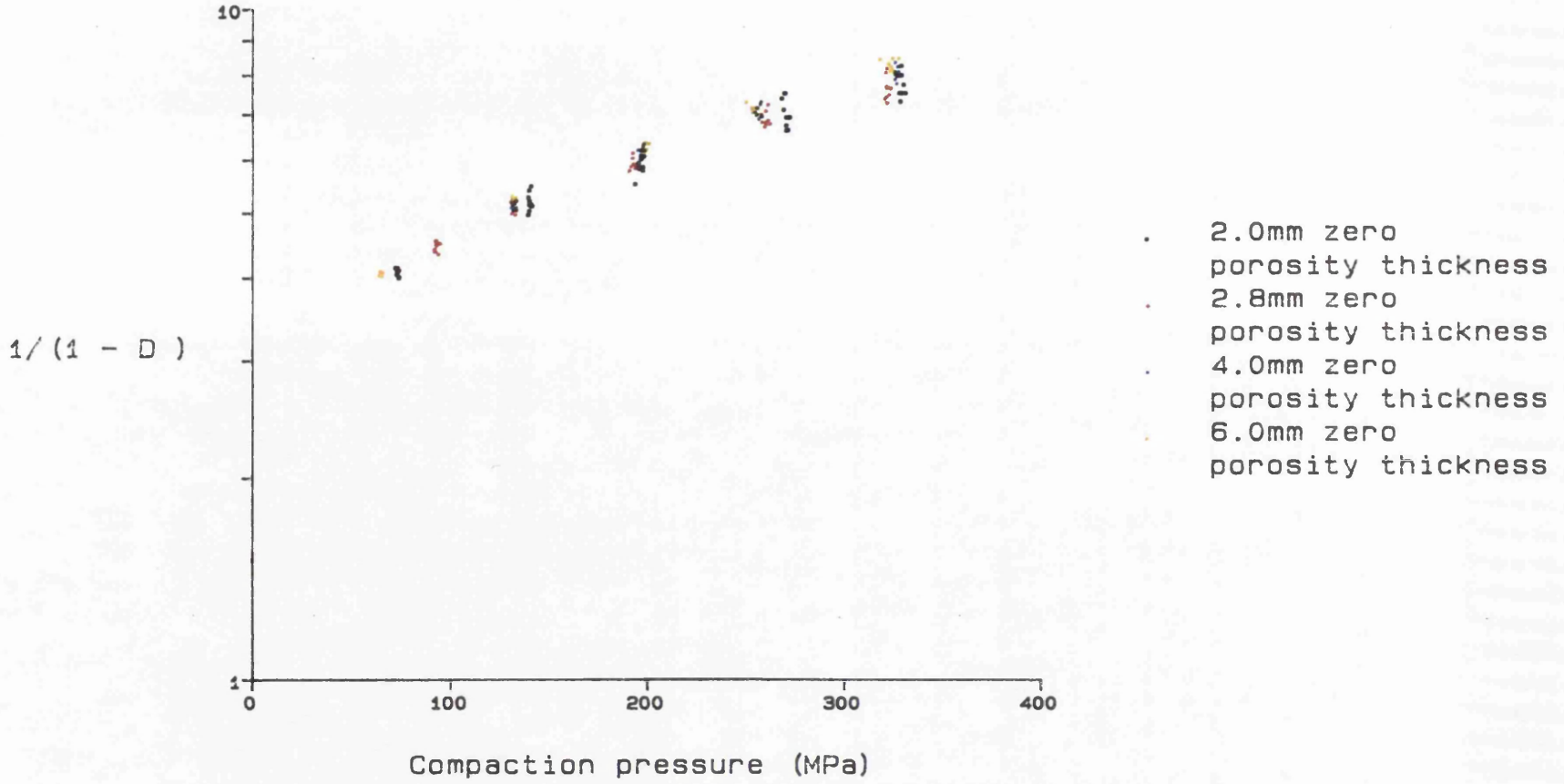

Figure 3.29 Heckel plot for Emcompress 10mm diameter circular compacts

3.3.3 Comparison of the compaction properties of circular and shaped compacts

3.3.3.1 Compact appearance

Square and hexagonal compacts having theoretical zero porosity thicknesses of 2mm and 2.8mm could be produced satisfactorily with all the materials tested. Square compacts of Emcompress could not be prepared with zero porosity thicknesses in excess of 2.8mm. On ejection the lower surface of such compacts had a characteristic pattern with the four corners displaying curved faults (Figure 3.30). These areas became detached on handling.

3.3.3.2 Diametral compression

Figures 3.31 to 3.41 illustrate the compaction pressure/tensile strength profiles of 10mm and 20mm circular, square and hexagonal compacts of Avicel PH-102, Lactose DMV 100, Lactose DCL 21 and Emcompress. These results indicate that the shape does not affect the tensile strength, determined by diametral compression, of compacts prepared using the same compaction pressure. Analysis of covariance indicated that there were no significant differences between the different shapes of compact for each excipient compared. This method could only be used to compare compacts of Avicel produced in the range of compaction pressures that produced a linear response. Above this level there is evidence that the maximum tensile stress is greater for square and hexagonal compacts than for circular compacts (Figures 3.35 to 3.37). Similarly Figures 3.42 to 3.45 illustrating log tensile strength versus porosity, and Figures 3.46 to 3.47 showing Heckel plots, demonstrate no difference between shapes.

Figure 3.30
Appearance of square compacts of Emcompress with theoretical zero porosity of 4mm prepared on the single punch machine

a. Appearance on ejection

b. Appearance after handling

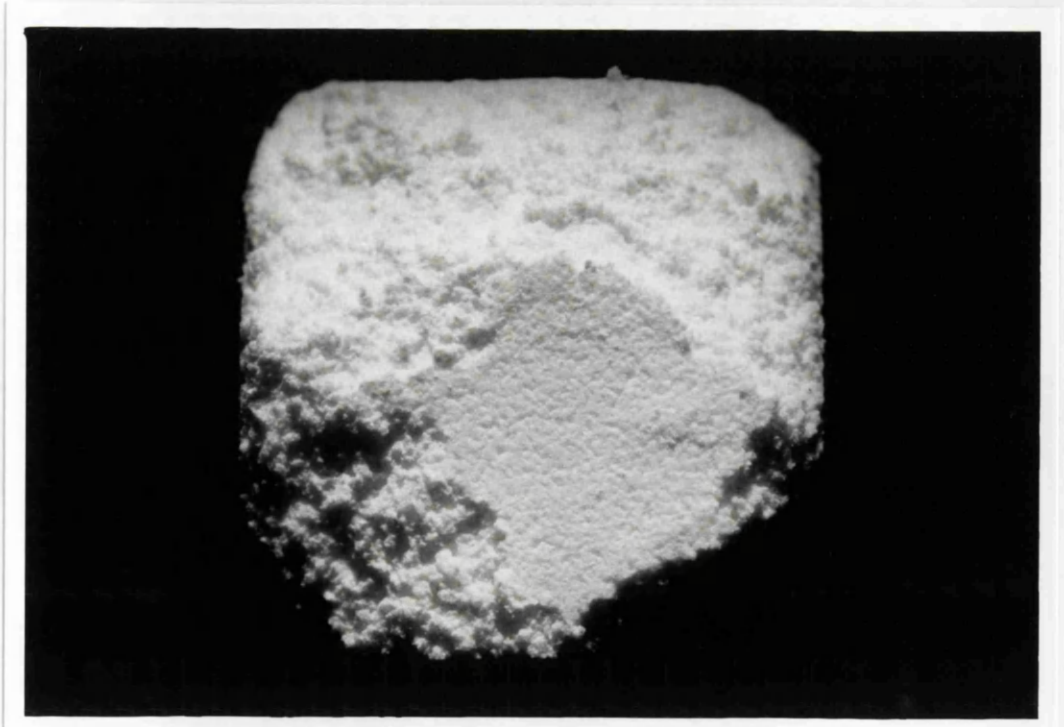

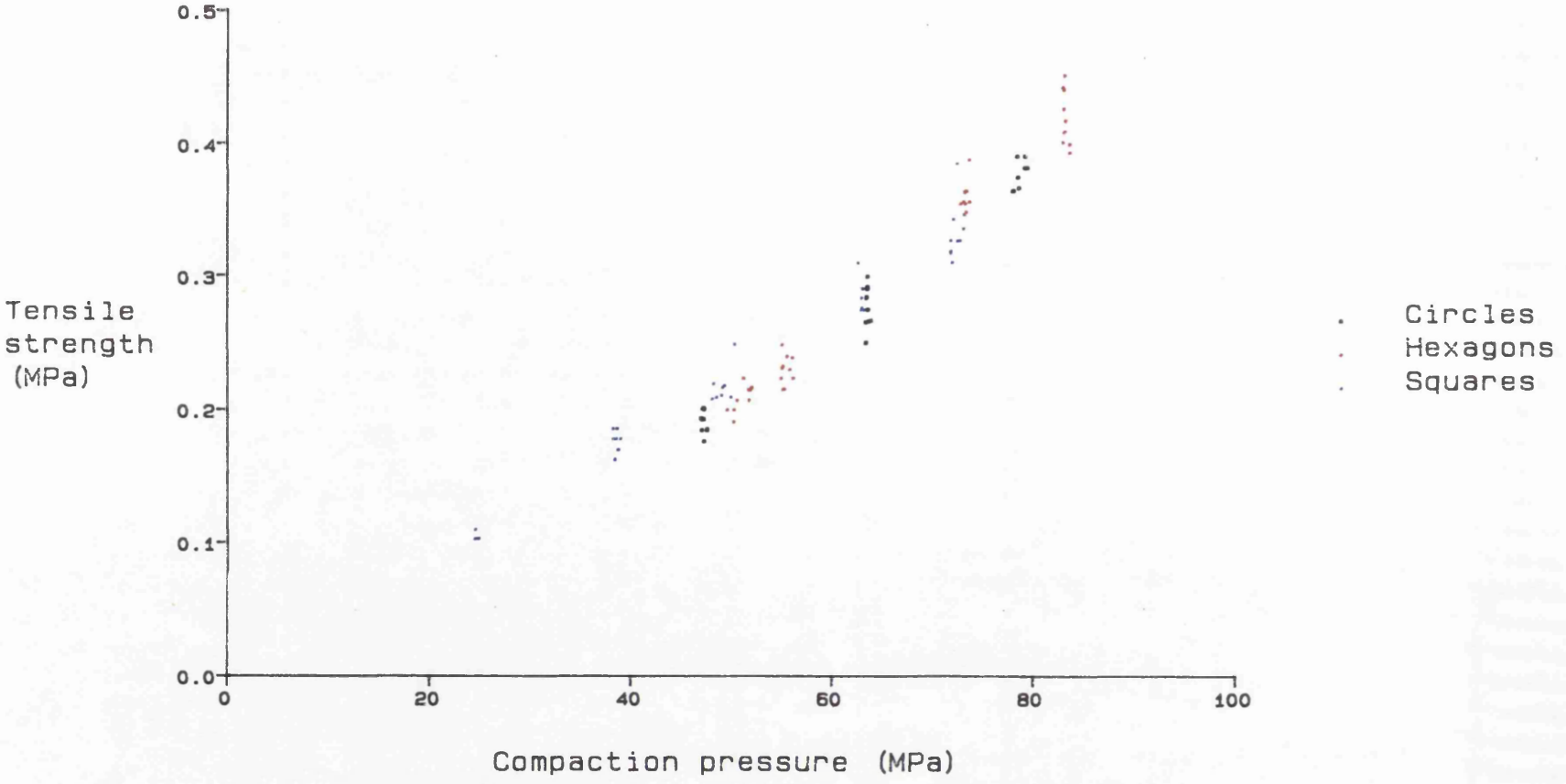

Tensile strength determined by diametral compression using semicircular platens.
Theoretical thickness of compacts at zero porosity = 2.8mm.

Figure 3.31 Effect of shape on the compaction pressure/ tensile strength profile of Emcompress 20mm compacts

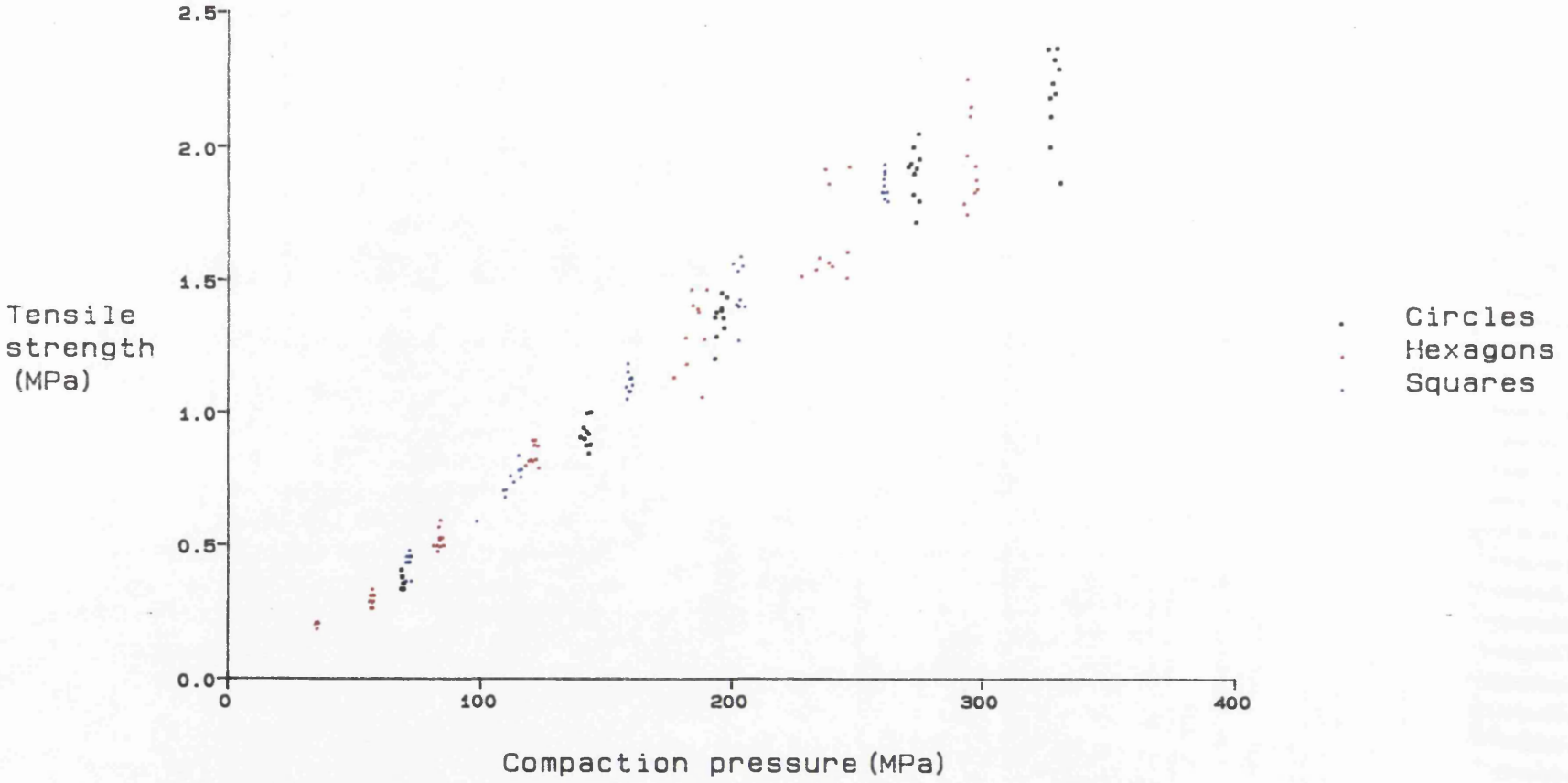

Tensile strength determined by diametral compression using semicircular platens.
Theoretical thickness of compacts at zero porosity = 2.0mm.

Figure 3.32 Effect of shape on the compaction pressure/ tensile strength profile of Emcompress 10mm compacts

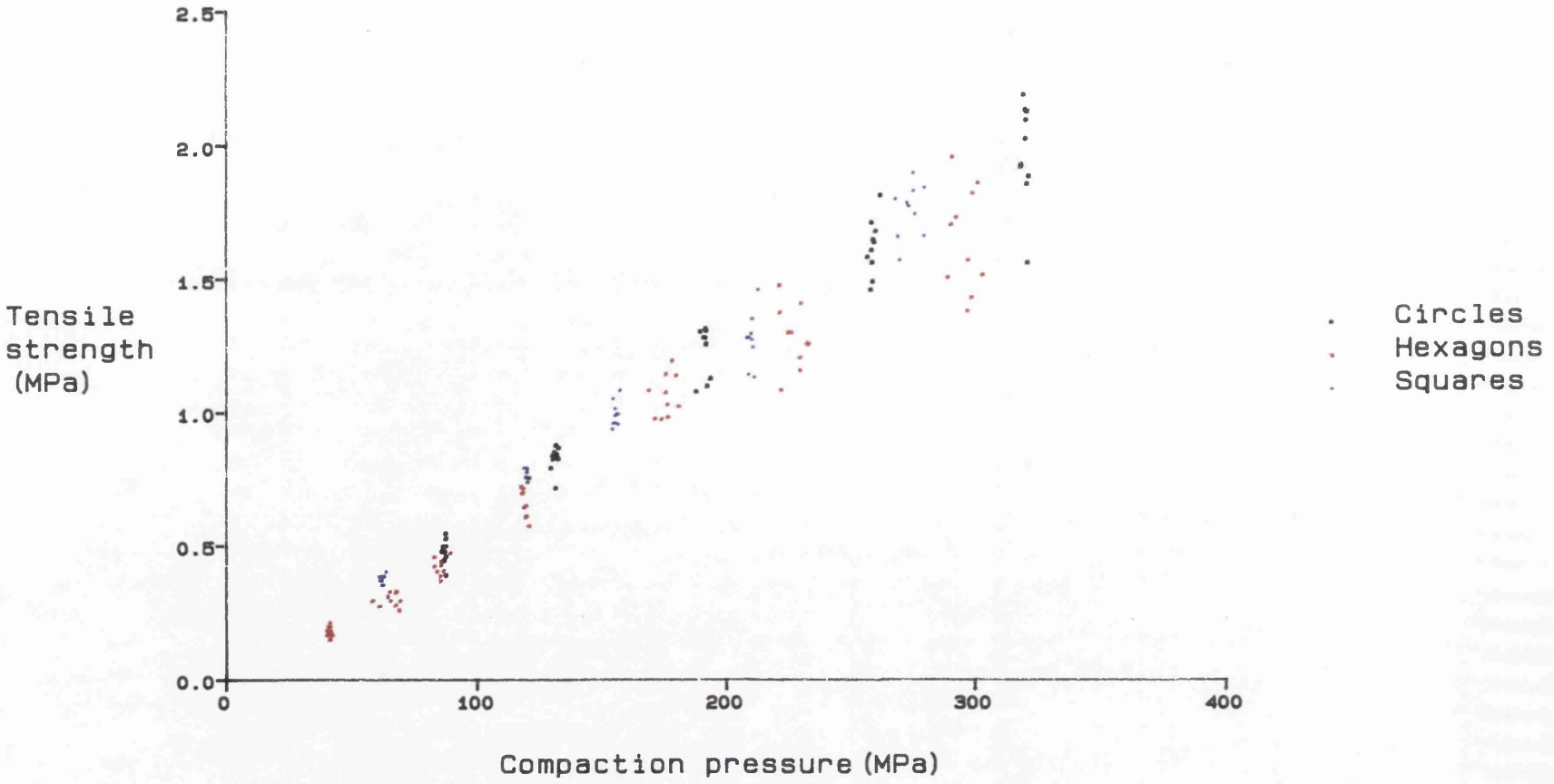

Tensile strength determined by diametral compression using semicircular platens.
Theoretical thickness of compacts at zero porosity = 2.8mm.

Figure 3.33 Effect of shape on the compaction pressure/ tensile strength profile of Emcompress 10mm compacts

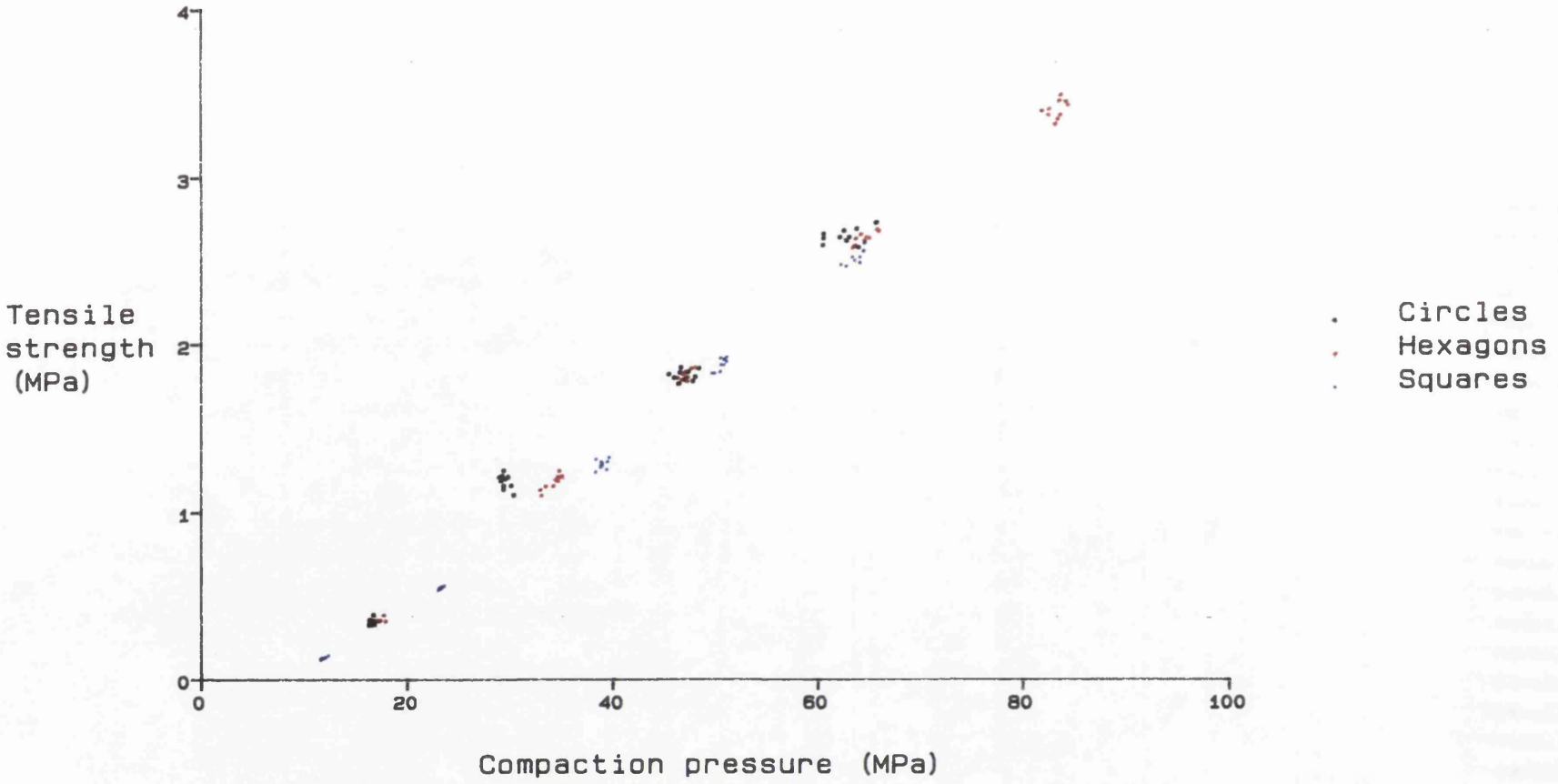

Tensile strength determined by diametral compression using semicircular platens.
Theoretical thickness of compacts at zero porosity = 2.8mm.

Figure 3.34 Effect of shape on the compaction pressure/ tensile strength profile of Avicel 20mm compacts

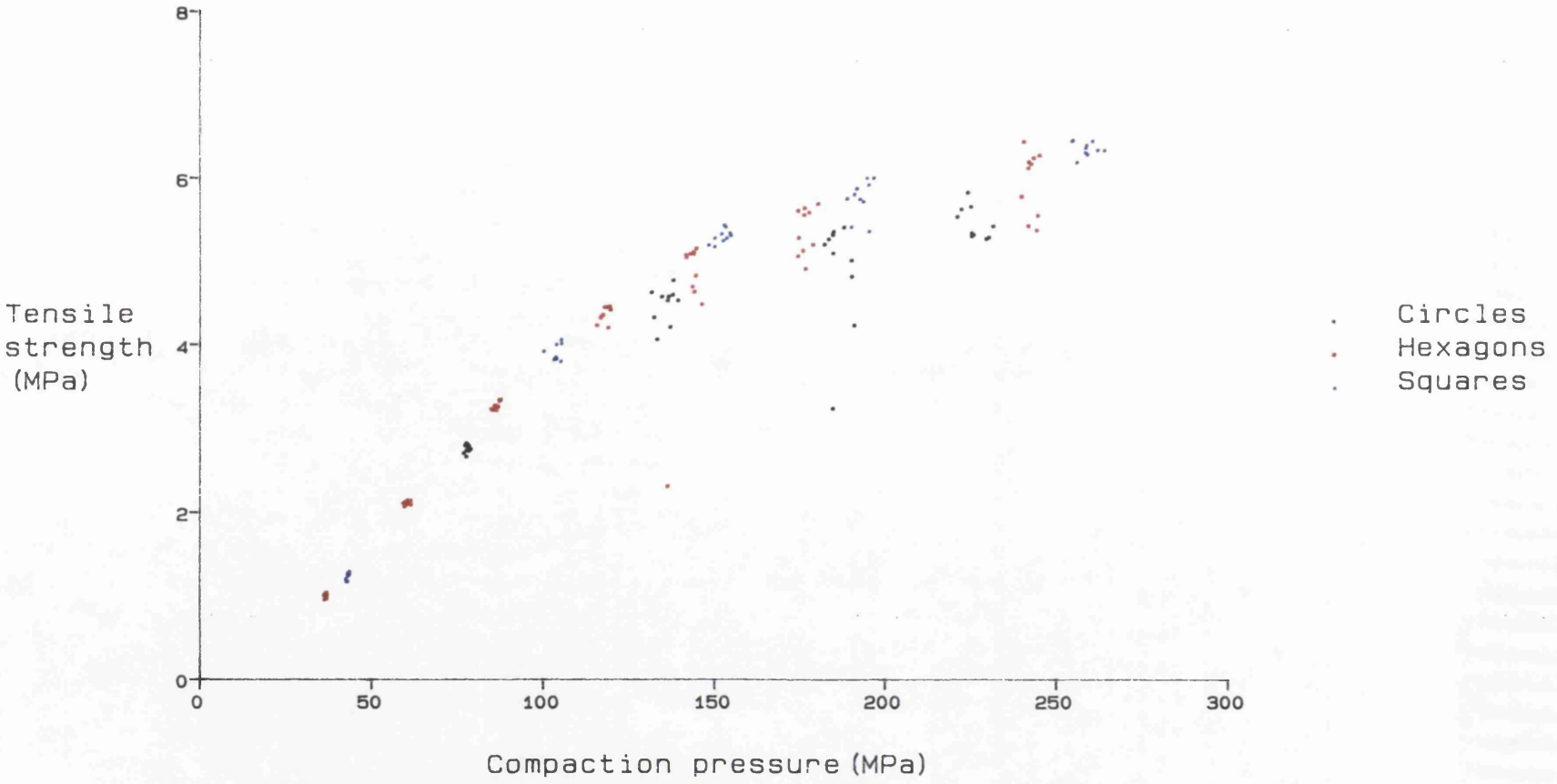

Tensile strength determined by diametral compression using semicircular platens.
Theoretical thickness of compacts at zero porosity = 2.0mm.

Figure 3.35 Effect of shape on the compaction pressure/tensile strength profile of Avicel 10mm compacts

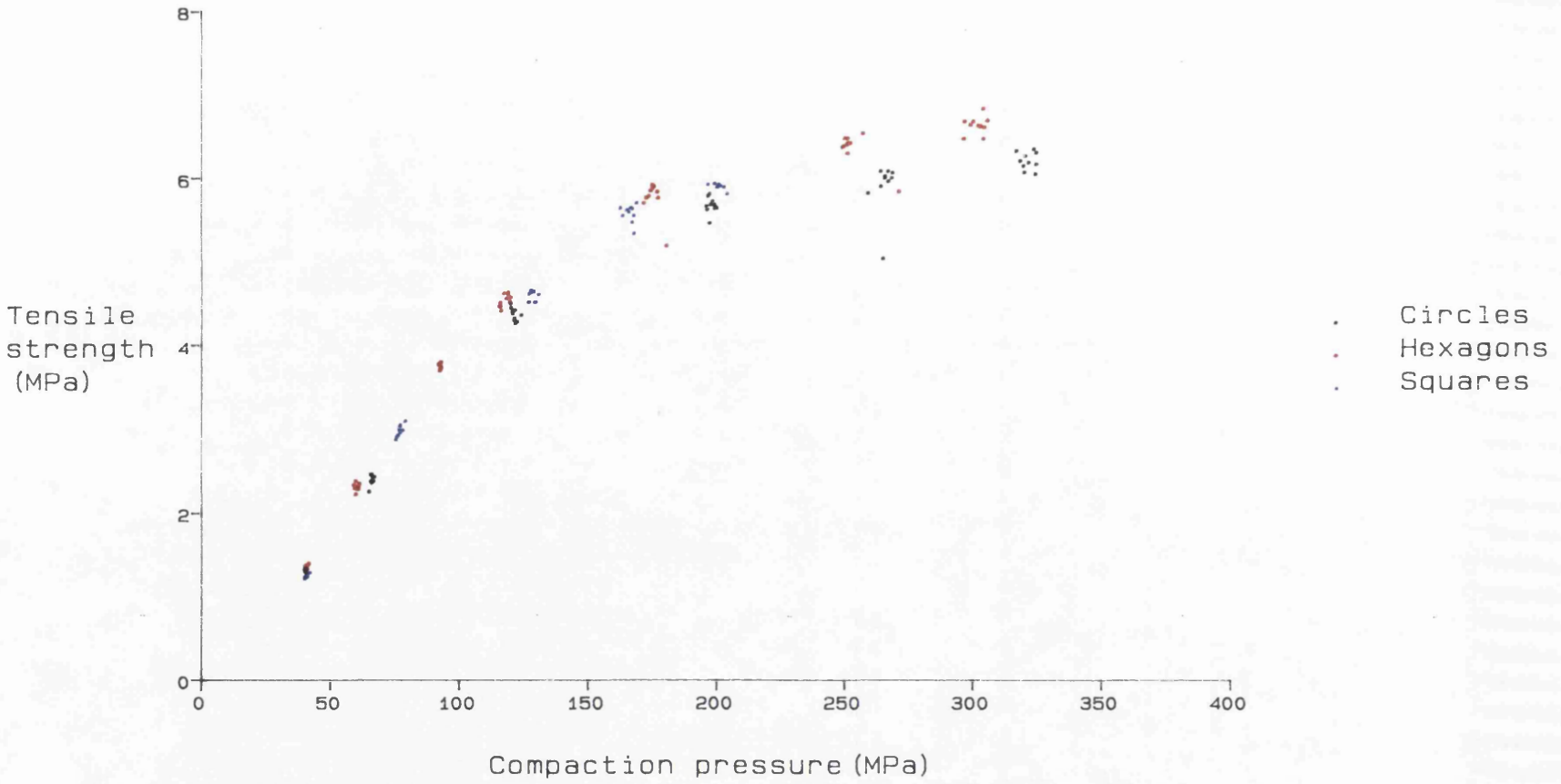

Tensile strength determined by diametral compression using semicircular platens.
Theoretical thickness of compacts at zero porosity = 2.8mm.

Figure 3.36 Effect of shape on the compaction pressure/ tensile strength profile of Avicel 10mm compacts

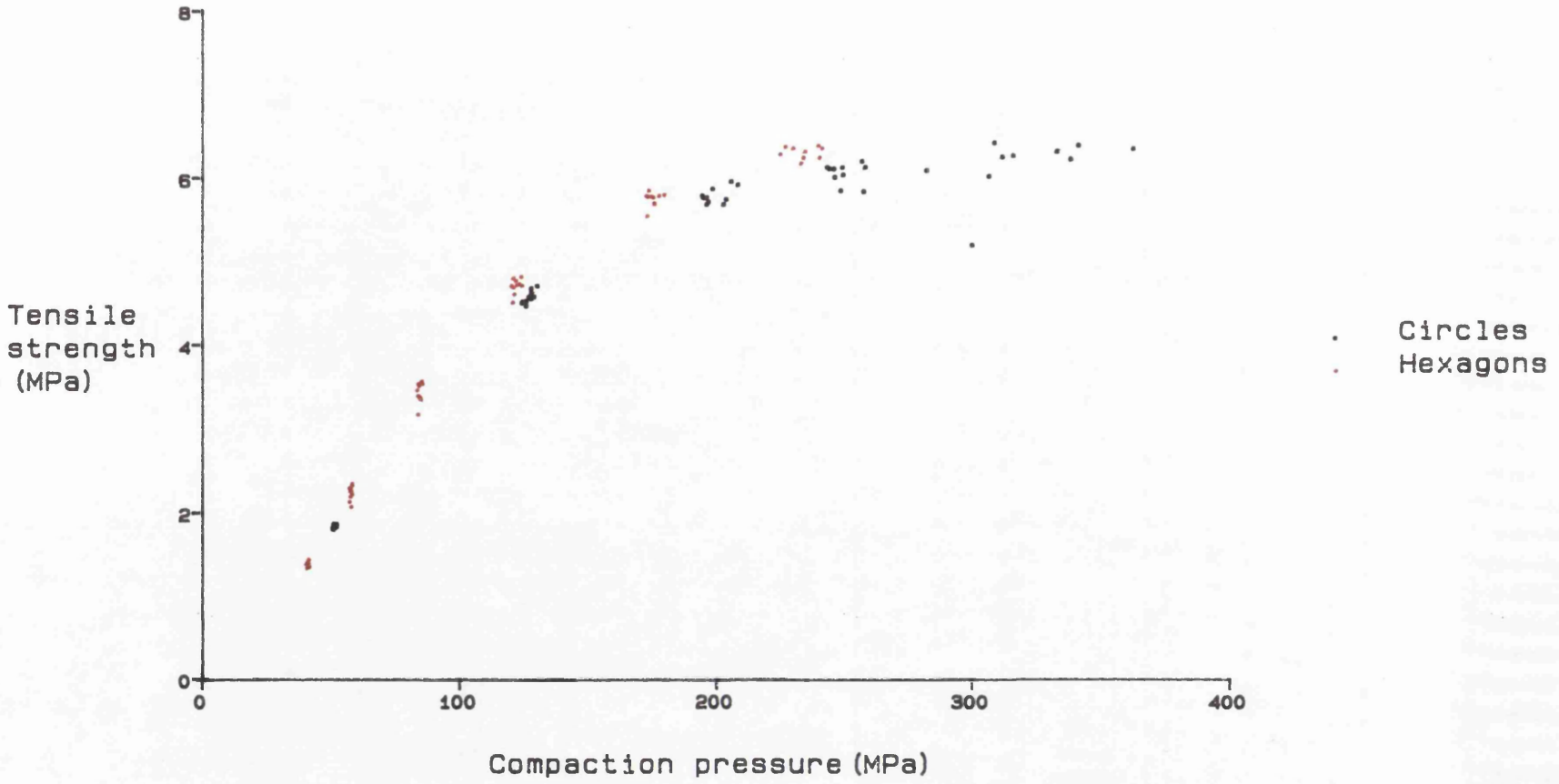

Tensile strength determined by diametral compression using semicircular platens.
Theoretical thickness of compacts at zero porosity = 3.2mm.

Figure 3.37 Effect of shape on the compaction pressure/ tensile strength profile of Avicel 10mm compacts

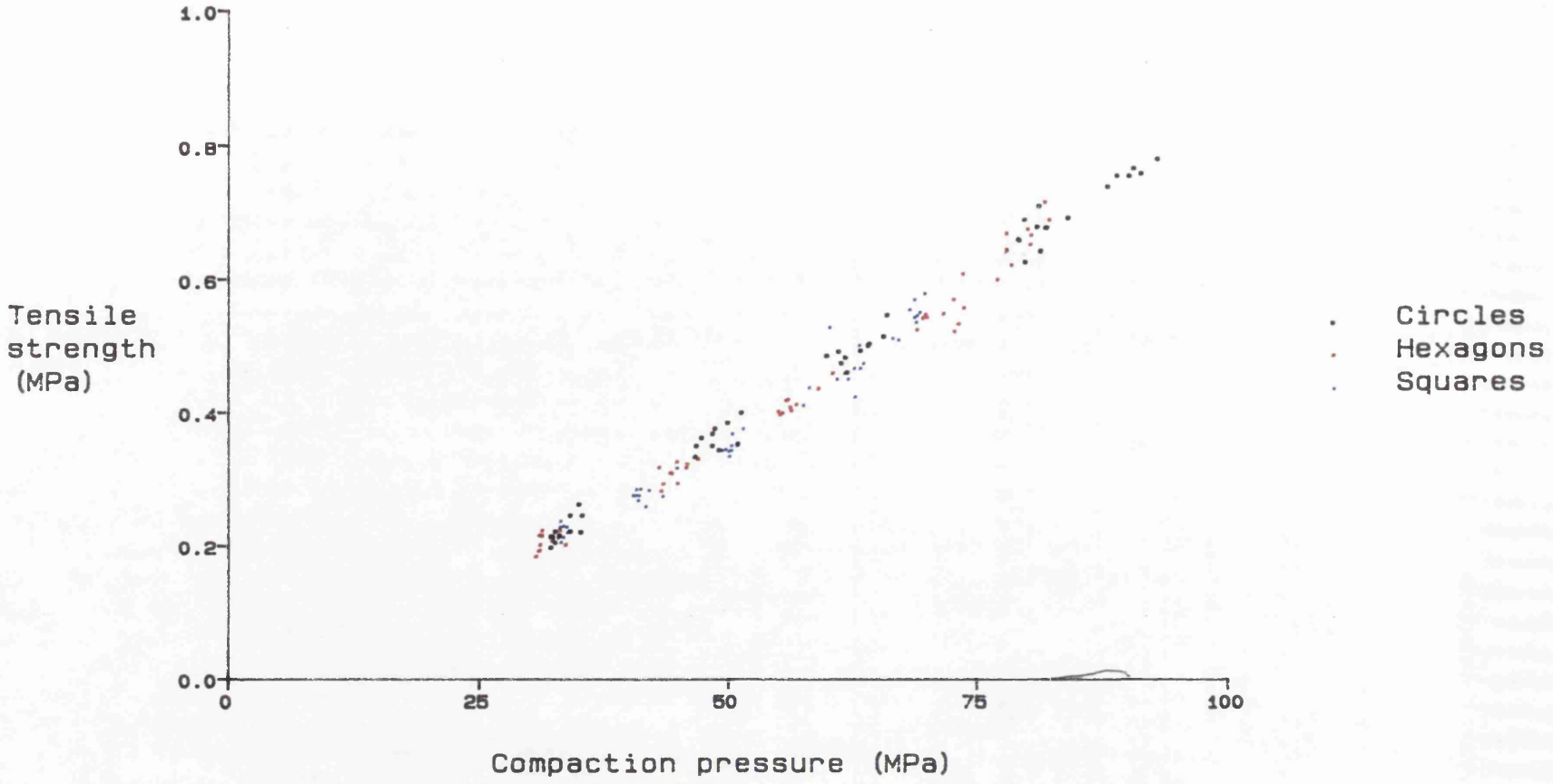

Tensile strength determined by diametral compression using semicircular platens.
Theoretical thickness of compacts at zero porosity = 2.8mm.

Figure 3.38 Effect of shape on the compaction pressure/ tensile strength profile of Anhydrous Lactose DCL 21 20mm compacts

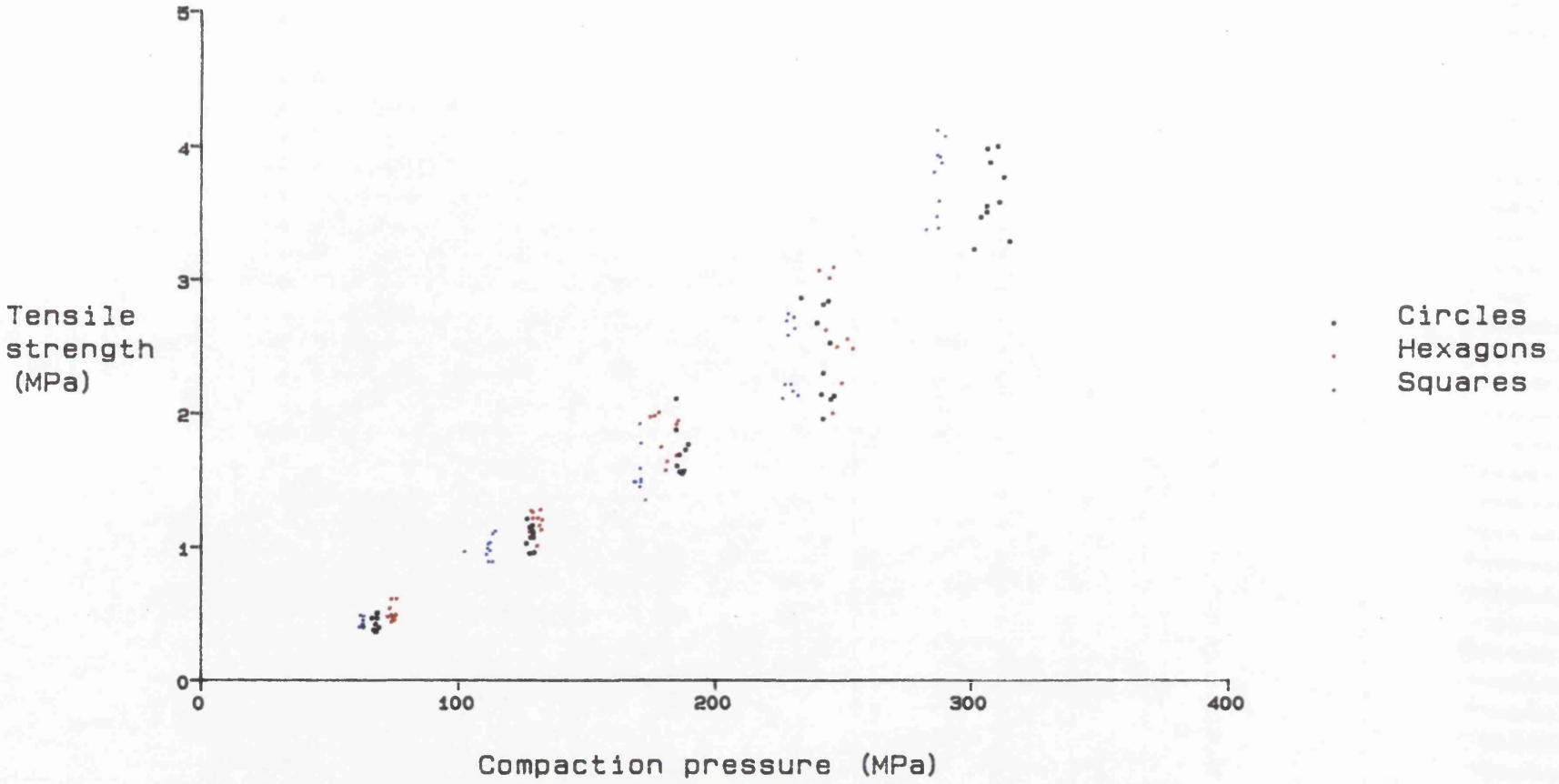

Tensile strength determined by diametral compression using semicircular platens.
Theoretical thickness of compacts at zero porosity = 2.8mm.

Figure 3.39 Effect of shape on the compaction pressure/ tensile strength profile of Anhydrous Lactose DCL 21 10mm compacts

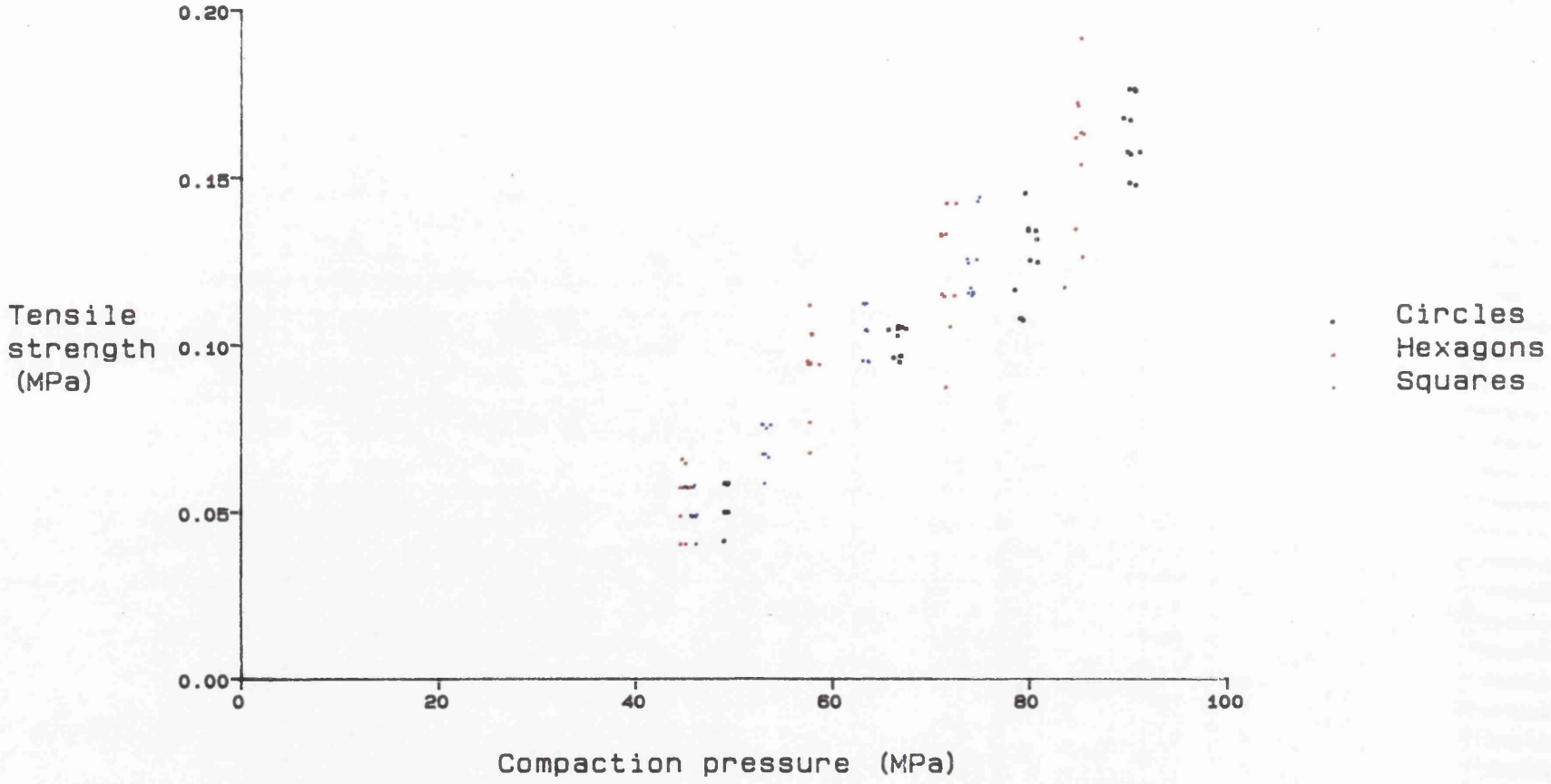

Tensile strength determined by diametral compression using semicircular platens.
Theoretical thickness of compacts at zero porosity = 2.8mm.

Figure 3.40 Effect of shape on the compaction pressure/ tensile strength profile of Lactose DMV 100 20mm compacts

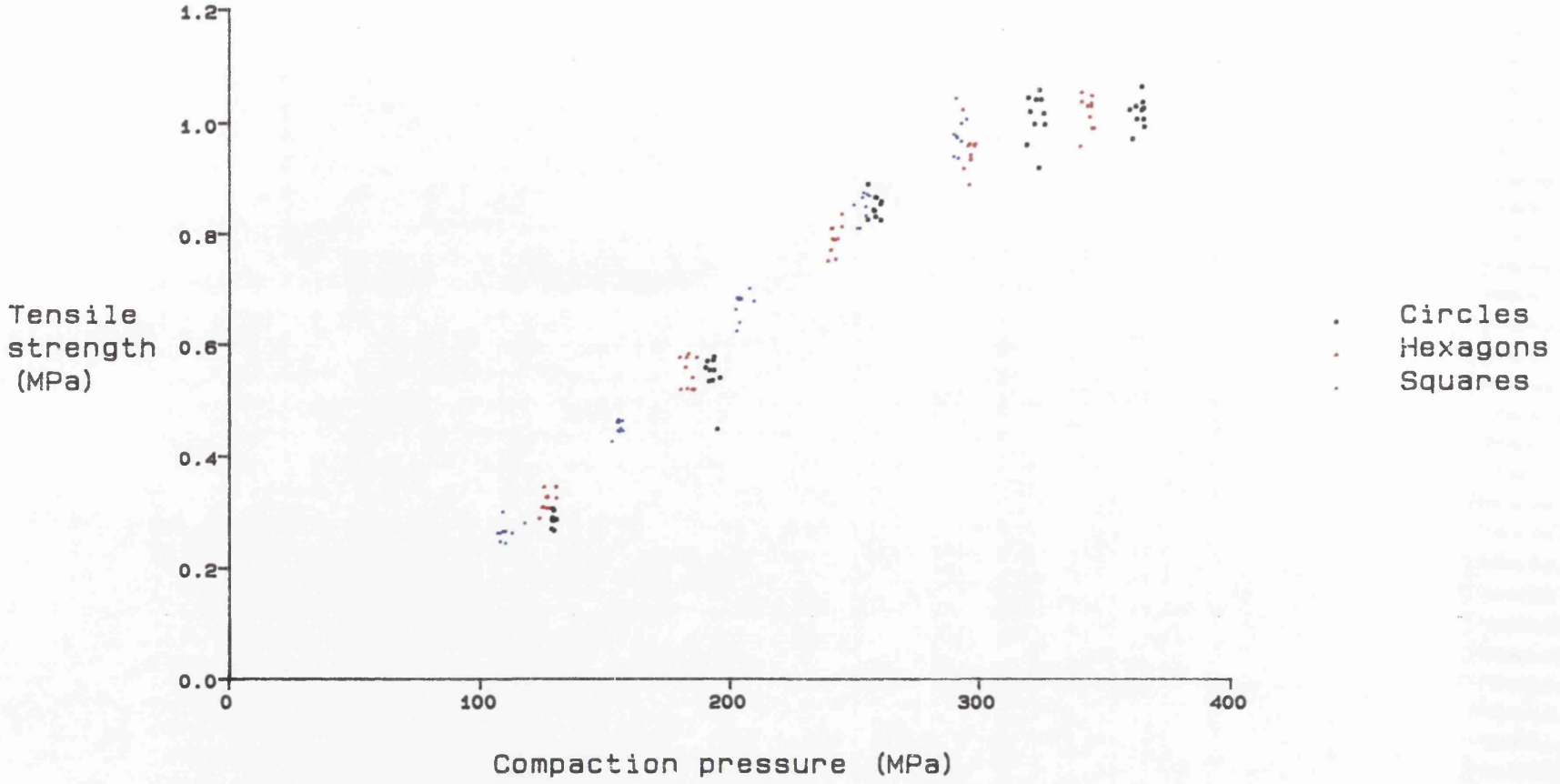

Tensile strength determined by diametral compression using semicircular platens.
Theoretical thickness of compacts at zero porosity = 2.8mm.

Figure 3.41 Effect of shape on the compaction pressure/ tensile strength profile of Lactose DMV 100 10mm compacts

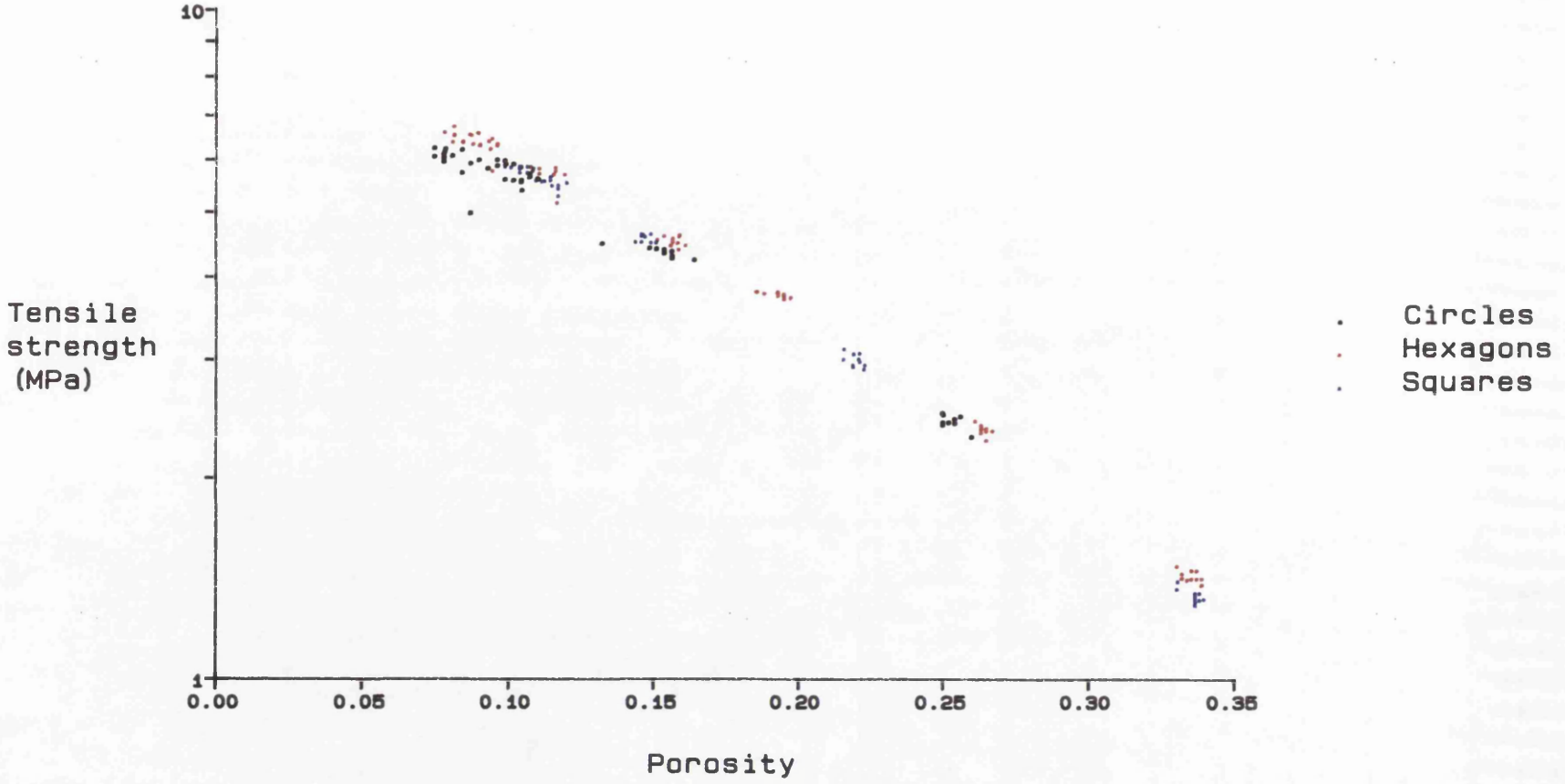

Tensile strength determined by diametral compression using semicircular platens
Theoretical thickness of compacts with zero porosity = 2.8mm.

Figure 3.42 Plot of tensile strength versus porosity for 10mm Avicel compacts

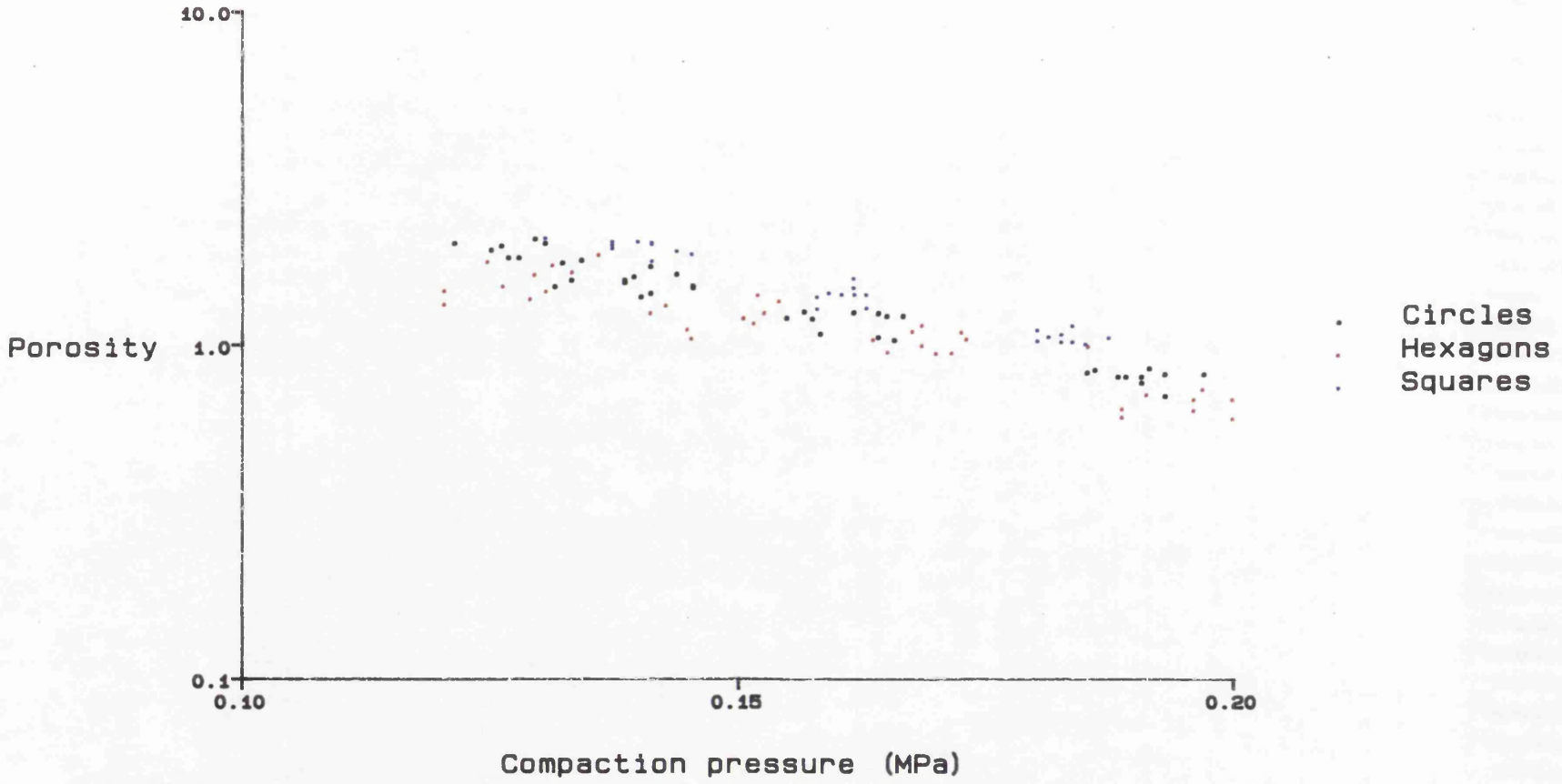

Tensile strength determined by diametral compression using semicircular platens
Theoretical thickness of compacts with zero porosity = 2.8mm.

Figure 3.43 Plot of tensile strength versus porosity for 10mm Emcompress compacts

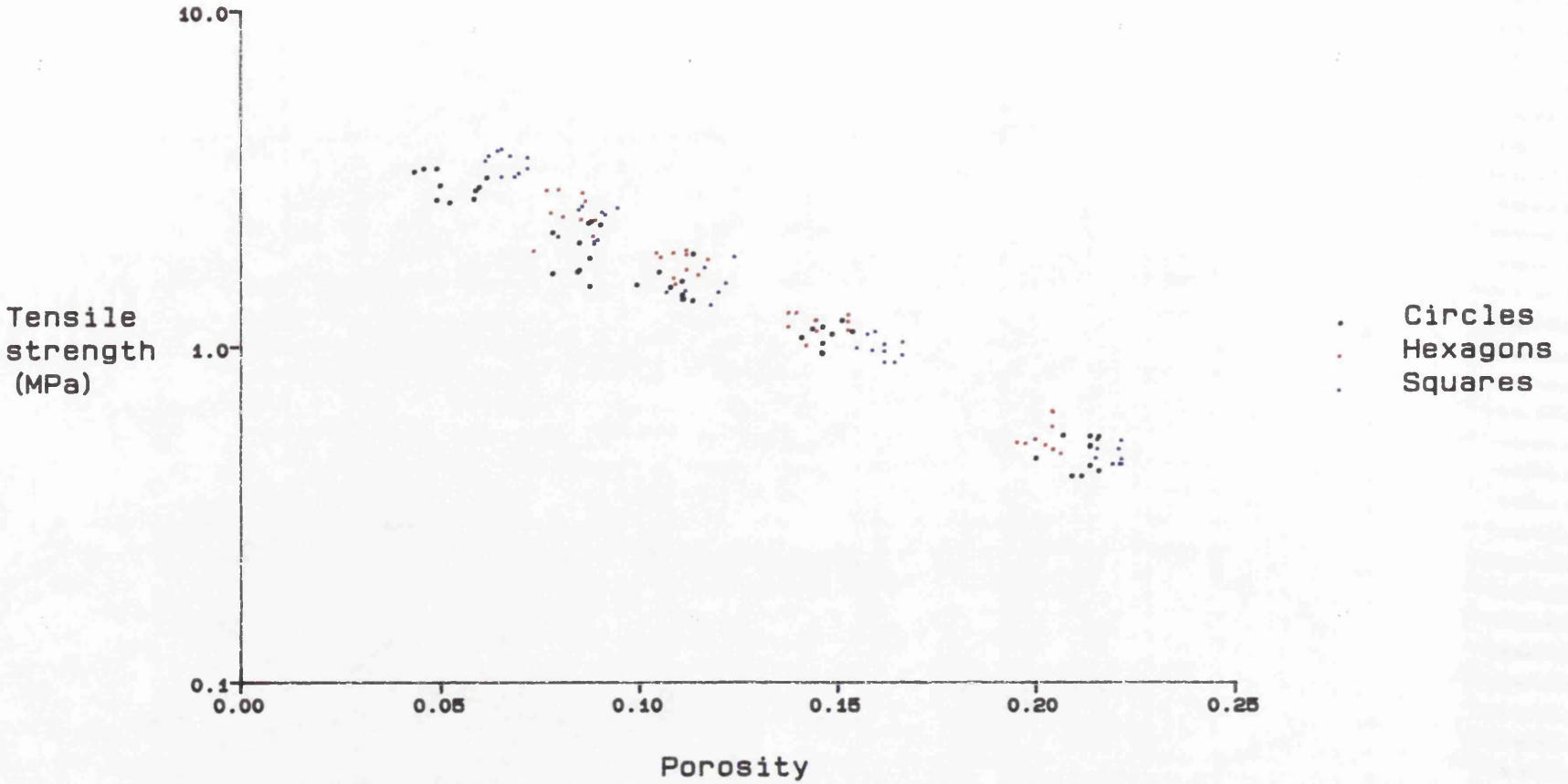

Tensile strength determined by diametral compression using semicircular platens
Theoretical thickness of compacts with zero porosity = 2.8mm.

Figure 3.44 Plot of tensile strength versus porosity for 10mm Anhydrous Lactose DCL 21 compacts

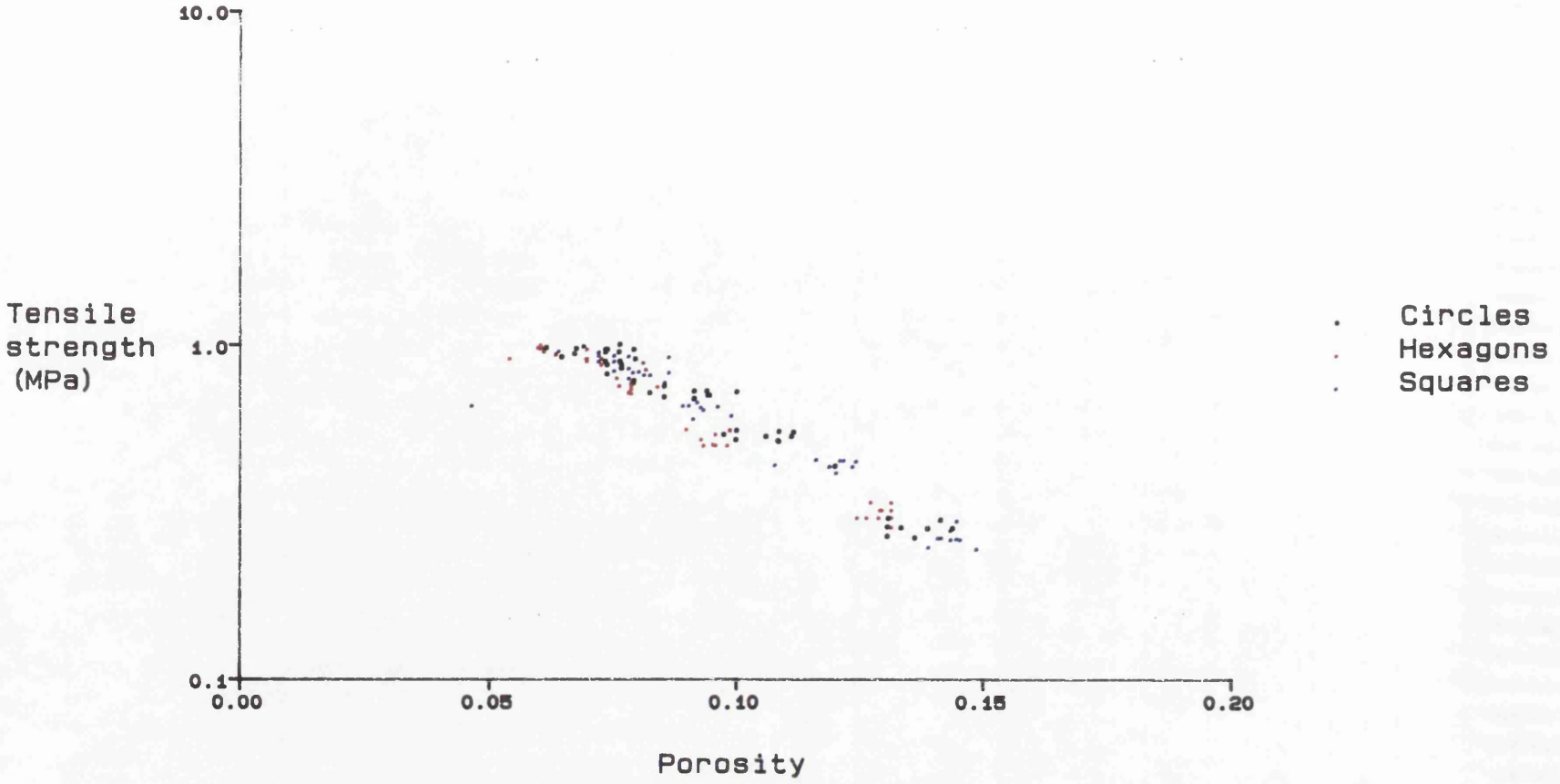

Tensile strength determined by diametral compression using semicircular platens
Theoretical thickness of compacts with zero porosity = 2.8mm.

Figure 3.45 Plot of tensile strength versus porosity for 10mm Lactose DMV 100 compacts

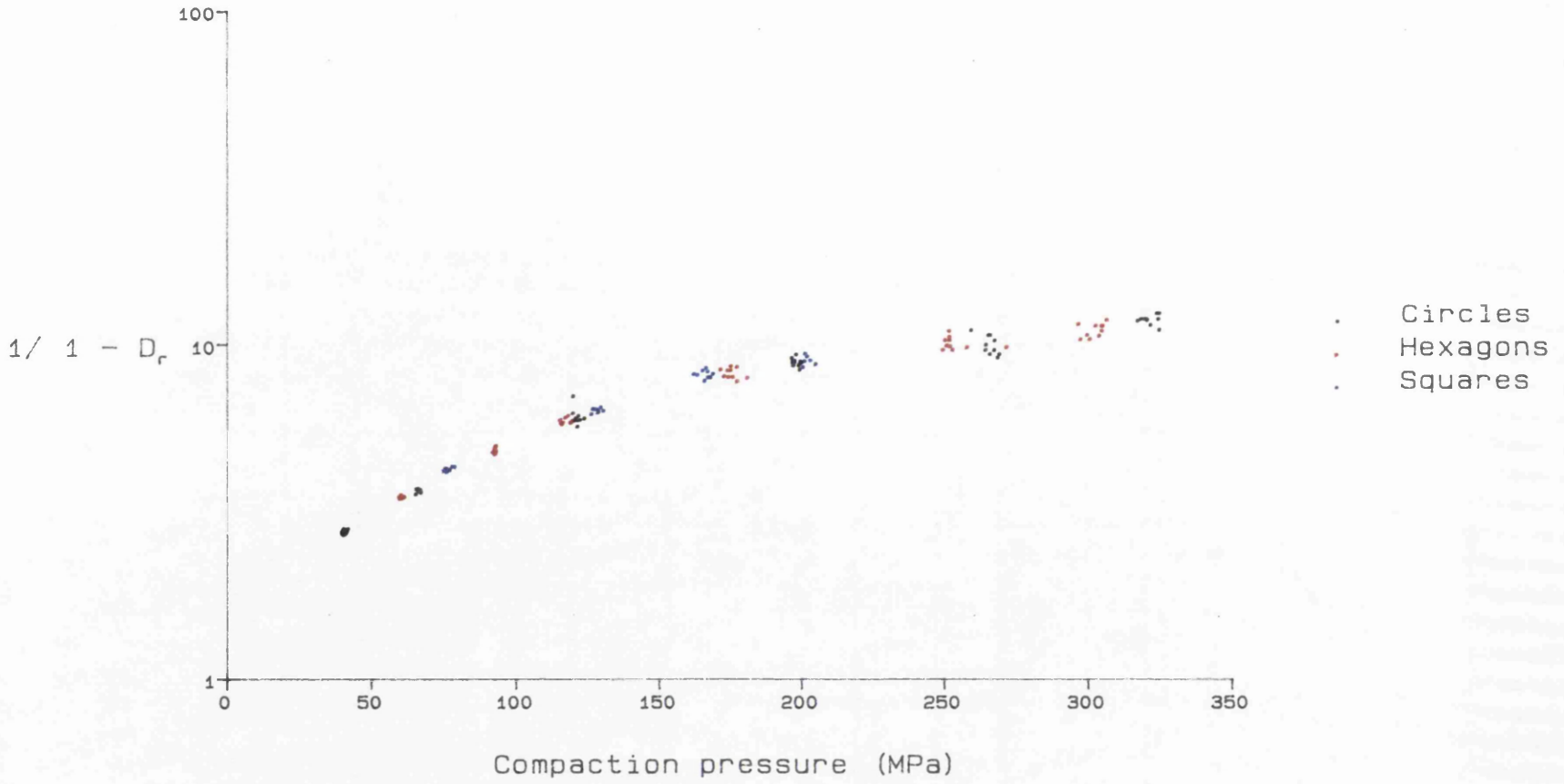

Figure 3.46 Heckel plots for 10mm Avicel shaped compacts

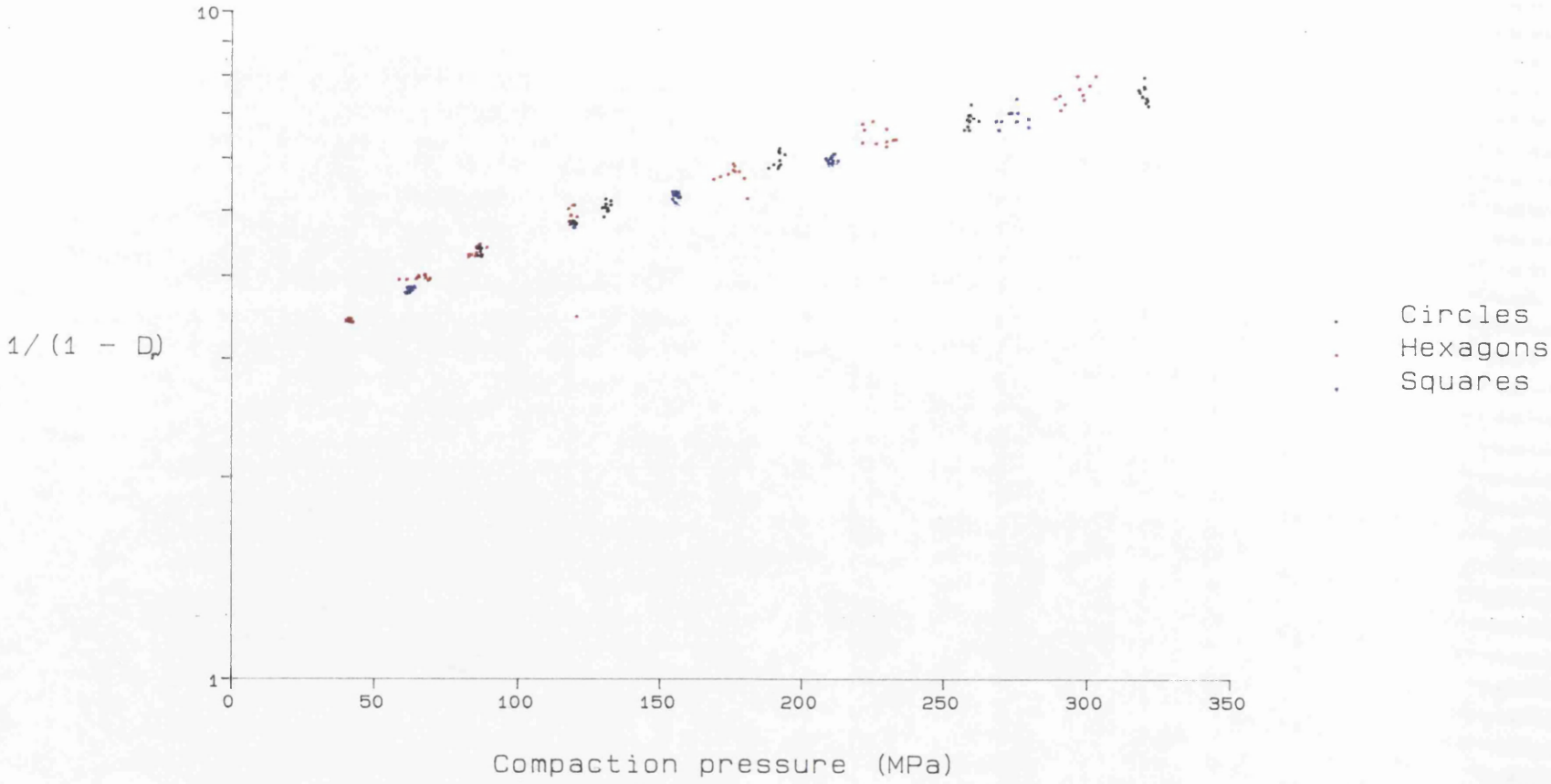

Figure 3.47 Heckel plots for 10mm Emcompress shaped compacts

The results of testing hexagonal and square compacts using notched platens are listed in Tables 3.16 and 3.17. With the compacts held in position by the notches slippage did not occur at the points of loading and the compacts failed along the line of loading, indicative of tensile failure. The loads required to produce failure with the notched platens were greater than for the face to face test using semicircular platens. This was to be expected as the distance between the loading points had increased, therefore for a given load the magnitude of the maximum tensile stress would be reduced. Davies and Bose (1968) investigated this loading configuration for cube specimens using the method of finite element analysis. It was concluded that the maximum tensile stress occurs at the centre of the specimen and is 0.77 of the value indicated by equation 2.1. A similar analysis has not been reported for hexagonal specimens.

If the value of 0.77 is used as a correction factor in Equation 2.1 to calculate the tensile strengths of square compacts similar values are obtained to those from the face to face diametral compression test using semicircular platens (Figure 3.48). If the distances between the loading points are used as the value of D in Equation 2.1, the compaction pressure/tensile strength profiles of both the square and hexagonal compacts are similar for the two test methods (Figures 3.49 and 3.50). In the latter case the ratios of the maximum tensile strengths for the two methods would be 0.707 and 0.866 for the squares and hexagons respectively.

As there are likely to be differences in the contact widths in the two tests it is not possible to conclude which value is the most appropriate for

Table 3.16
Diametral compression results for shaped Avicel compacts tested using notched platens

Compact shape	Compact size[1] (mm)	Zero porosity thickness (mm)	Compaction pressure (MPa)	Thickness (mm)	Mean breaking load (kg)
Square	10	2.0	46.2	2.98	10.37
	10	2.0	103.6	2.45	22.13
	10	2.0	168.4	2.30	27.7
	10	2.8	51.0	3.95	17.22
	10	2.8	128.2	3.27	36.36
	10	2.8	167.4	3.14	41.03
	10	2.8	200.8	3.11	44.89
	10	2.8	255.1	3.07	45.83
Hexagonal	10	2.0	49.3	3.04	7.60
	10	2.0	119.4	2.46	18.18
	10	2.0	175.5	2.33	23.37
	10	2.0	222.7	2.24	24.42
	10	2.0	298.5	2.19	26.20

Table 3.17
Diametral compression data for shaped Emcompress compacts tested using notched platens

Compact shape	Compact size[1] (mm)	Zero porosity thickness (mm)	Compaction pressure (MPa)	Compact thickness (mm)	Mean breaking load (kg)
Square	10	2.0	72.2	2.71	3.40
	10	2.0	115.6	2.51	5.22
	10	2.0	150.7	2.46	6.98
	10	2.0	204.4	2.39	9.99
	10	2.8	58.7	3.75	3.42
	10	2.8	126.0	3.48	8.24
	10	2.8	156.0	3.42	10.98
	10	2.8	206.9	3.28	14.84
Hexagonal	10	2.8	88.7	3.70	1.91
	10	2.8	110.9	3.61	2.44
	10	2.8	145.0	3.56	3.30
	10	2.8	175.6	3.48	4.32

1. Size is defined as the diameter of an inscribed circle, i.e. the distance between the mid points of two opposite faces.

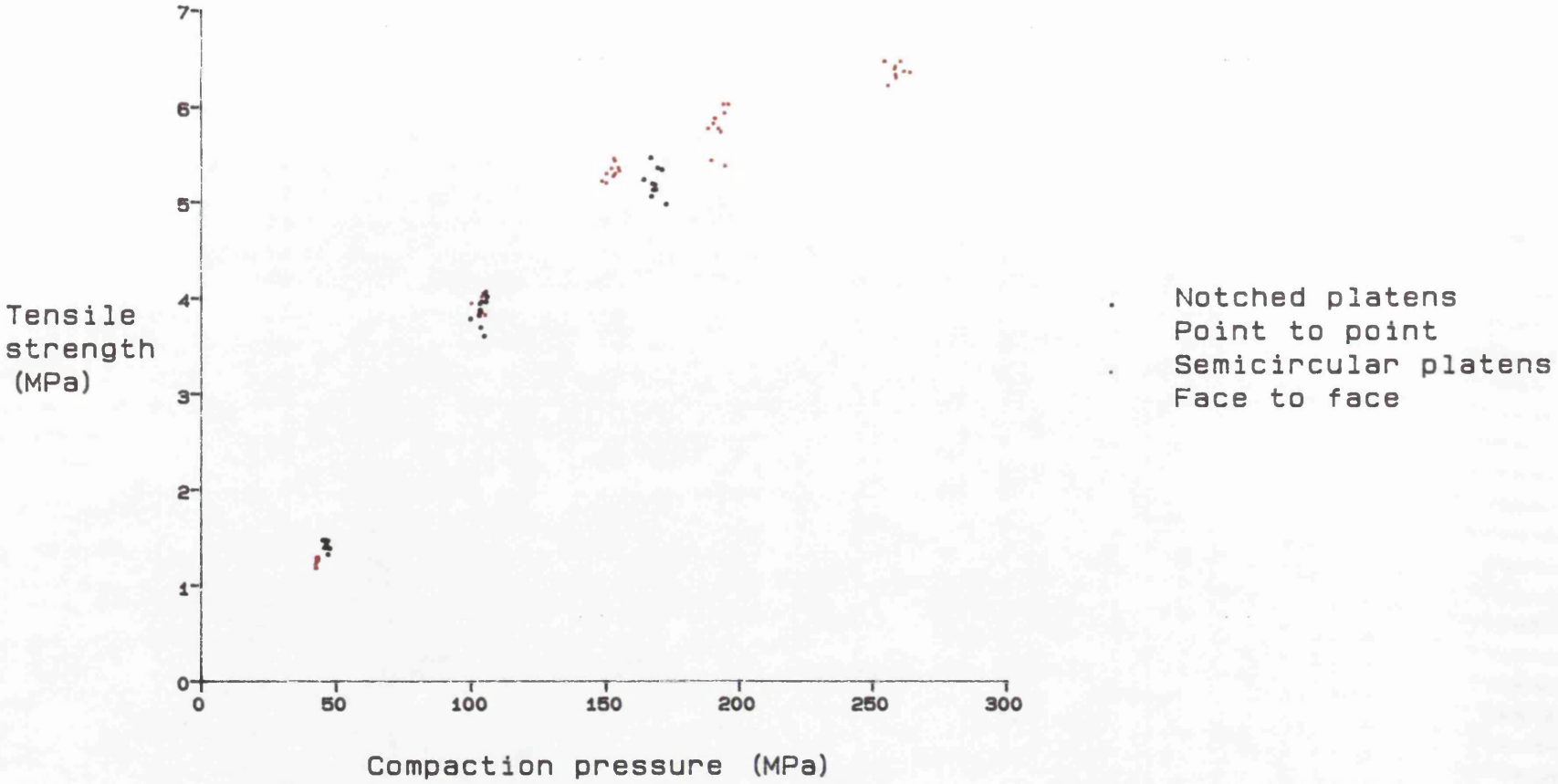

Correction value for tensile strength determination of notched platen test = 0.77

Figure 3.48 Effect of platen shape and test configuration on the compaction pressure/tensile strength profile of Avicel 10mm square compacts tested by diametral compression

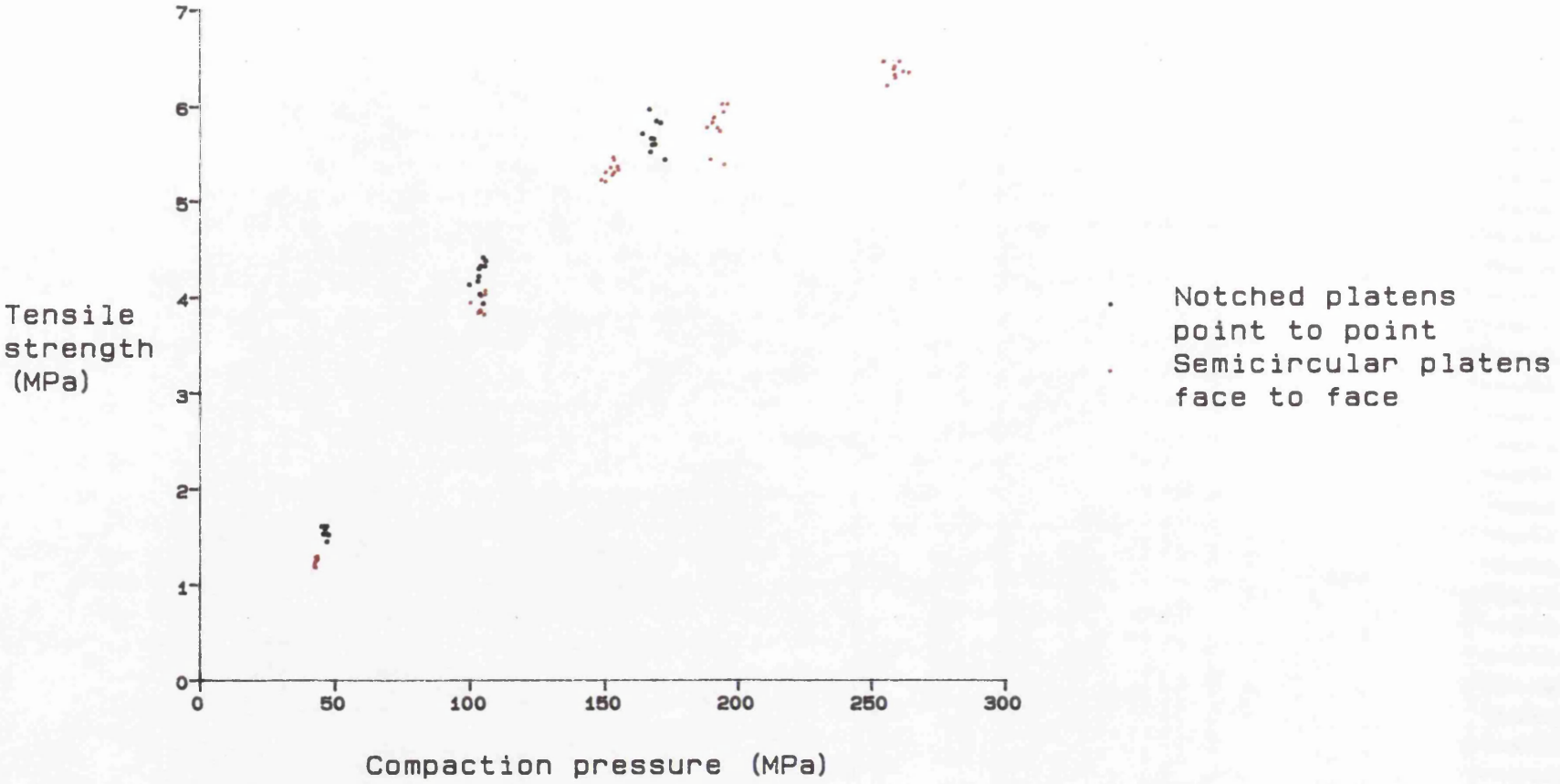

Correction value for tensile strength determination of notched platen test = 0.707

Figure 3.49 Effect of platen shape and test configuration on the compaction pressure/tensile strength profile of Avicel 10mm square compacts tested by diametral compression

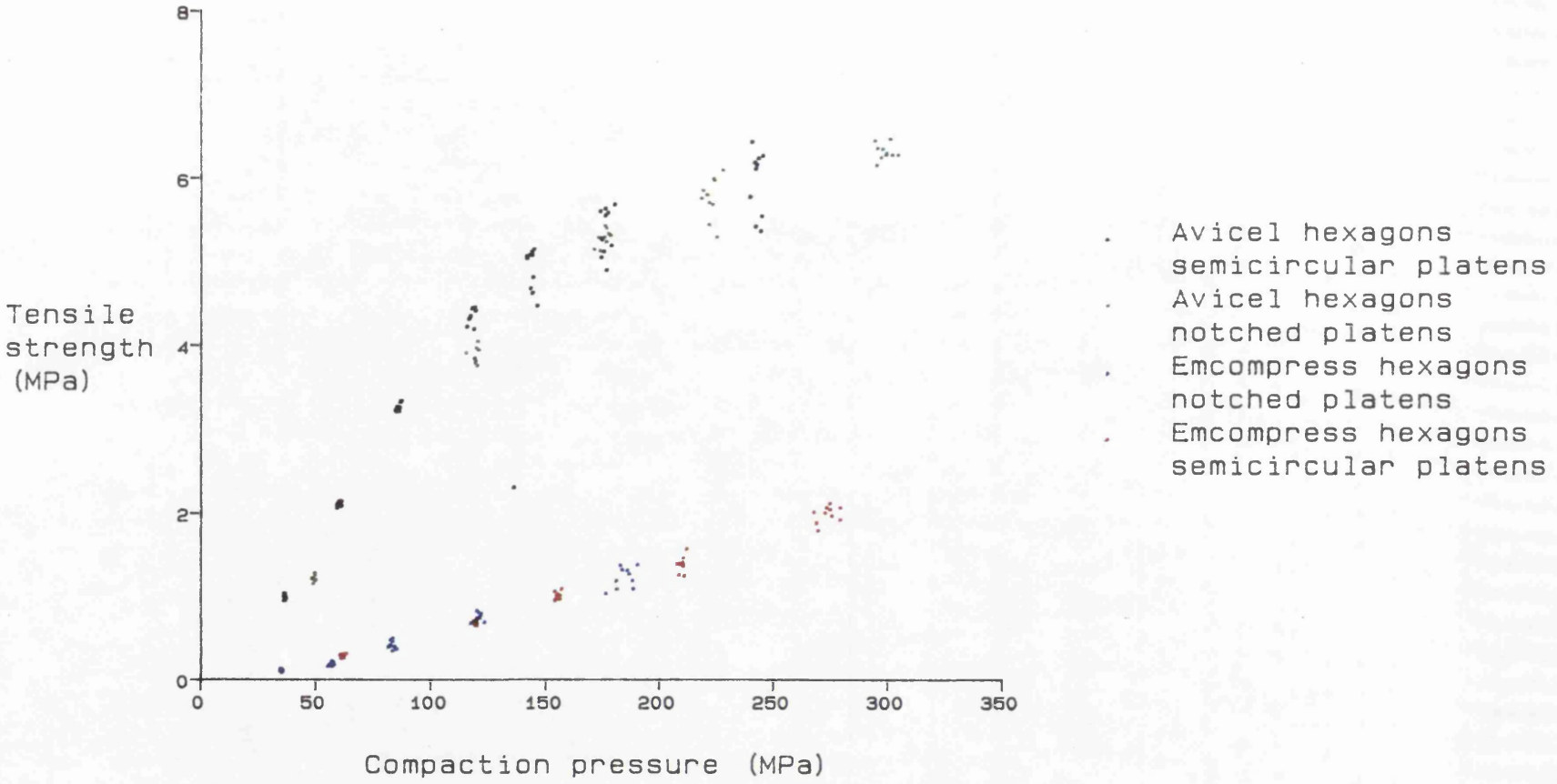

Figure 3.50 Effect of platen shape and test configuration on the compaction pressure/tensile strength profile of hexagonal shaped compacts

substitution into the equation. As such the test is of little value if used to detect minor differences between square and circular compacts.

3.3.3.3 Axial compression

Figures 3.51 to 3.54 illustrate the compaction pressure/ tensile strength profiles of Avicel and Emcompress 10mm compacts using the axial compression test to determine the tensile strength. For Avicel the compact shape again appears to have no effect on the tensile strength. However, the Emcompress results indicate that for a given compaction pressure the circular compacts have a greater tensile strength than the hexagons, which in turn are stronger than the squares. The compaction pressures used in the graphs are the lower punch pressures, i.e the transmitted pressure. The use of upper punch pressures increases the difference between the shapes as the proportion of the applied pressure transmitted to the lower punch (known as the R-value) is lowest for the square compacts (Table 3.18).

3.3.3.4 Transverse compression

The transverse compression test applies a compressive stress parallel to the upper and lower faces of the compact producing a tensile stress along the axis of compaction. The direction of the tensile stresses are the same as those produced by the axial tensile strength test described by Nystrom et al (1978), although the distribution of the stresses will be different. Nystrom used the test to measure the capping tendency of formulations. The transverse compression test cannot be considered a measure of capping tendency as the tensile stresses will be concentrated along the line of loading, which will not necessarily be the area in which capping occurs.

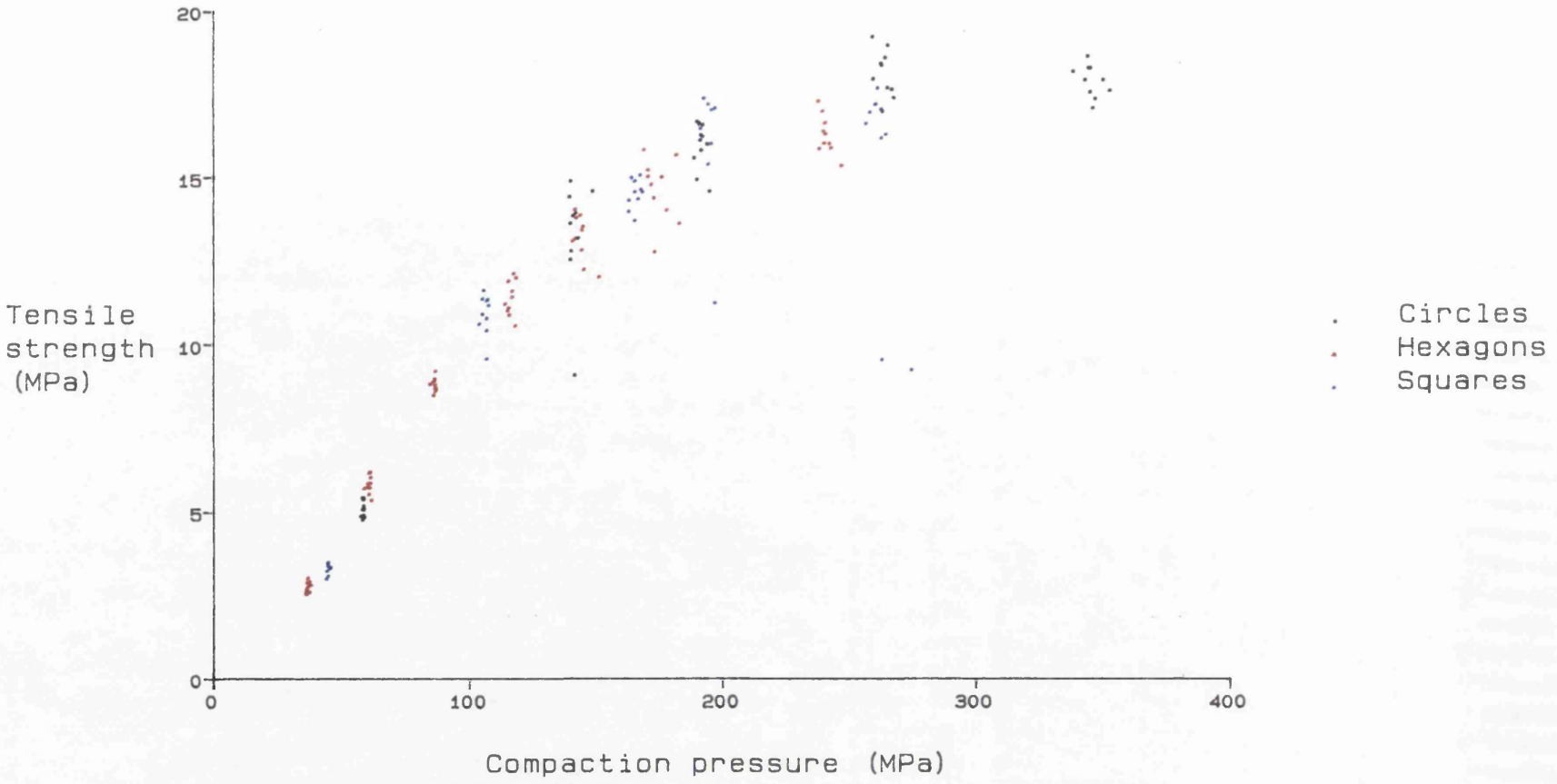

Tensile strength determined by axial compression.
Theoretical thickness of compacts with zero porosity = 2.0mm

Figure 3.51 Effect of compact shape on the compaction pressure/tensile strength profiles of Avicel 10mm compacts

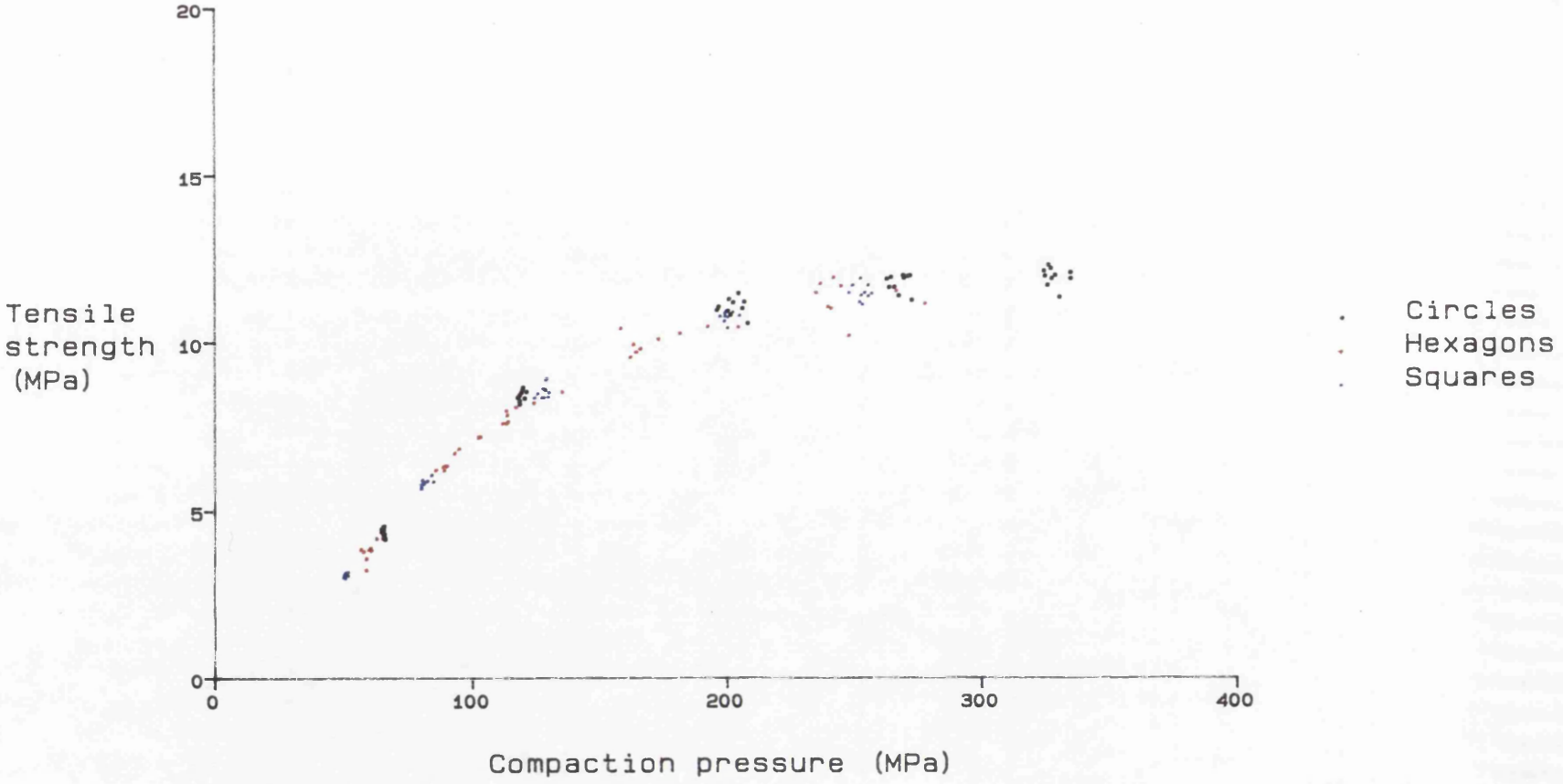

Tensile strength determined by axial compression.
Theoretical thickness of compacts with zero porosity = 2.8mm

Figure 3.52 Effect of compact shape on the compaction pressure/tensile strength profiles of Avicel 10mm compacts

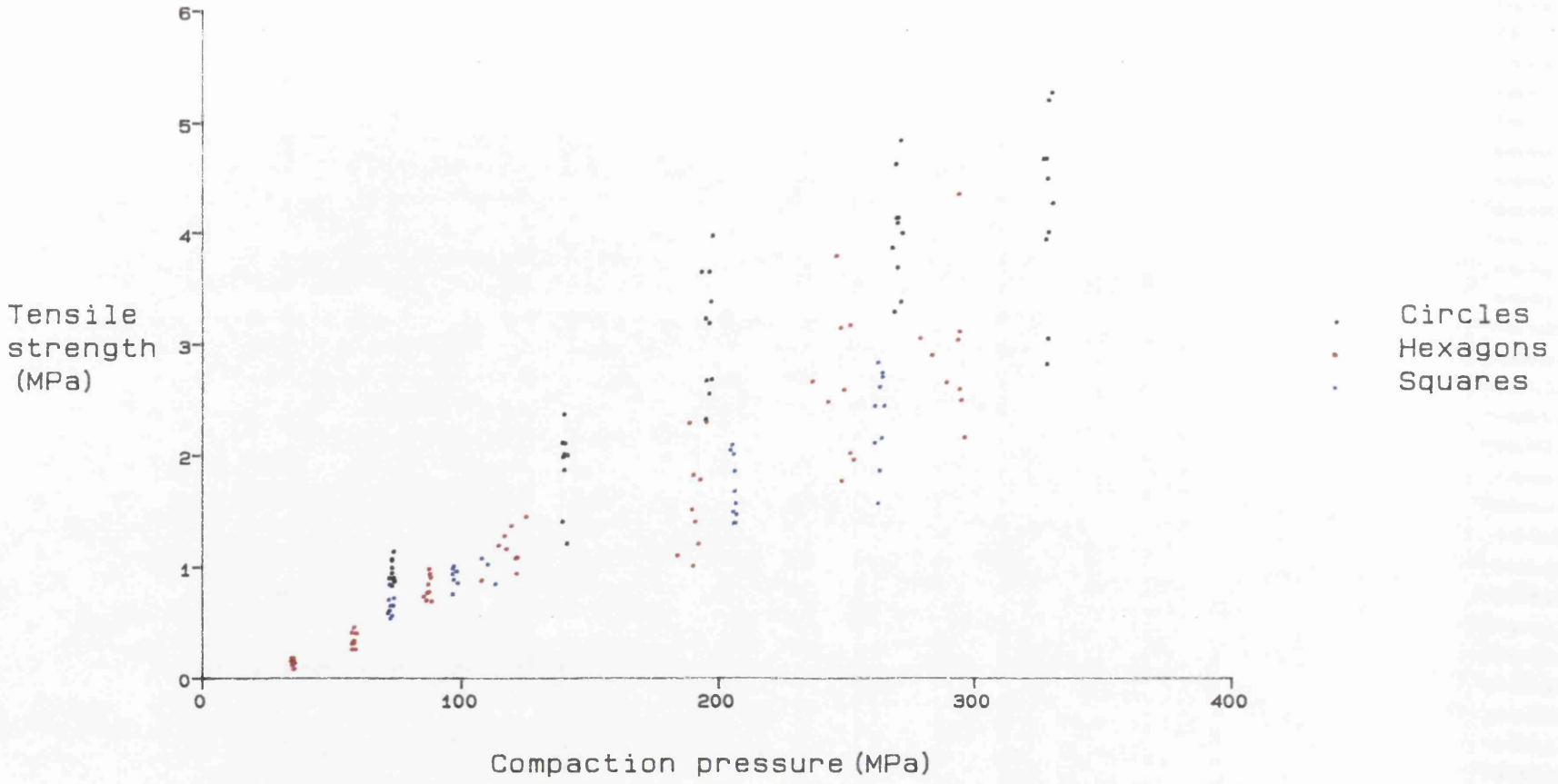

Tensile strength determined by axial compression.
Theoretical thickness of compacts with zero porosity = 2.0mm

Figure 3.53 Effect of compact shape on the compaction pressure/tensile strength profiles of Emcompress 10mm compacts

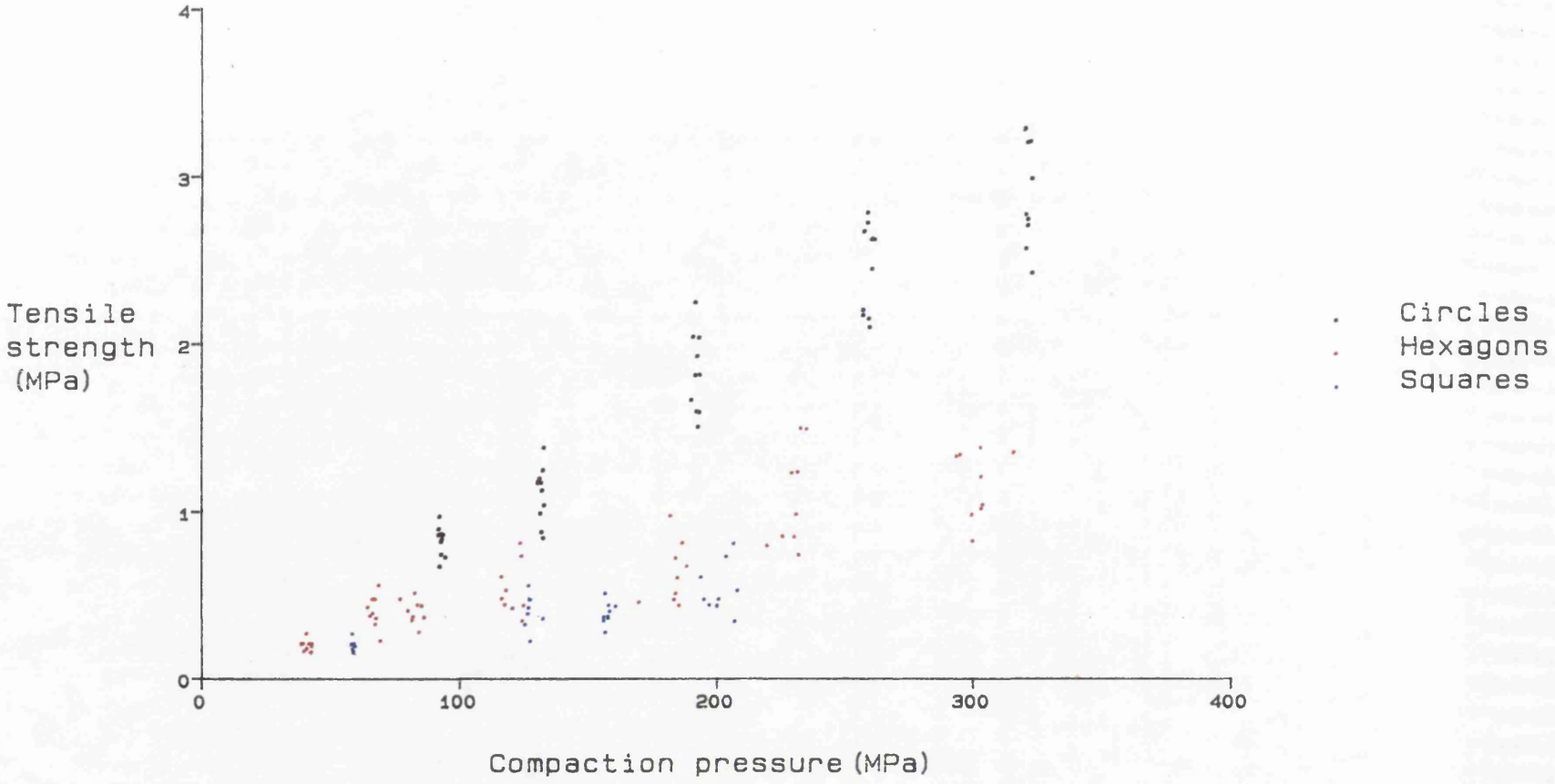

Tensile strength determined by axial compression.
Theoretical thickness of compacts with zero porosity = 2.8mm

Figure 3.54 Effect of compact shape on the compaction pressure/tensile strength profiles of Emcompress 10mm compacts

Table 3.18
Comparison of the R-values obtained for square and circular compacts

Table 3.18a Emcompress compacts

Zero porosity thickness (mm)	Circular compacts			Square compacts		
	Lower punch pressure (MPa)	Upper punch pressure (MPa)	R-value	Lower punch pressure (MPa)	Upper punch pressure (MPa)	R-value
2.0	69.1	72.8	0.95	71.4	76.6	0.93
	142.3	147.9	0.96	111.4	117.4	0.95
	195.4	202.8	0.96	159.0	185.3	0.86
2.8	86.9	92.8	0.94	62.0	74.7	0.83
	131.2	138.8	0.94	119.7	138.0	0.87
	191.3	221.8	0.86	155.5	190.0	0.82

Table 3.18b Avicel compacts

Zero porosity thickness (mm)	Circular compacts			Square compacts		
	Lower punch pressure (MPa)	Upper punch pressure (MPa)	R-value	Lower punch pressure (MPa)	Upper punch pressure (MPa)	R-value
2.0	77.7	80.0	0.97	42.8	45.3	0.94
	135.8	138.6	0.98	103.5	107.4	0.96
	186.3	203.9	0.91	152.3	172.2	0.88
2.8	66.0	69.0	0.96	40.5	44.8	0.91
	121.2	125.5	0.96	76.8	82.6	0.93
	198.2	226.5	0.88	128.2	138.0	0.93

A drawback of the transverse compression test is that comparison of results between square and circular compacts is complicated by the different loading arrangements. The square compacts are in contact with the platens along the entire length of the sides (Figure 3.4), producing tensile stresses across a plane equivalent to the cross sectional surface area of the compact. The testing of the circular compacts results in point loading with the platens. This results in tensile stresses being established over a much smaller part of the compact which would be expected to increase the mean breaking load. A further complication of the test on circular compacts is that the point loading conditions will produce tensile stresses in a plane normal to the direction of loading. Failure could therefore occur in directions analogous to either the diametral compression test or the transverse compression test depending on the relative strengths of the bonds in the two directions. To enable a comparison of the circular and square compacts the ball bearing diametral compression test was introduced. In this test both shapes of compact will be subjected to point loading.

The results of the transverse compression test for Emcompress squares with a zero porosity thickness of 2.8mm are illustrated in Figure 3.55. It can be seen that the diametral compression test produces higher values for the tensile strength of circular compacts than the square compacts. The results for the ball bearing test are similar to those of the transverse compression test indicating that failure is occurring in the weakest direction.

A comparison of results for the different modes of tensile strength test

(Figure 3.56) shows for Emcompress that the transverse compression results give slightly higher tensile strength values than the diametral compression results, which were similar to the ball bearing results. The difference between the ball bearing and transverse compression results indicates differences in the stresses established by the two methods, probably due to deformation at the platen edge for the transverse test. While it is interesting that the transverse compression results are greater than the diametral compression results for circular compacts and that the opposite effect is seen for square compacts, the aforementioned differences in the loading prevent conclusions being drawn regarding structural differences between shapes.

The ball bearing results are interesting as they are similar to the lower of the two test results for both shapes. While the mode of failure would be expected to mirror the test producing the lowest tensile strength the similarity of the values obtained is surprising considering the differences in loading conditions. It was not possible to determine the mode of failure for the ball bearing test as the cracks produced in the compacts did not reach the surface before the load was removed by the CT40.

3.3.3.5 Three point bending test

The axial, diametral and transverse compression tests all produce failure of the compacts due to tensile stresses produced by the application of a compressive stress. There is no area within the compact that is subject to a pure tensile stress; all points are exposed to a combination of shear, compressive and tensile stresses. A second feature of the three tests is that the maximum tensile stress occurs at the centre of the compacts. There is

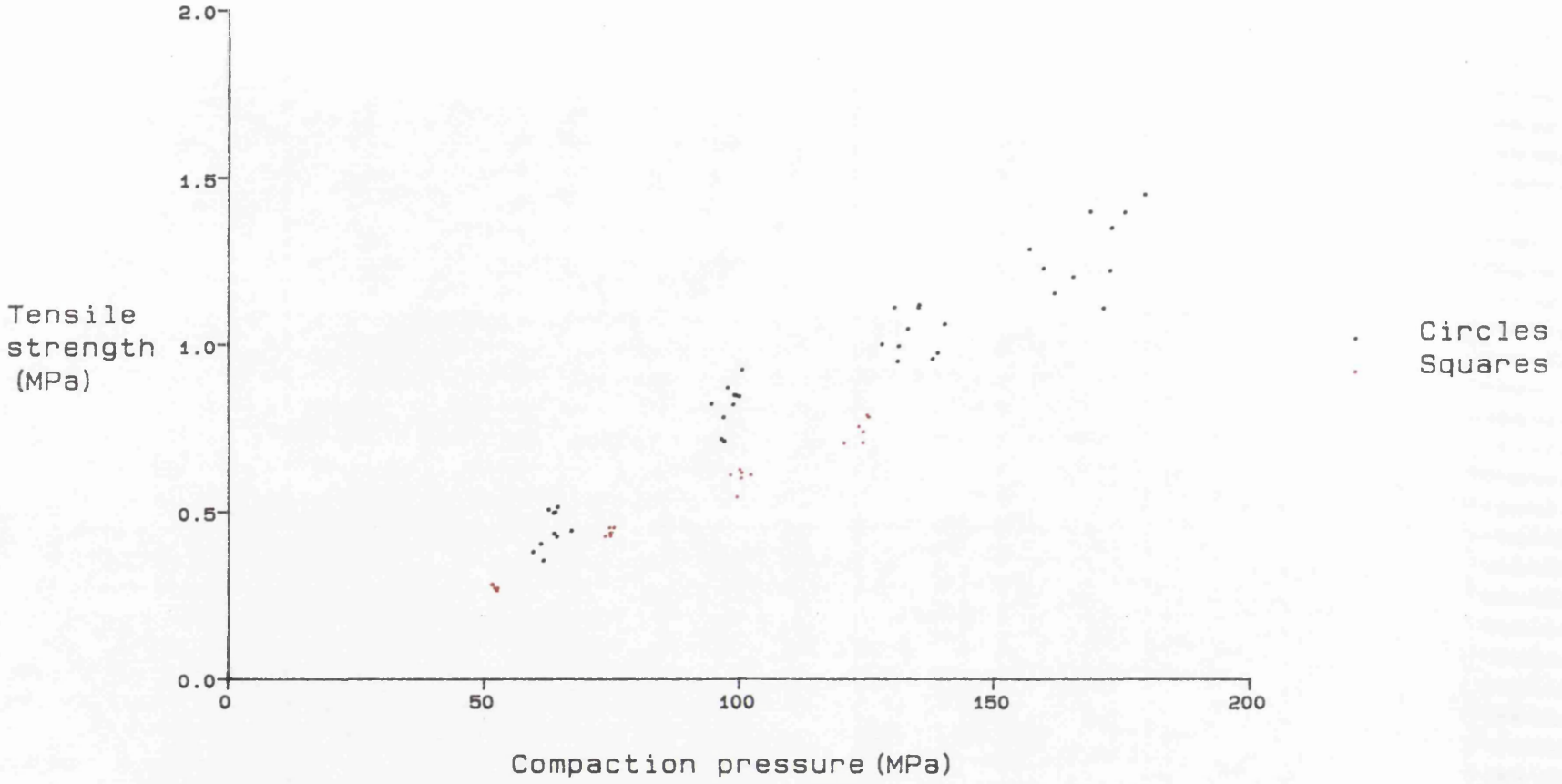

Tensile strength determined by transverse compression.
Theoretical thickness of compacts with zero porosity = 2.8mm

Figure 3.55 Effect of compact shape on the compaction pressure/tensile strength profiles of Emcompress 10mm compacts

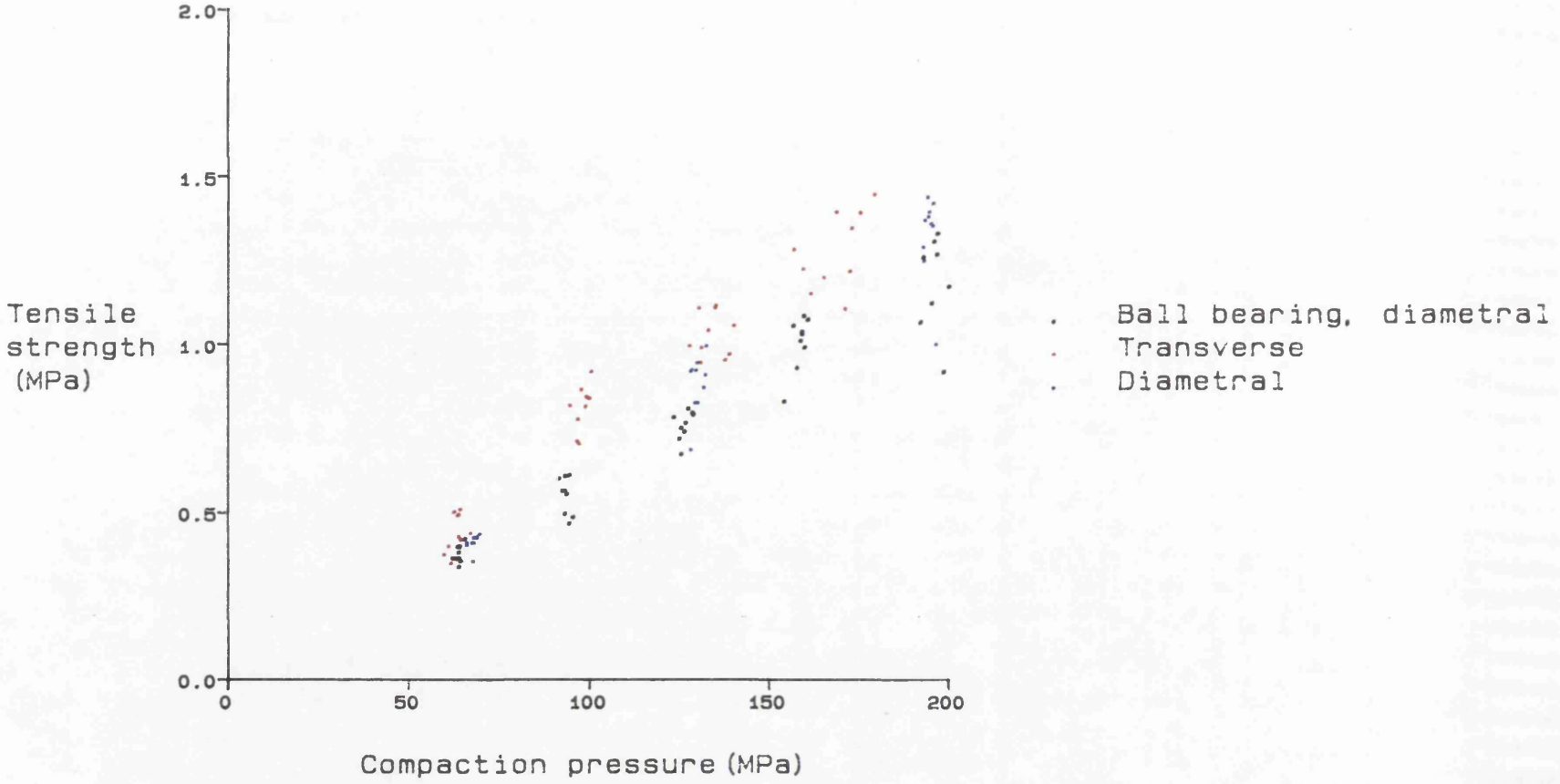

Theoretical thickness of compacts with zero porosity = 6.0mm

Figure 3.56 Effect of test method on the value of tensile strength obtained for 10mm diameter circular Emcompress compacts

evidence that there are differences in the structure of the compacts near the lower surfaces that are not fully reflected in the tensile strength values.

The 3 point bending test offers advantages over the indirect tensile strength tests because the point at which the maximum tensile strength occurs, on the lower test surface beneath the upper platen, is exposed to a pure tensile stress. Furthermore, as this point is on the surface of the compact the test offers the possibility of comparing the strengths of the upper and lower surfaces.

When compacts were tested using the 3 point bending rig failure did not occur at the mid point of the lower surface. The line of failure was from one of the lower rollers to the upper platen. Such a pattern is indicative of failure due to shear stresses adjacent to the roller. The upper platen speed and distance between rollers were varied but compacts continued to fail in the same manner. Although the successful use of the 3 point bending rig has been reported for circular compacts (David and Augsburger 1974) the low length to thickness ratio of the compacts results in greater shear stresses than are encountered by the traditional beam samples for which the test was originally designed.

3.3.3.6 Effect of varying platen position on the tensile strength

The positioning of the platens away from the centres of the compacts in the diametral compression test did lead to some changes in the values obtained for the tensile strength but the relevance of the changes is open to question.

The diametral compression test carried out on square compacts by

applying the platens to the specimen 2.5mm from a corner is compared with the usual test in Figure 3.57. The re-positioning of the platens did not result in a significant change in the tensile strength values but there was an increase in the variance.

The effect of moving the platens away from the centre in the transverse compression test was to increase the breaking load and thus the tensile strength value (Figure 3.58). The effect was the same whether the platens were moved towards the upper or lower surface of the compacts. A similar effect was seen with the square compacts tested axially away from the centre.

In all 3 tests a number of samples were excluded from any analysis as they did not fail in a manner indicative of tension. To minimise shear stresses the correct alignment of the specimens was important. The re-positioning of the platens appeared to make the alignment even more critical. In a number of cases incorrect alignment resulted in movement of the specimen during the test. The problem of alignment is an explanation for at least part of the increase in variance. The increase in mean value seen for the axial and transverse compression tests may indicate that the compacts are stronger away from the centre but could also be due in part to alignment problems. In the absence of stress analyses for these tests it is difficult to assess the relevance of the increase in strength values.

3.3.3.7 Effectiveness of Magnesium Stearate as a die wall lubricant

Holzer and Sjøgren (1978) examined the effect of compact thickness on the ratio of upper and lower punch forces (R-value) when preparing circular compacts of Lactose, Sodium Chloride and Aspirin. The R-value was shown

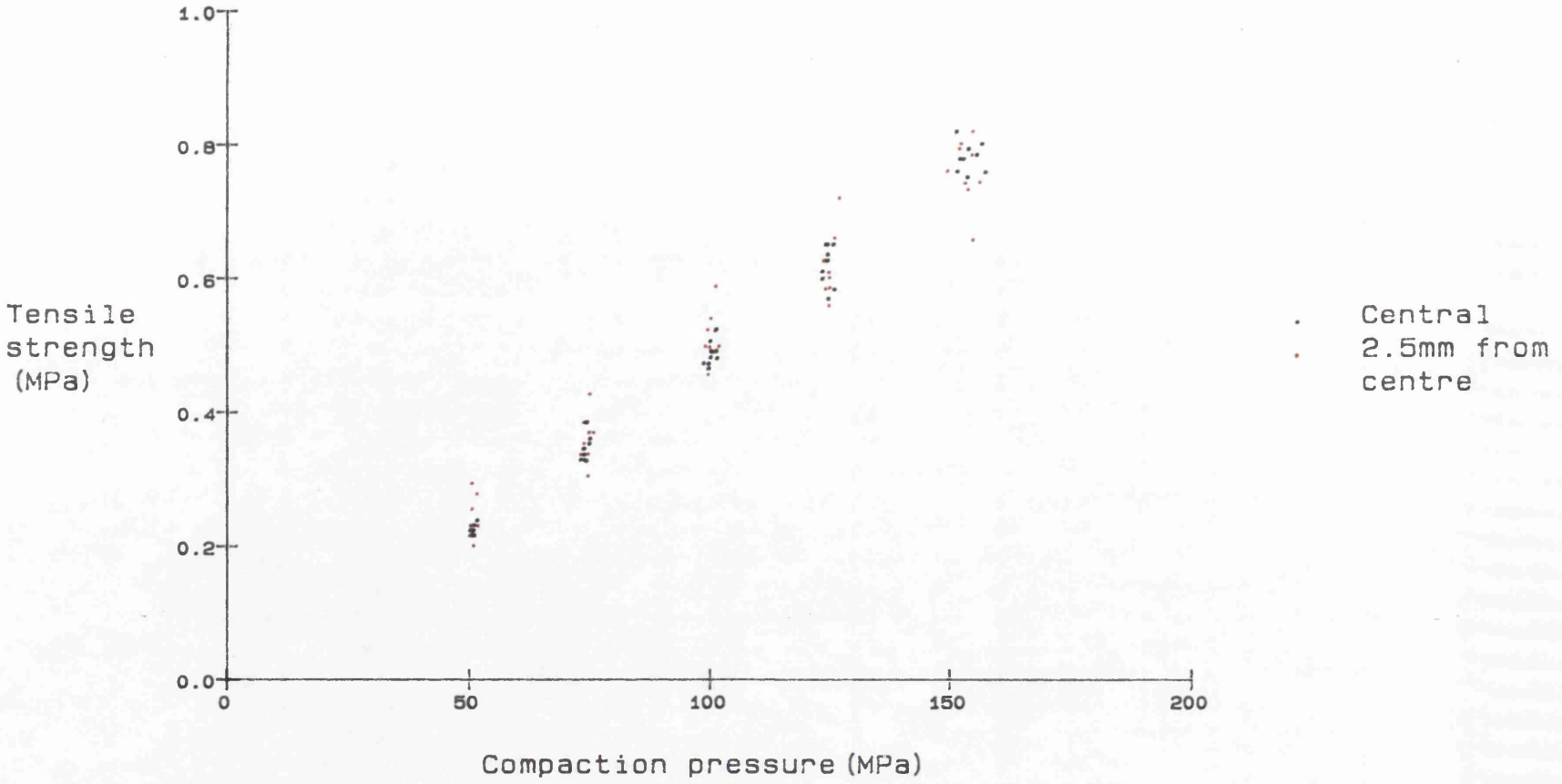

Theoretical thickness of compacts with zero porosity = 2.8mm
Compacts tested by diametral compression

Figure 3.57 Effect of platen position on the value of tensile strength obtained for 10mm square Emcompress compacts

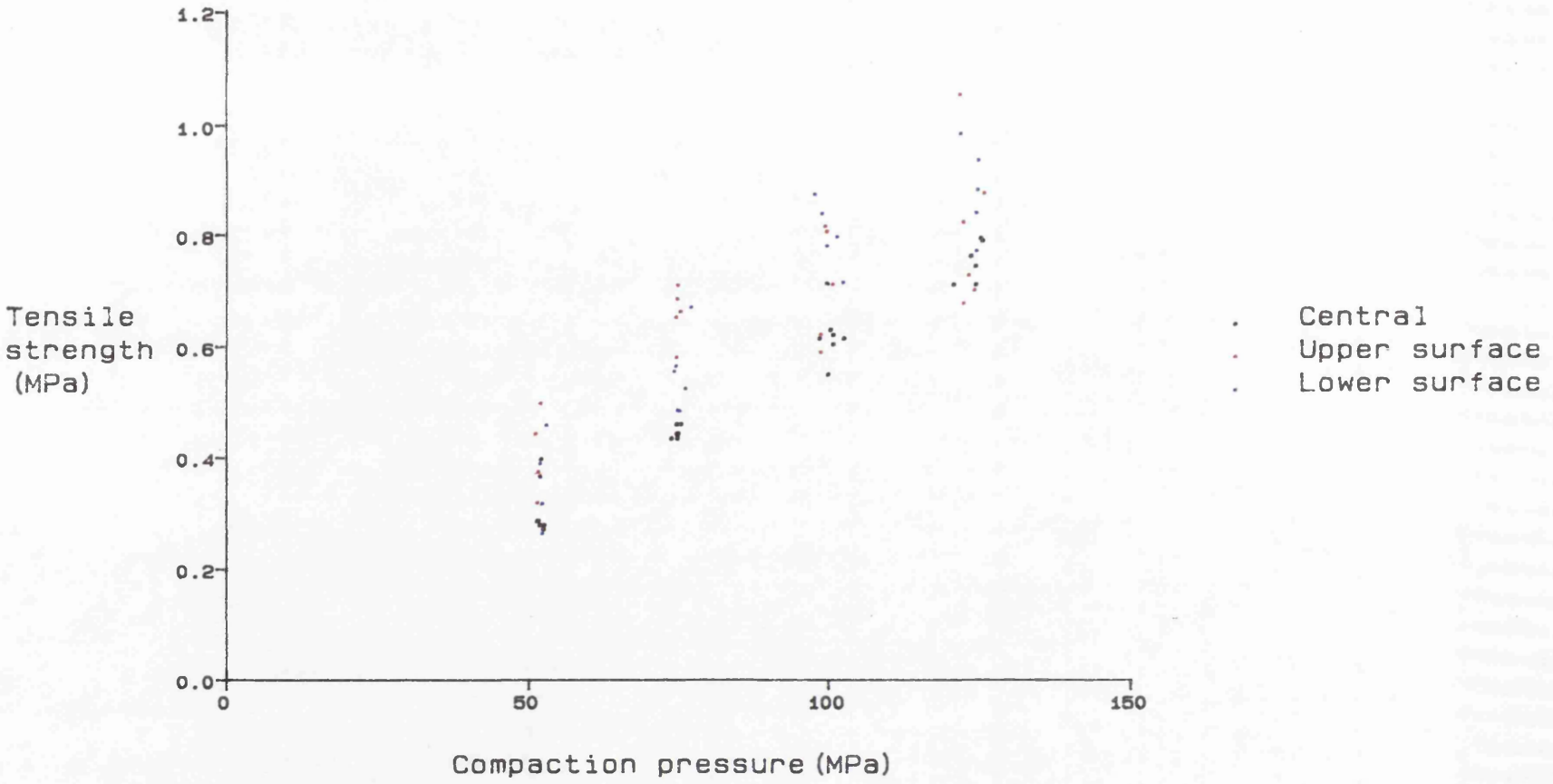

Theoretical thickness of compacts with zero porosity = 2.8mm
Compacts tested by transverse compression

Figure 3.58 Effect of platen position on the value of tensile strength obtained for 10mm square Emcompress compacts

to decrease as the compact thickness increased. The drop in force across the compacts was shown to be related to the contact area between the compact and the die wall. The R-value for Emcompress and Avicel compacts is thickness dependent for both circular and square compacts (Figures 3.59 and 3.60). Figure 3.61 illustrates the drop in force between the punches per unit area for 2 thicknesses of circular and square Emcompress compacts. The force loss per unit area remains constant for the two thicknesses of circles but increases substantially as the thickness of the square compacts increases.

Rubinstein and Moody (1985) investigated the distribution of Magnesium Stearate on the surface of compacts using X-Ray Photoelectron Spectroscopy. It was shown that the levels of Magnesium Stearate on the surface of the compacts adjacent to the die wall were up to 5 times the level expected if the lubricant was evenly distributed throughout the compact. Experiments were performed that indicated that the migration of the lubricant to the die wall was due to electrostatic forces. Electrostatic forces are related to distance by an inverse square law, i.e. the magnitude of the forces decrease rapidly as the distance between the charged particle increases. In a circular compact, assuming the electrostatic forces were constant around the circumference of the die, the migration of the Magnesium Stearate would be such that a uniform concentration would be present at the die wall. The geometry of the square die is such that the concentration of Magnesium Stearate along the faces of the square would be similar to the concentration found on the surface of the circular compacts. Near the corners of the square die a larger surface area of the

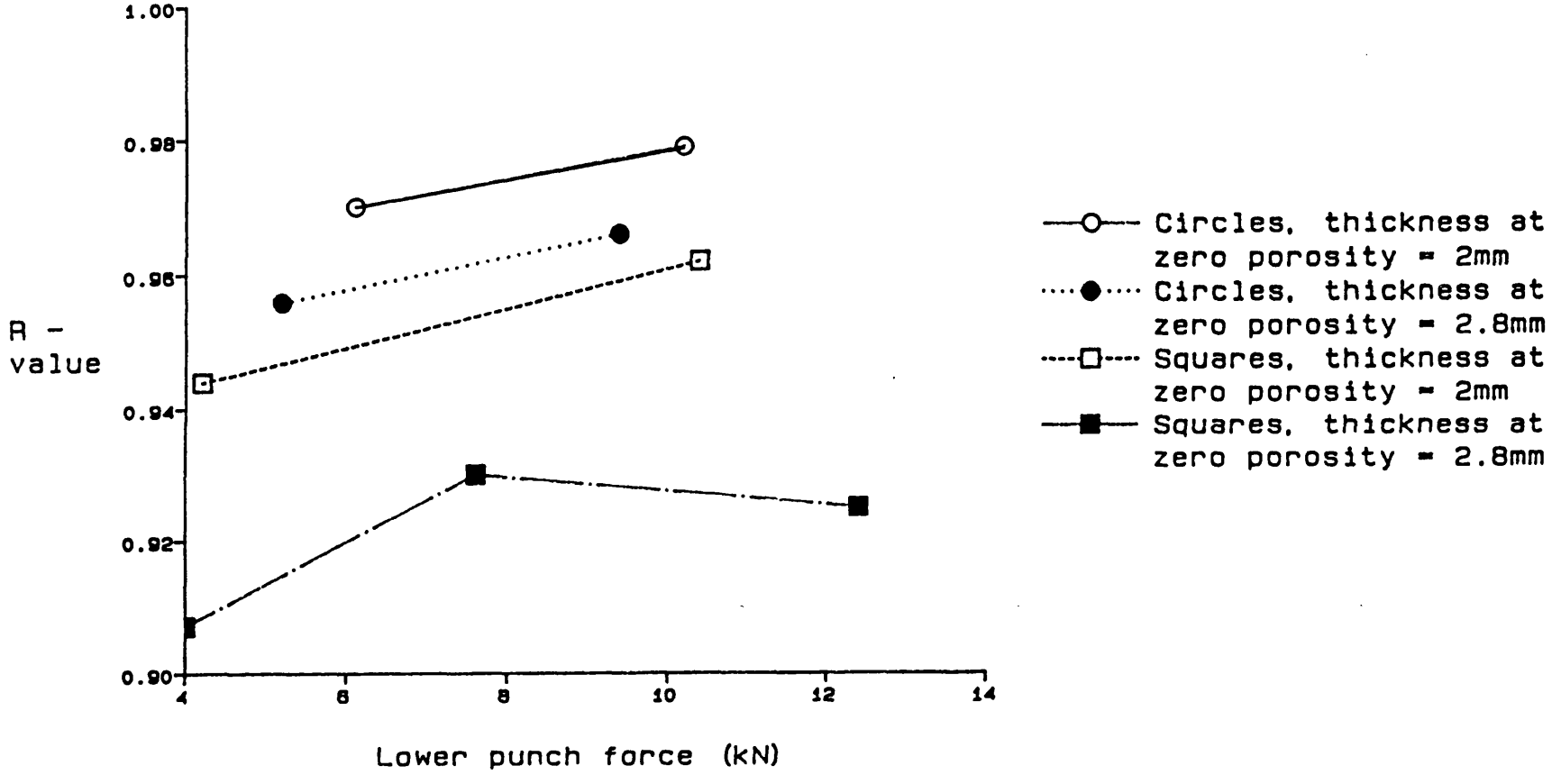

Figure 3.59 Effect of shape and thickness on the R-value of Avicel 10mm compacts

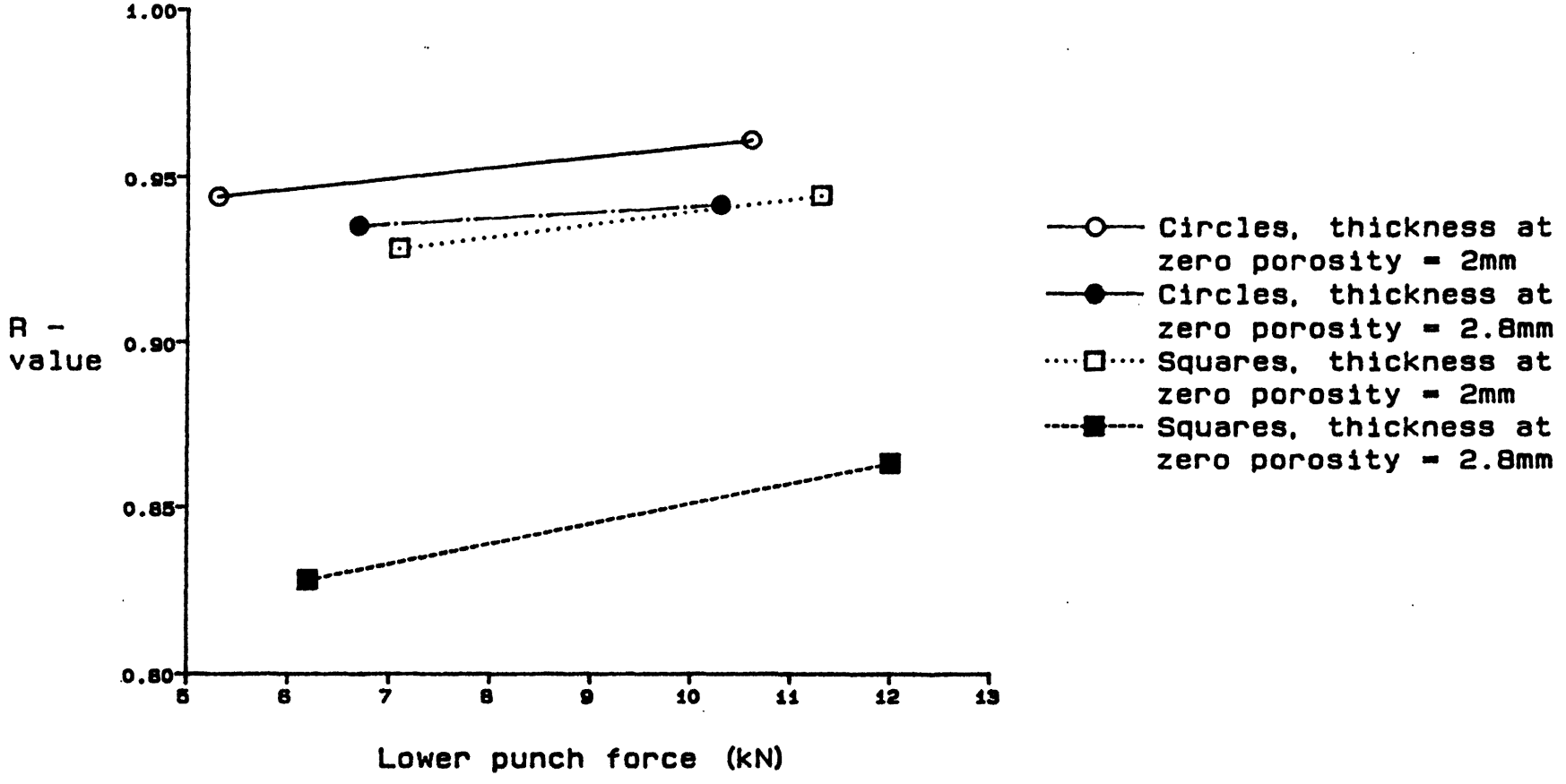

Figure 3.60 Effect of shape and thickness on the R-value of 10mm Emcompress compacts

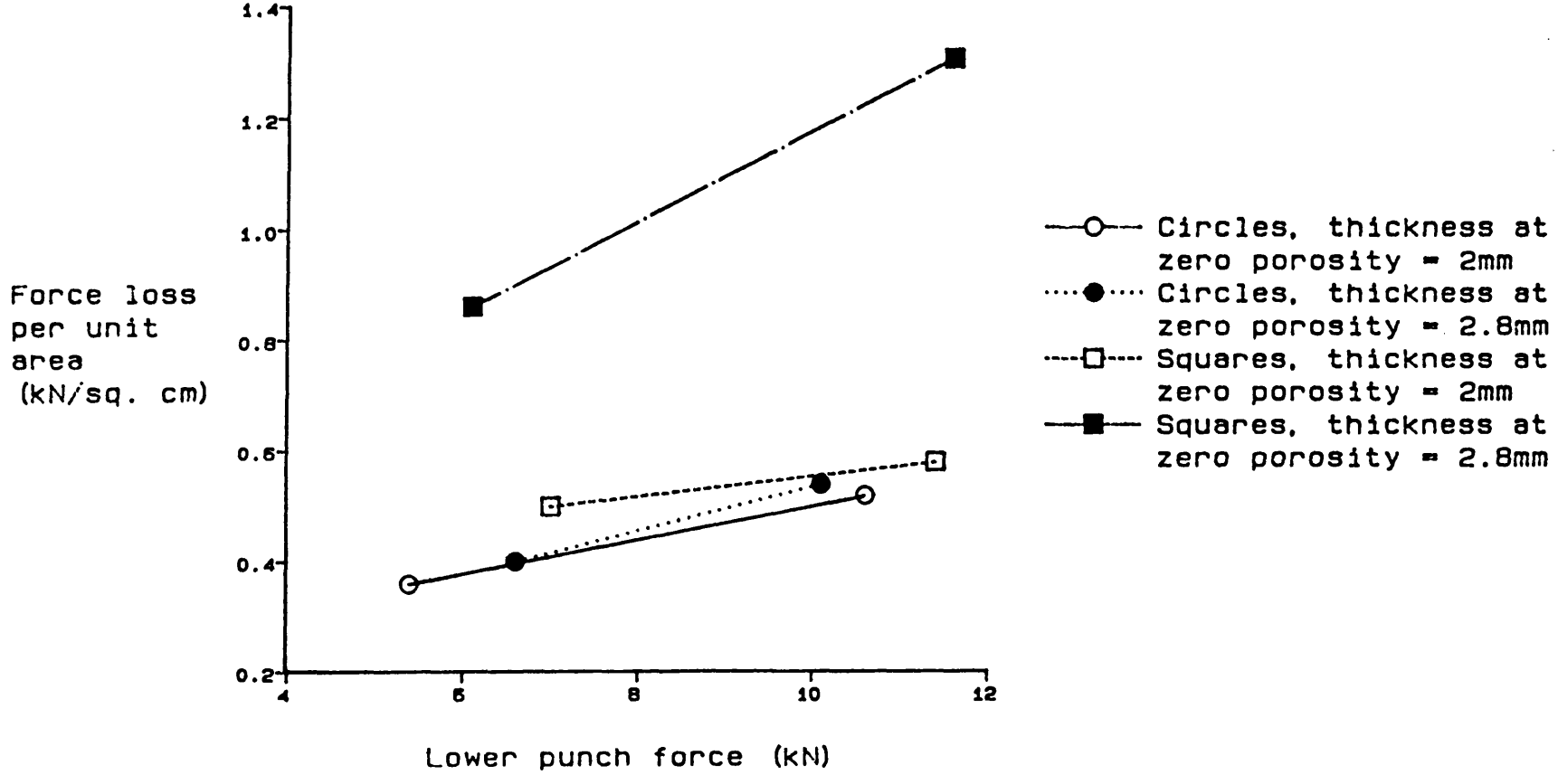

Figure 3.61 Effect of shape on the force loss/die area for Emcompress compacts

die will be competing for a smaller quantity of lubricant with the result that the concentration at the die wall will be reduced.

The low R-values for Emcompress square compacts, the appearance of square compacts with zero porosity thicknesses above 2.8mm and the difference in the axial compression results between the shaped compacts may all be due to the effectiveness of the lubricant at the die wall.The experiments preparing compacts with unlubricated Emcompress using tooling previously coated with Magnesium Stearate were performed to determine whether lack of lubricant in the corners of the square die was responsible for the problem. Unlubricated Emcompress compacts were compressed using tooling that had been painted with a saturated solution of Magnesium Stearate in acetone. The lubricant was not replaced between compressions so the level decreased as compacts were produced. The effect of this decrease in lubrication on the R-value and the tensile strength of the resultant compacts was assessed.As the initial level of lubricant applied was not controlled the experiment was repeated 10 times. The diametral compression test was used on compacts from five of these runs, the axial compression test on the remainder. The results for Emcompress are illustrated in Figure 3.62. As the lubricant level on the die wall decreases there is an increase in the upper punch pressure, a decrease in the lower punch pressure and an increase in the ejection force. The trend is common to the circular and square compacts but more pronounced with the latter. The axial compression test results decrease markedly as the R-value falls while the diametral compression results only decrease as the physical appearance of the compacts noticeably deteriorates.

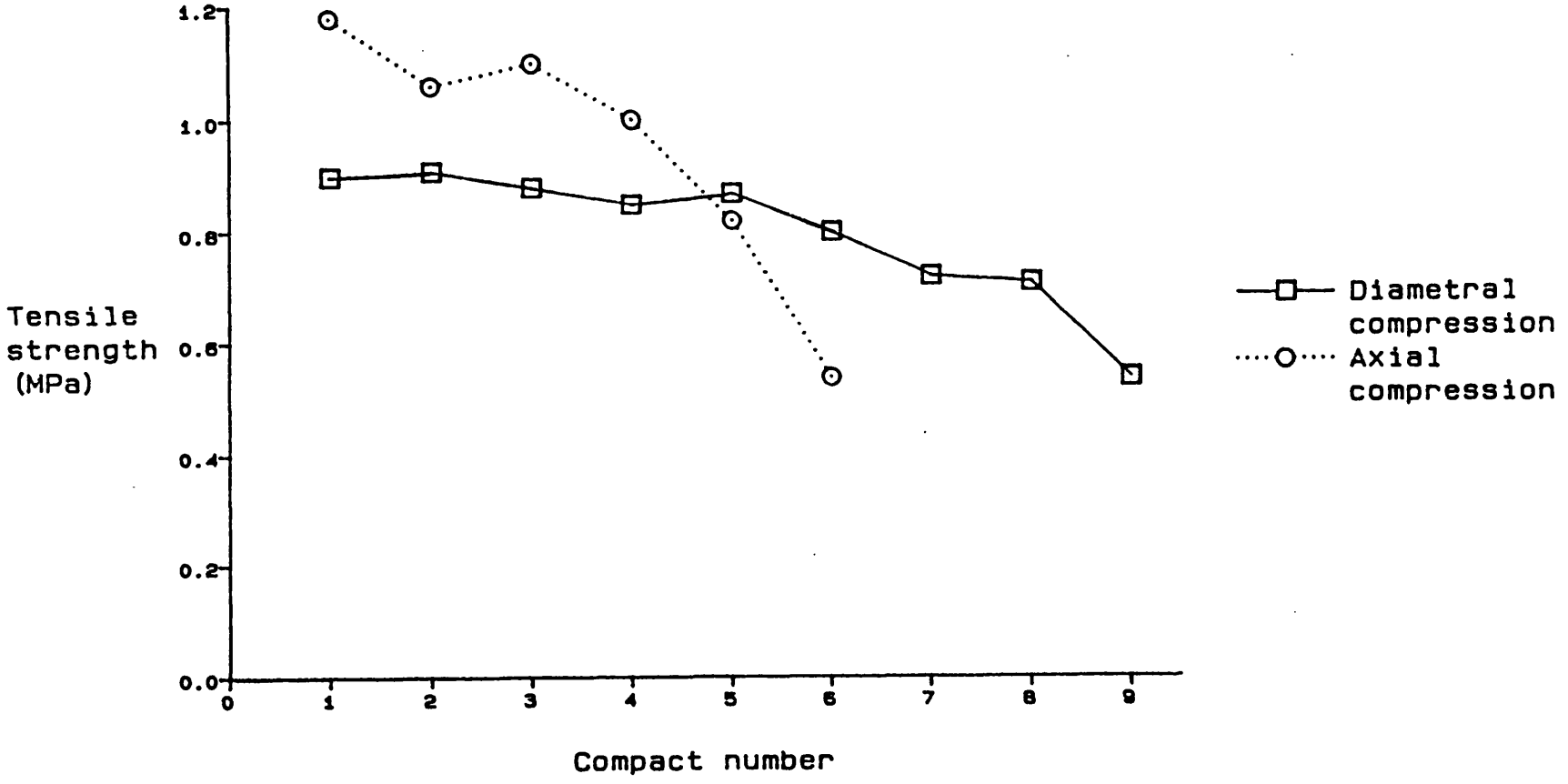

Lubricant applied to the die wall as a solution in acetone prior to compact number 1

Figure 3.62 Effect of diminishing die wall lubricant levels on the tensile strength of Emcompress 10mm square compacts

The running of unlubricated Avicel compacts produced a similar, but less pronounced, trend in the punch pressure levels (Figure 3.63). The axial compression results did not, however, decrease as the lubricant level dropped. Even when the thickness of the Avicel compacts was increased, resulting in a considerable drop in the R-value, the axial compression test results remained constant.

When applying the lubricant to the square die, care was taken to ensure that the corners were adequately coated. If the differences between square and circular compacts were solely due to a reduced level of lubricant in the corners they would be eliminated by the application of adequate lubricant. The rapid deterioration in the quality of the square compacts as the lubricant level diminished suggests that other factors are involved. To explain the changes that are occurring as the lubricant levels decrease it is necessary to consider what happens within a powder bed as a force is applied.

Macleod (1974) examined the density distributions present in compacts of uranium dioxide by contact autoradiography of longitudinal compact sections. A description of the relative movements of particles within the die and the resultant forces was proposed to explain the density distributions found. Figure 3.64 illustrates the proposed process. At the very early stage of compaction (Figure 3.64a) a pressure bulb exists. Immediately material begins to move at the die wall, adjacent to the upper punch, it dilates and expands away from the die wall. As frictional forces develop, densification begins and the process is repeated continuously in successive elements to the limit of the material movement. The extent of material movement is

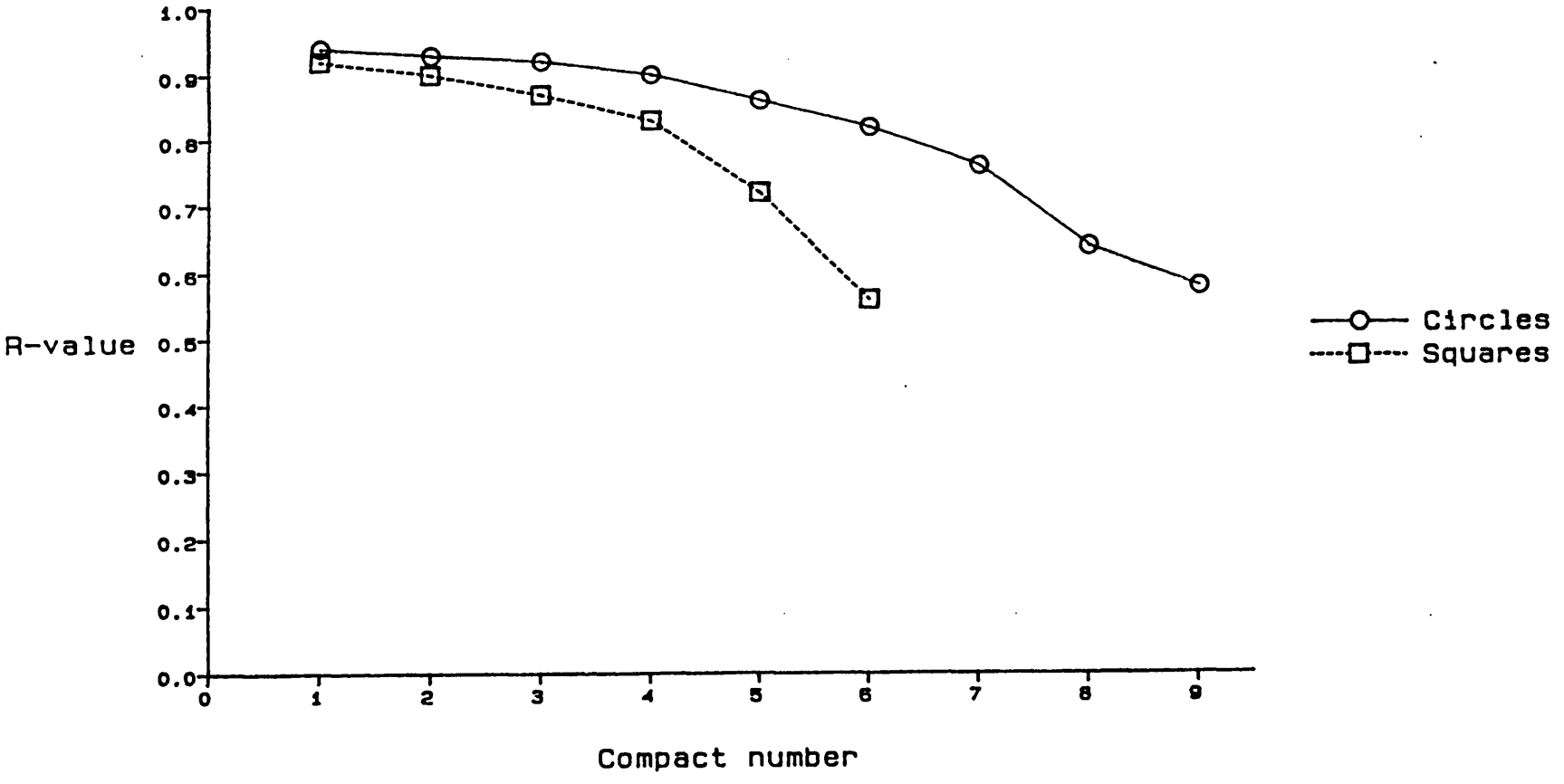

Lubricant applied to the die wall as a solution in Acetone prior to compact number 1

Figure 3.63 Effect of diminishing die wall lubricant levels on the R-values obtained when preparing 10mm Emcompress compacts

governed by the applied compaction pressure and by the resistance to inward movement produced by the densification and consequent tendency to outward movement at the axis of the compact (Figure 3.64b). Material on the compact axis is driven down into the unconsolidated material below it, exhibiting a hemispherical pressure front (Figure 3.64c). This process persists until the reaction from the lower punch exceeds the radial reaction from the die wall. Material from the centre begins to move outwards at the point of minimum radial pressure, which coincides approximately with the limit of material movement at the die wall (Figure 3.64d). This material has undergone less consolidation than material in the lower corners of the compact because of the predominance of the axial pressure front at this stage. The change of direction of powder movement induces high local forces which produce an area of high density just above the lower punch (Figure 3.64e). A secondary area of high density is formed between the primary area and the upper punch when the axial reaction from the primary area exceeds the radial pressure at any point between it and the moving punch.

The Emcompress compacts were prepared using a single machine setting. The position of the lower punch was identical for the circular and square compacts as was the penetration depth of the upper punch. As the lubricant on the die wall was reduced by successive compressions the resistance to movement of the adjacent Emcompress particles increased. The force required for the upper punch to overcome this resistance therefore increased. The larger frictional forces that need to be overcome result in a reduction in the proportion of the force reaching the lower

Figure 3.64
The development of density patterns within compacts
(after Macleod 1974)

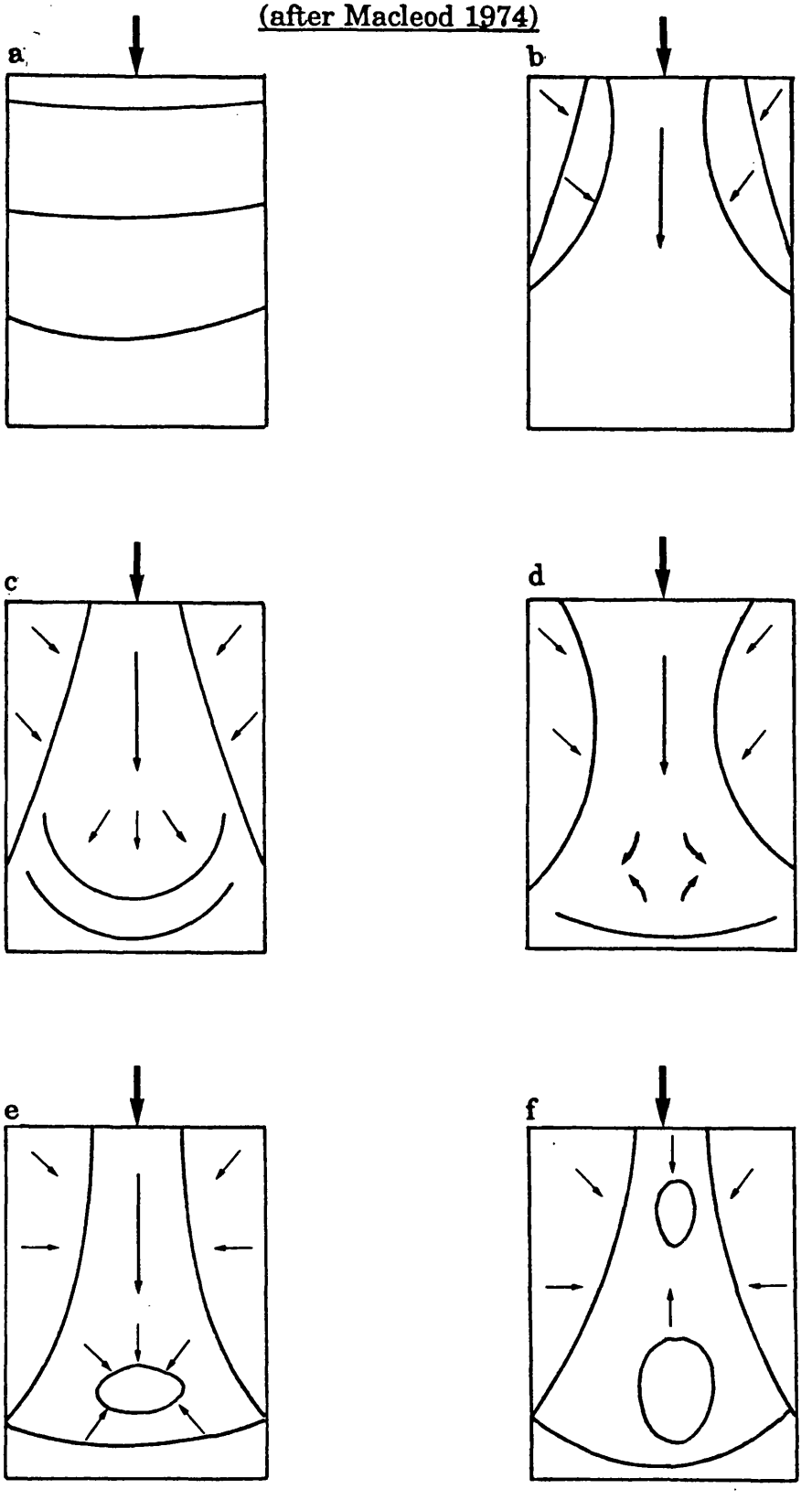

Arrows indicate the direction of the compacting forces

punch. One effect of increased frictional forces is to exaggerate the density variations within a compact. Macleod (1974) compared the density distributions in compacts prepared without lubricant, with an internal lubricant added and with die wall lubrication. The use of a combination of die wall lubrication and internal lubricant resulted in compacts with the lowest density variations, followed by die wall lubricant alone and then internal lubricant.

The square compacts of Emcompress require greater levels of Magnesium Stearate to be present on the die wall than circular compacts. This indicates that the die shape affects the ability of a material to flow under pressure. In a circular compact the resistance to movement will be constant around the circumference assuming a uniform level of lubricant is present. In the corners of a square die the area of material affected by die wall friction is increased by the presence of two surfaces. This effect will be exacerbated if the concentration of lubricant at the die wall is reduced in the corners.

The lower edges of circular compacts are formed primarily by the axial hemispherical pressure front as illustrated in Figure 3.64e. In a square compact the distance to the corners is greater and hence the force applied by the pressure front will be reduced. The combination of this reduced force with the effects of the increased die wall friction results in the production of compacts with areas of such low density that on removal of the upper punch the interparticulate forces are not sufficiently strong to maintain a coherent compact. The shape of the faults resemble the low density contours predicted by Macleod (1974).

The actual density variations seen by Macleod (1974) were relatively small. This is due to the density distributions being determined from the mean activity of large sections of the Uranium Dioxide compacts. The detection method was not sufficiently sensitive to allow small samples to be taken and any local variations in density would be disguised by the averaging out involved in the calculations. The reason for the apparent sensitivity of the axial compression test to the density differences in Emcompress compacts is unclear. Comparison of the regions exposed to the maximum tensile stress by diametral and axial compression does not reveal any areas of low density that would not be equally stressed by both methods. The failure of Emcompress to form coherent square compacts indicates that the local variations in density are considerable. The axial compression test may be more sensitive to these local variations.

The axial compression test is not solely a measure of poor force transmission. If this were the case the unlubricated Avicel compacts would be expected to produce different values for square and circular compacts as low R-values are obtained and the lower surface of the squares are noticeably softer than the upper surface. That differences are not seen may be due to the behaviour of Avicel during compaction or differences in the failure mechanism of Avicel in the compressive tests.

Avicel is known to have self lubricating properties and it is possible to prepare compacts on a single punch machine without any added lubricant. The Avicel should therefore be less sensitive to changes in lubricant levels in the corner of a square die. Such behaviour should reduce the density variations within the compact and it is likely that the extreme variations

that appear to be present in the Emcompress compacts would not be seen with Avicel.

Avicel and Emcompress are likely to behave differently under diametral compression. Mashadi and Newton (1987) examined the nature of failure of materials using high speed video techniques. Deforming materials such as Avicel were shown to fail initially at the centre of the compact with the crack spreading towards the platens. Crack initiation for a fragmenting material occurred near the platens moving into the centre. Such differences in the way failure occurs may alter the sensitivity of materials to density variations.

The density distributions may explain the effect of platen position on the transverse compression results. The lowest tensile strength values for the test were obtained when the platens were positioned centrally. Positioning the platens midway between the centre and either the upper or lower surface resulted in increased tensile strength values. Examination of the density distributions reveals that such tests involve the maximum tensile stresses occurring in the areas of highest density.

3.4 Conclusions

Circular, hexagonal and square compacts of a range of pharmaceutical excipients have been prepared using a single punch tablet machine and tested by the diametral compression test, axial compression test and transverse compression test.

The results of the tests were shown to be dependent on the shape of platen used. The differences were related to the width of contact between the

platen and compact. Increasing the contact width resulted in an increase in the mean tensile strength. Semicircular platens were shown to be suitable for comparing the tensile strengths of the circular and shaped compacts.

For the materials tested the compact shape did not affect the value of tensile strength obtained by the diametral compression test for compacts produced at the same compaction pressure.

Differences in the structure of square and circular compacts of Emcompress were detected by the axial compression test. These differences were attributed to an increase in the die wall friction with the square compacts. This increase in friction results in poor force transmission to the lower corners of the compact producing visible flaws. Such differences were not detected between the circular and square compacts of Avicel PH-102, Lactose DMV 100 or Anhydrous Lactose DCL 21.

CHAPTER 4

COMPACTION STUDIES USING THE ROTARY TABLET MACHINE

4.1 Introduction

The previous chapter examined the compaction properties of a number of materials using a single punch eccentric press. While such presses are still used extensively in product development almost all commercial tablet production is carried out on rotary machines, since they are capable of producing tablets at a much higher rate. The formation of compacts is achieved on both types of machine by compressing a powder in a die between two punches. The relative velocities and displacements of the punches do vary between machine types and may affect the compaction properties of materials. This Chapter examines the properties of Emcompress and Avicel PH-102 compacts produced on a Manesty D3B rotary tablet machine.

4.2 Materials and methods

4.2.1 Materials

Compaction studies were carried out using powder mixes of Avicel PH-102 and Emcompress, each lubricated with Magnesium Stearate. The 75 micrometre to 250 micrometre sieve fraction of Emcompress was used while the Avicel PH-102 was used as received. Mixes of the excipients with 1% Magnesium Stearate were prepared in the manner described in Section 3.3.2. Compacts of unlubricated Avicel PH-102 were also prepared.

4.2.2 Tooling

Two sets of tooling were used in the studies; 10mm diameter flat faced circular punches and flat faced square punches with an inscribed diameter of 10mm. The specifications for the surface hardness of the punches and

the punch/die clearances were the same as for the single punch machine tooling described in Section 3.2.3.

4.2.3 Force monitoring

The instrumentation of a rotary tablet machine to enable measurement of the forces involved in the compaction and ejection of compacts is less straightforward than for an eccentric single punch machine. In the latter the punches do not move relative to the punch holder assemblies. This allows the punch holders to be adapted to house the load measuring devices which can measure directly the forces applied. The relatively small movement of the punches during the compaction cycle allows connection to the data processing/acquisition devices to be made using appropriately screened cables.

On a rotary tablet machine the punches move within their holders and the force exerted on the punches is not transferred to the holders. When a rotary press is operated the punches pass between two stationary rollers exerting a force between them. This force is resisted by the frame, which is designed to maintain the rollers at a constant separation, and varying amounts of strain are thereby induced within the elements that constitute the frame. Measurement of the compaction forces can be achieved by either the direct measurement of the punch forces, using suitably gauged punches, or indirectly by measuring the strain on the frame.

The drawback with measuring the punch forces is that a suitable pathway is required from the rotating components to a stationary control unit. This problem has been approached in at least three ways; radio telemetry, rotary slip-ring gear and optical linkage.

Indirect measurement of the forces by monitoring the strain on part of the machine frame allows the signals generated to be passed to the control electronics by cable. The drawback of such a system is that the relationship between these strains and the forces at the punch tips is not always straightforward.

The instrumentation of a number of frame parts have been reported. Knoechel et al (1967) measured the compaction forces using gauged adjusting screws on the upper overload systems. In 1968 Goodhart et al published an account of the instrumentation of a Manesty Rotapress, concluding that the most satisfactory site was the upper end of the compression column, just below the pin supporting the upper roll carriage. The adjusting wheel eyebolts, which support the lower roll carriers on the Stokes BB2 press have been used (Wray 1969) and (Salpekar and Augsburger 1974). The tie rod, which joins the upper and lower roll carriages, has been a popular site; so too, in some machines, has been the end of the compression column where load washers can be used under the securing nuts. The roll pins, on which the compression rolls are mounted have been used (Ridgeway et al 1979). The roll pin itself may be gauged or the pin may be mounted on gauged supports.

The Manesty D3B machine used in this study was instrumented by modifying the eyebolt assembly to house a piezoelectric load cell. The cast iron eye bolt was replaced by a two piece hardened steel eyebolt between which a piezoelectric load cell (Kistler Instruments, type 9041) was mounted, under compression (Figure 4.1).

The ejection forces were measured using an instrumented ejection ramp.

Figure 4.1
Diagram illustrating the location of the piezoelectric load cell for monitoring compaction forces on a Manesty D3B rotary tablet machine

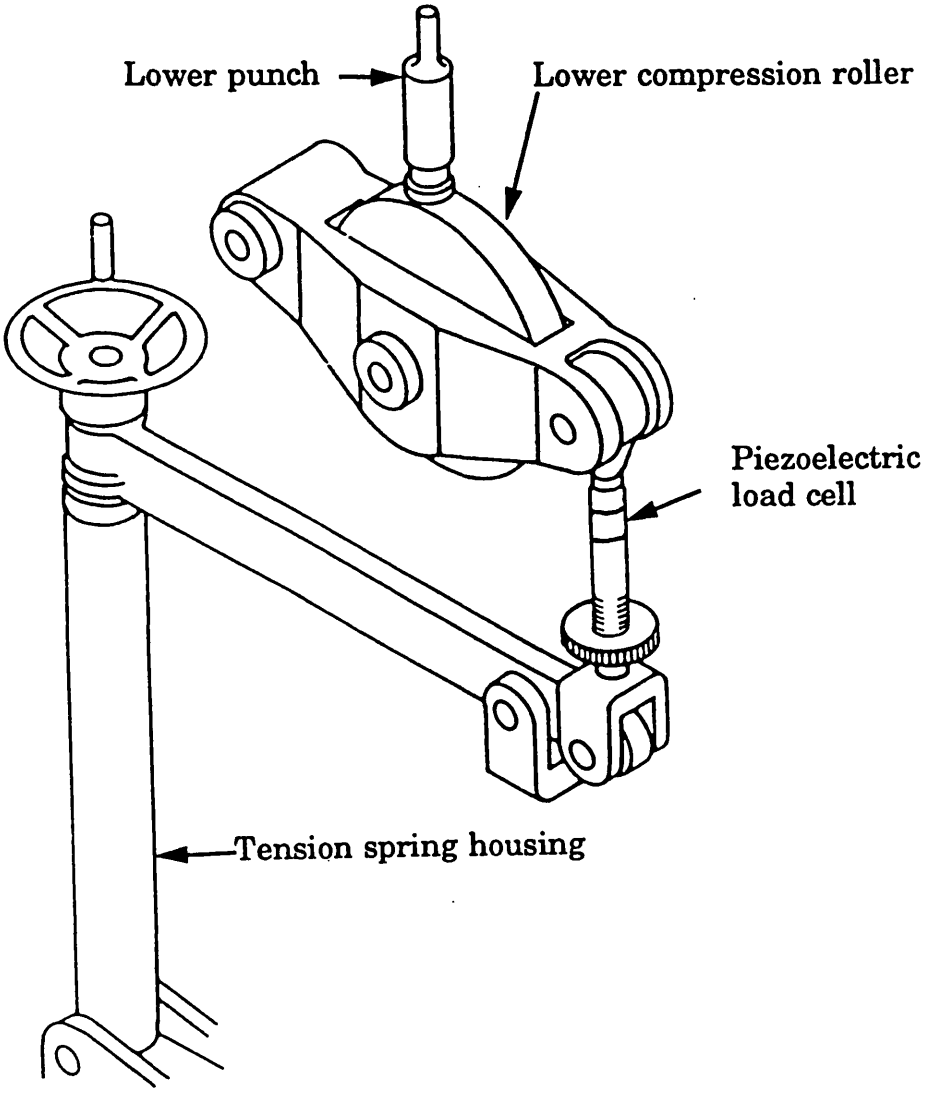

Early studies using such ramps (Knoechel et al 1967) were difficult to interpret as the loading on the gauged bolts varied continuously as the punch head moved along the ejection track. The ejection ramp used in this study was machined to allow 3 piezoelectric load cells (Kistler Instruments, type 9011) to be positioned on the underside (Figure 4.2). The ramp was bolted to the machine frame through the centre of the 3 load cells. The outputs of the load cells were wired in series and passed through the bolt hole of the original ejection ramp for connection to the charge amplifier. This approach overcomes the problem of positional variability, since the sum of the 3 signals will be independent of the point at which the load is applied. The ejection force for each punch can only be determined if one punch is on the ejection ramp at any one time. If a full complement of 16 punches were used up to 3 punches could be on the ejection ramp simultaneously and the output from the load cells would be the sum of the forces exerted by the 3 punch heads. In this study the machine was operated with just one station in position so the problem of summed responses did not occur.

Ridgway Watt and Rue (1980) reported that running a rotary tablet machine with only one station in use led to cyclic variations in tablet weight and compression force. This effect was attributed to overfilling of the feed frame. The machine used in that study, a Manesty Betapress, used a feed frame fitted with a feeder paddle. On such a machine, when the lower punch travels up the weight setting ramp at the filling stage it expels the excess powder back into the frame, underneath the rotating fingers of the feeder paddle. As the fingers pass over the top of the moving

dies, they partly obstruct the return flow of the powder and induce a small amount of pre-compression within the die. The cyclic variation of the weights could be correlated with the relative positions of the dies and feeder fingers. The Manesty D3B does not have a paddle feeder so such effects would not be anticipated. Nevertheless at the end of each run excess powder was removed from the feed frame to minimise any effect of overfilling. The compact weights and compaction forces did not reveal any trends involving weight change either during or between runs.

The load cell outputs were calibrated using short dummy punches between which a calibrated load cell was positioned. The machine was turned cautiously by hand in small increments, and simultaneous readings taken from the two transducer systems. The output from the load cell positioned in the eyebolt gave a linear response ($r = 0.98$) over the operating range of the tablet machine (0 to 50kN). The ratio of applied force to the measured force on the eyebolt was 0.356. The ejection load cells gave a linear response over the range 0 to 2.5kN ($r = 0.99$).

The outputs from the load cells were fed into charge amplifiers (Kistler Instruments, type 5054A) which convert the input charge to an output in the range of 0 to 10 volts. The load cell positioned in the eyebolt produced an output of 1.56pC per Newton of applied force and the charge amplifier was calibrated to give an output of 0.128mV per pC which corresponded to a 10 volt response for a force of 50kN. The summed output of the 3 load cells beneath the ejection ramp was 3.60pC per Newton and the charge amplifier was calibrated to give an output of 1.11mV per pC providing a range of 0 to 2.5kN.

Figure 4.2
Diagram of the ejection ramp modifications enabling the insertion of 3 piezoelectric load cells

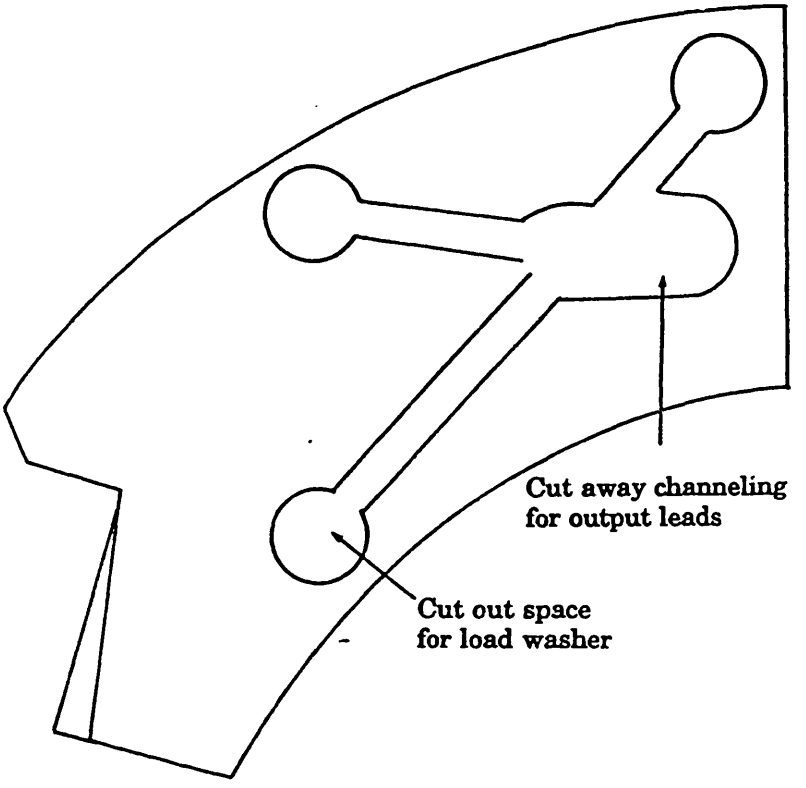

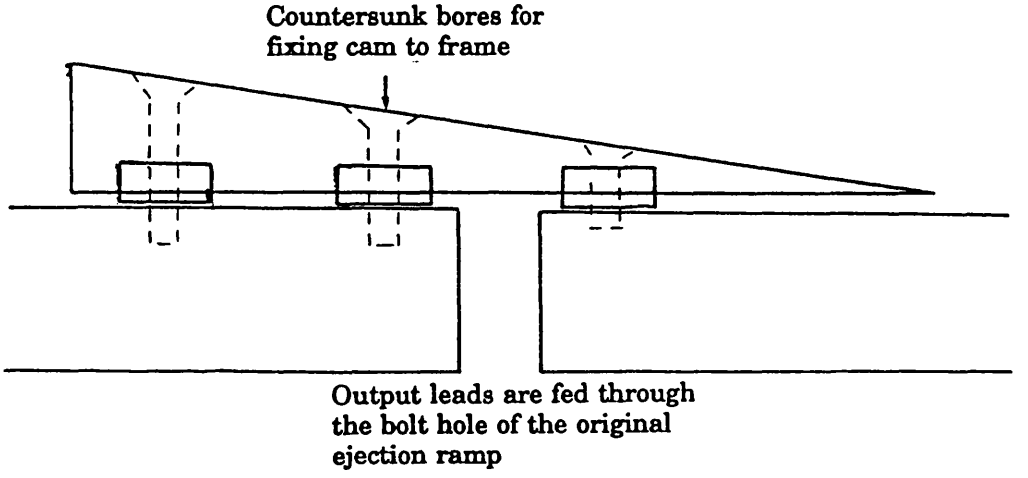

Data collection was performed using either an IBM PC XT fitted with a 12 bit analogue to digital convertor or a Digital Storage Oscilloscope (Gould Electronics, type 1602). To permit comparison of square and circular compacts the force measurements were converted to pressures by dividing by the surface area of the punch faces.

4.2.4 Preparation of compacts

The aim of this section of work was to prepare compacts on the rotary machine that could be compared with the compacts previously prepared on the single punch machine. The compression weights used for the two materials were, therefore, kept as close as possible to those used in the earlier studies. The maximum depth of fill on the rotary machine is smaller than on the single punch and it was not possible to prepare compacts of Emcompress with a zero porosity thickness of 6mm. The largest compacts produced on the rotary machine had a zero porosity thickness of 5mm. The full range of compacts produced are listed in Table 4.1.

The powder mixes were compacted by running the Manesty D3B machine under power with one set of tooling in position, the remaining 15 positions on the die table being fitted with blank dies. The machine was run at a speed of 24 r.p.m.(see Section 5.2.2). With the software in the "set-up" mode the compaction force was adjusted to the desired value and the data capture mode initiated. The compacts produced over an 18 second period were collected in the order they were produced and the values of their peak compaction and ejection forces recorded.

Lubricated and unlubricated compacts of Avicel PH-102 were also prepared

Table 4.1

Compression weights of excipients used in rotary machine studies

Material	Zero porosity thickness (mm)	Compression weight (mg)	
		Circle	Square
Avicel	2.0	245	312
	2.8	343	437
	3.2	392	499
Emcompress	2.0	361	460
	5.0	903	1150

by running the machine under power and collecting the compaction data on the digital storage oscilloscope.

All the compression work was performed in an environment where the temperature was controlled between 17°C and 22°C and the relative humidity was in the range of 30-45% RH.

4.2.5. Compact storage

After preparation all compacts were stored as before in tightly closed amber glass bottles for a period of 14 days prior to testing.

4.2.6 Testing the compacts

The compacts were tested in the same manner as those produced on the single punch machine. Due to the speed of the rotary machine and the presence of just one set of tooling only 8 compacts were produced at each compaction force during each data collection period, so all compacts were tested. Batches where the coefficient of weight variation exceeded 1% were excluded from tests.

4.2.6.1 Diametral compression test

The circular and square compacts were tested by diametral compression using semicircular platens by the method described in Section 2.2.5.

4.2.6.2. Axial compression test

The circular and square compacts were tested by axial compression using the method described in Section 3.2.7.2.

4.3 Results and discussion

4.3.1 Compact appearance

Satisfactory Emcompress compacts were produced with square and circular tooling over the range of compression weights and pressures tested.

Lubricated Avicel compacts were prepared satisfactorily at low compaction pressures. As the compaction pressure increased both circular compacts and square compacts exhibited laminar cracks approximately halfway between their upper surface and centre. Unlubricated compacts of Avicel could be produced over the range of compaction pressures tested (0 to 300MPa).

The capping pressures for the two shapes (defined here as the pressure at which laminar failure is visibly apparent following ejection) were determined by running the tablet machine under power and slowly increasing the compaction pressure until failure occurred. The results indicated that capping occurs at pressures of about 110MPa for the circular compacts and at about 160MPa for square compacts. Ritter and Sucker (1980) reported the capping of compacts of Avicel PH-102 lubricated with 1% Magnesium Stearate prepared on a rotary machine. The capping tendency was related to the compaction pressure, reaching a maximum at 175MPa. At higher pressures it was possible to produce intact compacts. Such a reduction in the capping tendency was not detected in the present study where increases in the compaction pressure up to 300MPa resulted in an increase in the number of laminar flaws per compact.

Capping occurs when a material is unable to relieve stresses present within a compact following compression by plastic deformation (Hiestand

1984). The nature and cause of such stresses has been the subject of many studies. Apart from the intrinsic properties of the material being compressed the presence of entrapped air within a compact has been implicated. Mann et al (1981) provided evidence that the capping pressure for a given formulation could be related to the clearance between the punch and die. The circular and square punches used in this study were manufactured to produce similar clearances. Furthermore the clearances were the same for both the single punch and rotary machines. As capping only occurred in this study on the rotary machine, and there is a substantial difference in the capping pressures of the circular and square compacts, it is unlikely that air entrapment is responsible in this example. When a material is compressed within a die by means of two opposing punches, the axial load that is applied through the upper punch is transmitted to the die as a shearing force. In addition, force is transmitted radially to the die wall. The nature of this radial force is determined by the elastic or plastic behaviour of the compact. On removal of the upper punch there will be a degree of axial elastic recovery resulting in expansion of the compact within the die. Following ejection expansion may also occur in a radial direction. This elastic recovery is considered to be the most likely cause of capping.

Train (1956) attributed capping to the strain imposed by elastic recovery of the areas of high density within the compact on ejection. Milosovich (1963) postulated that capping was due to the expansion of elastically deformed particles and the subsequent rupture of interparticulate bonds. This proposal was supported by the observation that capping occurs in a

peripheral ring parallel and near to the upper surface, i.e. at the points of greatest pressure and elastic deformation. Carless and Leigh (1974) showed that the granulation of paracetamol with binders that eliminated capping resulted in both an increase in residual die wall pressure and a decrease in elastic recovery. Elastic recovery following the removal of the upper punch is therefore considered the most likely cause of capping. Capping will occur if the stresses caused by the elastic recovery are sufficient to rupture the interparticulate bonds formed during the compaction process.

Attempts have been made to predict the capping tendencies of materials. Krycer et al (1982) proposed a Capping Index, C, defined as the slope of the percentage elastic recovery versus radial die wall pressure. Nyström et al (1978) compared the axial and radial tensile strengths of different compacts. It was proposed that the ratio of axial to radial tensile strength should be close to unity for a good formulation. Malamataris et al (1984) proposed that the ratio of elastic recovery to plastic compression was a useful parameter to measure capping tendency.

Capping was initially thought to occur on ejection of the compact from the die (Train 1956). Rue et al (1979) measured acoustic emissions from compacts during compaction cycles and were able to correlate the incidence of capping to an acoustic signal that appeared immediately after compaction. This finding suggests that capping occurs within the die and not on ejection. As a general rule it could be said that capping within the die is associated with uniaxial relaxation while capping outside the die as the compact is ejected may take place when the relaxation is anisotropic.

The role of die shape on the capping process in Avicel compacts is unclear. If capping occurs due to uniaxial recovery the square die may reduce the capping tendency by restricting movement due to possible increased die wall friction due to the increased die wall surface area. Alternatively the increased resistance to movement at the die wall during the compression of the powder bed may produce areas of low density within the square compacts that could act as a pressure relief system for the tightly compressed central core of the compact. On the single punch machine the ratio of the upper to lower punch pressures was used as an indication of the die wall friction during the compaction cycle. On the rotary machine only one load cell is used to measure compaction pressures so such measurements were not feasible. Furthermore, as both punches move on the rotary machine the force loss due to die wall friction would not necessarily be represented by differences in the punch pressures. This will be discussed further in Chapter 5.

4.3.2 Diametral compression

The results are summarised in Tables 4.2 and 4.3 while the compaction pressure/tensile strength profiles of the Avicel and Emcompress compacts are presented in Figures 4.3 to 4.8. As with the compacts produced using the single punch machine the variance in the tensile strength values tended to increase with the compaction pressure. A weighted linear regression, using the reciprocal of the variance as the weighting, was performed on the results and the regression coefficients are presented in Table 4.4. Two sets of values are given for some of the Avicel results where the tensile strength values at the higher compaction pressures deviate

Table 4.2
Summary of diametral compression data for Emcompress compacts prepared on the Manesty D3B rotary tablet machine

Compact shape	Zero porosity thickness (mm)	Mean compaction pressure (MPa)	Mean compact thickness (mm)	Mean breaking load (kg)	Mean tensile strength (MPa)	Mean porosity
Circle	2.0	64.7	2.64	1.59	0.38	0.238
		98.7	2.49	2.53	0.63	0.201
		123.8	2.45	3.21	0.82	0.184
		159.7	2.38	4.14	1.08	0.159
		184.2	2.35	4.76	1.26	0.152
		261.4	2.30	6.59	1.79	0.126
		316.7	2.27	7.91	2.19	0.113
Circle	5.0	61.6	6.50	3.13	0.30	0.237
		93.4	6.23	4.84	0.48	0.203
		124.9	6.03	6.39	0.66	0.181
		158.1	5.93	8.43	0.89	0.165
		189.2	5.85	9.93	1.06	0.152
		251.8	5.69	14.86	1.63	0.131
		314.0	5.62	17.73	1.97	0.117
Square	2.0	50.0	2.65	1.29	0.30	0.246
		75.6	2.54	1.90	0.47	0.216
		97.8	2.49	2.44	0.61	0.199
		122.8	2.43	2.99	0.77	0.180
		145.7	2.38	3.84	1.01	0.162
		193.7	2.34	4.33	1.16	0.146
		256.9	2.29	5.99	1.63	0.127
Square	5.0	34.5	7.11	1.63	0.14	0.298
		51.4	6.77	2.00	0.18	0.260
		77.7	6.44	3.03	0.29	0.223
		100.2	6.28	3.96	0.39	0.203
		129.4	6.15	5.17	0.54	0.183
		157.3	6.05	6.03	0.65	0.169
		210.6	5.89	7.87	0.88	0.147
		247.1	5.79	10.88	1.8	0.133

Table 4.3
Summary of diametral compression data for Avicel compacts prepared on the Manesty D3B rotary tablet machine

Compact shape	Zero porosity thickness (mm)	Mean compaction pressure (MPa)	Mean compact thickness (mm)	Mean breaking load (kg)	Mean tensile strength (MPa)	Mean porosity
Circle	2.0	49.8	3.09	1.64	0.33	0.329
		68.8	2.82	2.93	0.65	0.257
		101.3	2.52	3.93	0.97	0.183
Circle	2.8	50.2	4.18	2.34	0.35	0.317
		64.1	3.79	3.47	0.57	0.264
		100.5	3.44	5.93	1.08	0.186
Circle	3.2	51.4	4.73	3.00	0.40	0.314
		67.1	4.35	4.81	0.69	0.259
		99.6	4.05	6.44	0.99	0.194
Square	2.0	38.7	3.19	1.20	0.24	0.369
		52.2	2.90	1.89	0.41	0.305
		74.7	2.66	3.00	0.70	0.240
		101.2	2.47	4.23	1.07	0.188
		124.9	2.42	4.24	1.09	0.164
Square	2.8	36.6	4.53	1.53	0.21	0.386
		53.9	3.99	3.07	0.48	0.302
		82.1	3.58	5.26	0.92	0.216
		108.3	3.36	7.11	1.32	0.170
		125.2	3.27	7.74	1.48	0.151
		154.6	3.24	6.94	1.34	0.144
Square	3.2	39.2	5.13	2.32	0.27	0.439
		60.2	4.51	4.60	0.64	0.363
		75.9	4.14	5.86	0.88	0.320
		102.8	3.95	8.69	1.37	0.274
		120.2	3.76	9.91	1.65	0.251
		158.6	3.77	10.04	1.66	0.239

Table 4.4

Weighted linear regression data for compacts prepared on the Manesty D3B rotary tablet machine and tested by diametral compression

Material	Compact shape	Zero porosity thickness (mm)	Intercept (MPa)	Slope	Regression coefficient
Avicel	Circle	2.0	-0.298	1.27×10^{-2}	0.972
	Circle	2.8	-0.341	1.41×10^{-2}	0.979
	Circle	3.2	-0.204	1.23×10^{-2}	0.954
	Square	2.0	-0.241	1.23×10^{-2}	0.979
	Square[1]	2.0	-0.289	1.34×10^{-2}	0.995
	Square	2.8	-0.218	1.22×10^{-2}	0.971
	Square[2]	2.8	-0.356	1.55×10^{-2}	0.997
	Square	3.2	-0.370	1.65×10^{-2}	0.991
	Square[3]	3.2	-0.393	1.69×10^{-2}	0.996
Emcompress	Circle	2.0	-0.0860	7.24×10^{-3}	0.998
	Circle	5.0	-0.0935	6.31×10^{-3}	0.986
	Square	2.0	-0.0150	6.38×10^{-3}	0.995
	Square	5.0	-0.0409	4.37×10^{-3}	0.995

1. Based on data obtained at compaction pressures up to 105MPa.

2. Based on data obtained at compaction pressures up to 115MPa.

3. Based on data obtained at compaction pressures up to 123MPa.

from linearity, the second values presented are regression coefficients for the linear portion of the profiles. The gradients of the lines obtained for different shaped compacts were compared by analysis of covariance as described in Section 3.2.8.2

The compact shape does not influence the compaction pressure/tensile strength profile of Avicel compacts below the capping pressure for circular compacts (Figures 4.3 to 4.5). Tensile strength results are not presented for compacts that did not fail in tension under diametral compression. Compacts that had capped were not tested.

Comparison of the compaction pressure/tensile strength profiles of unlubricated Avicel with lubricated material implicates Magnesium Stearate in the capping process (Figure 4.6) The deleterious effect of Magnesium Stearate on the tensile strength of Avicel compacts is well documented (Jarosz and Parrot 1984).The strength of compact depends on the area of intimate contact between the particles. The strongest bonds are formed between clean surfaces so the addition of the lubricant interferes by acting as a physical barrier between the Avicel particles. The role that Magnesium Stearate plays in the capping process is to weaken the bonds formed by plastic deformation thus altering the ratio of elastic recovery to plastic compression. Elastic recovery stresses will also be present in the unlubricated compacts of Avicel but in such compacts the bonds produced by plastic deformation are strong enough to withstand them. A comparison of the effects of Magnesium Stearate on Emcompress compaction properties could not be performed in the same manner because Emcompress does not have any lubricant properties of its own and could not be run on the

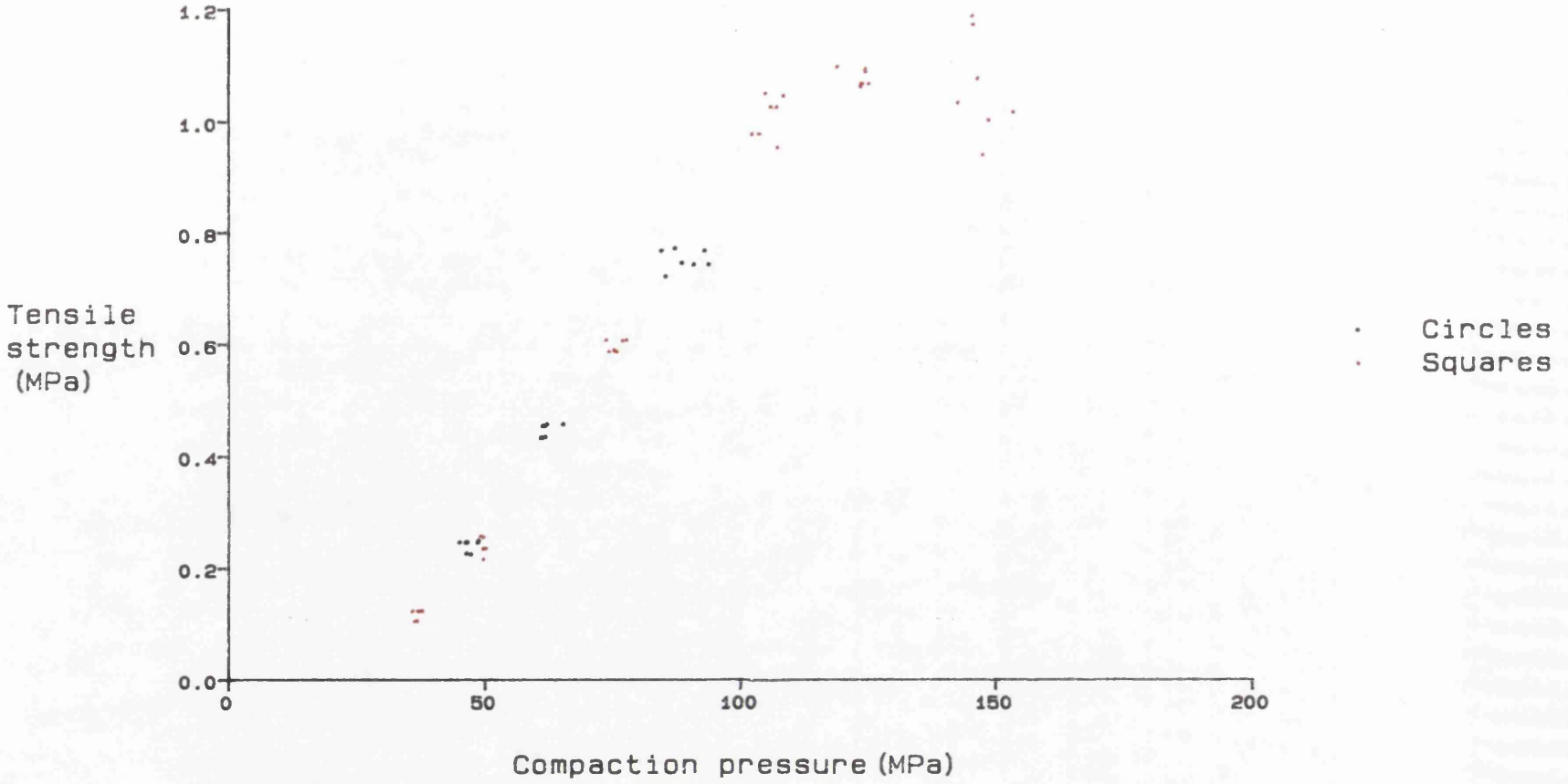

Compacts tested by diametral compression.
Theoretical thickness of compacts with zero porosity = 2.0mm.

Figure 4.3 Effect of shape on the compaction pressure/tensile strength profile of Avicel compacts produced on a rotary tablet machine

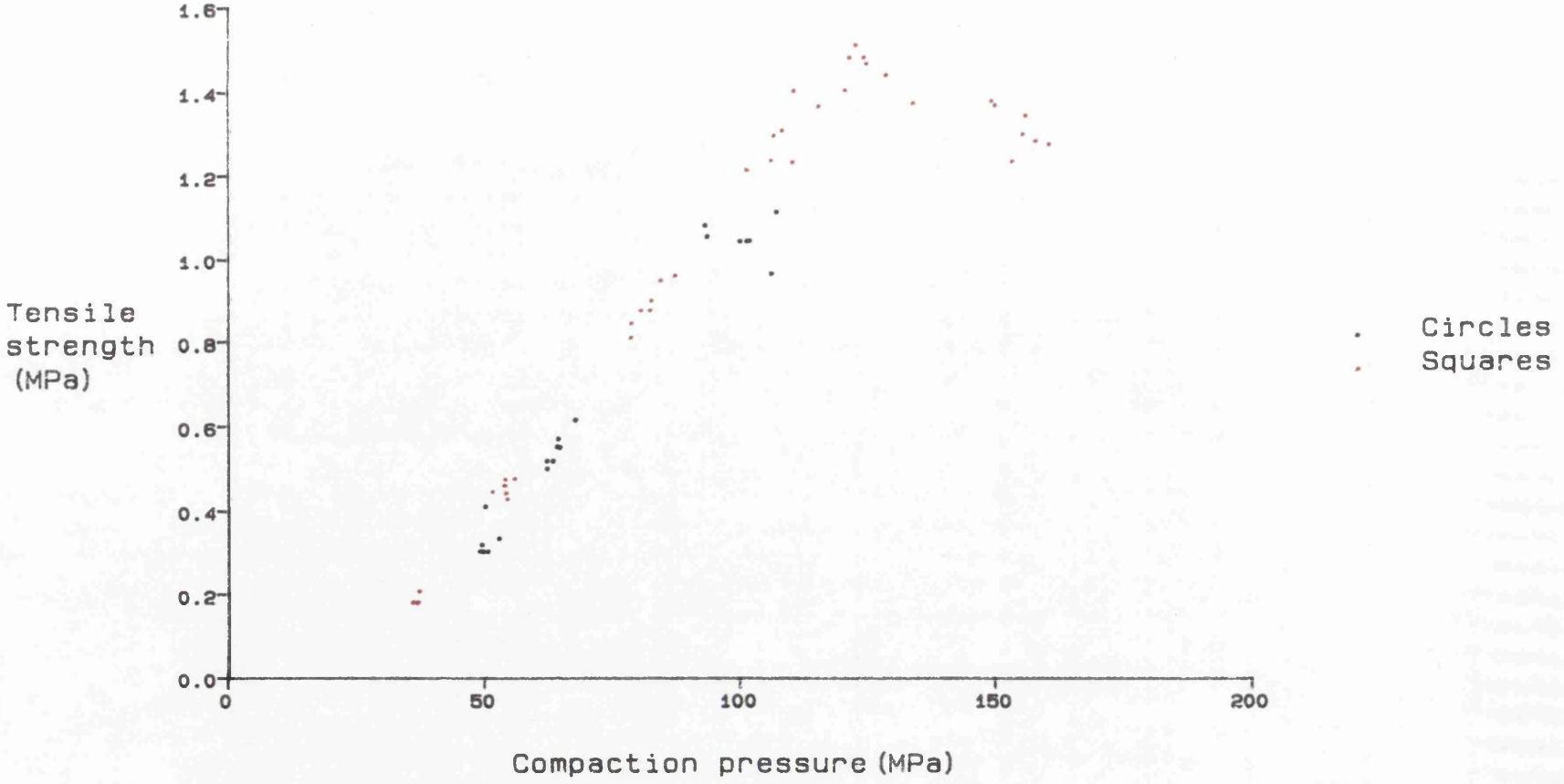

Compacts tested by diametral compression.
Theoretical thickness of compacts with zero porosity = 2.8mm.

Figure 4.4 Effect of shape on the compaction pressure/tensile strength profile of Avicel compacts produced on a rotary tablet machine

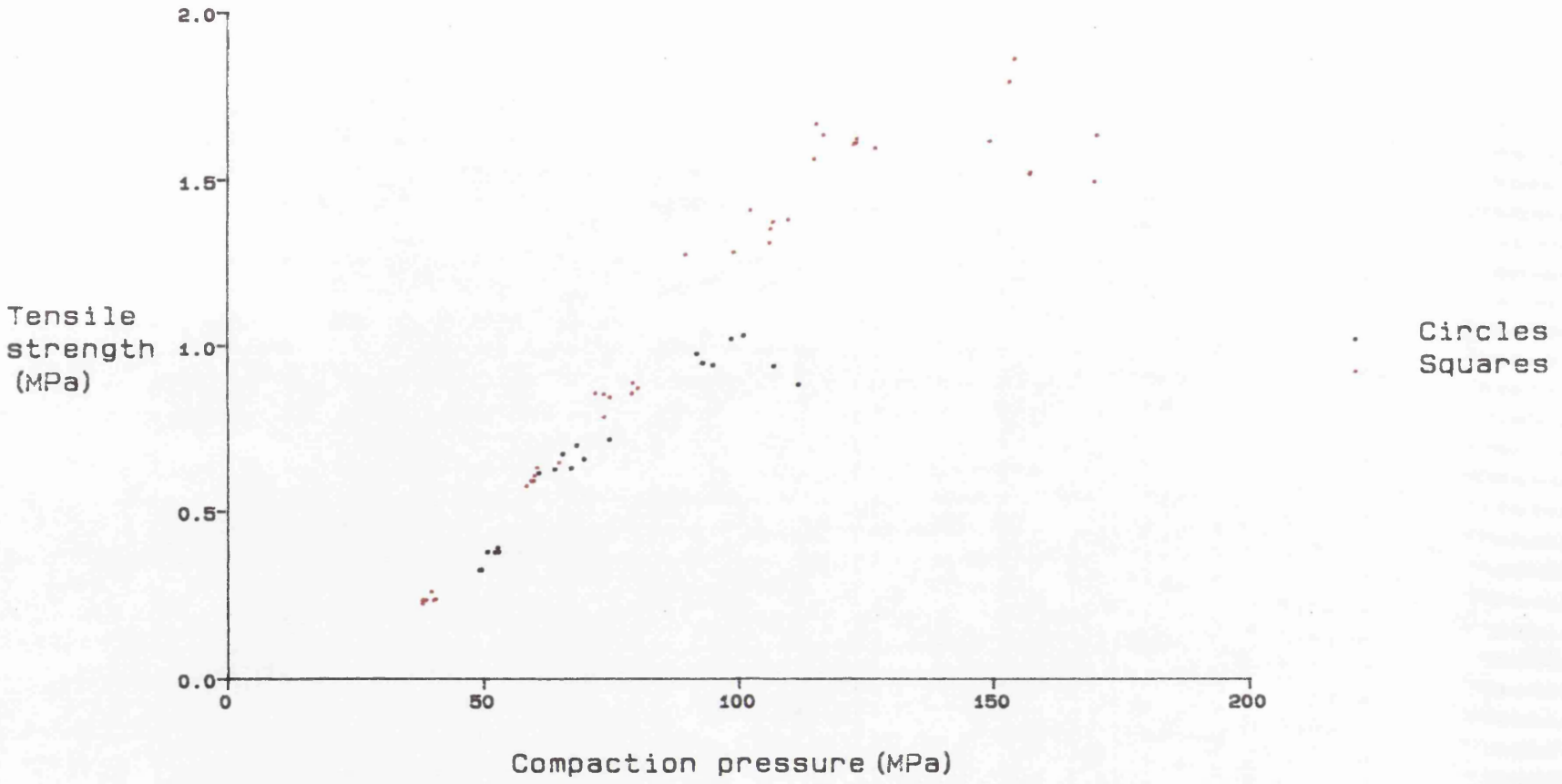

Compacts tested by diametral compression.
Theoretical thickness of compacts with zero porosity = 3.2mm.

Figure 4.5 Effect of shape on the compaction pressure/tensile strength profile of Avicel compacts produced on a the rotary tablet machine

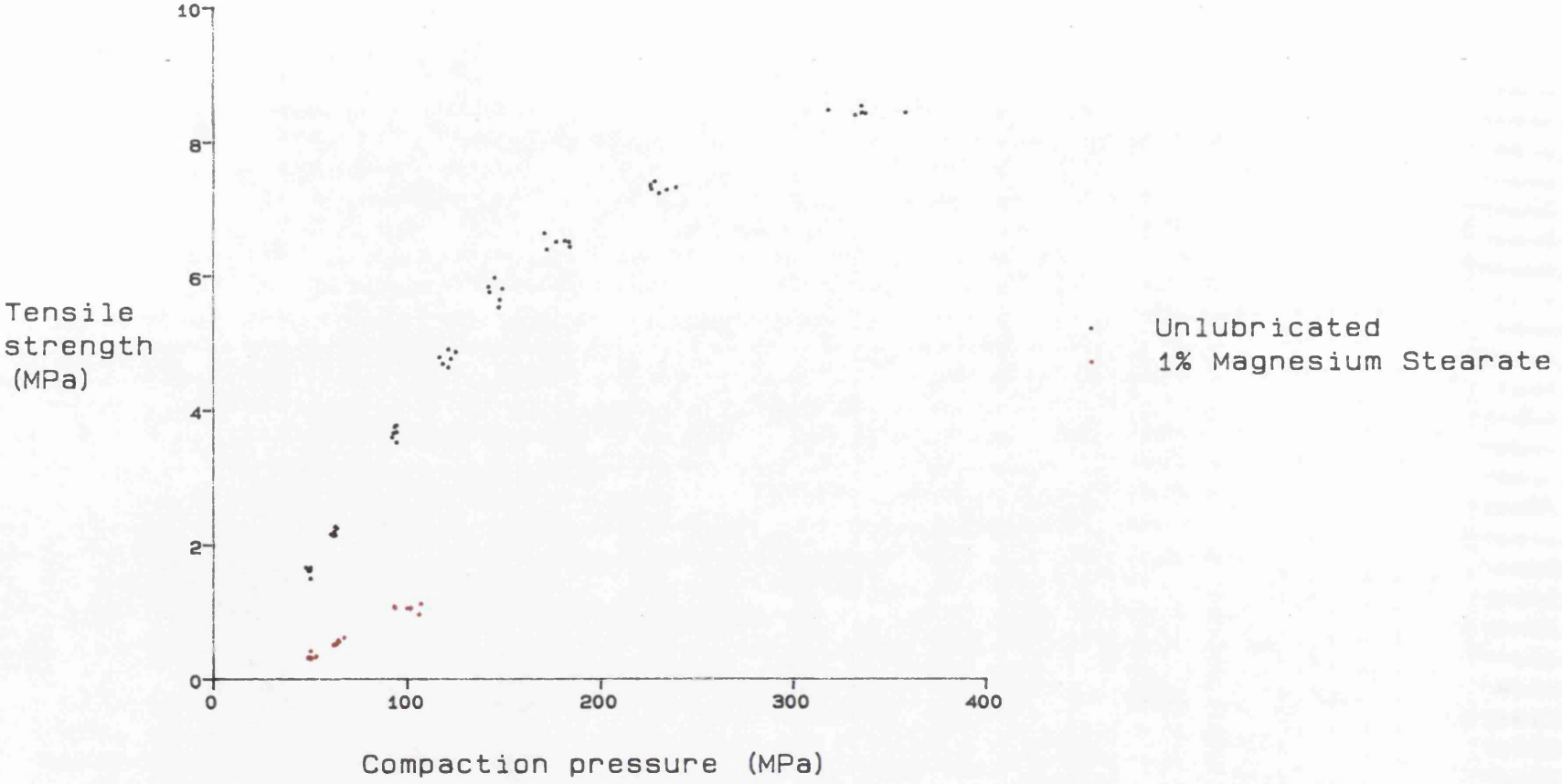

Compacts tested by diametral compression.
Theoretical thickness of compacts with zero porosity = 2.8mm.

Figure 4.6 Effect of Magnesium Stearate on the compaction pressure/tensile strength profile of Avicel circular compacts produced on a rotary tablet machine

machine without an external lubricant present.

The Emcompress compacts with a zero porosity thickness of 2mm produce similar compaction pressure/tensile strength profiles for squares and circles (Figure 4.7). The compacts with a zero porosity thickness of 5mm did show significant ($p > 0.05$) shape differences with the circular compacts producing stronger compacts than the squares (Figure 4.8). Plots of log diametral tensile strength versus porosity (Figure 4.9) indicate that there is a difference in the strengths of compacts of the two shapes with similar porosities. These results indicate that under the compaction conditions exerted by the rotary machine the shape of the tooling does influence the structure of the final compact for Emcompress.

The thickness of the compact affects the tensile strength of Emcompress compacts prepared at similar pressures (Figures 4.10 and 4.11). As the thickness increases the tensile strength decreases. This relationship is true for both square and circular compacts. This differs from the single punch machine work where the tensile strength, derived by diametral compression, of Emcompress compacts produced using a given compaction pressure appeared to be independent of compact thickness. The tensile strength values for Avicel circular compacts (Figure 4.12) are not thickness dependent. The Avicel square compacts with a zero porosity thickness of 3.2mm are significantly stronger than the compacts with 2mm and 2.8mm zero porosity thicknesses (Figure 4.13). This is the reverse of the trend seen with Emcompress compacts. The increase in strength for the thicker compacts may be associated with the increase in their capping pressure.

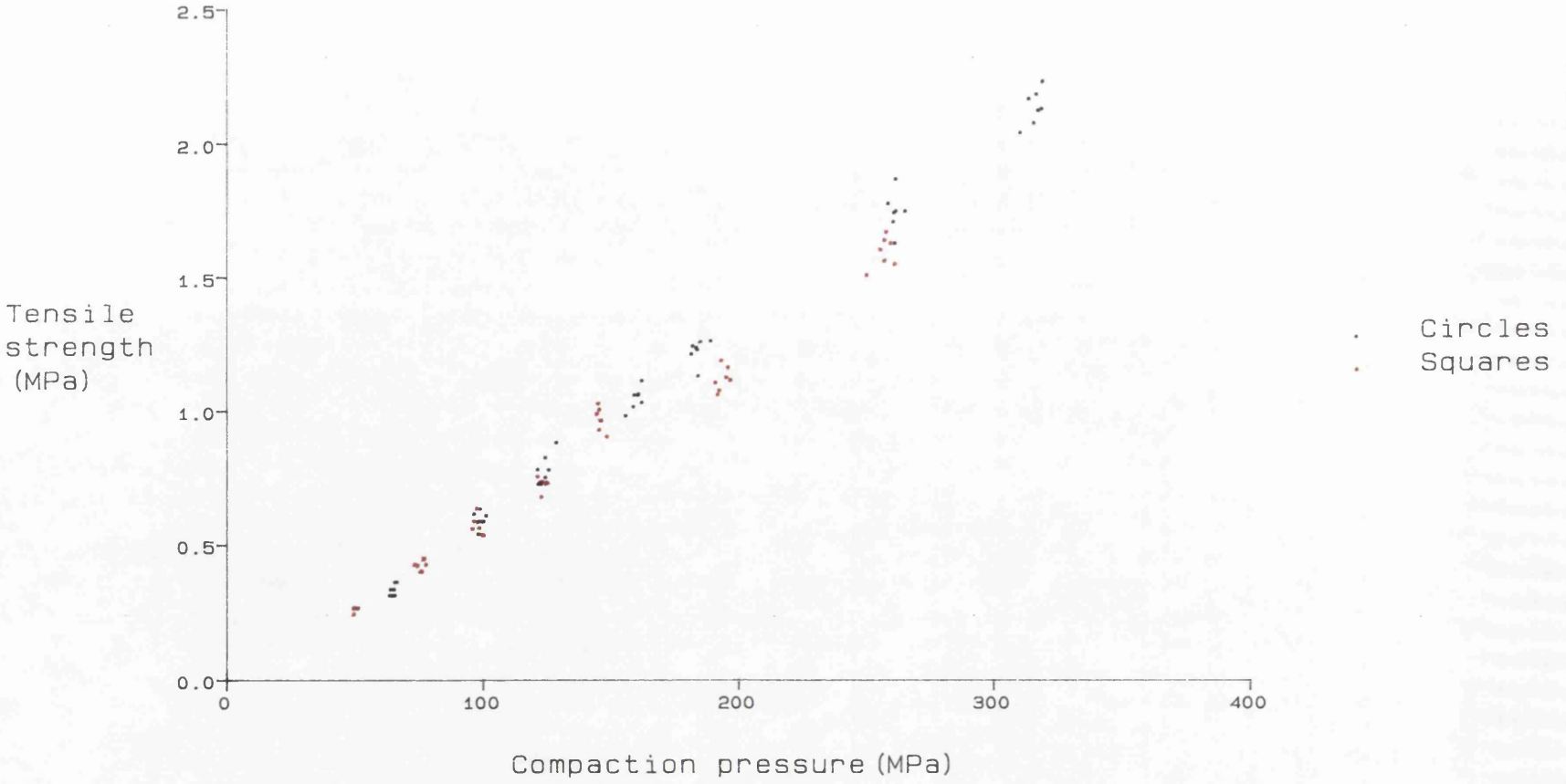

Compacts tested by diametral compression.
Theoretical thickness of compacts with zero porosity = 2.0mm.

Figure 4.7 Effect of shape on the compaction pressure/tensile strength profile of Emcompress compacts produced on a rotary tablet machine

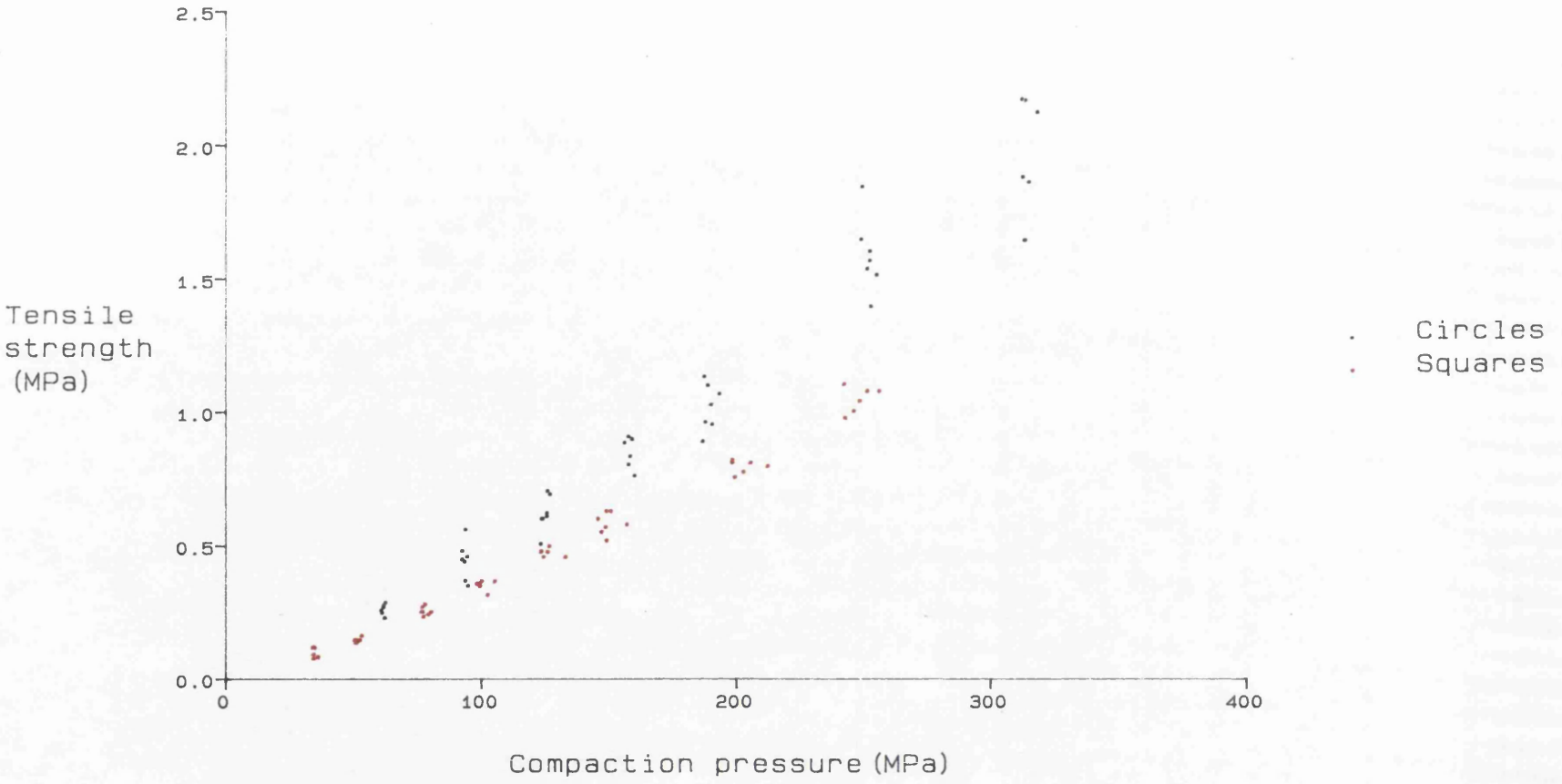

Compacts tested by diametral compression.
Theoretical thickness of compacts with zero porosity = 5.0mm.

Figure 4.8 Effect of shape on the compaction pressure/tensile strength profile of Emcompress compacts produced on a rotary tablet machine

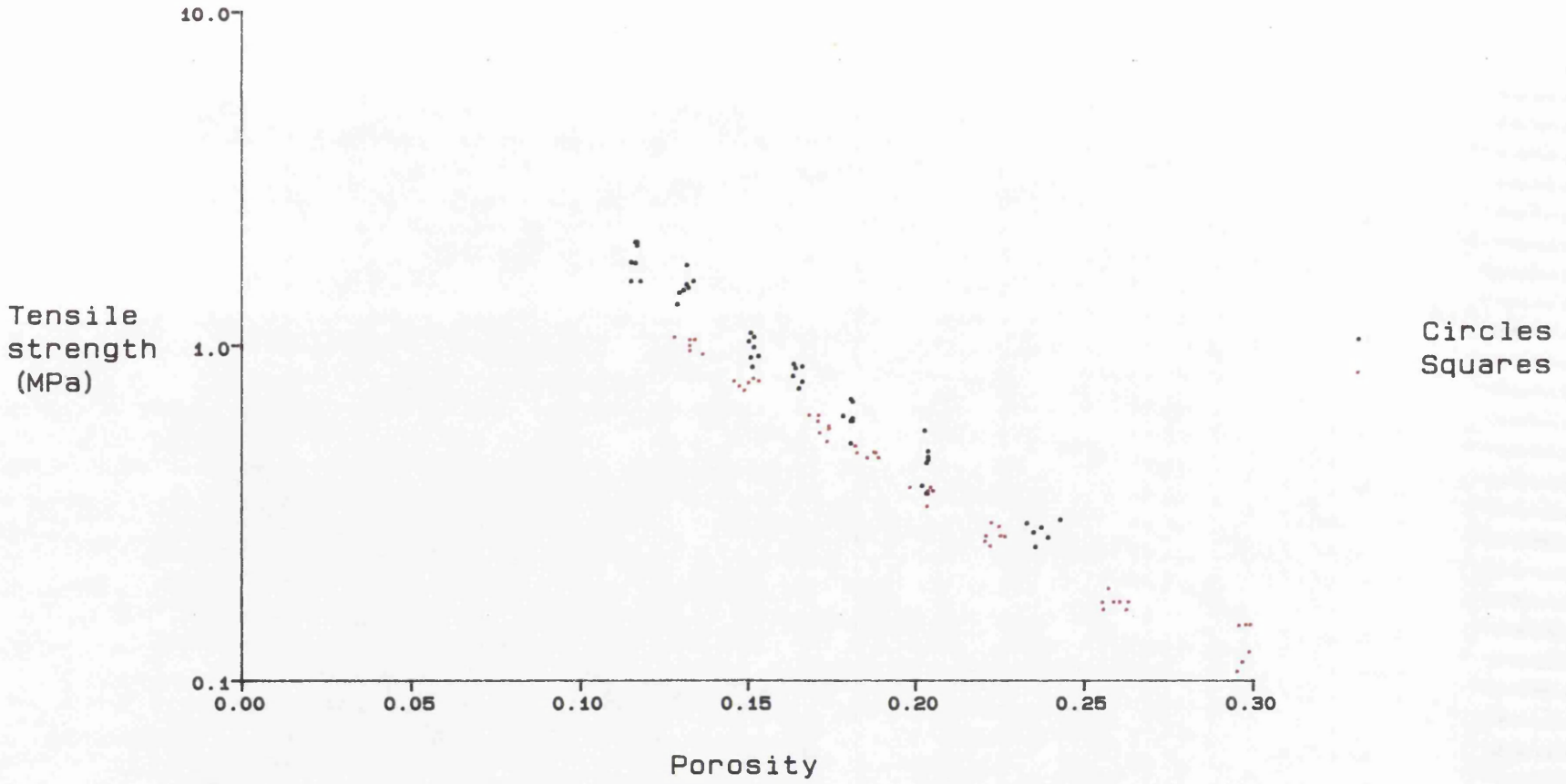

Compacts tested by diametral compression.
Theoretical thickness of compacts with zero porosity = 5.0mm.

Figure 4.9 Plot of tensile strength versus porosity for Emcompress compacts produced on a rotary tablet machine

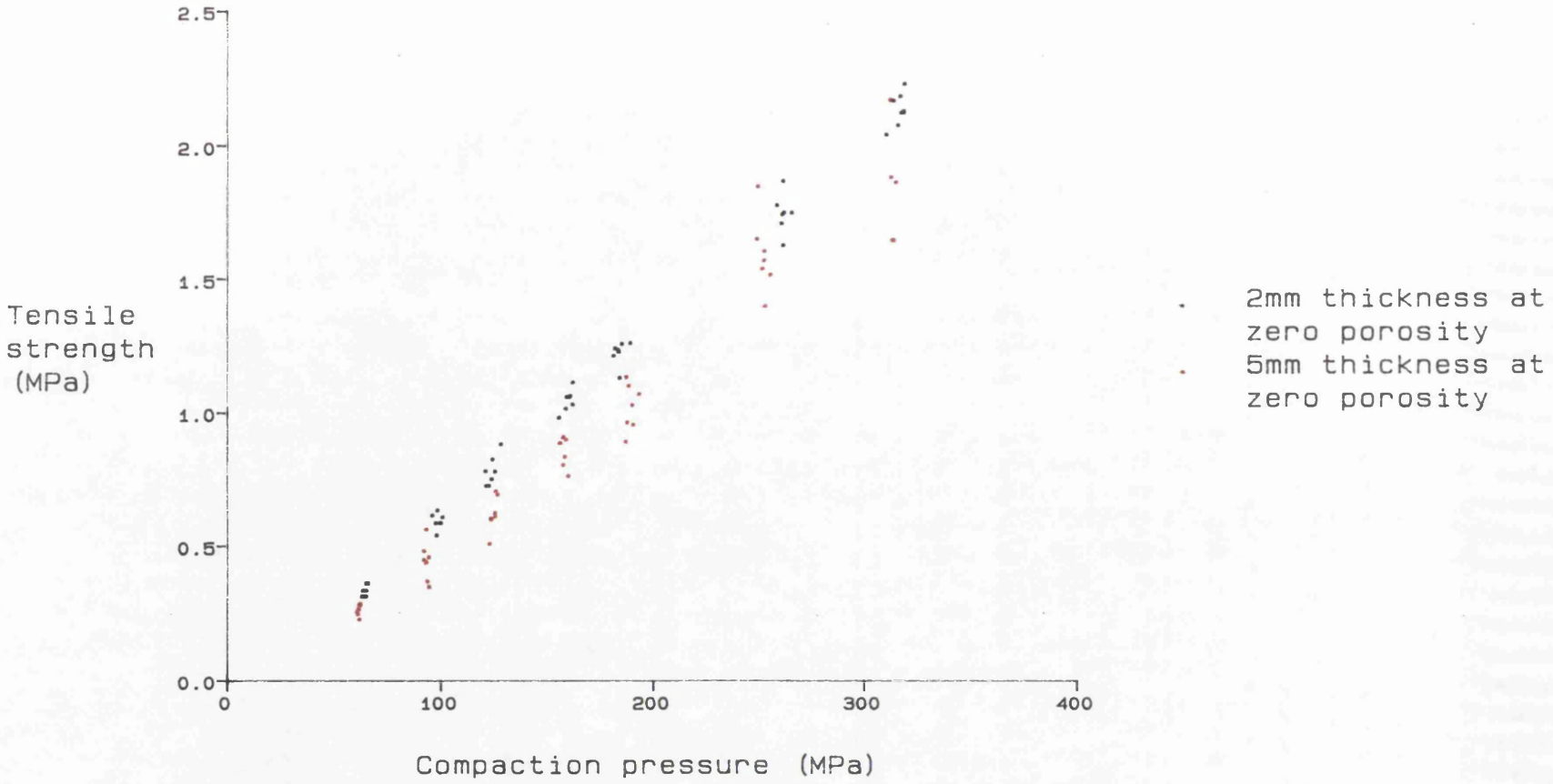

Tensile strength determined by diametral compression.

Figure 4.10 Effect of thickness on the compaction pressure/tensile strength profile of circular Emcompress compacts produced on a rotary tablet machine

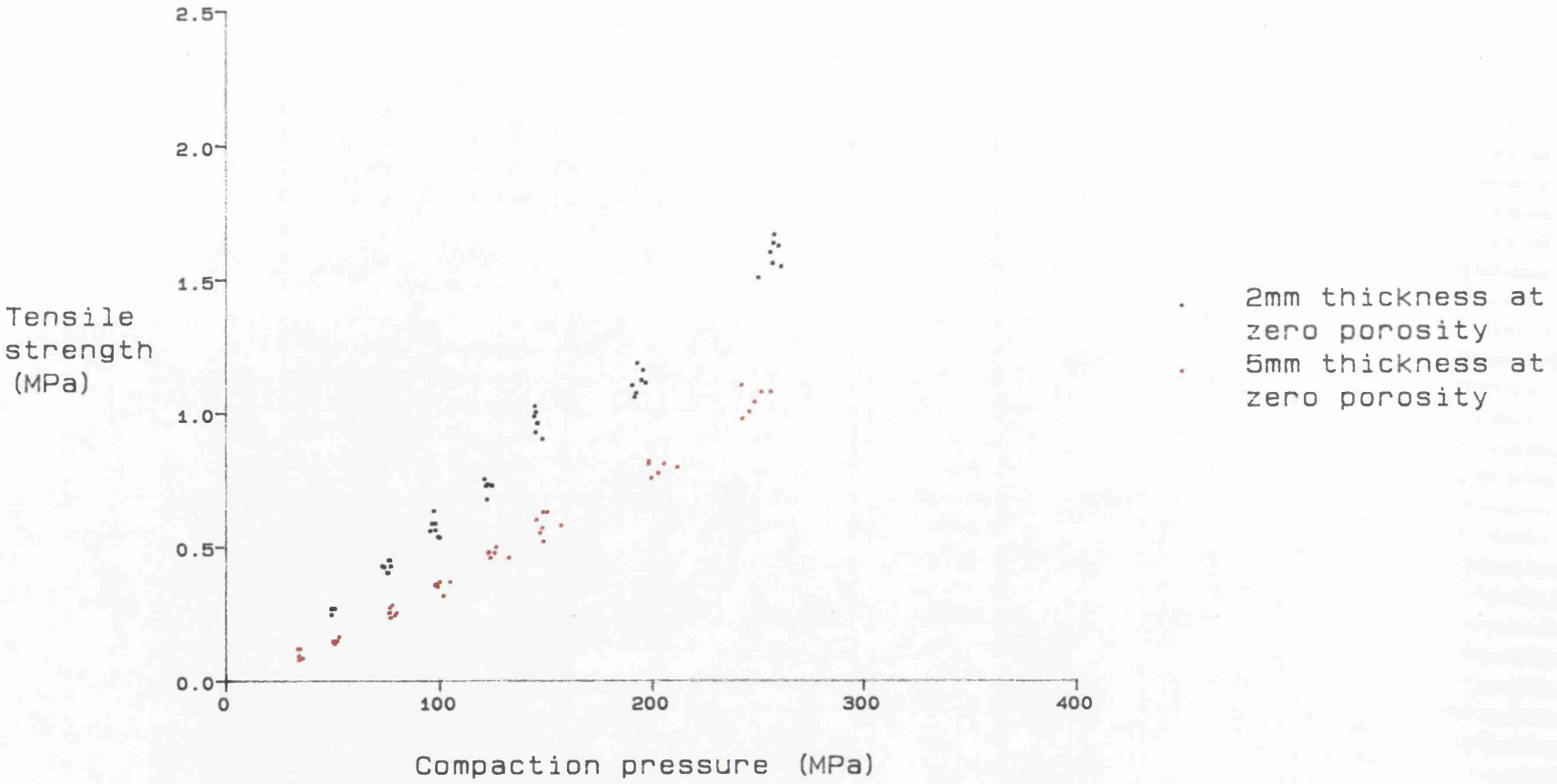

Tensile strength determined by diametral compression.

Figure 4.11 Effect of thickness on the compaction pressure/tensile strength profile of square Emcompress compacts produced on a rotary tablet machine

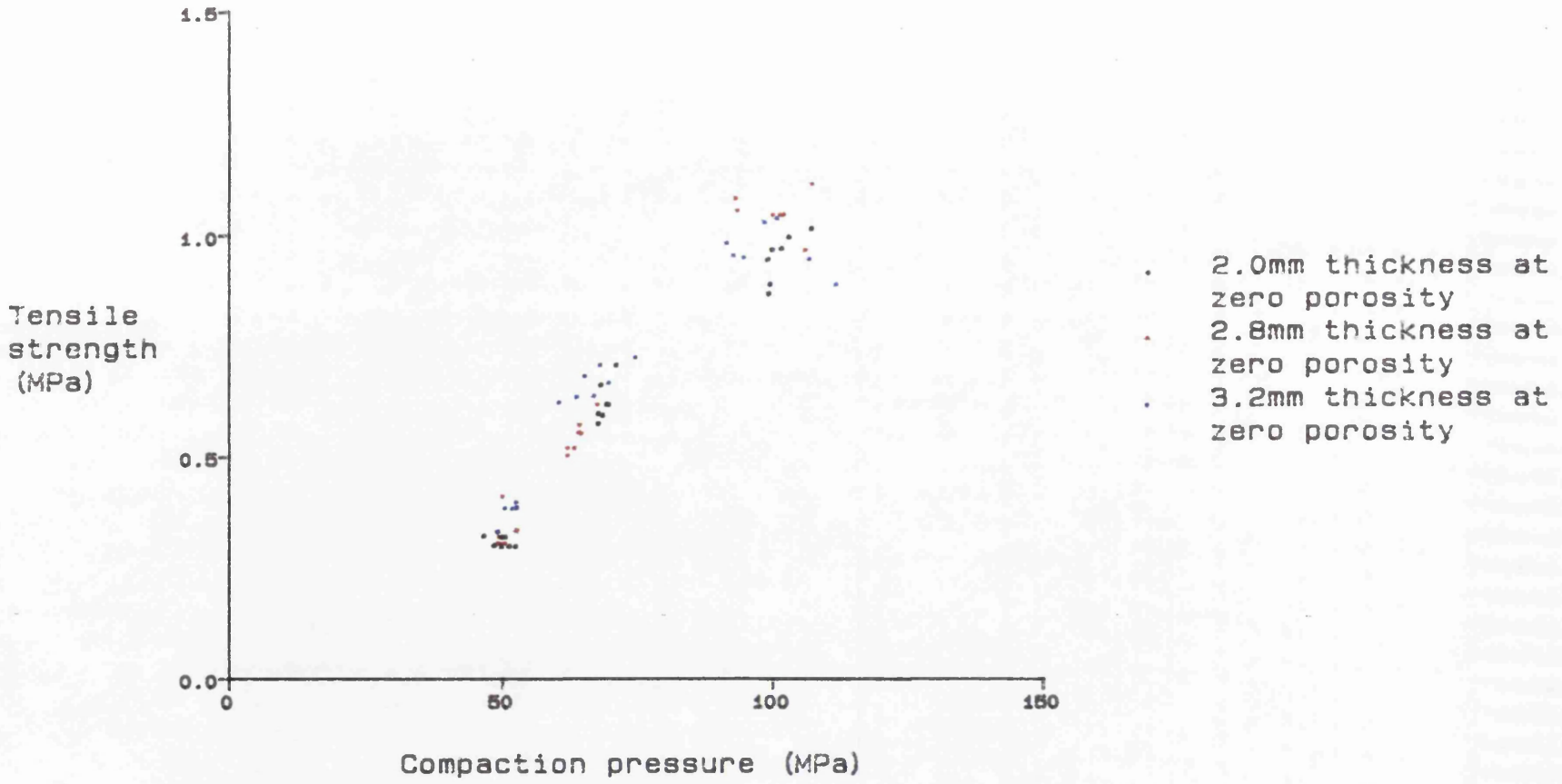

Tensile strength determined by diametral compression.

Figure 4.12 Effect of thickness on the compaction pressure/tensile strength profile of circular Avicel compacts produced on a rotary tablet machine

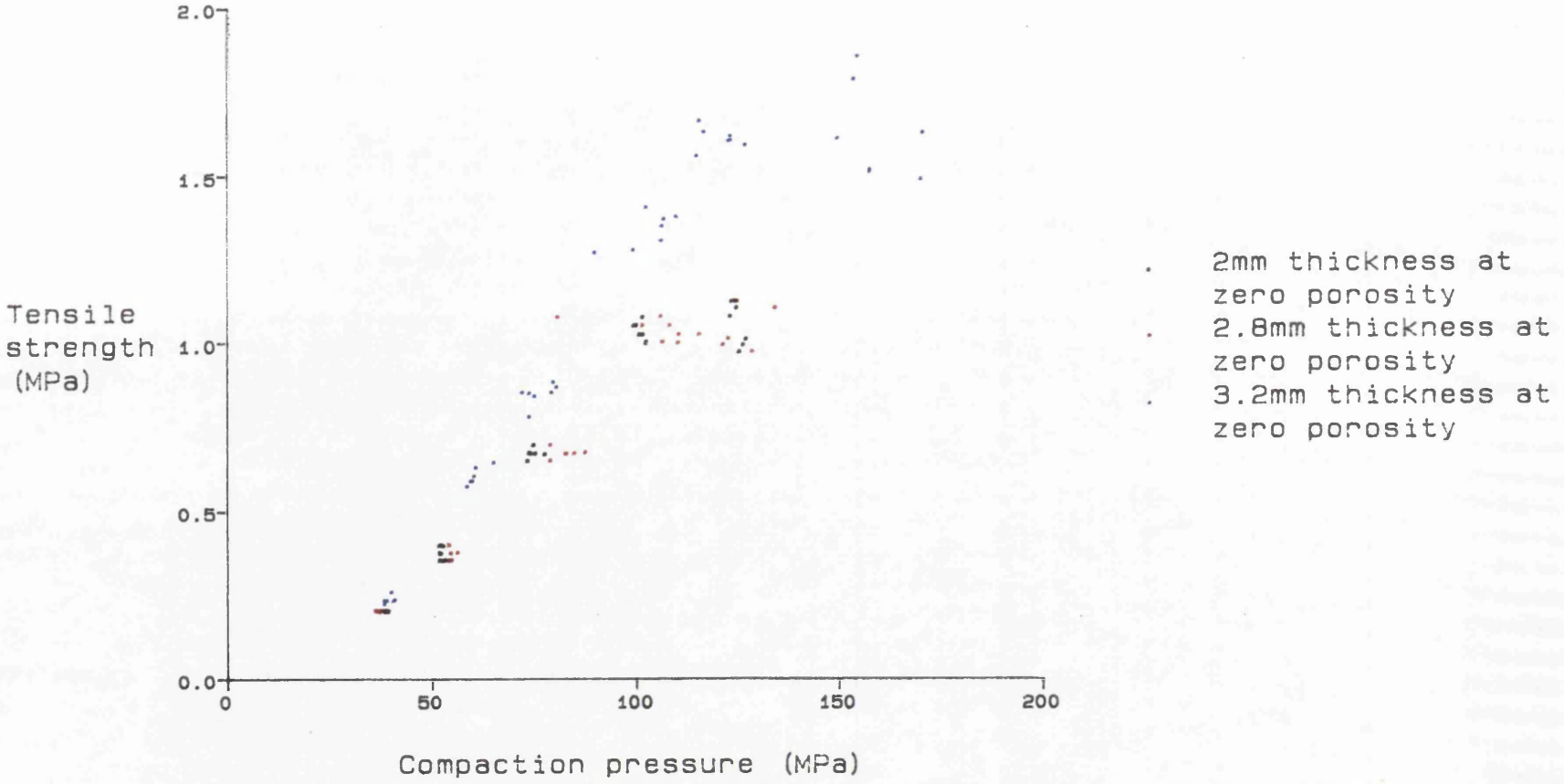

Tensile strength determined by diametral compression.

Figure 4.13 Effect of thickness on the compaction pressure/tensile strength profile of square Avicel compacts produced on a rotary tablet machine

4.3.3 Axial compression test

The results for the axial compression test are summarised in Tables 4.5 to 4.7 with the regression coefficients presented in Table 4.8. The compaction pressure/tensile strength profiles are shown in Figures 4.14 to 4.18.

The results for Avicel compacts again indicate that the tensile strength is not shape dependent prior to capping occurring.

The Emcompress results (Figures 4.17 and 4.18) indicate that the tensile strengths of the circular compacts are greater than the squares at both thicknesses. These results are also reflected by differences in the plots of log axial tensile strength versus porosity (Figures 4.19 and 4.20).

In Chapter 3 it was postulated that the reason for the square Emcompress compacts having lower axial compression tensile strength values may be due to poor force transmission to the lower surface of the compact. On a rotary machine both the upper and lower punches move within the die during the compaction cycle so the density variations within the compacts prepared on the two machines will differ. The differences between the compaction cycles of the two machines will be discussed in greater detail in Chapter 5.

It is clear, however, that the punch and die shape is again influencing the final structure of Emcompress compacts.

Table 4.5

Summary of axial compression data for Emcompress circular compacts prepared on the Manesty D3B rotary tablet press

Zero porosity thickness (mm)	Mean compaction pressure (MPa)	Mean compaction thickness (mm)	Mean breaking load (kg)	Mean tensile strength (MPa)	Mean porosity
2.0	66.9	2.64	2.61	0.62	0.236
	100.5	2.49	3.74	0.94	0.198
	125.4	2.45	4.38	1.12	0.183
	161.0	2.39	5.63	1.47	0.163
	186.0	2.35	6.86	1.82	0.151
	264.9	2.31	6.97	1.88	0.127
	317.1	2.27	9.71	2.67	0.114
5.0	64.7	6.50	3.32	0.32	0.291
	97.4	6.24	4.60	0.46	0.261
	129.9	6.04	5.62	0.58	0.240
	164.0	5.94	6.48	0.68	0.226
	192.1	5.86	7.21	0.77	0.214
	260.6	5.71	9.49	1.04	0.196
	323.1	5.63	11.50	1.27	0.183

Table 4.6
Summary of axial compression data for Emocompress square compacts prepared on the Manesty D3B rotary tablet machine

Zero porosity thickness (mm)	Mean compaction pressure (MPa)	Mean compact thickness (mm)	Mean breaking load (kg)	Mean tensile strength (MPa)	Mean porosity
2.0	50.4	2.65	1.79	0.42	0.246
	77.2	2.56	2.21	0.54	0.217
	98.2	2.50	2.57	0.64	0.199
	127.5	2.44	2.77	0.71	0.180
	145.6	2.39	3.09	0.81	0.165
	195.1	2.36	4.96	1.31	0.150
	257.6	2.30	5.64	1.53	0.126
5.0	34.5	7.11	1.61	0.14	0.298
	51.2	6.77	2.11	0.20	0.259
	78.0	6.42	3.24	0.31	0.223
	100.2	6.29	3.67	0.33	0.203
	126.7	6.15	3.91	0.40	0.180
	149.7	6.06	4.99	0.51	0.173
	202.2	5.90	5.47	0.58	0.150
	247.6	5.79	6.30	0.68	0.134

Table 4.7
Summary of axial compression data for Avicel PH-102 compacts prepared on the Manesty D3B rotary tablet machine

Compact shape	Zero porosity thickness (mm)	Mean compaction pressure (MPa)	Mean compact thickness (mm)	Mean breaking load (kg)	Mean tensile strength (MPa)	Mean porosity
Circle	2.0	48.7	3.10	7.34	1.48	0.326
		66.9	2.83	12.61	2.78	0.265
		97.4	2.51	19.86	4.94	0.192
		128.6	2.44	21.92	5.60	0.174
Circle	2.8	48.6	4.19	7.76	1.16	0.324
		66.0	3.80	12.13	1.99	0.260
		102.6	3.48	19.63	3.52	0.191
Circle	3.2	50.2	4.75	8.21	1.08	0.318
		68.4	4.35	12.86	1.84	0.254
		88.0	4.04	18.90	2.92	0.196
Square	2.0	39.7	3.18	7.44	1.46	0.361
		53.3	2.90	9.11	1.96	0.304
		75.4	2.66	13.44	3.15	0.238
		103.1	2.48	17.61	4.43	0.184
		125.2	2.41	19.19	4.97	0.159
Square	2.8	37.4	4.51	4.67	0.65	0.380
		52.9	4.00	8.05	1.26	0.304
		79.9	3.60	14.19	2.46	0.222
		111.4	3.37	18.89	3.49	0.168
		125.7	3.28	20.93	3.98	0.154
		153.4	3.23	23.87	4.62	0.142
Square	3.2	39.2	5.13	2.21	0.27	0.367
		59.7	4.50	11.10	1.54	0.288
		74.1	4.13	16.36	2.47	0.216
		104.9	3.94	22.61	3.58	0.179
		136.1	3.82	26.51	4.33	0.147
		163.9	3.79	29.76	4.90	0.147

Table 4.8

Linear regression data for compacts prepared on the Manesty D3B rotary tablet machine and tested by axial compression

Material	Compact shape	Zero porosity thickness (mm)	Intercept (MPa)	Slope	Regression coefficient
Avicel	Circle	2.0	-1.458	6.16×10^{-3}	0.979
	Circle	2.8	-0.528	3.35×10^{-3}	0.973
	Circle	3.2	-0.243	2.95×10^{-3}	0.767
	Square	2.0	-0.315	4.41×10^{-3}	0.983
	Square	2.8	-0.703	3.67×10^{-3}	0.994
	Square	3.2	-1.492	1.54×10^{-3}	0.963
Emcompress	Circle	2.0	0.141	7.57×10^{-3}	0.932
	Circle	5.0	0.084	3.67×10^{-3}	0.978
	Square	2.0	0.161	4.81×10^{-3}	0.891
	Square	5.0	0.055	2.64×10^{-3}	0.985

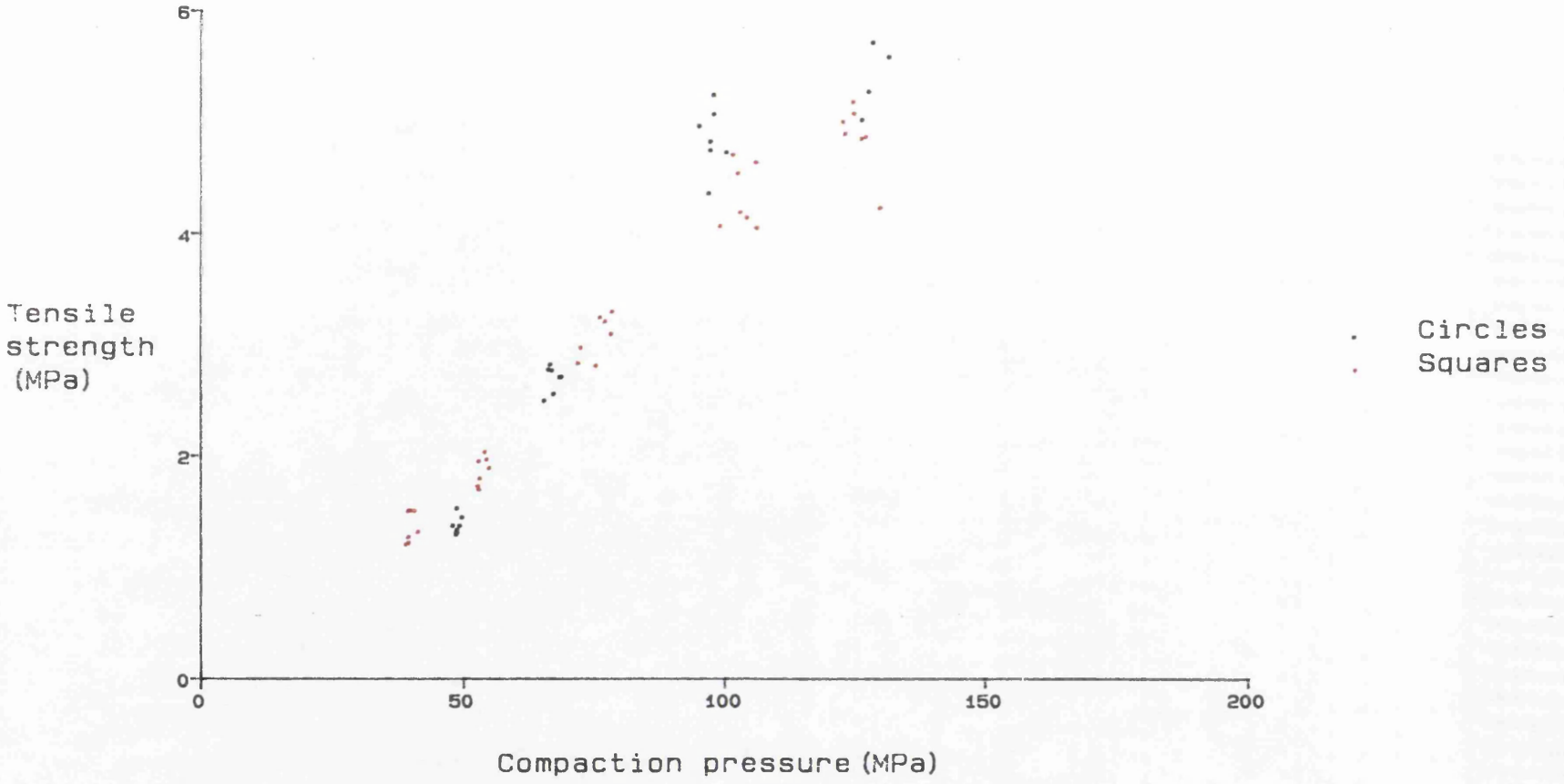

Compacts tested by axial compression.
Theoretical thickness of compacts with zero porosity = 2.0mm.

Figure 4.14 Effect of shape on the compaction pressure/tensile strength profile of Avicel compacts produced on a rotary tablet machine

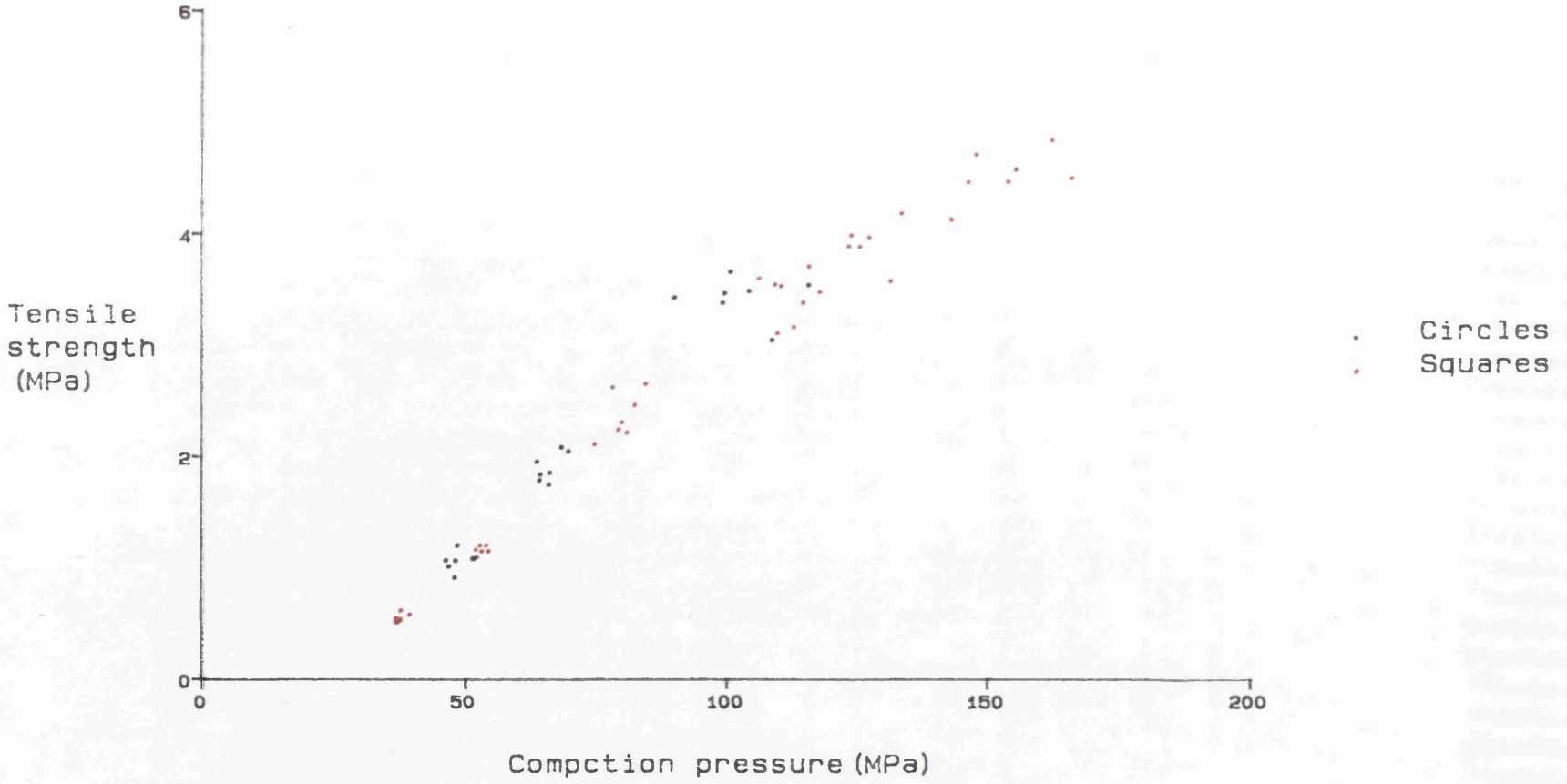

Compacts tested by axial compression.
Theoretical thickness of compacts with zero porosity = 2.8mm.

Figure 4.15 Effect of shape on the compaction pressure/tensile strength profile of Avicel compacts produced on a rotary tablet machine

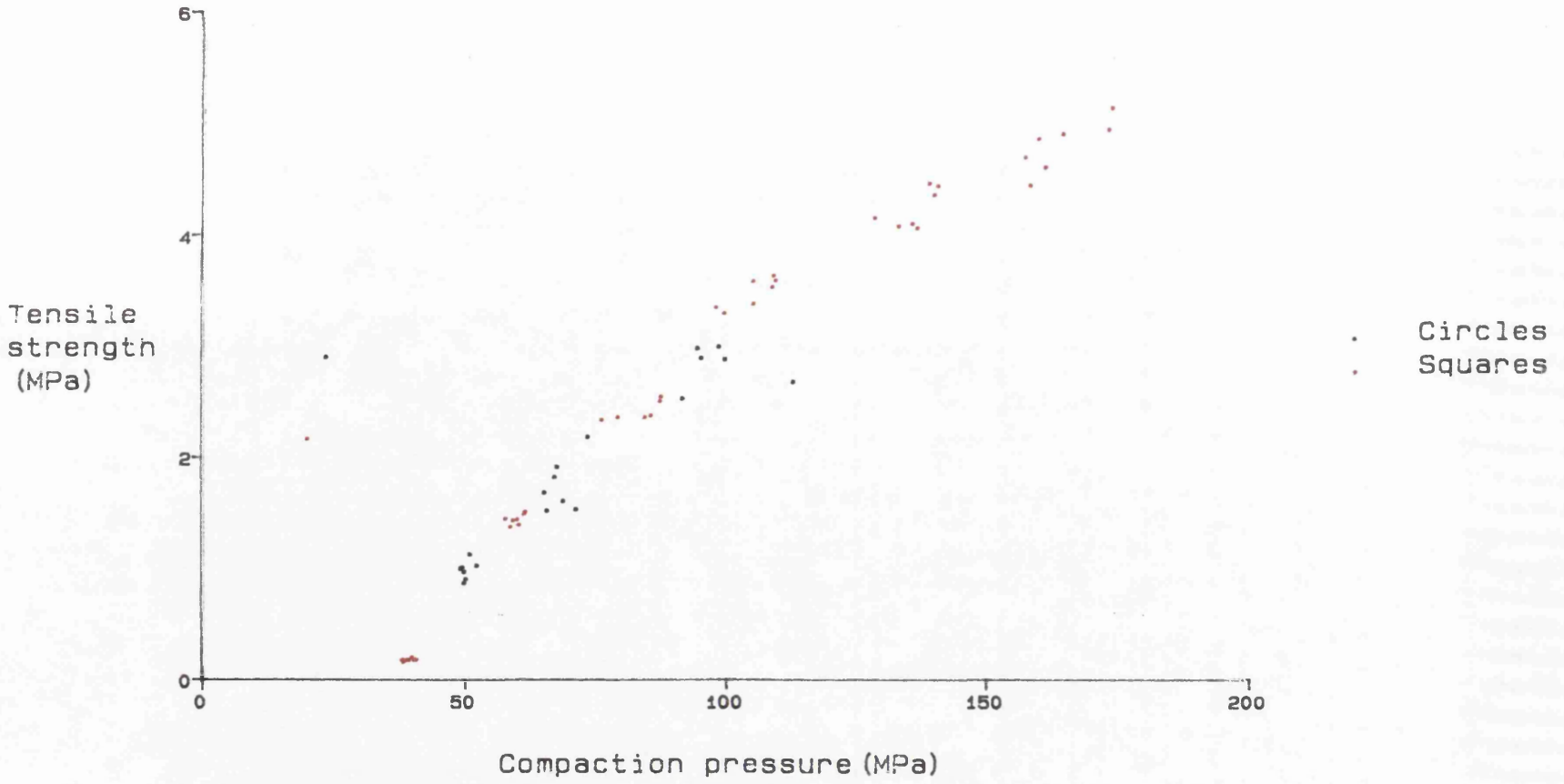

Compacts tested by axial compression.
Theoretical thickness of compacts with zero porosity = 3.2mm.

Figure 4.16 Effect of shape on the compaction pressure/tensile strength profile of Avicel compacts produced on a rotary tablet machine

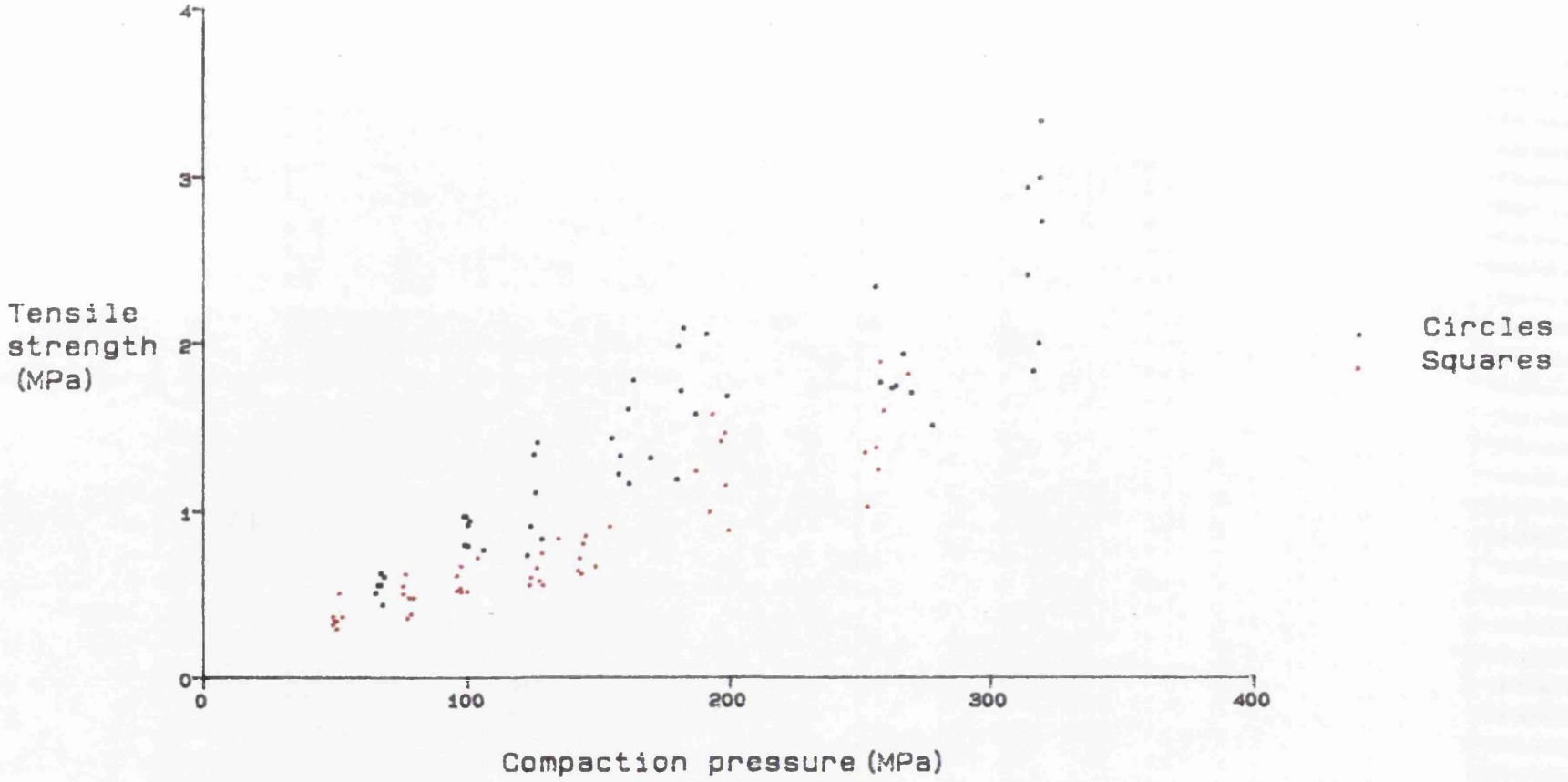

Compacts tested by axial compression.
Theoretical thickness of compacts with zero porosity = 2.0mm.

Figure 4.17 Effect of shape on the compaction pressure/tensile strength profile of Emcompress compacts produced on a rotary tablet machine

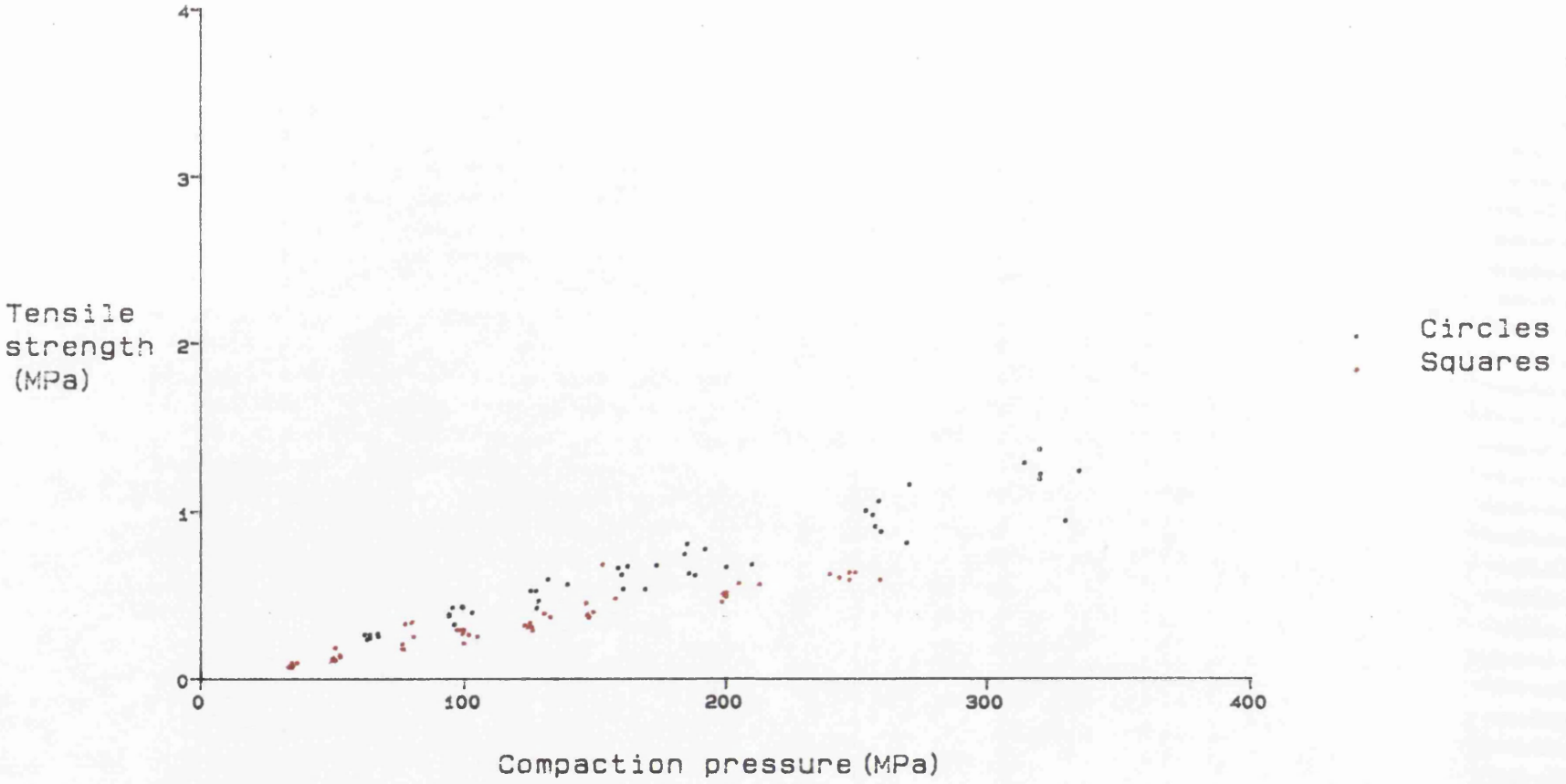

Compacts tested by axial compression.
Theoretical thickness of compacts with zero porosity = 5.0mm.

Figure 4.18 Effect of shape on the compaction pressure/tensile strength profile of Emcompress compacts produced on a rotary tablet machine

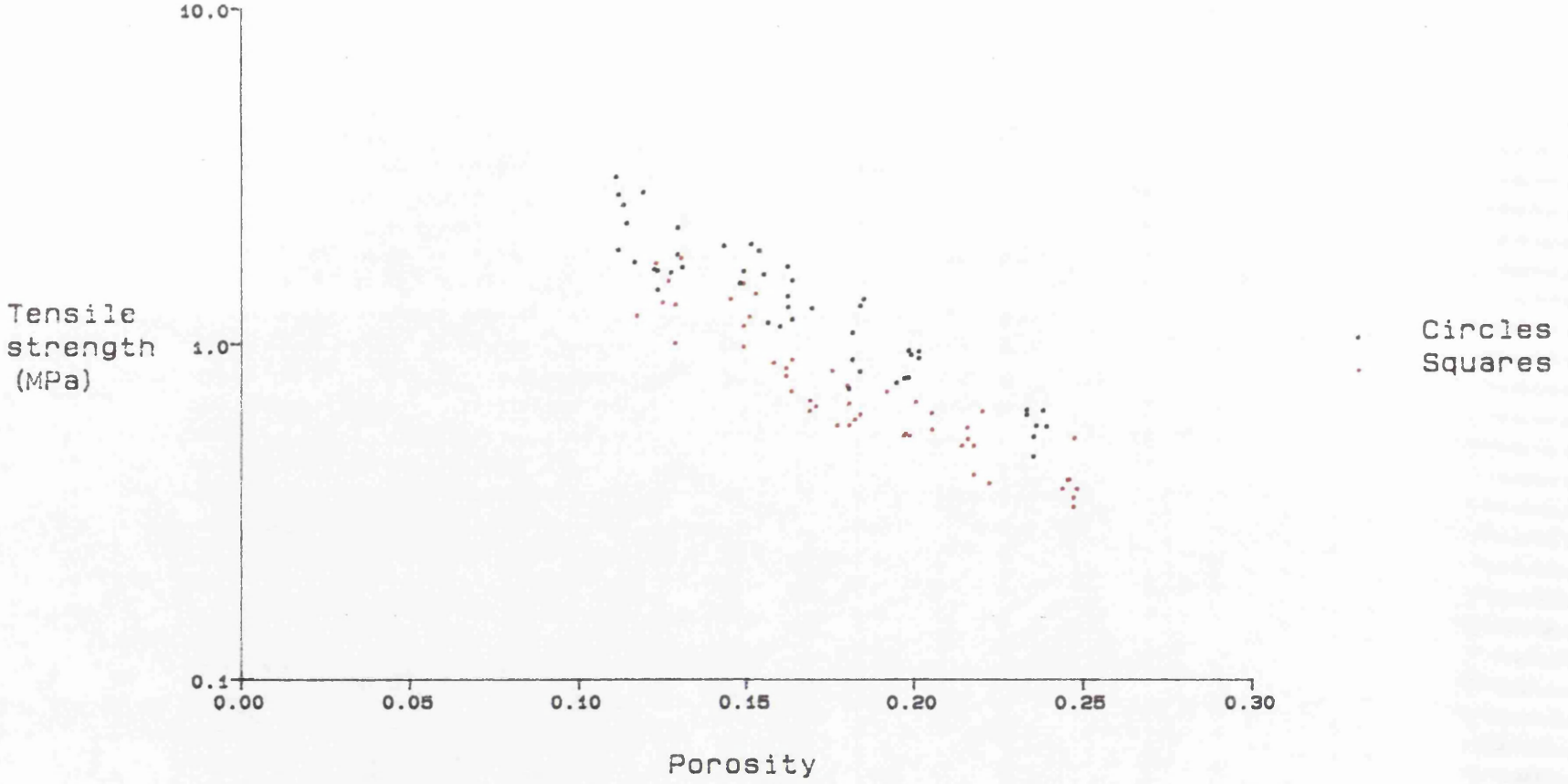

Compacts tested by axial compression.
Theoretical thickness of compacts with zero porosity = 2.0mm.

Figure 4.19 Plot of tensile strength versus porosity for Emcompress compacts produced on a rotary tablet machine

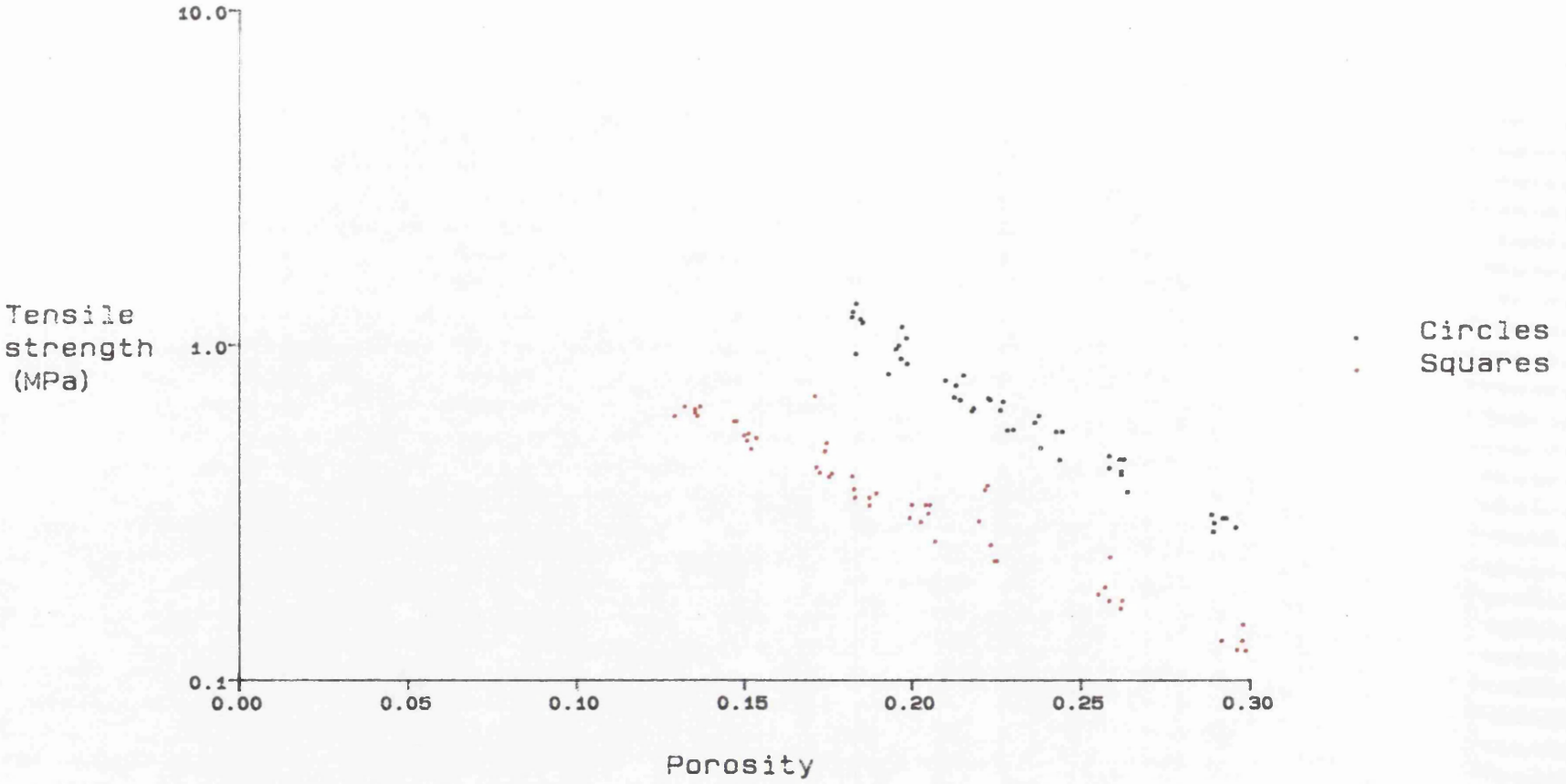

Compacts tested by axial compression.
Theoretical thickness of compacts with zero porosity = 5.0mm.

Figure 4.20 Plot of tensile strength versus porosity for Emcompress compacts produced on a rotary tablet machine

4.4 Conclusions

The compaction properties of Avicel PH-102 and Emcompress have been examined using a Manesty D3B rotary tablet machine.

The lubricated Avicel PH-102 mix displayed a capping tendency that was related to the compaction pressure. The pressure at which capping first occurred appears to be dependent on the shape of tooling used, the square tooling displaying a higher capping pressure than the circular tooling.

The maximum thickness of square Emcompress compacts that could be produced was only limited by the maximum depth of fill of the die; there were no apparent problems of force transmission. The tensile strengths of the Emcompress square compacts were lower than those of circular compacts produced with similar porosities, indicating differences in their structures.

The results of the Avicel compacts clearly indicate that the final properties of a compact depend not only on the pressure used to form the compact but also on the way in which that pressure is applied.

CHAPTER 5

COMPARISON OF THE SINGLE PUNCH AND ROTARY TABLET MACHINES

5.1 Introduction

The previous two chapters have dealt separately with the formation of compacts using a single punch machine and a rotary tablet machine. A number of differences were seen in the results obtained from the two machines in terms of the ability to form compacts and the strengths of those formed. The aim of this chapter is to compare the two sets of results and consider the reasons for any differences seen.

The single punch and rotary machines differ in a number of respects from the die filling mechanism to the manner and speed with which the punches move together. While the initial distribution of powders within the dies may differ due to the filling mechanisms it is unlikely that these will significantly affect the properties of the final compacts. The particle rearrangement that occurs at low compression pressures will reduce initial variations in powder fill. The final compact properties are more likely to arise from the differences in the compaction cycles. Before comparing the compacts prepared with the two machines the mechanisms of their compaction cycles will be reviewed.

5.2 The eccentric single punch tablet press

A single punch machine compresses a powder by the movement of the upper punch relative to a stationary lower punch. The motion of the upper punch is produced by having the punch holder attached to an arm which is carried on an eccentric cam. This is demonstrated in a simplified form in Figure 5.1, where D is the distance of the cam off-set, L the length of the eccentric strap, O the centre of the driving wheel and P and J are the

Figure 5.1
Schematic representation of the upper punch mechanism on a single punch machine

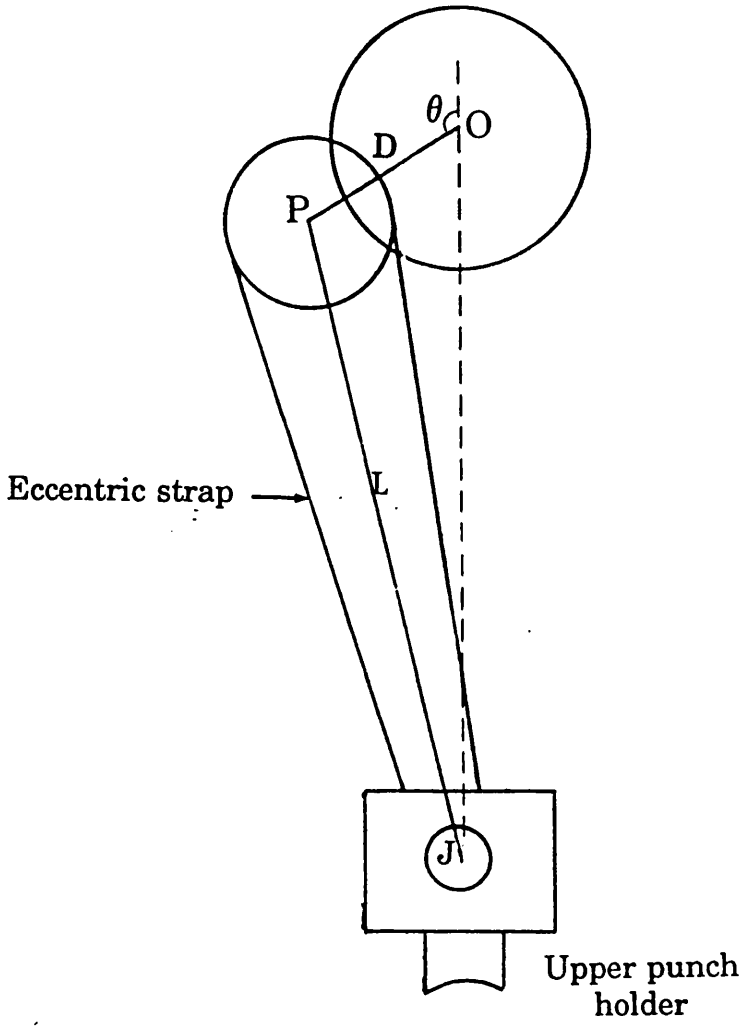

pivots. The motion of the punch will be the same as the motion of the pivot J.

Charlton and Newton (1984) analysed the motion of point J relative to O and derived the following formula for the punch velocity, V_p;

$$V_p = D.\sin\theta.\omega(1 - A.[1 - A^2.\sin^2\theta]^{-0.5}.\cos\theta) \quad (5.1)$$

where A = D/L

θ = angle between line PO and vertical

ω = dθ/dt the angular velocity of the driving wheel.

An equivalent formula was derived separately by Armstrong et al (1983). For the Manesty F3 machine used in this study L and D were measured using a cathetometer (Model 2022, Precision Tool and Instrument Co. Ltd). Values of 21.00cm for L and 2.29cm for D were obtained yielding a value of 0.109 for A. The angle of the eccentric strap, θ, at the point of entry into the die is dependent on the depth of penetration of the punch during the compaction cycle. This, in turn, is a function of the initial powder bed and the final compact thickness. Measurement of the initial powder bed height and the extent of punch penetration into the die enables the angle of the eccentric strap θ, at which the punch enters the die to be determined. The punch velocity at this point, which is the maximum velocity during the compression process, can then be determined using equation 5.1. The initial powder bed height was measured using a caliper gauge. Using the compact thickness measured immediately after ejection to determine the extent of punch penetration the maximum punch velocities for Avicel and Emcompress circular compacts were calculated. The results are presented in Table 5.1. The contact times (t_c) listed in the table represent the time

Table 5.1
Maximum punch velocities for Avicel and Emcompress circular compacts prepared on a single punch machine

Material	Zero porosity thickness (mm)	Compaction pressure (MPa)	Initial punch velocity (mms^{-1})	Compaction time (s)
Avicel PH-102	2.0	76	9.17	0.122
		127	9.36	0.125
	2.8	64	10.50	0.143
		121	10.68	0.147
	3.2	51	11.20	0.156
		124	11.51	0.162
Emcompress	2.0	64	6.10	0.078
		191	6.38	0.082
	5.0	64	10.21	0.139
		191	10.50	0.143

that elapses from the entry of the punch into the die to the point of maximum penetration, i.e. the time that the upper punch is in contact with the compact. This value is determined by;

$$t_c = \frac{2\pi - \theta}{\omega} \qquad (5.2)$$

where θ is the angle at the point of entry of the punch into the die.

This analysis is subject to errors due to assumptions made about the operation of the machine. The calculations assume that there is no deformation of the various components involved (e.g punches and cams). Changes in punch movements have been shown to occur in single punch machines due to the stiffness of the bearings of the machines. Any expansion of the compact following removal of the upper punch will result in inaccuracies in the measurement of the punch penetration, although the effect of such errors on the value obtained for the punch velocity will be minimal. Armstrong and Palfrey (1987) compared actual punch velocities in an eccentric press with theoretical values. It was found that the predicted and actual velocities were equal when an empty die was used. If the die was not empty deviations from the predicted velocity occurred as the presence of material in the die increased the deceleration of the punch. The deviations were dependent on machine speed, the material being compressed and the force being applied. The latter point is significant as the force required to produce a given compaction pressure is greater for square compacts than circular compacts with the same inscribed diameter due to the increased surface area of the square punches. The deviation from the theoretical punch velocities observed with square compacts may,

therefore, be greater than for circular compacts prepared under nominally similar conditions.

5.3 The rotary tablet press

Compaction on the rotary machine is effected by a pair of punches running between two rollers. The upper roller is fixed while the lower roller may be raised to control the vertical distance that the lower punch travels thus altering the compaction pressure. As with the single punch machine the theoretical motion of the two punches can be calculated from a geometrical analysis of the machine. For the purposes of this analysis the movements of the upper and lower punches will be assumed to be similar. The movements will be dependent on the height of the roller above the cam track on which the punch runs, the radius of the roller and the profile of the punch head (Figure 5.2).

Charlton and Newton (1984) showed that the vertical velocity (V_v) of the lower punch can be determined by;

$$V_v = \frac{2\pi R_p f}{\tan \phi} \qquad (5.3)$$

where R_p = radius of the horizontal circle in which the punches travel

f = frequency of rotation of the turret

ϕ = the angle between the horizontal cam track and the point of contact on the roller measured from the centre of the roller

The angle ϕ can be determined from the punch separation P_s, which at the

Figure 5.2
Geometry of a punch passing over the roller
of a rotary tablet machine

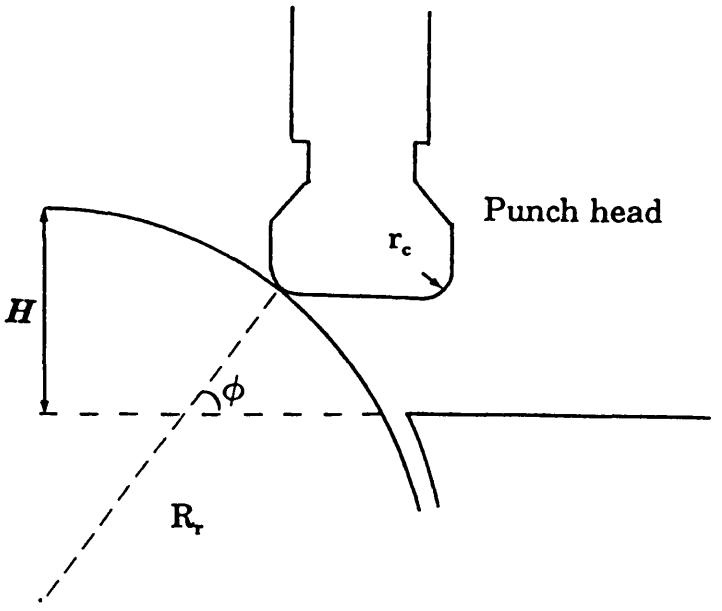

start of compression is equal to the thickness of the powder bed;

$$P_s = D_r - H - 2L_p + 2(R + r_c).(1 - \sin \phi) \qquad (5.4)$$

where D_r = height of the lower edge of the upper roller above the lower cam track.

L_p = punch length

R_r = radius of roller

r_c = radius of curved section of punch

H = height of lower roller above the cam track

Using the cathetometer values of 28.5cm, 13.4cm, 11.3cm and 1.2cm were obtained for D_r, L_p, R_r and r_c respectively. With these values it was possible to calculate the initial punch velocities for Avicel and Emcompress compacts. Table 5.2 presents figures for compaction times and total contact times. The compaction time quoted is the time taken between the start of compaction and achieving maximum die penetration. The punch position at this point is illustrated in Figure 5.3a. On the rotary machine there is a dwell time during which the punches are maintained at maximum die penetration while the flat heads of the punches pass over the roller. The total contact time quoted in Table 5.2 is the time that elapses from the start of compaction until the flat portions of the punches have completely passed over the rollers, i.e. when the punch reaches the position illustrated in Figure 5.3b. The assumptions regarding lack of deformation apply equally to the rotary machine as the single punch machine. Oates and Mitchell (1989) have proposed equations that allow for punch deformation during the compaction process. A further effect will arise from the assumption that the upper punch follows the profile of the upper roller. In

Figure 5.3a
Punch position on roller at start of dwell time

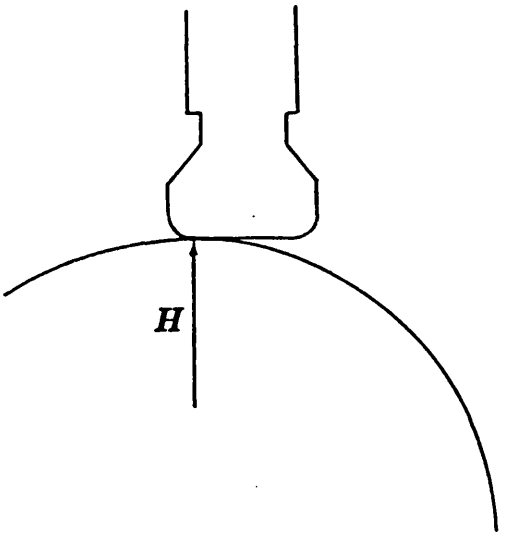

Figure 5.3b
Punch position on roller at end of dwell time

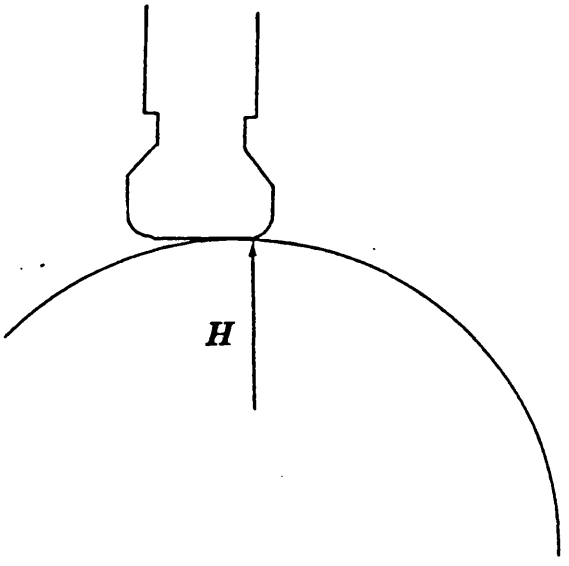

Table 5.2
Initial punch velocities for Avicel and Emcompress circular compacts prepared on the rotary tablet press

Material	Zero porosity thickness (mm)	Compaction pressure (MPa)	Initial punch velocity (mms^{-1})	Compaction time (s)	Total contact time (s)
Avicel PH-102	2.0	50	9.12	0.072	0.118
		99	9.15	0.075	0.121
	2.8	50	10.81	0.085	0.131
		102	11.28	0.088	0.134
	3.2	51	11.91	0.093	0.139
		99	12.30	0.095	0.141
Emcom-press	2.0	64	6.13	0.049	0.095
		185	6.33	0.051	0.097
	5.0	62	9.85	0.078	0.124
		191	10.26	0.081	0.127

practise the upper punch falls from the cam back onto the powder under its own weight before running under the roller. The powder bed will thus be subjected to a small amount of pre-compression reducing the thickness of the powder bed. The effect of this will be to reduce the punch velocity at the start of compaction and reduce the compaction time.

Comparison of values in Tables 5.1 and 5.2 shows that the initial/maximum punch velocities are similar for the two machines. The machine speed of 24 r.p.m. for the rotary machine was selected so that the punch velocities would be similar to those of the single punch machine run at 60 r.p.m. The period during which the compacts are in contact with both punches is also similar for both machines. The main difference between the two machines is the time taken to achieve maximum punch penetration. For the rotary machine this period is labelled as the compaction time in Table 5.2 while for the single punch machine the period is the same as the contact time given in Table 5.1. It can be seen that this time is much shorter for the rotary machine. This is due to both punches moving together at the same speed, effectively doubling the relative velocities. The movement of each punch during compression on the rotary machine is lower than the movement of the upper punch on the single punch machine. The deceleration of the rotary punches is greater than that of the F-machine punch. Figures 5.4 and 5.5 demonstrate the theoretical motions of the upper punches during the compaction of a circular Avicel compact using a pressure of 64MPa. The plot of punch velocity versus time (Figure 5.4) illustrates the rapid deceleration of the rotary machine compared with the single punch. The punch separations, shown in Figure 5.5, indicate the

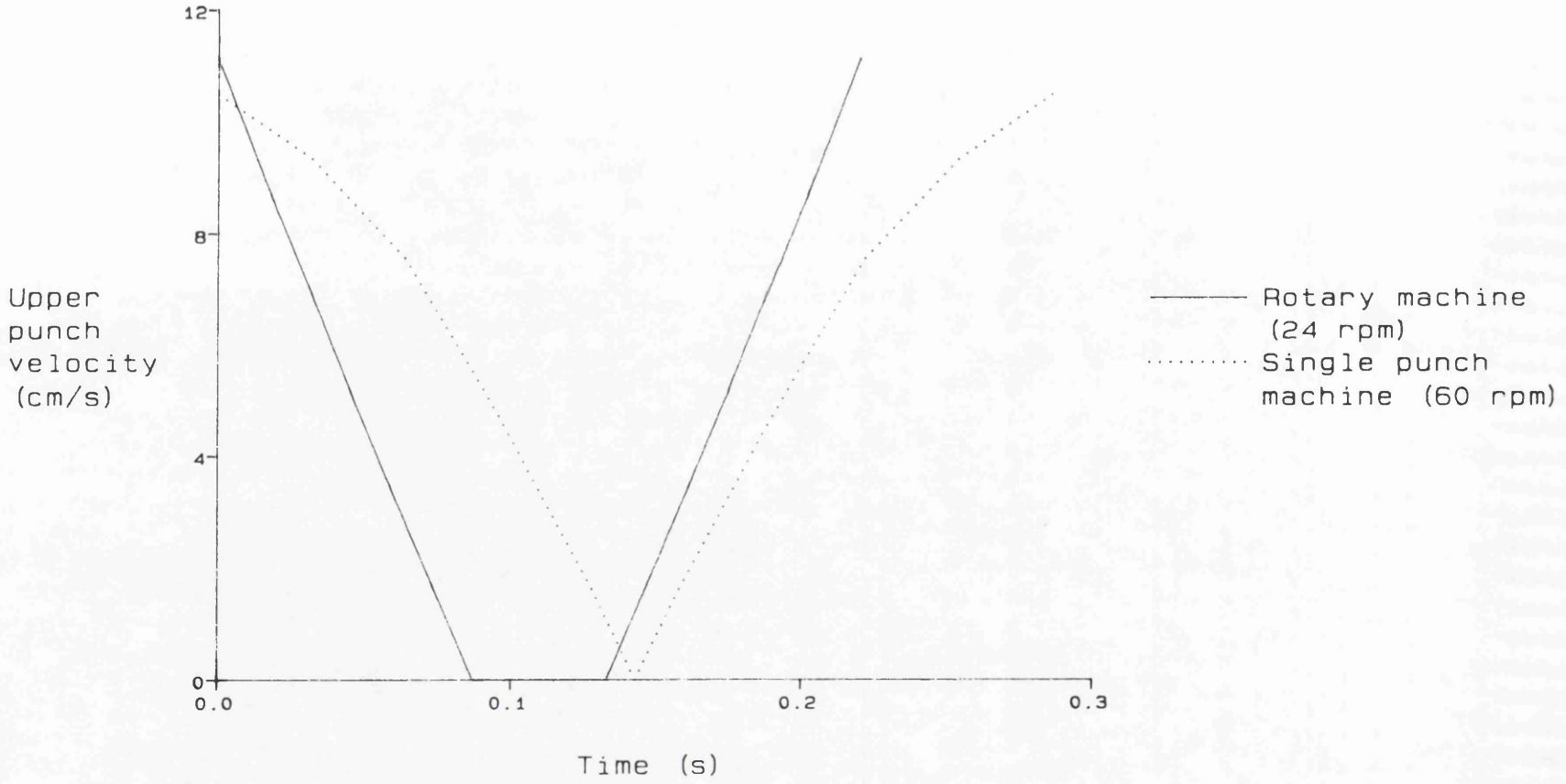

Theoretical thickness of compacts with zero porosity = 2.8mm.

Figure 5.4 Plot of punch velocity versus time for an Avicel circular compact compressed at 64MPa

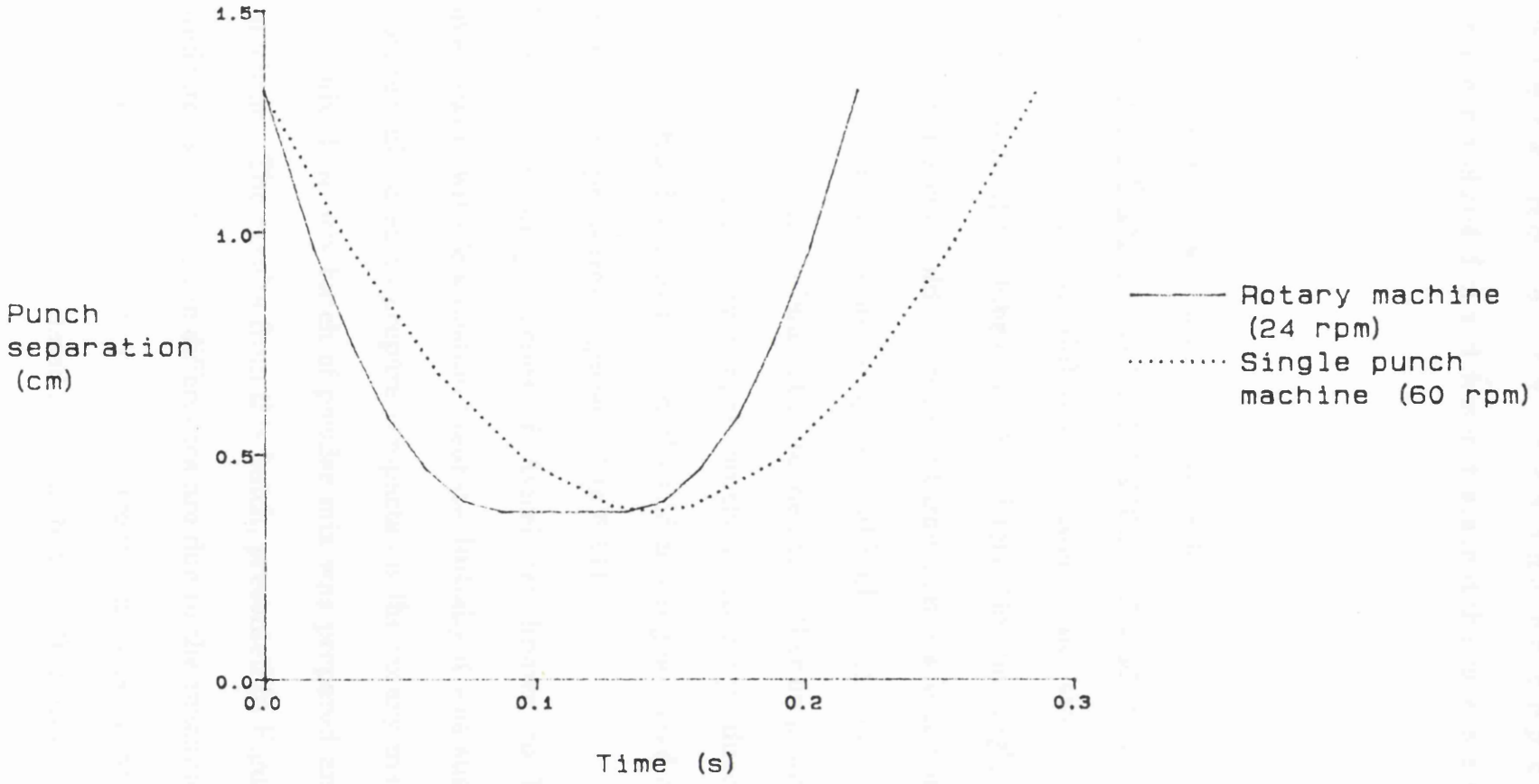

Theoretical thickness of compacts with zero porosity = 2.8mm.

Figure 5.5 Plot of punch separation versus time for an Avicel circular compact compressed at 64MPa

long dwell time present on the rotary machine. Figure 5.6 contains oscilloscope traces of force versus time for compacts prepared at approximately 64MPa and demonstrate that the force is held at or near the maximum for a more prolonged period on the rotary machine.

5.4 Effect of machine type on compaction properties

5.4.1 Effect of machine type on the compaction properties of Avicel PH-102

The most noticeable difference between the two machines is the performance of the lubricated Avicel mix. On the single punch machine Avicel compacts could be prepared throughout its force operating range (0 to 30kN). The resultant compacts had high tensile strength values and gave no indication of lamination tendencies either on production or during subsequent testing. By comparison the compacts produced on the rotary machine had low tensile strengths and capping occurred at relatively low compaction pressures (Figures 5.7 to 5.11)

The compaction properties of Avicel are known to be sensitive to overmixing with Magnesium Stearate. Initially it was suspected that the powder mix used to prepare compacts on the rotary machine had been overmixed. A new batch of powder mix was prepared and used on both machines. The results from this batch, presented in Figures 5.7 to 5.11., indicate again that the differences are due to the machines.

Avicel is a material that produces strong compacts by virtue of its ability to deform plastically (David and Augsburger 1977) due to the presence of numerous slip planes and dislocations in its structure (Lamberson and

Figure 5.6
Comparison of the force/time profiles obtained on the single punch and rotary tablet machines when compressing 10mm circular compacts of Avicel at approximately 95MPa (7.5kN)

Single punch machine (60r.p.m.)

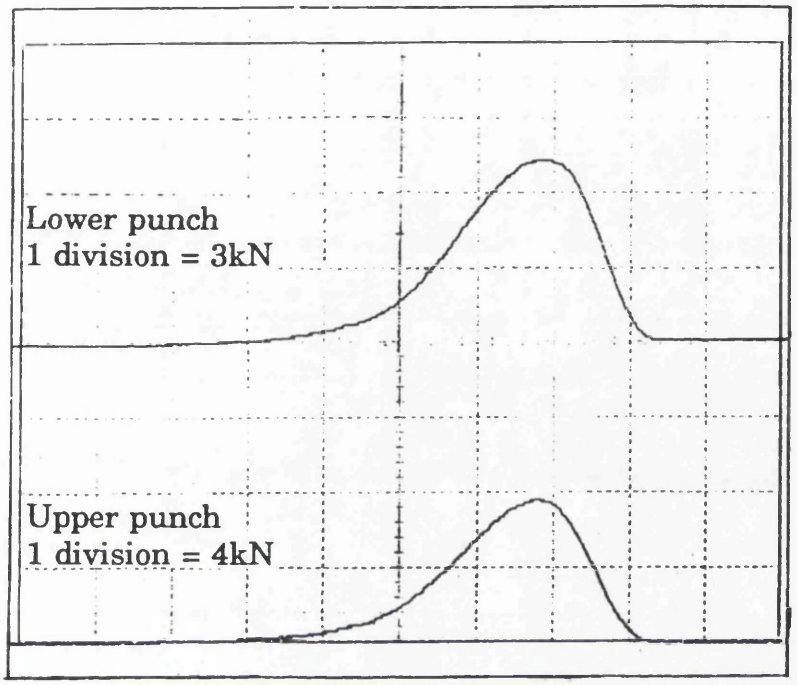

Rotary tablet machine (24r.p.m.)

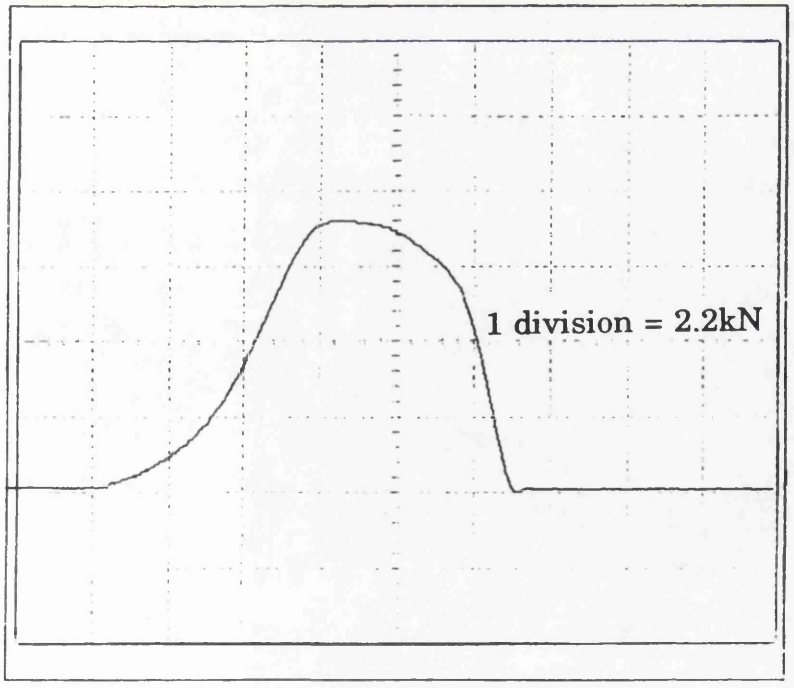

Time scale for both traces = 20ms/division

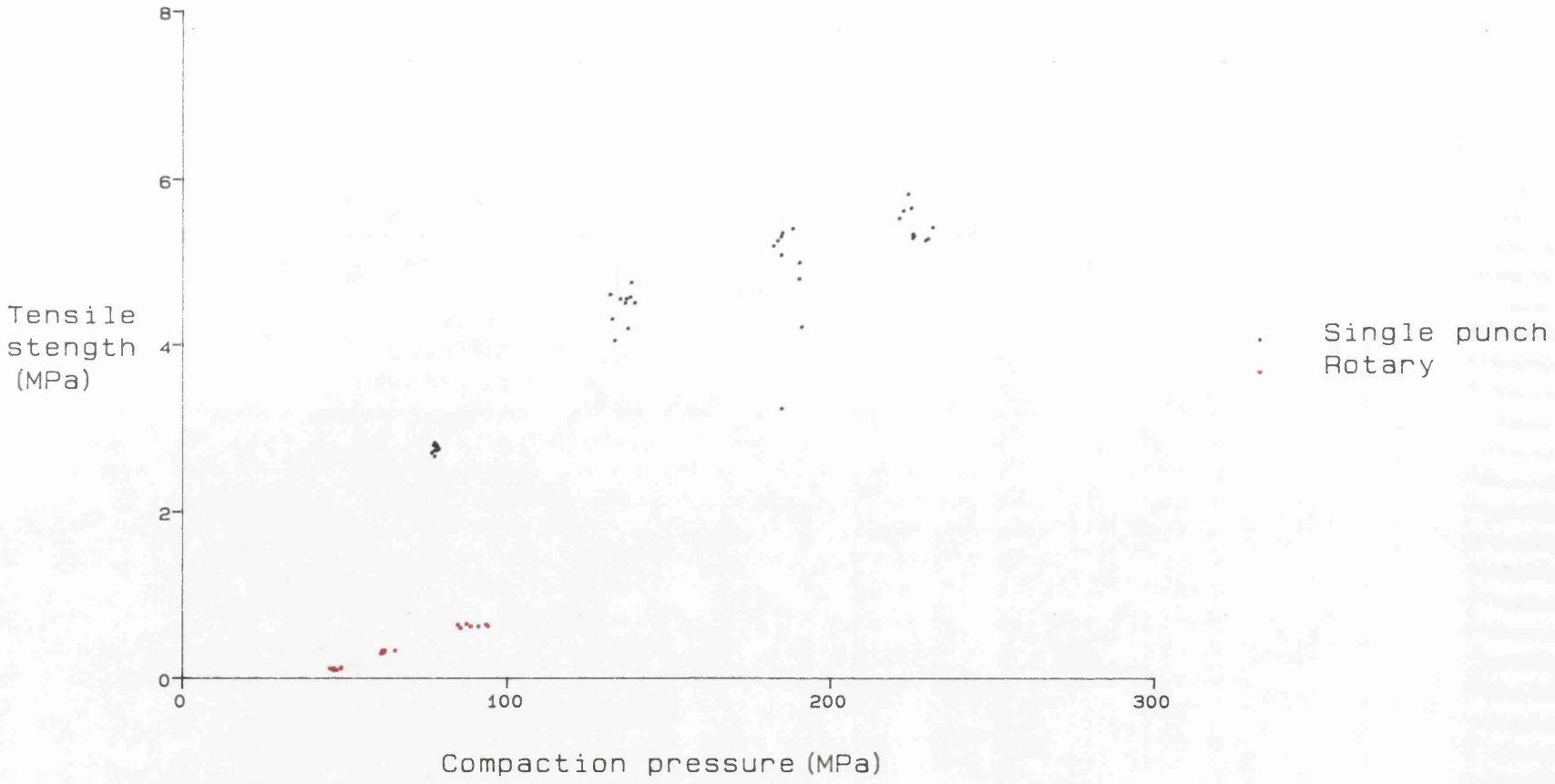

Tensile strength determined by diametral compression.
Theoretical thickness of compacts with zero porosity = 2.0mm.

Figure 5.7 Effect of machine type on the compaction pressure/tensile strength profile of circular Avicel compacts

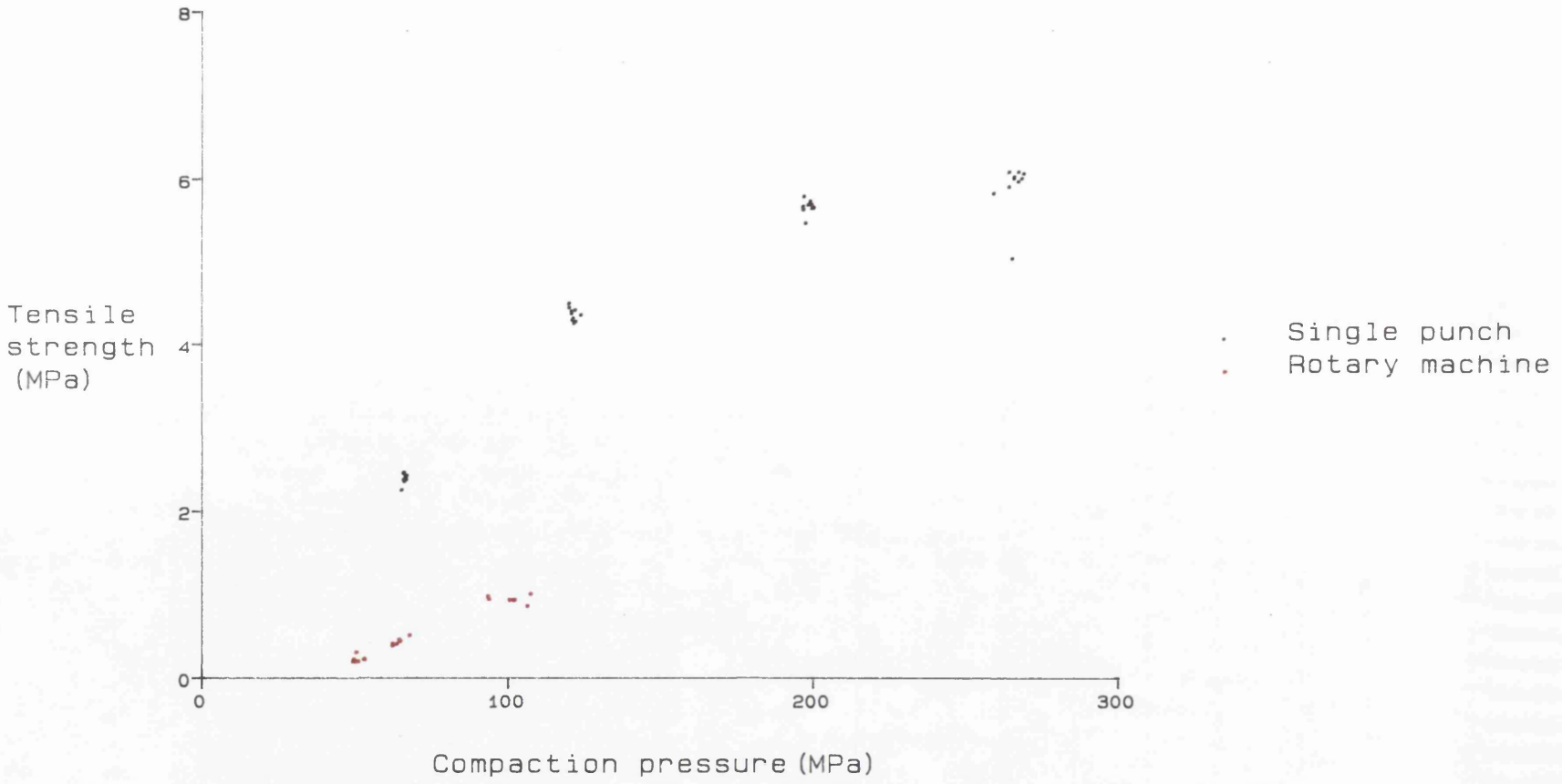

Tensile strength determined by diametral compression.
Theoretical thickness of compacts with zero porosity = 2.8mm.

Figure 5.8 Effect of machine type on the compaction pressure/tensile strength profile of circular Avicel compacts

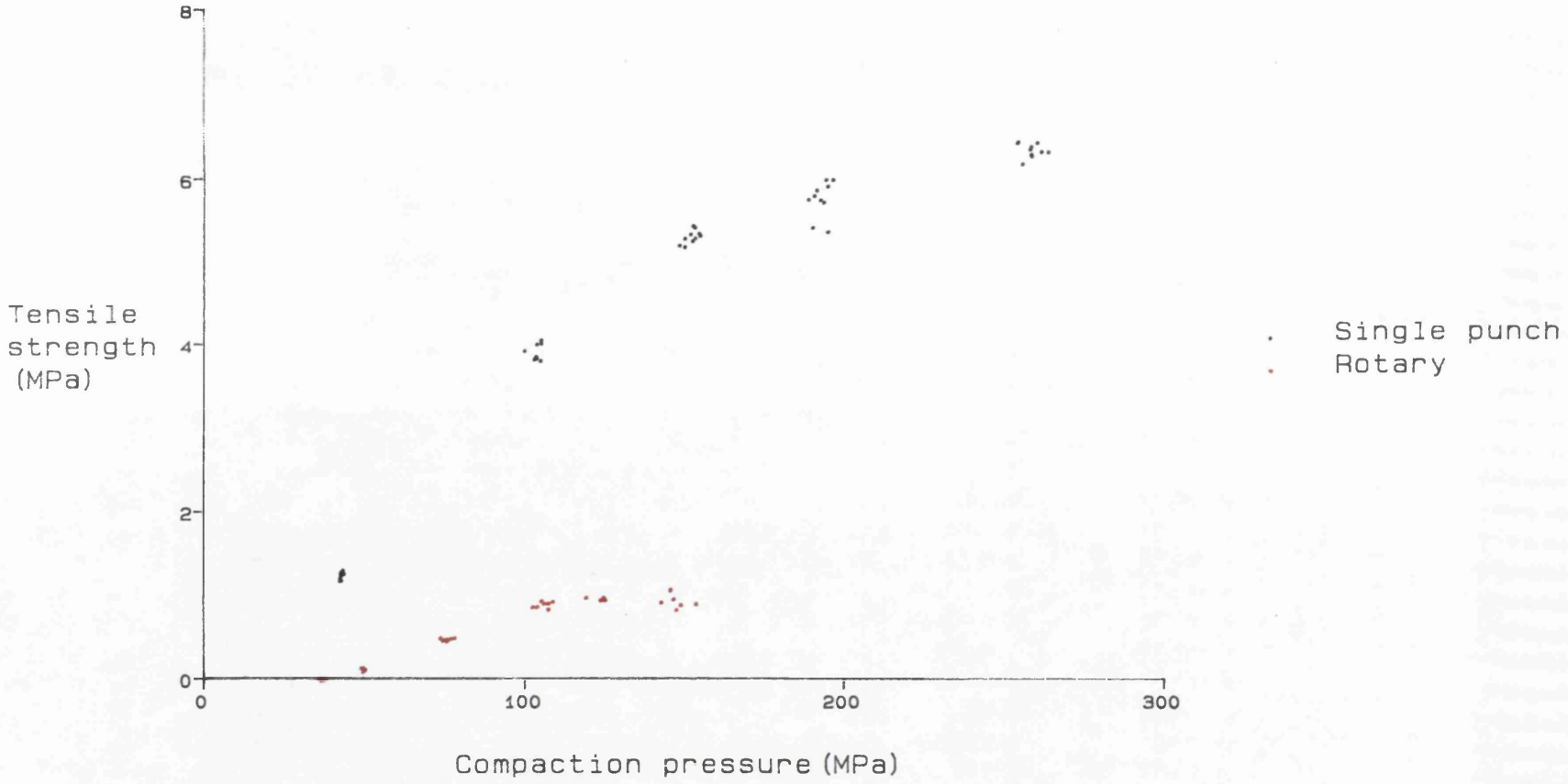

Tensile strength determined by diametral compression.
Theoretical thickness of compacts with zero porosity = 2.0mm.

Figure 5.9 Effect of machine type on the compaction pressure/tensile strength profile of square Avicel compacts

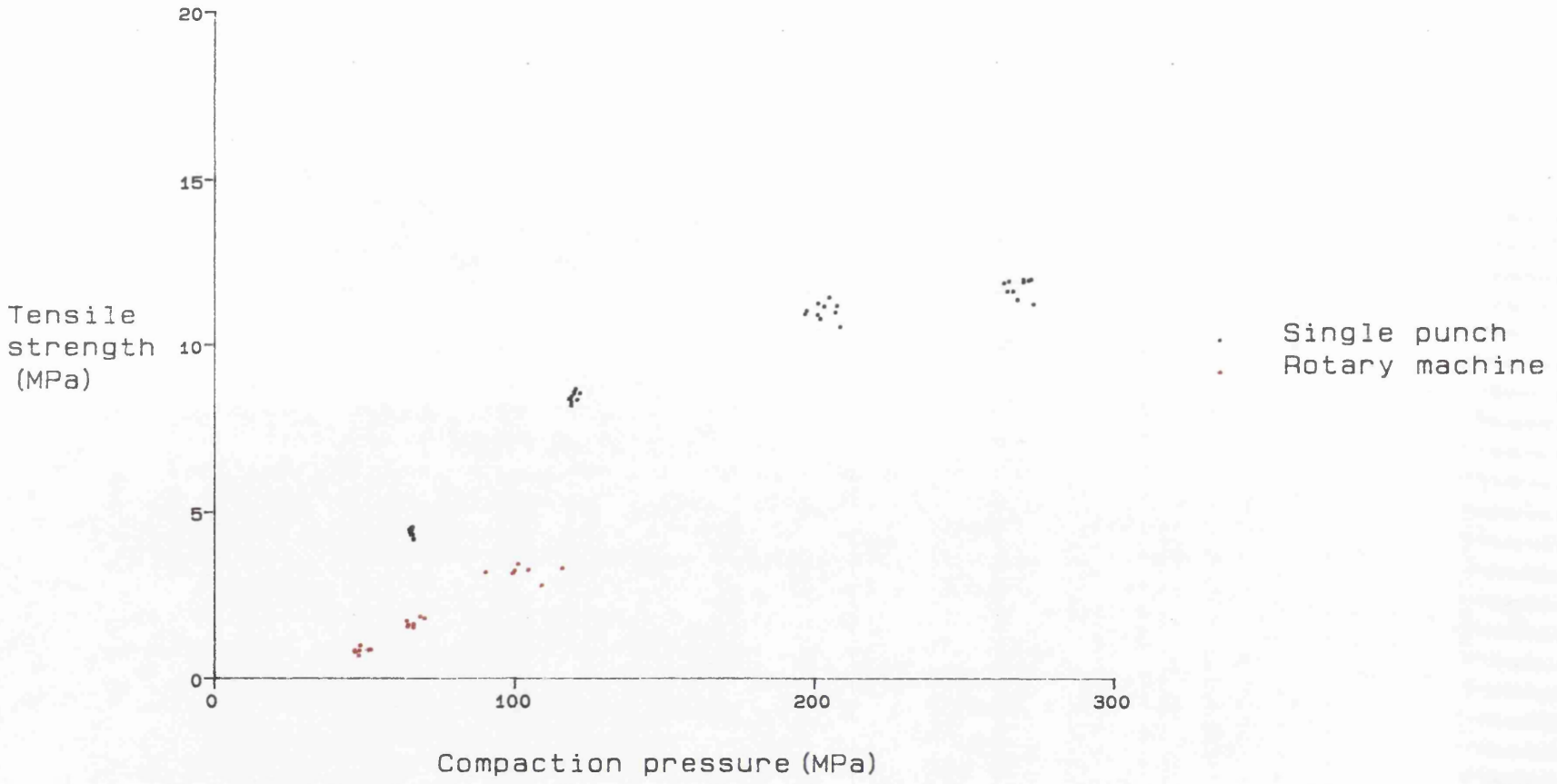

Tensile strength determined by axial compression.
Theoretical thickness of compacts with zero porosity = 2.8mm.

Figure 5.10 Effect of machine type on the compaction pressure/tensile strength profile of square Avicel compacts

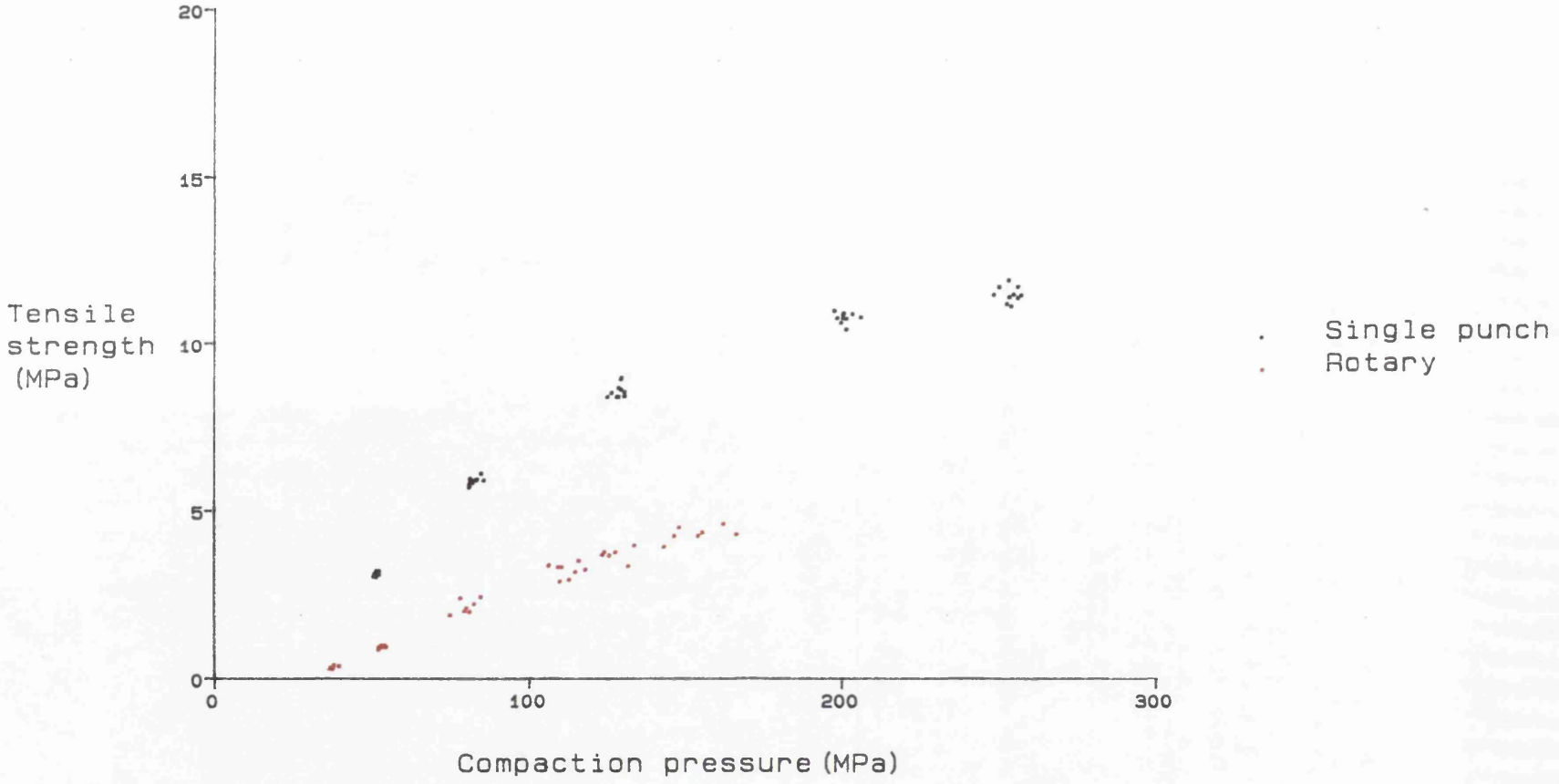

Tensile strength determined by axial compression.
Theoretical thickness of compacts with zero porosity = 2.0mm.

Figure 5.11 Effect of machine type on the compaction pressure/tensile strength profile of square Avicel compacts

Raynor 1976). Plastic deformation is time dependent so that materials which behave in this manner will be sensitive to variations in the strain rate. Roberts and Rowe (1984) investigated the effect of punch velocity on the Heckel plots of a range of materials. Materials known to consolidate by fragmentation demonstrated no change in yield pressure over the range of velocities examined ($0.033mms^{-1}$ to $400mms^{-1}$), while plastic deforming materials demonstrated an increase in yield pressure with increasing punch velocities. The authors proposed an index for the Strain Rate Sensitivity (SRS) of materials based on the percentage change in the yield pressure for compacts prepared at punch velocities of $0.033mms^{-1}$ to $300mms^{-1}$. Avicel PH-101 was found to have an SRS value of 38.9%. The mechanism for an increase in the yield pressure with punch velocity may be a reduction in the amount of plastic deformation, due to the time dependent nature of plastic flow and thus bond formation.

The change in compaction rate is therefore a possible cause of the capping seen on the rotary machine. While it may be a contributory factor there is evidence to suggest that this alone is unlikely to produce the dramatic decrease in compact strength seen at all compaction pressures and not only above the capping pressure. Firstly, although the volume reduction of the powder is much more rapid on the rotary machine, the punches retain the powder at the maximum pressure for a prolonged period during which plastic flow can occur (Figure 5.5). This maintenance of the compact at or near the maximum pressure for an extended time would be expected to produce an increase in the strength of compacts formed through plastic deformation. On the single punch machine the upper punch is removed as

soon as maximum penetration is reached.The machine does not, therefore, provide the dwell time seen on the rotary machine.

Secondly, on the single punch machine Avicel does not appear to be sensitive to changes in compaction rate. Figure 5.12 shows the compaction pressure/tensile strength profiles of circles produced at 2 machine speeds for each machine. A doubling of the machine speed (from 30 r.p.m. to 60 r.p.m.) and hence a doubling of the punch velocities and halving of the compaction time results in only a small increase in the strength of the compacts. Changing the speed of the rotary machine produces changes in the strength of the compacts produced, but does not appear to affect the capping pressure. If the differences between the rotary machine and single punch machine were solely related to the rate of compression, it would be likely that the changes in machine speed would produce greater changes in the compact strength.

The differences may be due to the manner in which the powder moves and hence how the force is transmitted during the compaction process. The movement of powder in a die when compressed between a moving punch and a stationary punch has been examined by Train (1955) and Macleod (1974) and is described in Chapter 3. As the punch enters the die the force applied is transmitted through the powder bed as a hemispherical pressure front, the powder in the centre of the compact moving to a greater extent than the material at the edge due to the die wall friction (Figure 5.13a). This pressure front continues until the reaction from the lower punch exceeds the radial reaction from the die wall. Typically this was found to occur about two thirds of the way down a compact. On a rotary machine

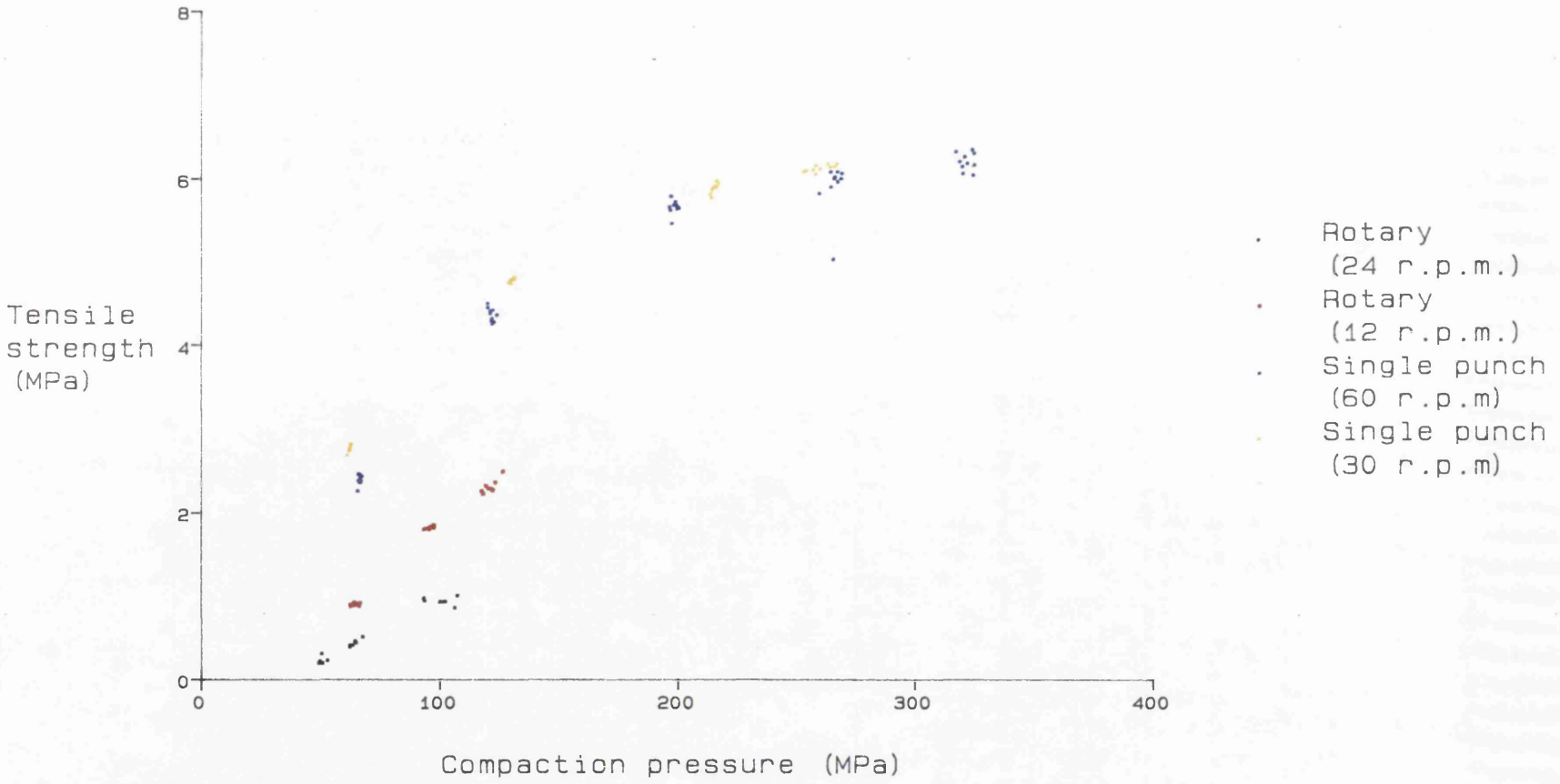

Tensile strength determined by axial compression.
Theoretical thickness of compacts with zero porosity = 2.8mm

Figure 5.12 Effect of machine speed on the compaction pressure/tensile strength profiles of Avicel circular compacts

there will be powder flow in 2 directions, due to the actions of both punches, from the start of compression. In the early stages of compression there will be 2 hemispherical pressure fronts moving towards each other (Figure 5.13b). It is likely that the maximum stresses will occur where the pressure fronts meet, i.e close to the centre of the compact. The interaction between the two pressure fronts is difficult to predict but it is evident that the structures of compacts produced by the two machines are likely to differ.

Macleod (1974) demonstrated that the level of die wall friction affects the density distribution within compacts altering the hemispherical nature of the pressure front (Figure 5.14). The increased ratio of die wall surface area to powder volume will increase the die wall friction. The movement of powder at the die wall in square compacts will therefore be lower than in circular compacts. At the point where the pressure fronts of the two punches meet the axial stresses at the die wall will be lower in the square compacts. This may provide a mechanism for the stresses produced in the centre of the compact to be relieved by radial movement. Such stress relief could account for the higher capping pressures seen in the square compacts compared to the circular compacts.

5.4.2 Effect of machine type on the compaction properties of Emcompress

The properties of the Emcompress compacts produced on the two machines were not as markedly different as the Avicel compacts but significant differences were evident. The main difference was that square compacts with zero porosity thicknesses of 5mm could be produced on the rotary machine but not the single punch machine. Differences were also seen in

Figure 5.13
Diagrammatic representation of powder movement during the early stages of compression

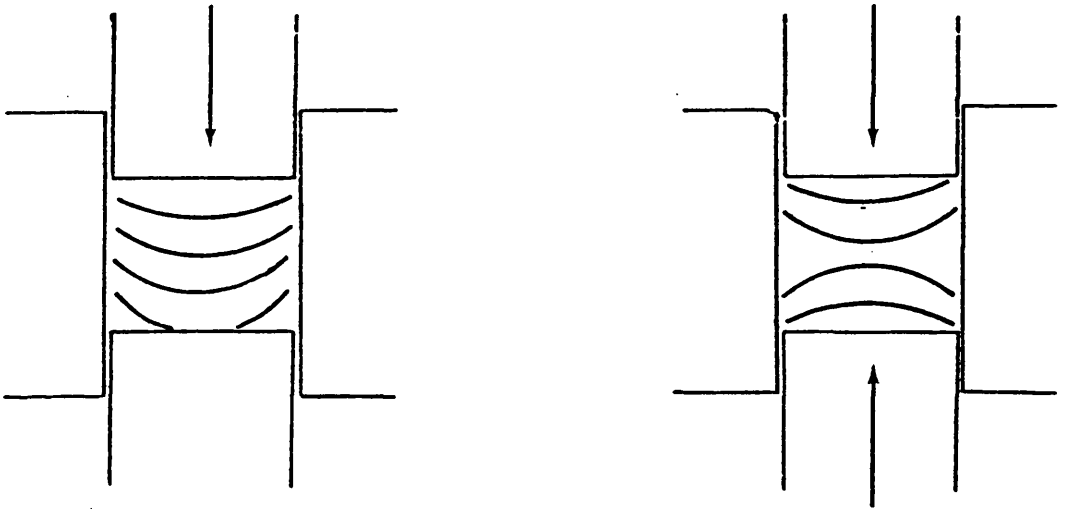

Single punch machine

Rotary tablet machine

Figure 5.14
Effect of die wall friction on powder movement on a rotary tablet machine

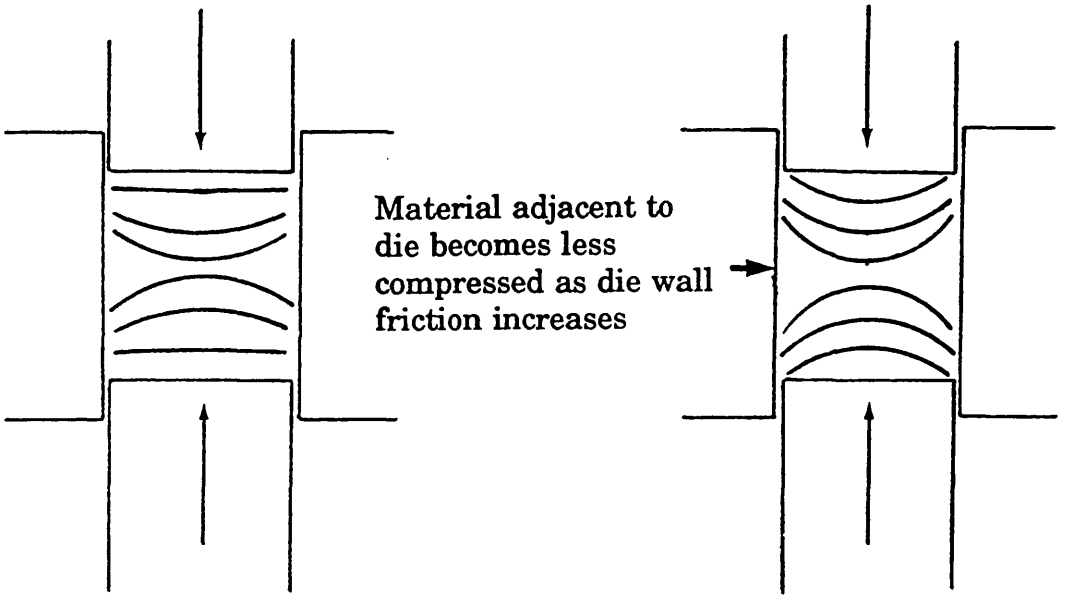

Low friction

High friction

the compaction pressure/tensile strength profiles of compacts produced on the two machines.

The ability to produce the square compacts can be explained by the differences in punch movement between machines. The failure to produce square compacts with zero porosity thicknesses above 2.8mm on the single punch machine was attributed to the die wall friction in the corners of the compacts producing exaggerated density differences within the compact. In particular at the limit of downward powder movement in the four corners the degree of compression was insufficient to produce a coherent compact. On the rotary machine the die wall friction will again reduce powder movement adjacent to the die. However, because both punches are moving, the distance moved by each punch during compression is less than the distance moved by the upper punch of a single punch machine, hence the point at which powder ceases to move at the die wall is not reached with the rotary machine.

The effect of machine type on the compaction pressure/tensile profiles of Emcompress compacts is illustrated in Figures 5.15 to 5.19. The rotary machine produces weaker compacts than the single punch machine at any given compaction pressure. As the compaction force on the rotary machine is measured at a point remote from the punches it is possible that such differences could be attributed to errors in the force measurement. Figures 5.20 to 5.24 show the log tensile strength versus porosity plots for compacts produced on the two machines. Again there are differences between the compacts produced on the two machines. This indicates that even if differences do exist between the two force monitoring systems there

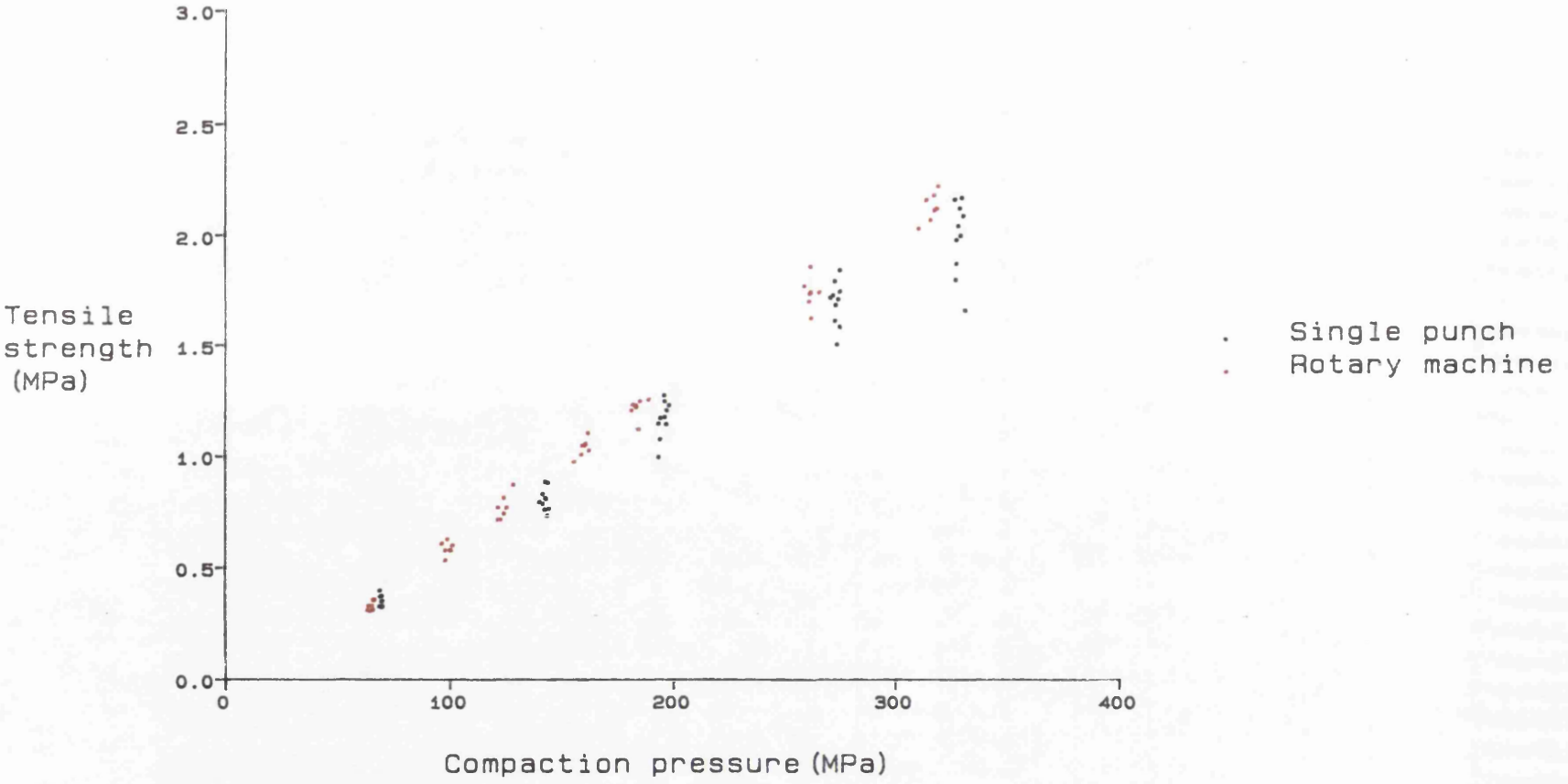

Tensile strength determined by diametral compression.
Theoretical thickness of compacts with zero porosity = 2.0mm.

Figure 5.15 Effect of machine type on the compaction pressure/tensile strength profile of circular Emcompress compacts

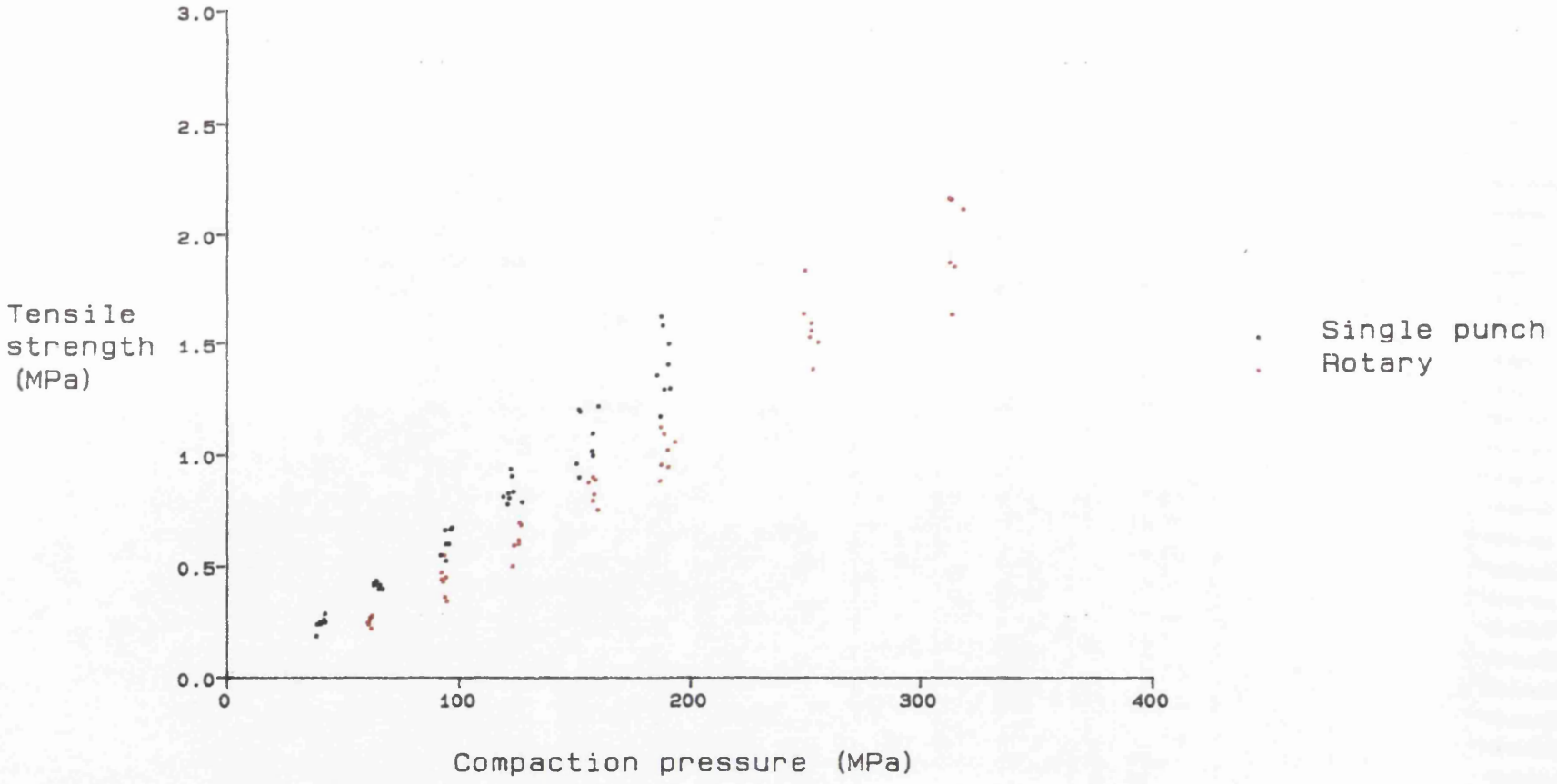

Tensile strength determined by diametral compression.
Theoretical thickness of compacts with zero porosity = 5.0mm.

Figure 5.16 Effect of machine type on the compaction pressure/tensile strength profile of circular Emcompress compacts

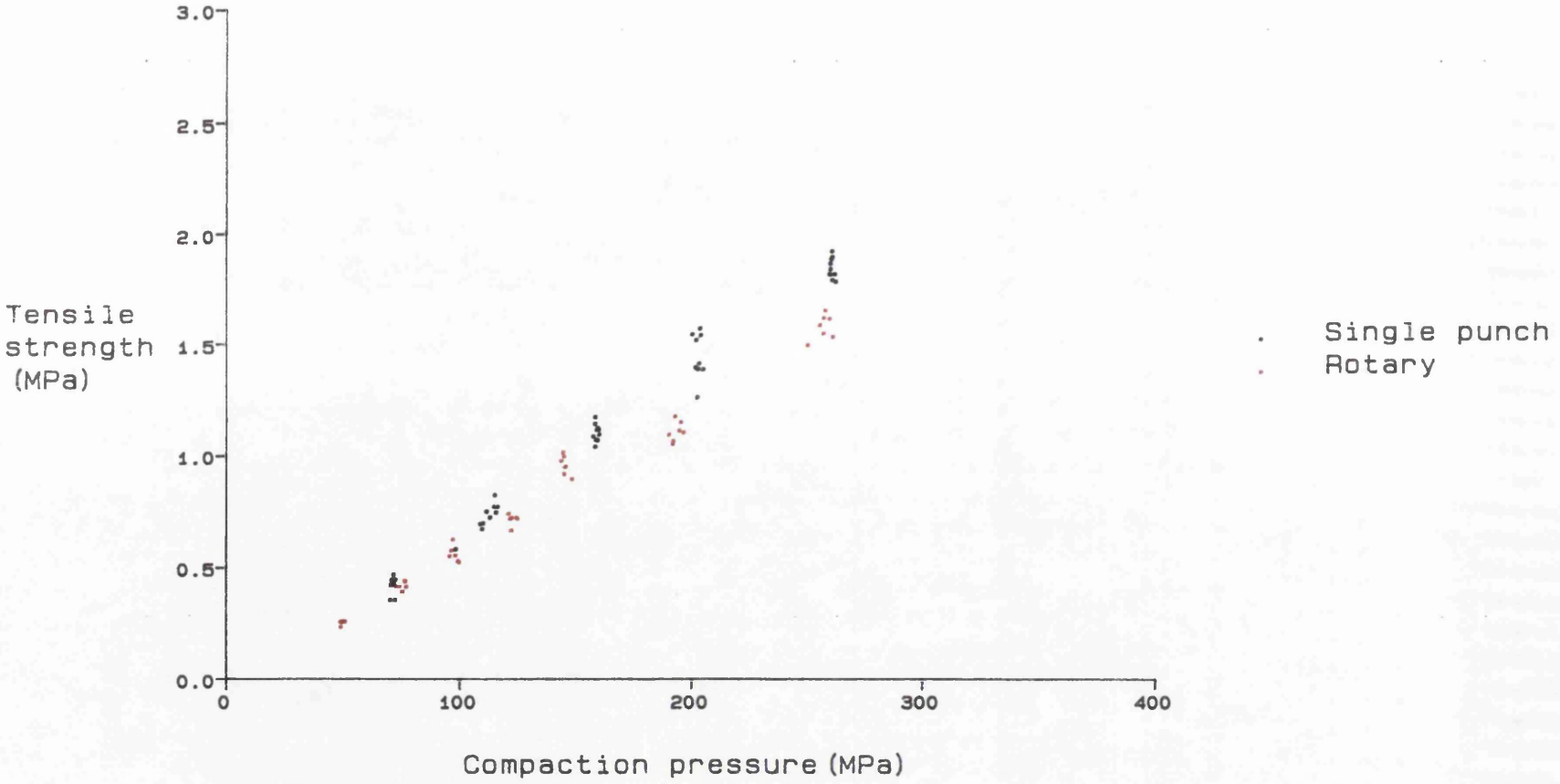

Tensile strength determined by diametral compression.
Theoretical thickness of compacts with zero porosity = 2.0mm.

Figure 5.17 Effect of machine type on the compaction pressure/tensile strength profile of square Emcompress compacts

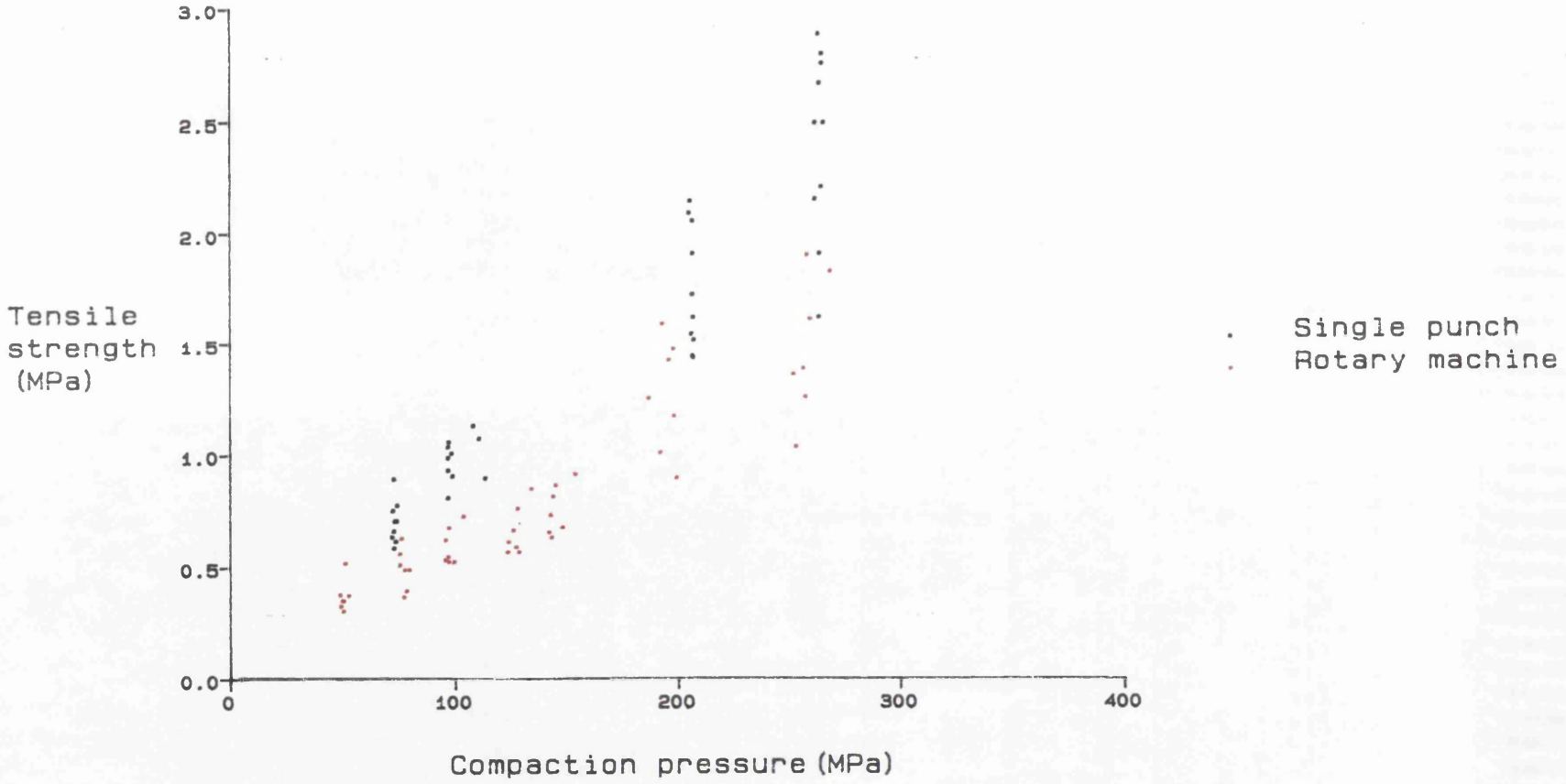

Tensile strength determined by axial compression.
Theoretical thickness of compacts with zero porosity = 2.0mm.

Figure 5.18 Effect of machine type on the compaction pressure/tensile strength profile of square Emcompress compacts

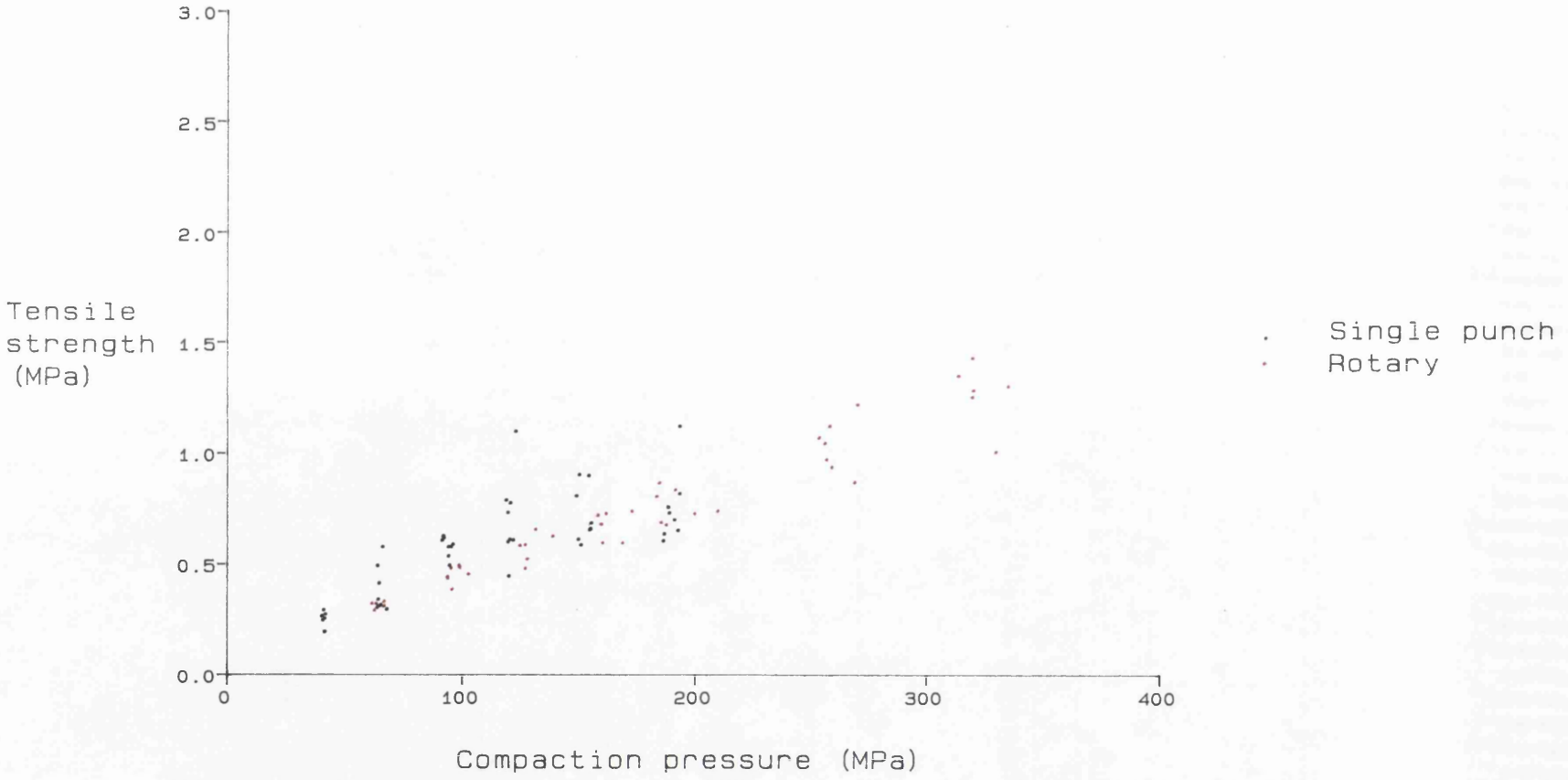

Tensile strength determined by axial compression.
Theoretical thickness of compacts with zero porosity = 5.0mm.

Figure 5.19 Effect of machine type on the compaction pressure/tensile strength profile of circular Emcompress compacts

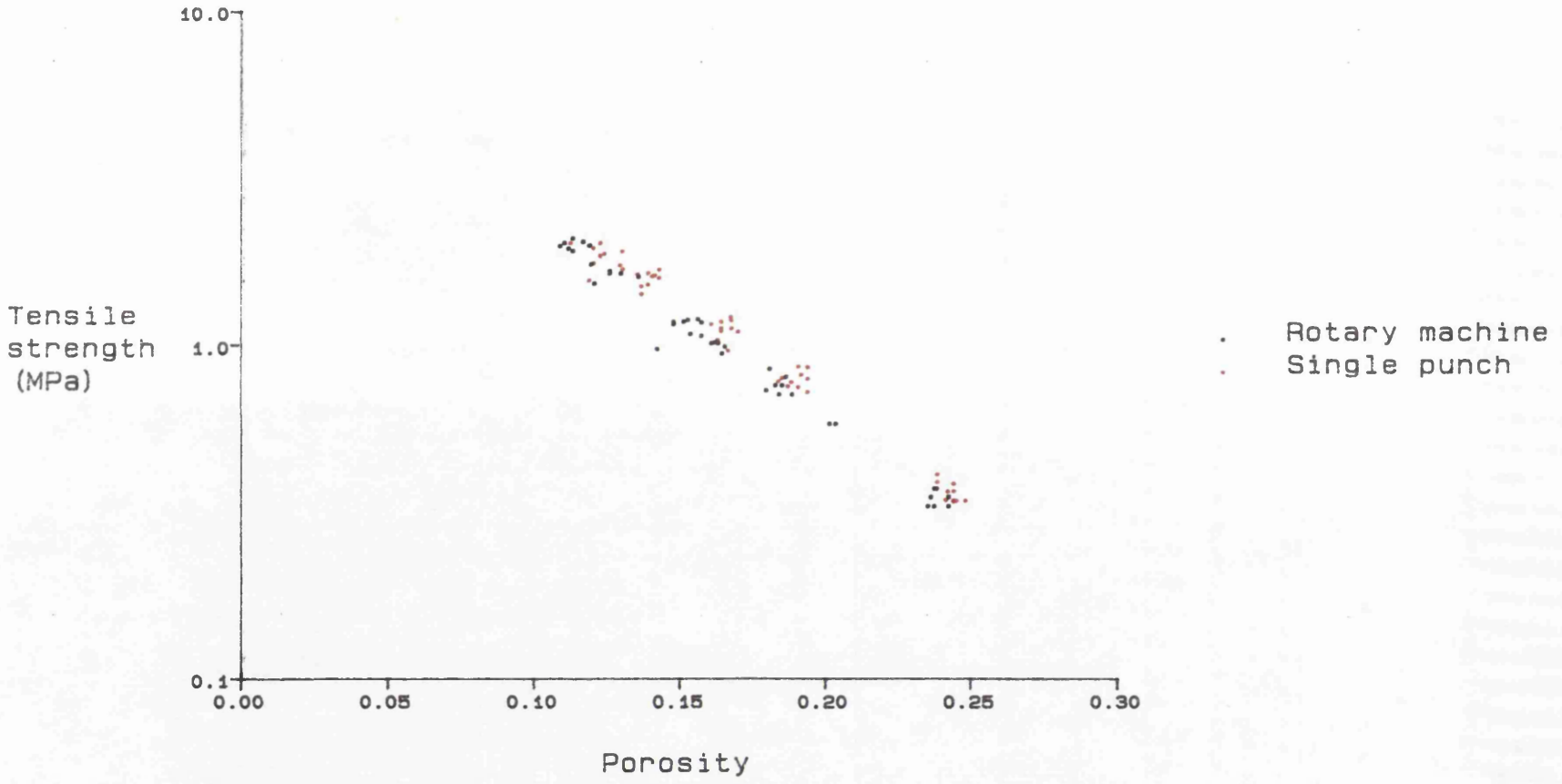

Tensile strength determined by diametral compression.
Theoretical thickness of compacts with zero porosity = 2.0mm.

Figure 5.20 Effect of machine type on the plot of tensile strength versus porosity for circular Emcompress compacts

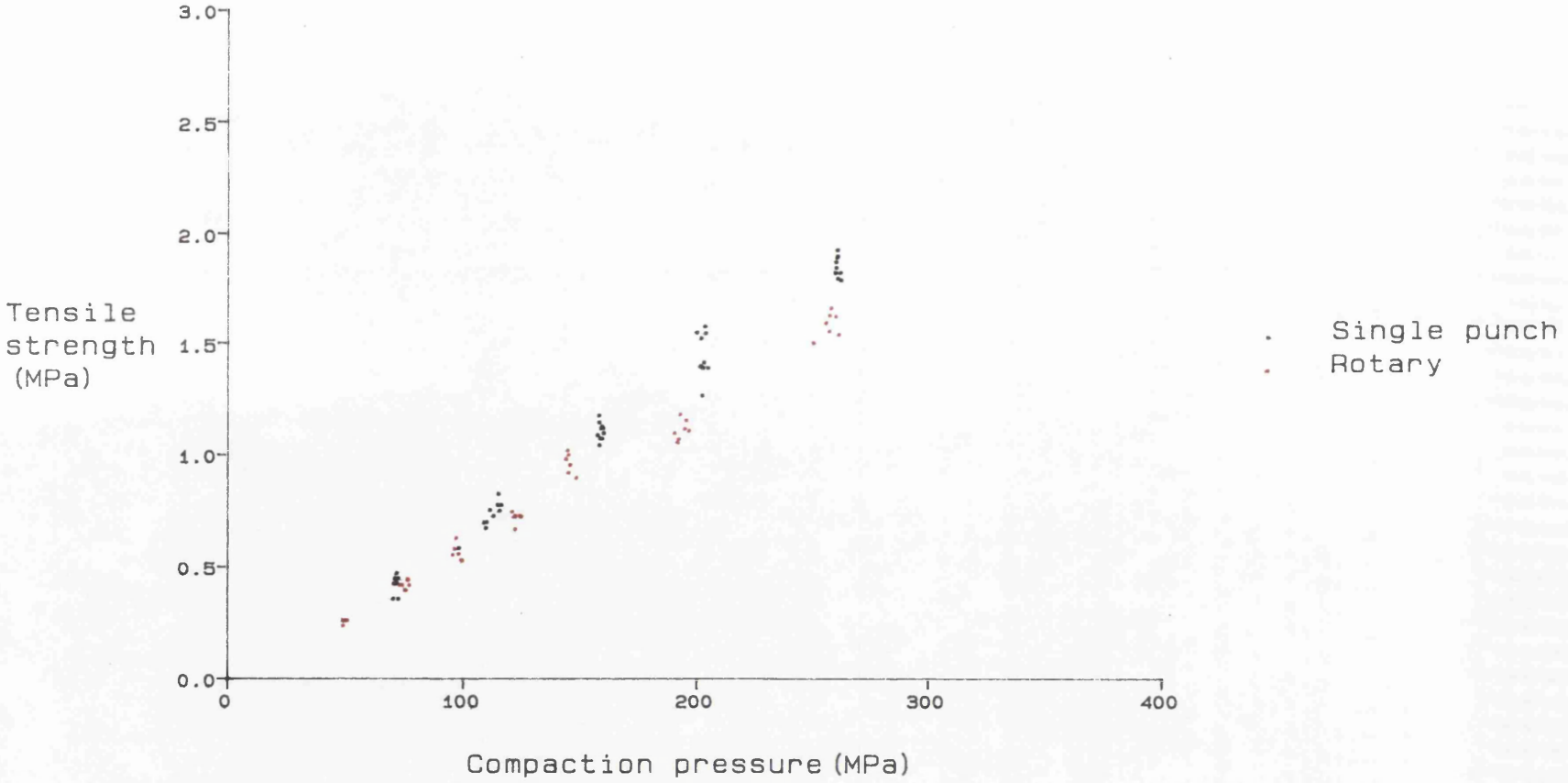

Tensile strength determined by diametral compression.
Theoretical thickness of compacts with zero porosity = 2.0mm.

Figure 5.21 Effect of machine type on the plot of tensile strength versus porosity for square Emcompress compacts

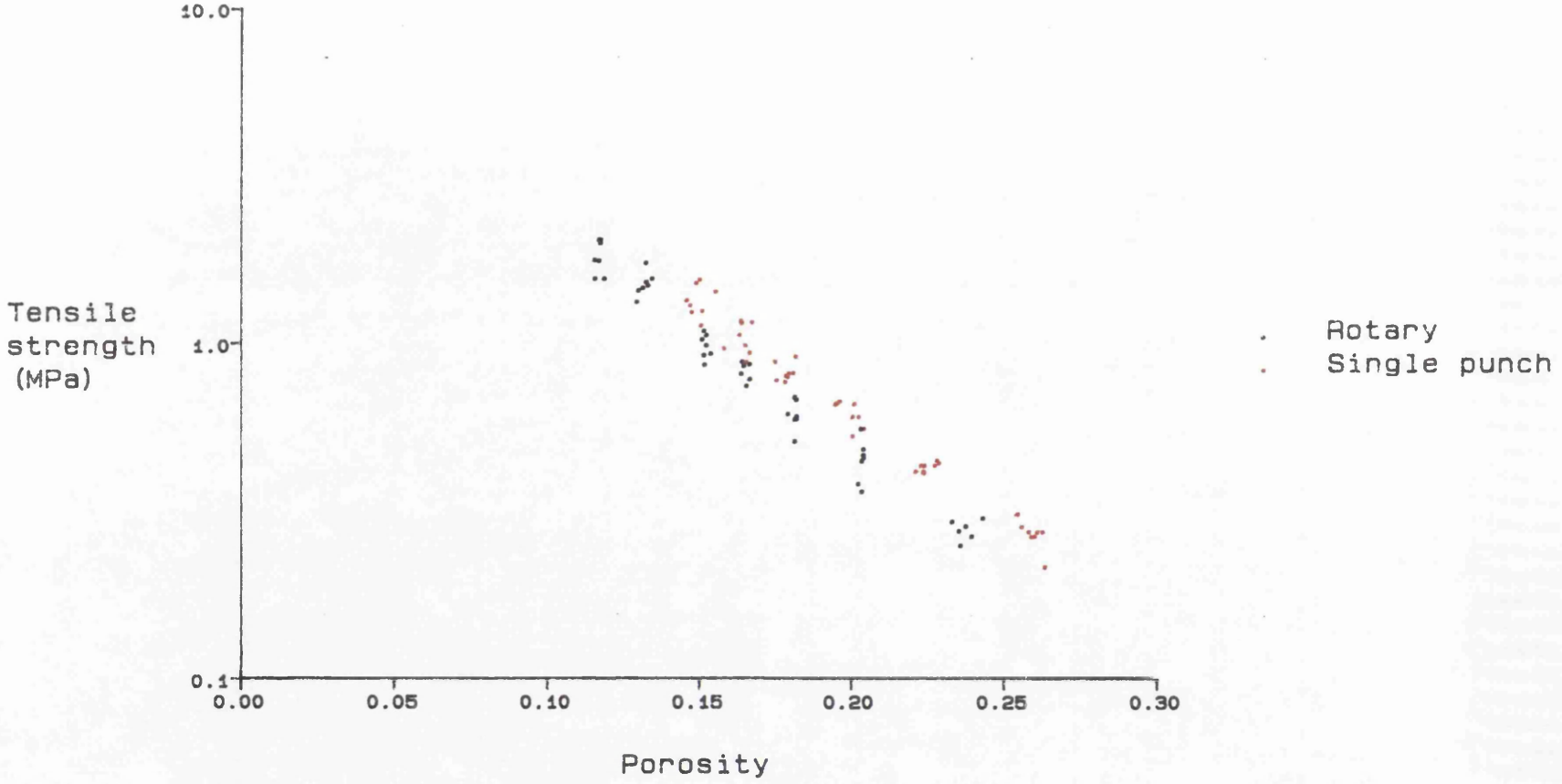

Tensile strength determined by diametral compression.
Theoretical thickness of compacts with zero porosity = 5.0mm.

Figure 5.22 Effect of machine type on the plot of tensile strength versus porosity for circular Emcompress compacts

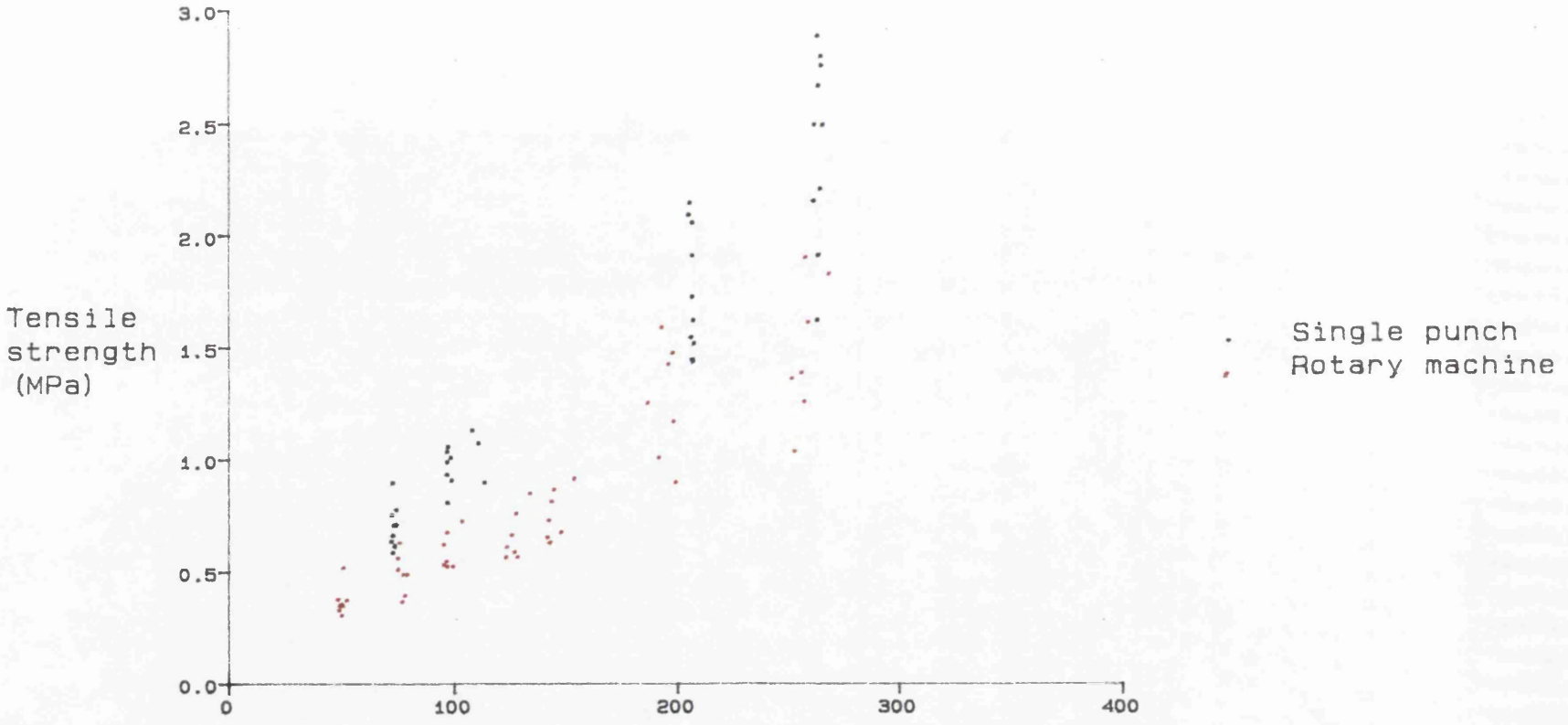

Tensile strength determined by axial compression.
Theoretical thickness of compacts with zero porosity = 2.0mm.

Figure 5.23 Effect of machine type on the plot of tensile strength versus porosity for circular Emcompress compacts

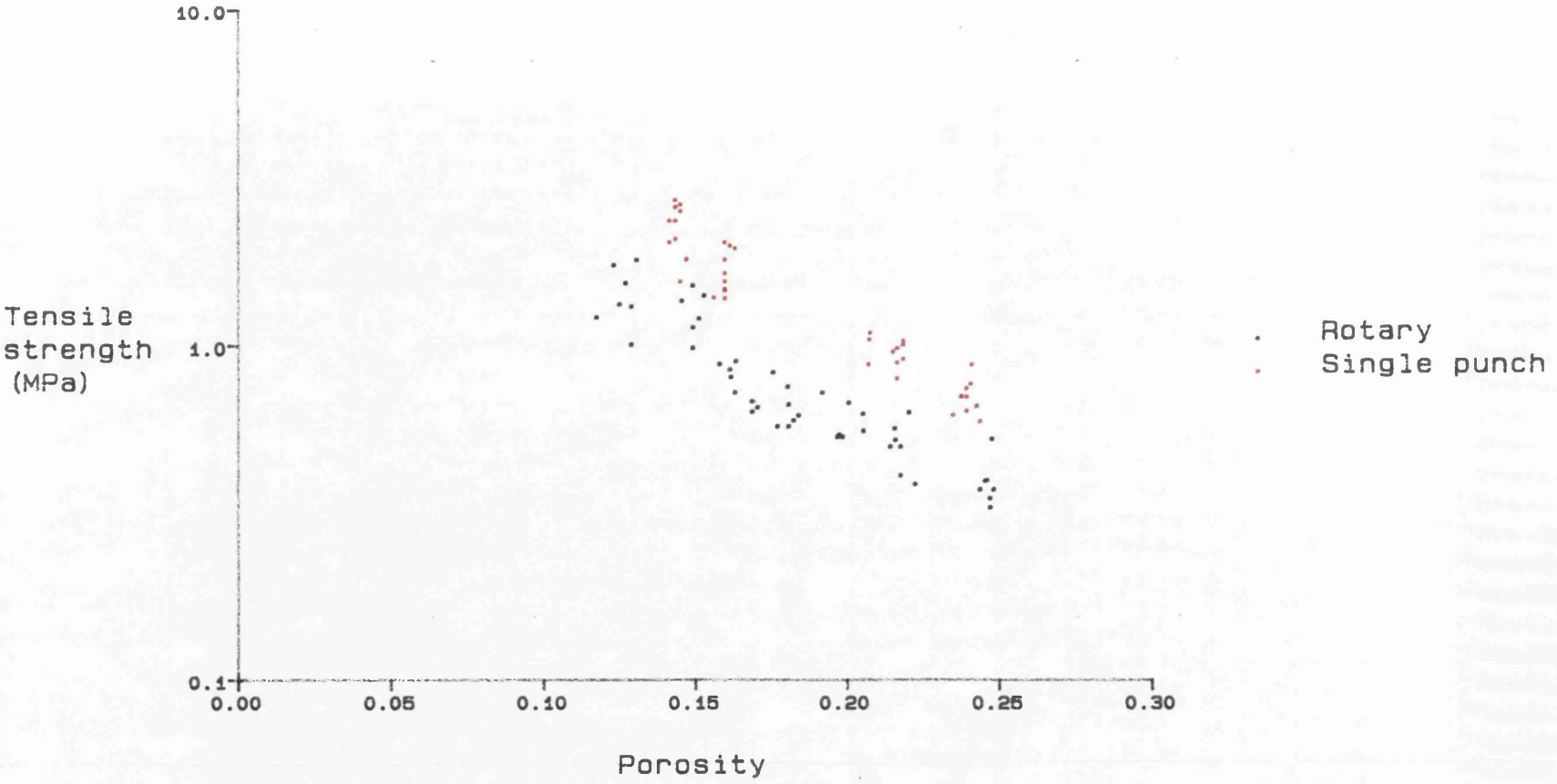

Tensile strength determined by axial compression.
Theoretical thickness of compacts with zero porosity = 5.0mm.

Figure 5.24 Effect of machine type on the plot of tensile strength versus porosity for square Emcompress compacts

are differences in the structures of the compacts produced by the machines. Unlike Avicel, Emcompress is considered a brittle material that consolidates by fragmentation. Rees (1980) showed that the strength of a perfectly elastic-brittle particle shows no rate dependence. Roberts and Rowe (1984) measured the strain rate sensitivity of calcium phosphate and obtained a value of zero, indicating no time dependence. The differences seen between the Emcompress compacts prepared on the two machines is unlikely, therefore, to be due to changes in the rate of compaction. Again the differences are probably due to the changes in punch movement. The structural differences between the square and circular compacts responsible for the different tensile strength values cannot be described without a more detailed knowledge of the way in which the stresses are distributed within the compacts during the compaction process. It is likely, however, that the differences in powder movement adjacent to the die wall are implicated in the differences observed between compact shapes.

5.5 Conclusions

The type of tablet machine used to prepare compacts of Avicel PH-102 and Emcompress has been shown to affect their tensile strength. An analysis of the punch velocities obtained on the single punch and rotary machines indicates that the maximum punch velocities were similar at the machine speeds used in this study. However, due to the movement of both punches on the rotary machine the period over which volume reduction is achieved is lower than for the single punch machine. The differences in the punch velocities and compaction times for the two machines are not considered

sufficient to account for the differences in compact properties. These differences have been attributed to the manner in which the forces are transmitted through the compact by the two compression systems. It is postulated that the density distributions within compacts will be machine dependent, and that it is these which lead to the changes seen in compact properties.

CHAPTER 6

THE INFLUENCE OF SHAPE ON THE STRENGTH OF COMPACTS PREPARED FROM GRANULATED FORMULATIONS

6.1 Introduction

The compaction studies described in Chapters 3 to 5 have been performed on single excipients and blends of each excipient with Magnesium Stearate to facilitate smooth running on a tablet machine. Such studies can provide useful information about the behaviour of materials during compression but do not realistically represent the situation present in pharmaceutical formulations where a number of excipients are combined. The compaction properties of the final formulation will be a function of the individual contributions of each excipient and any interactions that occur between them. The nature of such interactions cannot as yet be predicted from studies performed on the single materials, although an understanding of the compaction mechanisms of individual components may help to explain interactions when they are seen to occur.

Although some commercial tablet formulations are prepared using direct compression the majority still involve a granulation step. Reasons for granulating may include improvement of flow properties, reduction of content uniformity problems by locking a low dose drug within the larger particles thus reducing its ability to segregate and improvement of compaction properties. Avicel PH-102, although initially used as a direct compression excipient, is also used extensively as a compression aid in granulated pharmaceutical products. The work described in this chapter examines the behaviour of Avicel PH-102 and Magnesium Stearate in a granulated tablet formulation and attempts to relate the effects seen to the properties of the excipients per se. These formulations formed part of an optimisation study for a placebo tablet and a third variable, the level of the

disintegrant, Primojel, was also included in the study. Square and circular compacts produced using the single punch machine and rotary machine were tested using the diametral compression and axial compression tests. The aim of the study was to determine which factors affected the tensile strength of the final compact and the relative effects of the excipients and their interactions.

The calculation of the effects of each variable and interactions between variables depends on the use of an appropriate experimental design. Having selected an appropriate protocol, normally based on a factorial design, the resultant data can be analysed in a number of ways. If the purpose of the experiment was to assess which of the variables had a significant effect on the tensile strength and the relative importance of the effects the data could be analysed by the Yates method (Armstrong and James 1990). In this experiment the aim was to quantify the effects of the variables, so a model dependent optimisation procedure was considered more appropriate. Model dependent optimisation involves the fitting of a regression line to the experimental data that best explains the variance in tensile strength between formulations. Using the formula of the fitted line the effects of the variables can be presented graphically. The ultimate goal of such experiments is usually the selection of a formulation that will possess the optimum properties. For this study the aim is to attempt to explain any differences seen between compacts of different shape or compacts produced on different machines using the knowledge gained in Chapters 3 to 5.

6.2 Materials and methods

6.2.1 Materials

The compacts were prepared from granulates containing a blend of Anhydrous Lactose DCL 21 (PFW Ltd), Microcrystalline Cellulose (Avicel PH-102, Honeywell and Stein Ltd), Sodium Starch Glycollate (Primojel, Tunnel Avebe Starches Ltd) and Polyvidone (Kollidon 30, BASF UK Ltd) which were lubricated with Magnesium Stearate (Durham Chemicals Ltd).

6.2.2 Experimental design

The general formulation of the mixes used in the compaction studies was;

Anhydrous Lactose DCL 21	to 100%
Microcrystalline Cellulose (Avicel PH-102)	X_1%
Sodium Starch Glycollate (Primojel)	X_2%
Polyvidone (Kollidon 30)	2%
Magnesium Stearate	X_3%

where; X_1 = 8% to 24%

X_2 = 0% to 6%

X_3 = 0.2% to 1.0%

The 3 independent variables being assessed were the levels of Avicel PH-102, Primojel and Magnesium Stearate. The 2 dependent variables being measured were the tensile strengths determined by the axial compression and diametral compression tests. In considering the experimental design to be used the following factors were taken into account. Firstly, it was felt that it could not be assumed that there would be linear relationships between the levels of the 3 excipients being varied and the tensile strengths. Secondly, it was considered likely that there would be

interactions between the excipients, e.g Magnesium Stearate is known to have a greater adverse effect on the compactibility of plastically deforming materials such as Avicel than on brittle materials that create new uncoated surfaces during compaction. The final assumption was that any changes seen between the formulations would be due to the varying levels of the 3 independent variables and not changes in the level of Anhydrous Lactose. This assumption was necessary to restrict the number of experiments to be performed and was justified on the basis that the Lactose formed the bulk of all the formulations examined. However, when comparing the behaviour of formulations on the 2 tablet machines the influence of the Anhydrous Lactose must be considered.

To assess the non-linearity of the response surfaces at least 3 levels of each of the independent variables must be used. This permits the relationships between the excipients and the tensile strengths to be expressed using equations which contain both linear and quadratic terms. The expression of all the interactions using linear and quadratic terms for each excipient would require a full factorial design to be performed. This would involve $3^3 = 27$ experiments.

If certain interactions are considered to be unimportant they can be excluded from any analyses by using a confounded system. Confounding is the term given to experiments in which it is not possible to differentiate the effects of two or more variables on a response due to an incomplete factorial design. Careful selection of the experiments to be performed allows the higher interactions, i.e. those involving more than two variables or the squares of the variables, to be confounded enabling the main effects

and lower order interactions to be determined with a reduced number of experiments. It has to be accepted that the use of such systems will result in a reduction in accuracy.

The design selected for this experiment was a Box Benkhen type experiment in which 13 different formulations were prepared. This design is represented diagrammatically in Figure 6.1 and the levels of the 3 dependent variables listed in Table 6.1. Using this design the responses can be expressed in the following form;

$$Y = B_0 + B_1X_1 + B_2X_2 + B_3X_3 + B_{12}X_1X_2 + B_{13}X_1X_3 + B_{23}X_2X_3 + B_{11}X_1^2 + B_{22}X_2^2 + B_{33}X_3^2 \quad (6.1)$$

Where; Y = Tensile strength

B = Regression coefficient

X = Level of excipient

The centre point of the box, which contains the intermediate levels of the 3 excipients, was prepared in triplicate to provide an estimate of the variance between batches.

6.2.3 Preparation of tablet mixes

Sufficient granulate to produce 1kg of the final tablet mix was prepared. The Anhydrous Lactose was passed through a 355 micrometre sieve and the remaining excipients were passed through a 250 micrometre sieve to remove any agglomerates. The Anhydrous Lactose, Avicel PH-102, Primojel and Kollidon 30 were blended in a Y-cone mixer (Apex Construction, Type 165) for 6 minutes and transferred to the bowl of a planetary mixer (Hobart Machinery Ltd, Model SE 200). Two hundred and twenty five millilitres of Purified Water was added to the granulate, at a rate of 15ml per minute using a peristaltic pump, while stirring at 30 r.p.m. Mixing

Table 6.1
Tablet formulations prepared in optimisation study

Formulation	X1 Avicel (%)	X2 Primojel (%)	X3 Magnesium Stearate(%)
1	8	0	0.6
2	8	3	0.2
3	8	3	1.0
4	8	6	0.6
5	16	0	0.2
6	16	0	1.0
7	16	6	1.0
8	16	6	0.2
9	24	0	0.6
10	24	6	0.6
11	24	3	1.0
12	24	3	0.2
13	16	3	0.6

Figure 6.1
Schematic representation of the Box-Benkhen experimental design

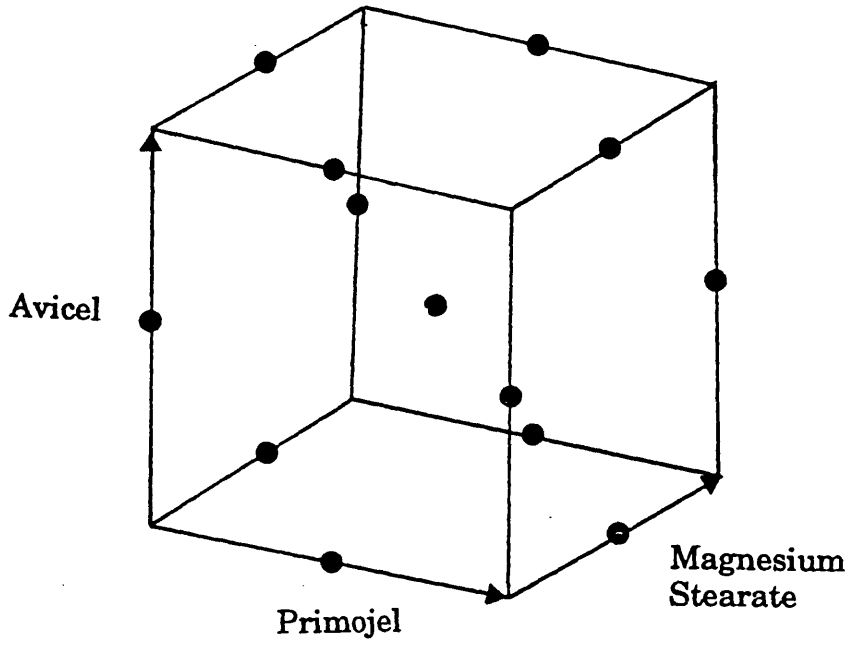

continued for 5 minutes after the addition of water was complete.

The wet mass was passed through a 1mm sieve by hand and transferred to the drying chamber of a fluid bed dryer (Anglo-Continental Machinery, Aeromatic Strea-1). The material was dried using an air inlet temperature of 50°C. Drying was continued until a loss on drying value below 1% was obtained, as determined by use of a balance fitted with an infra-red dryer (Mettler Instruments Ltd, Model LP-15). The end point for the loss on drying test was defined as a weight loss of less than 1mg per minute from a 5g sample being dried at 90°C.

The dried granulate was passed through a 900 micrometre sieve. Sieve analyses were performed on the granulates using a tapping sieve shaker (Inclyno Model 1, Pascall Engineering). The results are summarised in Table 6.2. demonstrating that differences exist between batches. Elimination of particle size as a variable by selecting a specific size fraction for the compaction studies was considered. However, the differences are likely to be due, at least in part, to the differences between the formulations. The selection of specific size fractions could significantly affect the final conclusions. Five hundred grammes of each tablet mix listed in Table 6.1 was prepared by blending a portion of each granulate with the appropriate quantity of Magnesium Stearate for 3 minutes in the Y-cone mixer.

6.2.4 Preparation of compacts

Compacts from each formulation were prepared using both the single punch and rotary machines fitted with 10mm square and circular flat faced tooling. The single punch machine was operated at a speed of 60 tablets

Table 6.2
Particle size data of granulates

Formulation	Avicel (%)	Primojel (%)	Magnesium Stearate (%)	Particle size (mirometres)		
				Cumulative % undersize		
				10	50	90
1	8	0	0.6	73	325	543
2	8	3	0.2	55	287	495
3	8	3	1.0	55	287	495
4	8	6	0.6	69	234	480
5	16	0	0.2	84	358	608
6	16	0	1.0	84	358	608
7	16	6	1.0	75	319	538
8	16	6	0.2	75	319	538
9	24	0	0.6	68	275	524
10	24	6	0.6	52	294	487
11	24	3	1.0	79	330	640
12	24	3	0.2	48	245	467
13	16	3	0.6	73	285	525

per minute while the rotary machine was run at 24 r.p.m. The compaction forces were monitored by the methods described in Sections 3.2.4 and 4.2.3 respectively. A compression weight of 400mg was selected for the circular compacts. The square compacts were prepared using a compression weight of 509mg so that square and circular compacts of the same formulation with equal thicknesses would have equal porosities. A mean compaction pressure of 60 ± 2 MPa was used for all formulations; this corresponds to a pressure that might typically be used to produce 10mm diameter tablets.

6.2.5 Testing of the compacts

After preparation the compacts were stored in well closed amber glass bottles for 14 days prior to testing. The thicknesses of the compacts were measured using a Mercer Dial Gauge. The compacts were tested using the diametral compression test described in Section 3.2.7.1 and the axial compression test described in Section 3.2.7.2. Semicircular platens were used for all the tests. Six compacts of each batch were tested by each of the two methods. The tensile strengths were determined using Equation 3.1.

6.2.6 Data analysis

The data was analysed using backward elimination regression to produce expressions relating the excipient levels to the tensile strength values obtained. The calculations were performed with RS-1 software (BBN Software Products Corporation) using the stepwise algorithm described by Draper and Smith (1981).

The basic steps in the procedure are;

1. A regression equation containing all the variables listed in Equation 6.1 is computed.

2. The significance of each variable is calculated. A t-value is determined for each variable and the significance level determined using the student t-distribution. The significance level is the probability of observing a t-value as large or larger than the one observed under the null hypothesis that the coefficient is zero.

3. The highest significance level is compared with a preselected significance level, in this instance 0.1. If the highest significance value is above 0.1 a new regression is computed omitting that variable. If the value is below 0.1 the regression equation is adopted as calculated.

The goodness of fit of the final model can be assessed using the F-value obtained from analysis of variance and the multiple R-squared value. The F-value can be used to determine the significance of the fit while the multiple R-squared value represents the proportion of the variation in the response explained by the regression model. A worked example of the backward elimination regression is presented in Appendix 1.

After the models had been determined they were used to prepare contour plots. A contour plot is a graph in which the combinations of independent variables producing a given theoretical response are joined. This provides a simple method of illustrating the effect that altering the individual variables will have. The points on the contour plots were determined by solving the quadratic equations generated by the regression procedure. Quadratic equations of the form;

$$aX^2 + bX + C = 0 \qquad (6.2)$$

can be solved using the equation;

$$X = \frac{-b \pm \sqrt{b^2 - 4ac}}{2a} \qquad (6.3)$$

Equation 6.1 can be rearranged to

$$0 = B_{11}X_1^2 + (B_1 + B_{12}X_2 + B_{13}X_3)X_1 + (B_0 + B_2X_2 + B_3X_3 + B_{23}X_2X_3 + B_{22}X_2^2 + B_{33}X_3^2 - Y) \qquad (6.4)$$

Substituting values of Y (tensile strength), X_2 (Primojel) and X_3 (Magnesium Stearate) and the values for the regression coefficients the equation can be solved in terms of X_1 using Equation 6.2. Substituting different values for Magnesium Stearate while keeping the Primojel and tensile strength values constant will produce a range of combinations of Avicel and Magnesium Stearate that give the same tensile strength. The calculations can be repeated for different values of tensile strength. Using the Avicel and Magnesium Stearate levels as axes, all points producing the same value of Y can be joined on a graph to produce contour plots.

6.3 Results and discussion

The results of the backwards stepwise regression analyses are listed in Tables 6.3 to 6.10. For each combination of compact shape, tablet machine type and test configuration a quadratic equation is presented together with details of the significance of each of the regression coefficients. The predicted values for each formulation are compared with the mean values obtained. The goodness of fit of the overall expression is described by the F-value, significance level and multiple R-squared terms.

The regression coefficients were used to prepare contour plots (Figures 6.2 to 6.9). Three contour plots were prepared for each combination of tablet

Table 6.3
Regression data describing the tensile strength of circular compacts prepared on the single punch machine and tested by diametral compression

6.3a Coefficients table

Variable name	Fitted coefficient	Standard deviation	t-value	Significance level
1	0.568			
X_1X_2	0.001	0.00052	1.87	0.0656
X_1X_3	-0.020	0.00289	-6.86	0.0001
X_2X_3	-0.102	0.0190	-5.39	0.0001
X_2^2	0.009	0.00178	5.10	0.0001
X_3^2	0.301	0.695	4.33	0.0001
F-value			17.47	
Significance level			6.3×10^{-11}	
Multiple R-squared value			0.573	

6.3b Residuals Table

Avicel PH-102 (%)	Primojel (%)	Magnesium Stearate (%)	Tensile strength (MPa)		
			Predicted	Experim-ental	Residual
8	0	0.6	0.58	0.62	-0.04
8	3	0.2	0.59	0.59	0.00
8	3	1.0	0.51	0.49	+0.02
8	6	0.6	0.59	0.59	0.00
16	0	0.2	0.52	0.50	+0.02
16	0	1.0	0.55	0.55	0.00
16	3	0.6	0.43	0.44	-0.01
16	6	1.0	0.36	0.36	0.00
16	6	0.2	0.81	0.80	+0.01
24	0	0.6	0.39	0.39	0.00
24	6	0.6	0.49	0.48	+0.01
24	3	1.0	0.24	0.29	-0.05
24	3	0.2	0.58	0.57	+0.01

Figure 6.2
Contour plots for circular compacts prepared on the single punch machine and tested by diametral compression

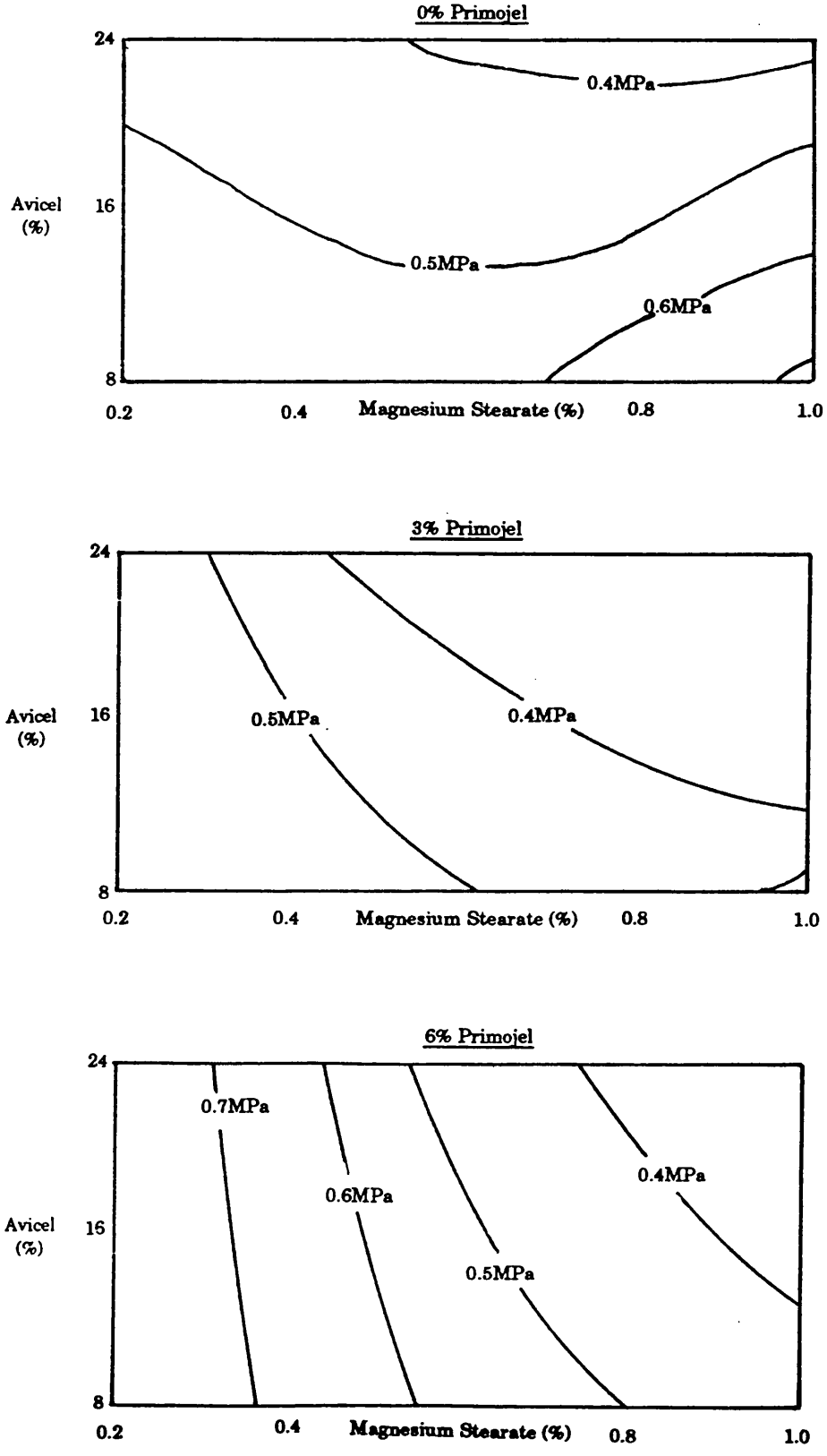

Table 6.4
Regression describing the tensile strength of circular compacts prepared on the single punch machine and tested by axial compression

6.4a Coefficients table

Variable name	Fitted coefficient	Standard deviation	t-value	Significance level
1	-0.640			
Avicel (X_1)	0.145	0.0274	5.30	0.0001
Primojel (X_2)	0.0447	0.0235	1.90	0.0619
Magnesium Stearate (X_3)	0.552	0.219	2.61	0.0115
X_1X_3	-0.0788	0.0134	-5.90	0.0001
X_2X_3	-0.326	0.0550	-5.93	0.0001
X_1^2	-0.00306	0.000712	-4.29	0.0001
X_2^2	0.0314	0.00470	6.67	0.0001
X_3^2	1.02	0.230	4.45	0.0001
F-value			8.34	
Significance level			1×10^{-7}	
Multiple R-squared value			0.518	

6.4b Residuals Table

Avicel PH-102 (%)	Primojel (%)	Magnesium Stearate (%)	Tensile strength (MPa)		
			Predicted	Experi-mental	Residual
8	0	0.6	0.65	0.62	+0.03
8	3	0.2	0.57	0.57	0.00
8	3	1.0	0.71	0.71	0.00
8	6	0.6	0.87	0.89	-0.02
16	0	0.2	0.80	0.80	0.00
16	0	1.0	1.22	1.12	+0.10
16	3	0.6	0.68	0.68	0.00
16	6	1.0	0.66	0.66	0.00
16	6	0.2	1.32	1.25	+0.07
24	0	0.6	0.67	0.66	+0.01
24	6	0.6	0.88	0.85	+0.03
24	3	1.0	0.21	0.35	-0.14
24	3	0.2	1.08	1.01	+0.07

Figure 6.3
Contour plots for circular compacts prepared on the rotary tablet machine and tested by diametral compression

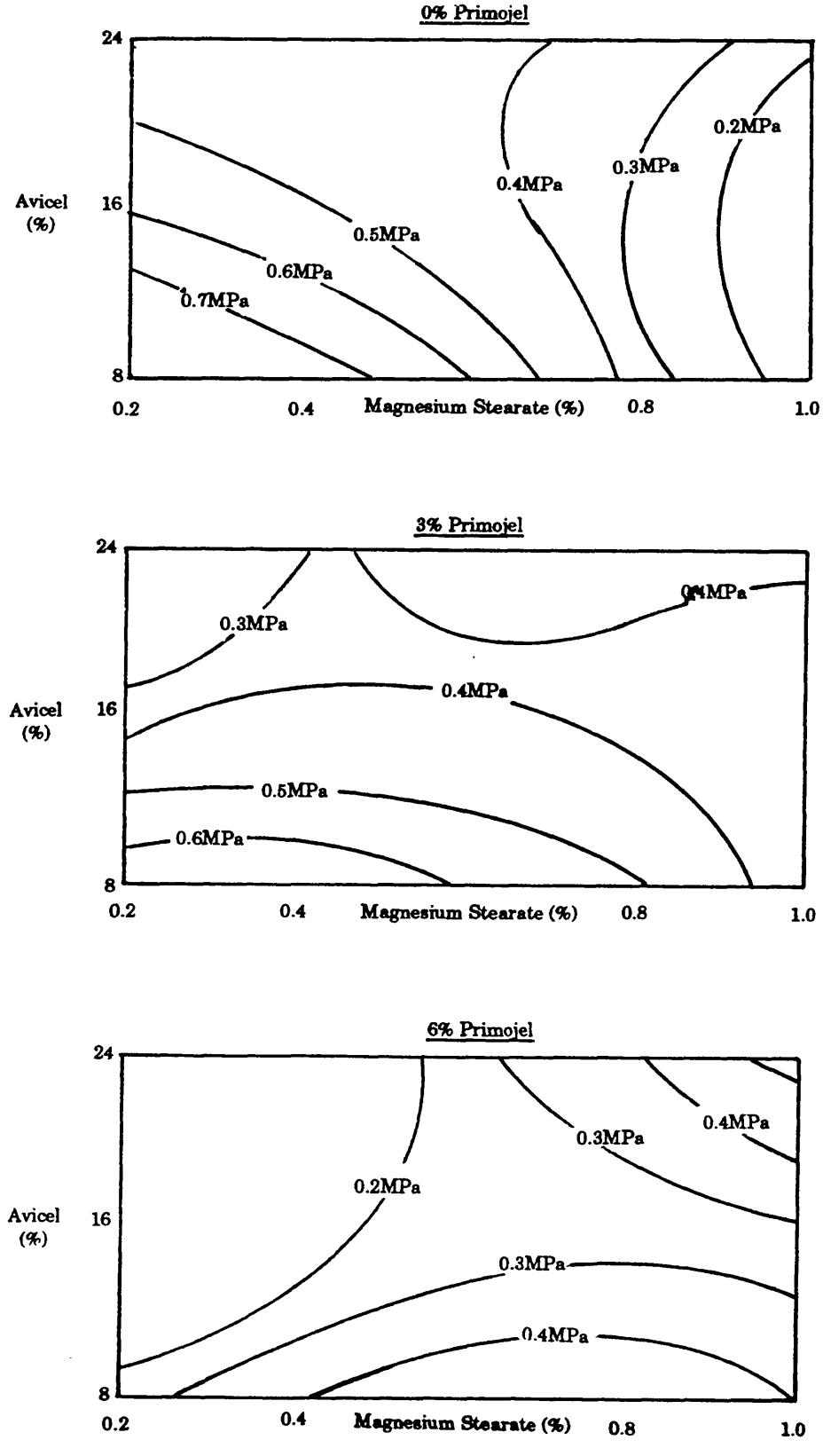

Table 6.5

Regression data describing the tensile strength of circular compacts prepared on the rotary machine and tested by diametral compression

6.5a Coefficients Table

Variable name	Fitted coefficient	Standard deviation	t-value	Significance level
1	1.68			
Avicel (X_1)	-0.0982	0.00950	-10.3	0.0001
Primojel (X_2)	-0.0912	0.0129	-7.409	0.0001
Magnesium Stearate (X_3)	-0.659	0.143	-4.62	0.0001
X_1X_3	0.0438	0.00510	8.60	0.0001
X_2X_3	0.191	0.0163	11.7	0.0001
X_1^2	0.00188	0.000245	7.65	0.0001
X_2^2	-0.00880	0.00157	-5.62	0.0001
X_3^2	-0.567	0.133	-4.27	0.0001
F-value			62.76	
Significance level			0	
Multiple R-squared value			0.892	

6.5b Residuals Table

Avicel PH-102 (%)	Primojel (%)	Magnesium Stearate (%)	Tensile strength (MPa)		
			Predicted	Experi-mental	Residual
8	0	0.6	0.63	0.62	+0.01
8	3	0.2	0.70	0.70	0.00
8	3	1.0	0.36	0.36	0.00
8	6	0.6	0.45	0.46	-0.01
16	0	0.2	0.58	0.58	0.00
16	0	1.0	0.18	0.21	-0.03
16	3	0.6	0.23	0.23	0.00
16	6	1.0	0.35	0.35	0.00
16	6	0.2	0.22	0.21	-0.01
24	0	0.6	0.44	0.44	0.00
24	6	0.6	0.26	0.25	-0.01
24	3	1.0	0.45	0.45	0.00
24	3	0.2	0.23	0.24	+0.01

Figure 6.4
Contour plots for square compacts prepared on the single punch machine and tested by diametral compression

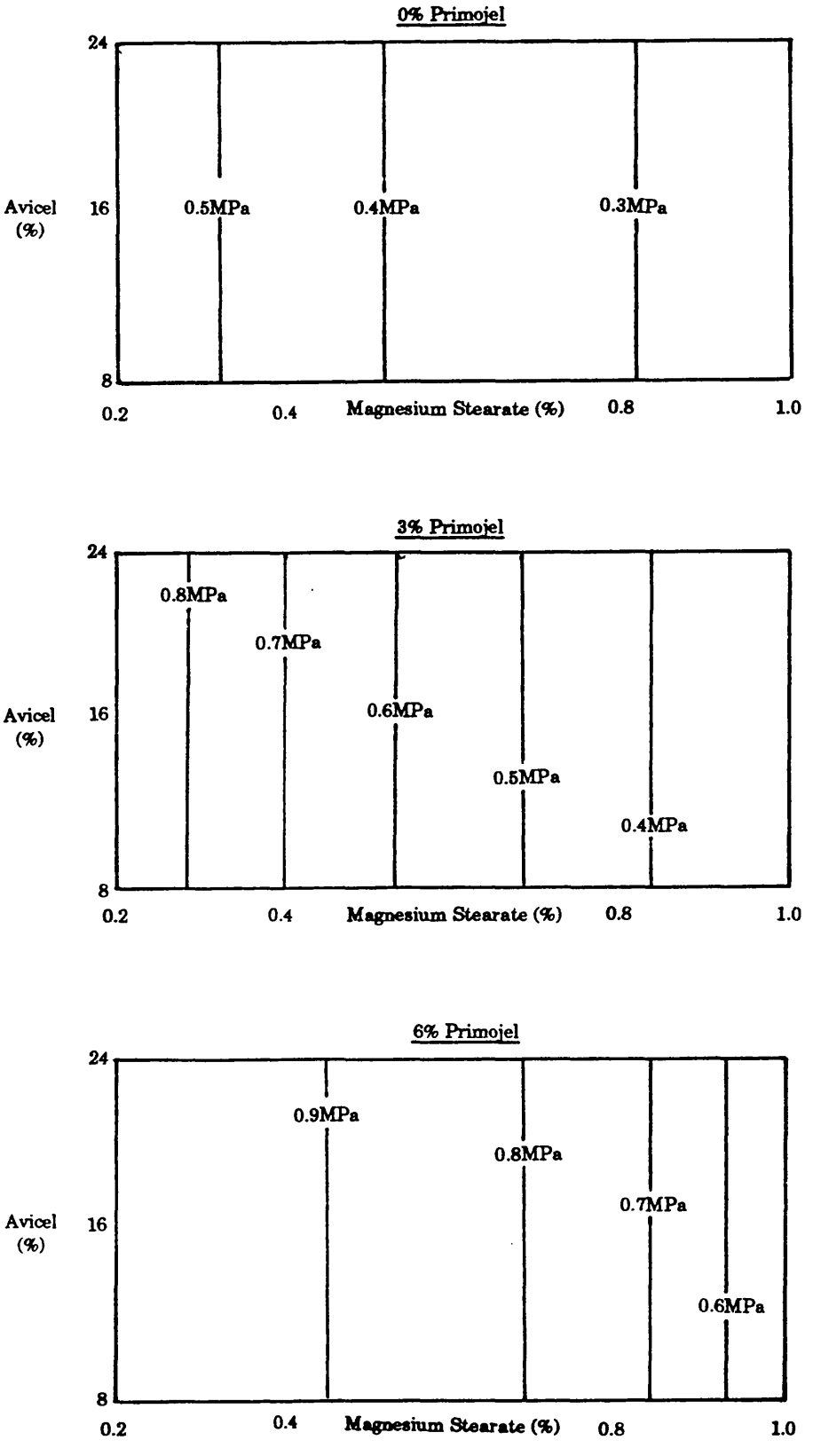

Table 6.6

Regression data describing the tensile strength of circular compacts prepared on the rotary machine and tested by axial compression

6.6a Coefficients Table

Variable name	Fitted coefficient	Standard deviation	t-value	Significance level
1	0.934			
Avicel (X_1)	-0.0427	0.0150	-2.86	0.0060
Primojel (X_2)	0.057137	0.0225	2.54	0.0141
X_1X_2	-0.00237	0.000666	-3.56	0.0007
X_1X_3	0.0380	0.00843	4.51	0.0001
X_2X_3	0.0916	0.0289	3.17	0.0025
X_1^2	0.000738	0.000411	1.79	0.0783
X_2^2	-0.0123	0.00255	-4.83	0.0001
X_3^2	-0.682	0.130	-5.24	0.0001
F-value			7.14	
Significance level			2×10^{-6}	
Multiple R-squared value			0.5	

6.6b Residuals Table

Avicel PH-102 (%)	Primojel (%)	Magnesium Stearate (%)	Tensile strength (MPa)		
			Predicted	Experi-mental	Residual
8	0	0.6	0.58	0.59	-0.01
8	3	0.2	0.73	0.70	+0.03
8	3	1.0	0.54	0.54	0.00
8	6	0.6	0.69	0.71	-0.02
16	0	0.2	0.53	0.53	0.00
16	0	1.0	0.37	0.37	0.00
16	3	0.6	0.67	0.68	-0.01
16	6	1.0	0.59	0.56	+0.03
16	6	0.2	0.32	0.31	+0.01
24	0	0.6	0.64	0.63	+0.01
24	6	0.6	0.52	0.52	0.00
24	3	1.0	0.73	0.74	-0.01
24	3	0.2	0.43	0.43	0.00

Figure 6.5
Contour plots for square compacts prepared on the rotary tablet machine and tested by diametral compression

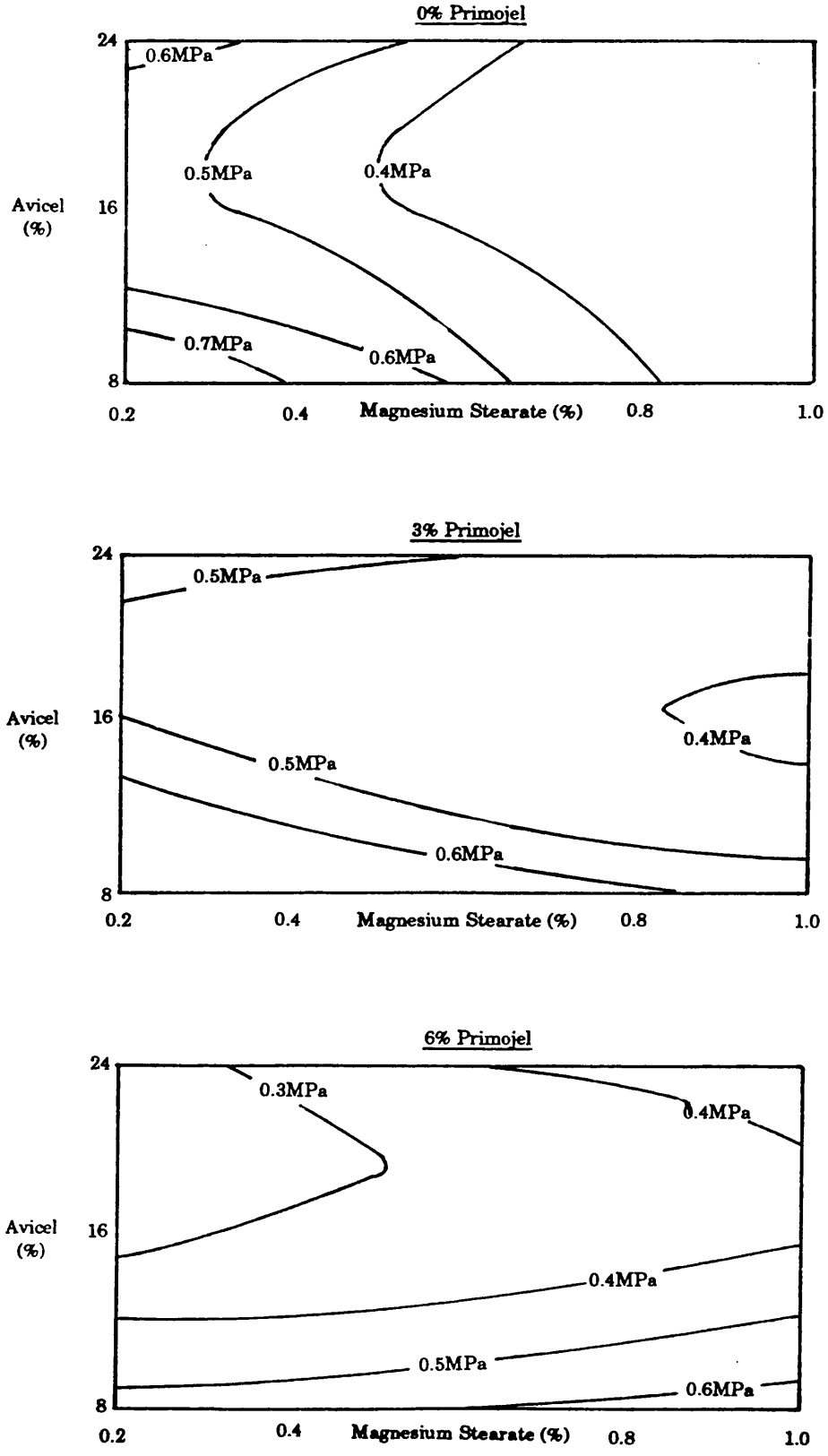

Table 6.7
Regression data describing the tensile strength of square compacts prepared on the single punch machine and tested by diametral compression

6.7a Coefficients table

Variable name	Fitted coefficient	Standard deviation	t-value	Significance level
1	0.705			
Primojel (X_2)	0.0924	0.0166	5.57	0.0001
Magnesium Stearate (X_3)	-0.744	0.158	-4.71	0.0001
X_2X_3	-0.0996	0.0197	-5.06	0.0001
X_2^2	-0.00683	0.00227	-3.01	0.0043
X_3^2	0.610	0.129	4.71	0.0001
F-value			24.23	
Significance level			9.57×10^{-12}	
Multiple R-squared value			0.729	

6.7b Residuals Table

Avicel PH-102 (%)	Primojel (%)	Magnesium Stearate (%)	Tensile strength (MPa)		
			Predicted	Experi-mental	Residual
8	0	0.6	0.49	0.50	-0.01
8	3	0.2	0.74	0.76	-0.02
8	3	1.0	0.49	0.51	-0.02
8	6	0.6	0.43	0.41	+0.02
16	0	0.2	0.58	0.56	+0.02
16	0	1.0	0.57	0.57	0.00
16	3	0.6	0.52	0.50	+0.02
16	6	1.0	0.28	0.28	0.00
16	6	0.2	0.77	0.76	+0.01
24	0	0.6	0.48	0.49	-0.01
24	6	0.6	0.43	0.46	-0.03
24	3	1.0	0.49	0.48	+0.01
24	3	0.2	0.74	0.75	-0.01

Figure 6.6
Contour plots for circular compacts prepared on the single punch machine and tested by axial compression

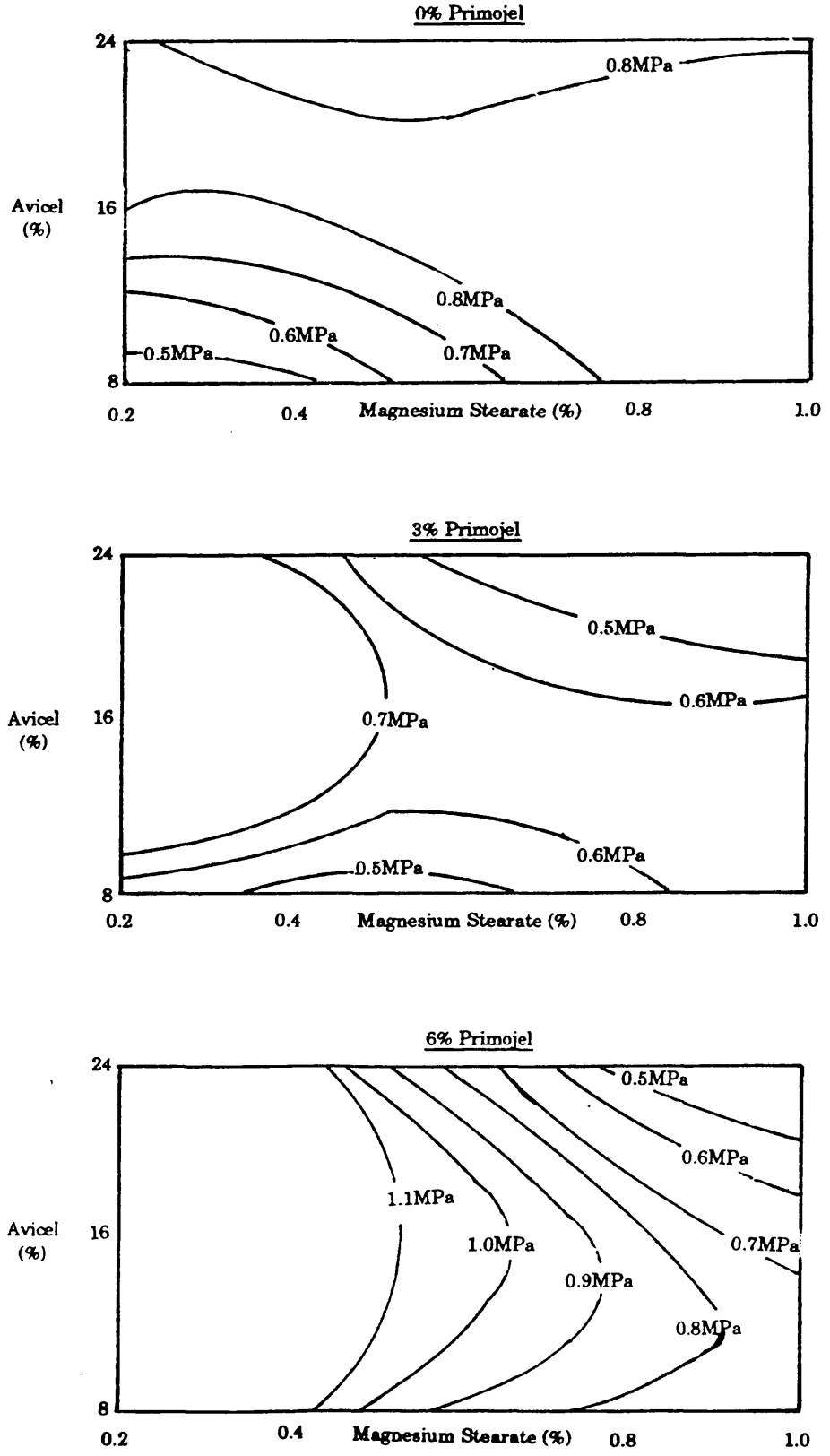

Table 6.8

Regression data describing the tensile strength of square compacts prepared on the single punch machine and tested by axial compression

6.8a Coefficients Table

Variable name	Fitted coefficient	Standard deviation	t-value	Significance level
1	0.357			
Avicel (X_1)	0.0216	0.00346	6.24	0.0001
Primojel (X_2)	0.116	0.0236	4.93	0.0001
X_1X_2	-0.00196	0.000971	-2.02	0.0497
X_2X_3	-0.115	0.0251	-4.58	0.0001
X_3^2	0.0873	0.0200	4.37	0.0001
F-value			15.03	
Significance level			2×10^{-8}	
Multiple R-squared value			0.641	

6.8b Residuals Table

Avicel PH-102 (%)	Primojel (%)	Magnesium Stearate (%)	Tensile strength (MPa)		
			Predicted	Experi-mental	Residual
8	0	0.6	0.56	0.54	+0.02
8	3	0.2	0.76	0.74	+0.02
8	3	1.0	0.57	0.59	-0.02
8	6	0.6	0.75	0.77	-0.02
16	0	0.2	0.71	0.77	-0.06
16	0	1.0	0.79	0.77	-0.02
16	3	0.6	0.96	1.02	-0.06
16	6	1.0	0.61	0.59	+0.02
16	6	0.2	1.08	1.02	+0.06
24	0	0.6	0.91	0.82	+0.08
24	6	0.6	0.91	0.91	0.00
24	3	1.0	0.83	0.83	0.00
24	3	0.2	1.02	1.00	+0.02

Figure 6.7
Contour plots for circular compacts prepared on the rotary tablet machine and tested by axial compression

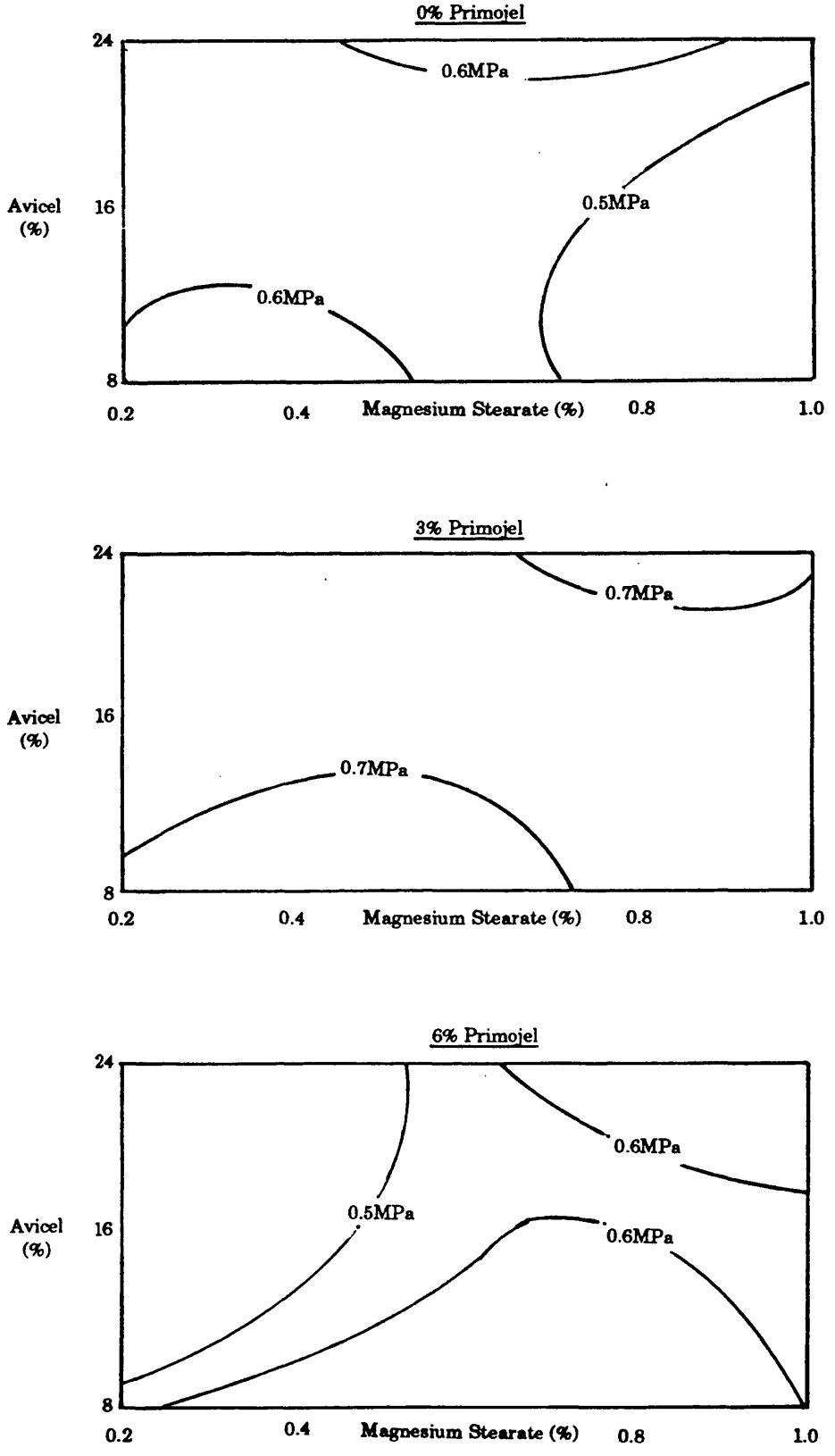

Table 6.9
Regression coefficents describing the tensile strength of square compacts prepared on the rotary machine and tested by diametral compression

6.9a Coefficients Table

Variable name	Fitted coefficient	Standard deviation	t-value	Significance level
1	1.25			
Avicel (X_1)	-0.0660	0.00819	-8.05	0.0001
Magnesium Stearate (X_3)	-0.443	0.0856	-5.18	0.0001
X_1X_2	-0.00134	0.000474	-2.82	0.0065
X_1X_3	0.00975	0.00470	2.08	0.0424
X_2X_3	0.0392	0.0127	3.09	0.0030
X_1^2	0.00158	0.000256	6.16	0.0001
F-value			44.15	
Significance level			0	
Multiple R-squared value			0.820	

6.9b Residuals Table

Avicel PH-102 (%)	Primojel (%)	Magnesium Stearate (%)	Tensile strength (MPa)		
			Predicted	Experi-mental	Residual
8	0	0.6	0.61	0.61	0.00
8	3	0.2	0.74	0.76	-0.02
8	3	1.0	0.55	0.58	-0.03
8	6	0.6	0.68	0.61	+0.07
16	0	0.2	0.67	0.66	+0.01
16	0	1.0	0.31	0.35	-0.04
16	3	0.6	0.43	0.43	0.00
16	6	1.0	0.42	0.40	+0.02
16	6	0.2	0.46	0.46	0.00
24	0	0.6	0.45	0.47	-0.02
24	6	0.6	0.40	0.38	+0.02
24	3	1.0	0.73	0.74	-0.01
24	3	0.2	0.46	0.47	-0.01

Figure 6.8
Contour plots for square compacts prepared on the single punch machine and tested by axial compression

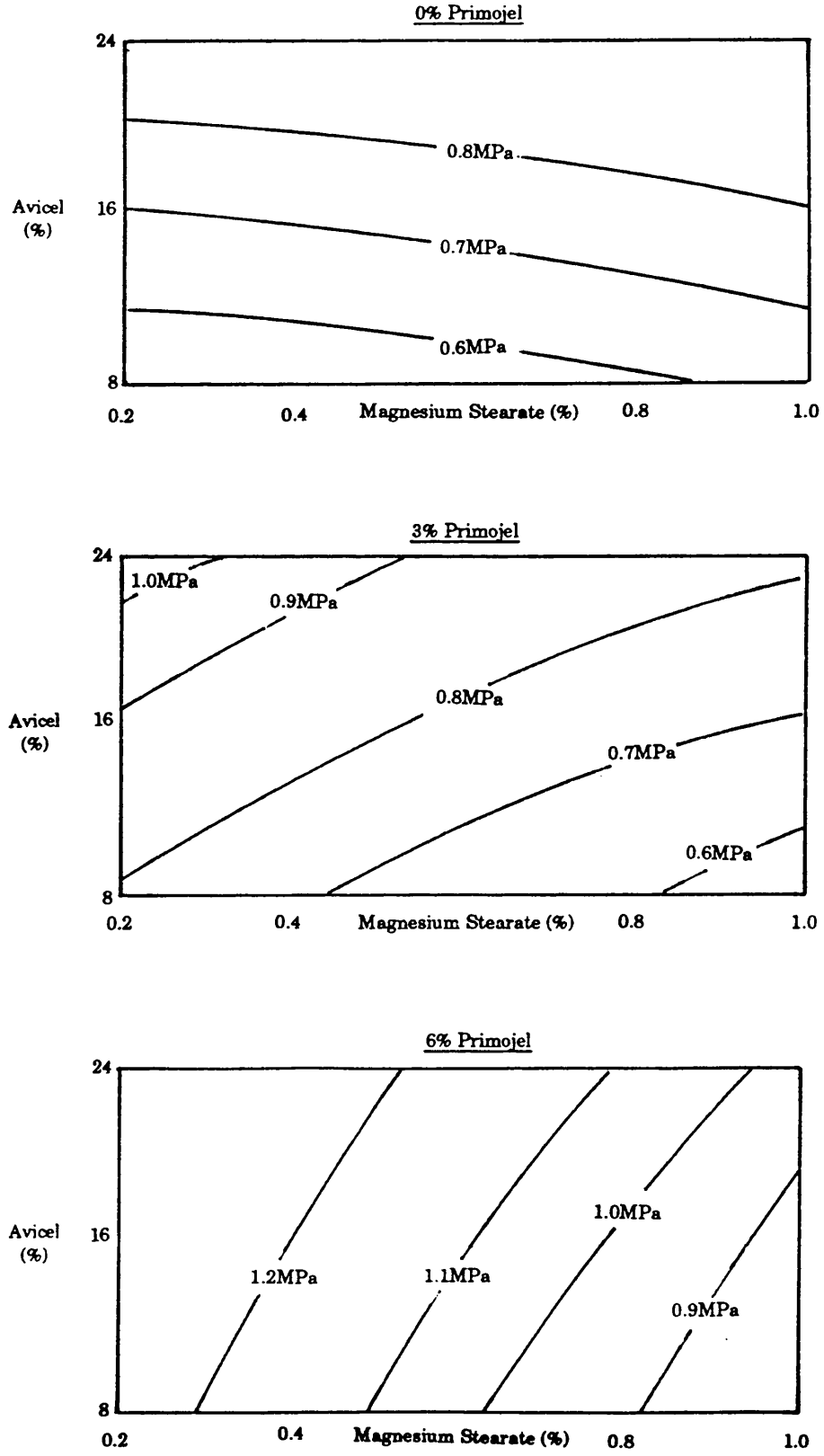

Table 6.10

Regression data describing the tensile strength of square compacts prepared on the rotary machine and tested by axial compression

6.10a Coefficients Table

Variable name	Fitted coefficient	Standard deviation	t-value	Significance level
1	1.40			
Avicel (X_1)	-0.118	0.0147	-7.60	0.0001
Primojel (X_2)	0.143	0.0222	6.44	0.0001
X_1X_2	0.00514	0.000645	-7.97	0.0001
X_1X_3	0.0256	0.00834	3.07	0.0033
X_2X_3	0.0911	0.0288	3.17	0.0025
X_1^2	0.00320	0.000406	7.88	0.0001
X_2^2	-0.0148	0.00251	-5.88	0.0001
X_3^2	-0.599	0.129	-4.64	0.0001
F-value			26.95	
Significance level			9.7×10^{-17}	
Multiple R-squared value			0.791	

6.10b Residuals Table

Avicel PH-102 (%)	Primojel (%)	Magnesium Stearate (%)	Tensile strength (MPa)		
			Predicted	Experi-mental	Residual
8	0	0.6	0.62	0.62	0.00
8	3	0.2	0.95	0.94	+0.01
8	3	1.0	0.76	0.76	0.00
8	6	0.6	1.02	1.03	-0.01
16	0	0.2	0.39	0.40	-0.01
16	0	1.0	0.24	0.36	-0.02
16	3	0.6	0.67	0.67	0.00
16	6	1.0	0.62	0.61	+0.01
16	6	0.2	0.43	0.42	-0.01
24	0	0.6	0.71	0.71	0.00
24	6	0.6	0.62	0.62	0.00
24	3	1.0	0.77	0.77	0.00
24	3	0.2	0.64	0.63	+0.01

Figure 6.9
Contour plots for square compacts prepared on the rotary tablet machine and tested by axial compression

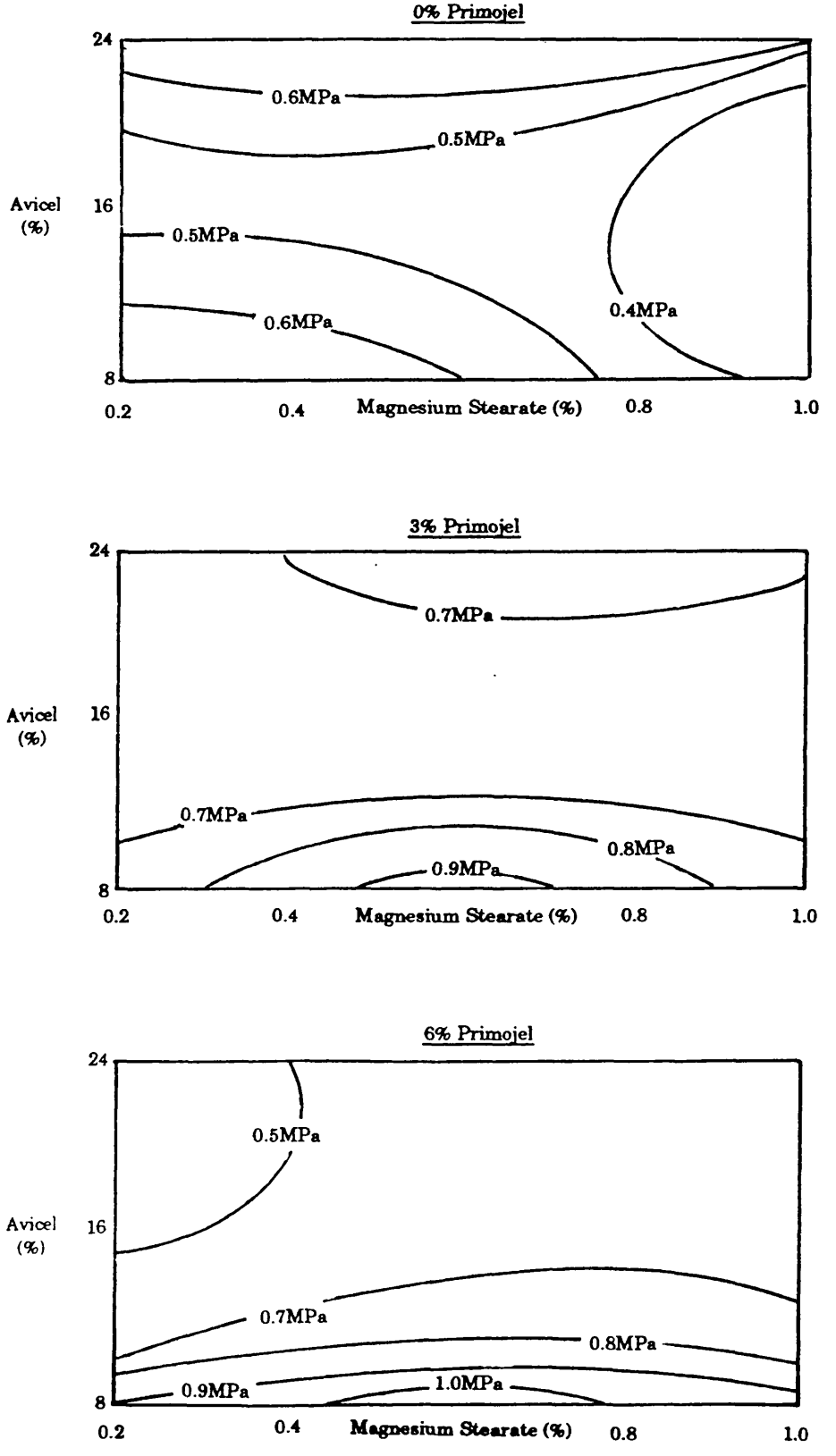

machine and test configuration representing the 3 levels of Primojel used in the studies. These plots demonstrate the effects that varying the levels of Avicel PH-102 and Magnesium Stearate will have on the 2 tensile strength values. The effect of Primojel on the tensile strengths can be gauged by comparing the contour plots of the 3 levels of disintegrant. Contour plots showing the effect of varying Primojel with either Magnesium Stearate or Avicel PH-102 could be prepared but the main purpose of this chapter of work was to see if the effects of Magnesium Stearate and Avicel in a typical formulation could be related to the results seen in earlier studies.

6.3.1 Effect of machine type on the relationship between Avicel PH-102 and Magnesium Stearate levels and tensile strength

6.3.1.1 Diametral compression

The results for circular compacts tested diametrally are presented in Figures 6.2 and 6.3 while the square compact results are shown in Figures 6.4 and 6.5. The results obtained for compacts prepared on the single punch machine (Figures 6.2 and 6.4) indicate that the main factor affecting the tensile strength is the level of lubricant. As the level of lubricant increases the tensile strength decreases. The deleterious effect of Magnesium Stearate on the strength of compacts determined by diametral compression is well documented (Jarosz and Parrot 1984) and has been described in Section 4.3.1.

The tensile strength of the square is unaffected by the Avicel PH-102 levels. The relationship for the circular compacts is more complex. At low levels of Primojel (Figure 6.2a) increasing the level of Avicel has a negative

effect on the tensile strength. As the level of Primojel increases the effect of the Avicel decreases and the Magnesium Stearate becomes the major factor influencing the strength.

In Chapter 2 Avicel was shown to produce very strong compacts on the single punch machine. From such results it may have been predicted that increasing the level of Avicel in the formulation would have a beneficial effect on the tensile strength. The results obtained may indicate that the presence of other excipients interfere with the bonding mechanism of Avicel. In the work described in Chapter 2 the compacts formed were held together predominantly by Avicel-Avicel bonds although there would also be Avicel-Magnesium Stearate and Magnesium Stearate-Magnesium Stearate bonds present. In the compacts formed in the optimisation trials the Avicel would be predominantly bonded with Anhydrous Lactose. The effect of Avicel will, to a degree, rely on the relative strengths of the Anhydrous Lactose-Anhydrous Lactose bonds and the Avicel-Anhydrous Lactose bonds. If the latter are not significantly stronger than the former the Avicel will not increase the compact strength.

The results obtained for Avicel in Chapter 2 were for a direct compression mix. In the current experiment the mixtures were prepared by wet granulation. Avicel is principally considered a direct compression excipient but inclusion in wet granulated formulations as a compression aid is commonplace. There is evidence that subjecting Avicel to the wet granulation process adversely affects compaction properties (Staniforth 1990). The magnitude of the effect was shown to be dependent on the method of drying employed. It was suggested that the effects may be due

to the way in which the cellulose fibres rearrange themselves during drying. Such changes may be an additional/alternative explanation for the inability of Avicel to improve the compaction properties of formulations prepared on the single punch machine.

The circular and square compacts produced on the rotary machine (Figures 6.3 and 6.5) are both affected by the Magnesium Stearate and Avicel levels in the same way. The addition of Avicel and Magnesium Stearate both adversely affect the tensile strength. The performance of the direct compression Avicel/Magnesium Stearate blend was very poor compared to the single punch machine. The addition of Avicel could not therefore be expected to have large beneficial effects on the tensile strengths. Such a trend may be as much influenced by the behaviour of Anhydrous Lactose as the Avicel, Magnesium Stearate and Primojel.

6.3.1.2 Axial compression test

The axial compression contour plots (Figures 6.6 to 6.9) indicate that the tensile strengths determined by this method vary less between formulations than the tensile strength determined by diametral compression. This may in part be due to the poorer fit of the regression coefficients, as described by the multiple R-squared values, not reflecting the full variation of the raw data.

The compacts containing no Primojel (Figures 6.6a and 6.8a) increase in tensile strength as the levels of Avicel and Magnesium Stearate increase. The effect of Magnesium Stearate is more pronounced on the circular compacts than the square compacts. The influence of lubricant levels on the axial compression results was discussed in Section 3.3.3.7 where it was

suggested that inadequate lubrication results in a decrease in the tensile strength values obtained due to the increase in the density variations within the compact.The beneficial effects of the additional lubricant would have been expected to be more pronounced with the square compacts. As the Primojel levels increase the beneficial effects of the Magnesium Stearate are reversed. The Avicel, however, continues to have a beneficial effect. Both the Primojel and Avicel reduce the ejection force of the compacts and it may be that a point is reached where the diminishing beneficial effect of the lubricant on die wall friction is countered by the adverse effect of the lubricant on interparticulate bonding.

The rotary machine data is harder to describe as the changes in tensile strength occurring within the design space are relatively small. The results for the compacts containing the high level of Primojel (Figures 6.6c and 6.8c) indicate that Avicel has an adverse effect on tensile strength.

Comparison of the compacts produced by the two machines shows that the single punch machine produces stronger compacts than the rotary machine, confirming the trend described in Sections 5.3.1 and 5.3.2.

6.3.2 Effect of compact shape on the tensile strength

In Sections 6.3.1.1 and 6.3.1.2 the similarities in the trends between square and circular compacts were mentioned. Although the trends and contour shapes are similar, there are differences in the actual values of tensile strength for compacts produced on the rotary machine. Comparing the contour plots of compacts produced on the rotary machine indicates that the square compacts produce higher tensile strength values than circular compacts over most of the design space for both axial and

diametral compression tests. The reasons for the differences in tensile strength are unclear and demonstrate a different trend to those seen in Chapter 4 where all differences detected involved the circular compacts being stronger than the square compacts.

The results show that the die geometry does influence the compaction mechanism. The nature of this influence cannot be predicted from the behaviour of the individual excipients lubricated with Magnesium Stearate. There may be interactions occurring between the excipients in the formulation that produce these differences. Alternatively the granulation process may dramatically alter the properties of a material or materials in the formulation. It would be interesting to examine the effect of Avicel and Magnesium Stearate in a direct compression formulation with Anhydrous Lactose, in particular the effect of the Avicel on the diametral compression results on compacts prepared on the single punch machine.

6.4 Conclusions

The optimisation work has demonstrated how experimental design can be used to assess the role of different variables on a response, in this instance tensile strength. It does not, however, explain why these effects take place. A number of effects were exposed by the technique, some of which could be explained by the findings in earlier chapters and some apparently contradicting earlier studies.

The experiments demonstrated that the behaviour of excipients within a formulation depends on the type of machine used for compaction. This

confirms the findings of the compaction studies performed with Avicel PH-102.

The compact shape is shown to affect the value obtained for the tensile strength of compacts produced on the rotary machine. The square compacts are generally stronger than circular compacts. This contrasts with the results of the single excipient studies performed on the rotary machine where circular compacts were the stronger for both Avicel and Emcompress.

From a practical viewpoint this study has demonstrated the importance of carrying out optimisation experiments for formulations on appropriate machinery, using tooling representative of that to be used for the final product.

The study has revealed that the shape of a compact does affect tensile strength and while the reason for the difference has not been identified, the need for further studies has been highlighted.

CHAPTER 7

CONCLUSIONS

7.1 Conclusions

Using casts of gypsum it has been demonstrated that the diametral compression test can be used to compare the tensile strength of circular, square and hexagonal specimens of similar size. The absolute value of tensile strength obtained for a given material will depend on the shape of platens used for testing and the specimen size.

The effect of platen shape on the tensile strength value obtained by the diametral compression test was investigated further using compacts of pharmaceutical excipients. The differences between tensile strength values were related to the width of contact between the platen and compact. The contact width depended on the shape of the platen and the degree of deformation of the test specimen. Deformation at the platen edge was greater for plastically deforming materials than for brittle materials. Semicircular convex platens were found to be suitable for testing pharmaceutical compacts.

A second test, the axial compression, test was developed. Compacts were compressed between two semicircular convex platens along the axis of compression. Failure occurred due to tension along the same plane as the diametral compression test.

The diametral compression test did not reveal differences between compacts of different shapes produced using the same compaction pressure on the single punch tablet machine. The tensile strength values obtained by the axial compression test for square compacts of Emcompress produced on the single punch tablet machine were significantly lower than for circular compacts produced under similar conditions, suggesting variations

in the structure of the compacts. The square compacts of Emcompress could only be formed using low compression weights. As the compression weight was increased flaws developed at the lower corners of the compacts. The differences in the axial compression test results and the flaws are attributed to increased die wall friction causing poor force transmission through the square compact and increased density variations within the compact.

The tensile strength of Emcompress compacts produced on the rotary tablet machine is influenced by shape. Higher tensile strength values are obtained for circular compacts than square compacts by both test methods. The compacts produced on the rotary machine are weaker than those compressed to a similar porosity on the single punch machine, indicating that the machine type affects the structure of the final compact. The compression weight of Emcompress square compacts that could satisfactorily be produced was limited only by the depth of the die. The ability to form such square compacts is related to the two sided compression that occurs on the rotary machine. This type of punch movement avoids the presence of a region within the compact, adjacent to the die wall near the lower punch, where powder movement is negligible. The difference between the punch movements on the single punch and rotary tablet machines results in compacts of lubricated Avicel PH-102 with very different properties. Compacts produced on the single punch tablet machine have very high tensile strength values and exhibit no tendency to cap. The tensile strength values of compacts produced on the rotary machine are very much lower and capping occurs at relatively low

compaction pressures. The shape does not influence the strength of Avicel compacts produced on the single punch machine. Below the capping pressure the tensile strength of compacts produced on the rotary machine is also independent of shape. However, the capping pressure of the compacts is shape dependent, capping occurring at lower compaction pressures for circular compacts than square compacts.

The influence of shape on the compaction properties of model granulated formulations has been investigated. Differences were seen between square and circular compacts produced on the rotary machine. Square compacts tended to exhibit higher tensile strength compacts than circular compacts. This finding contrasted with the experiments performed with the powder mixes. Again the properties of compacts was greatly influenced by the machine type used in their production.

7.2 Suggestions for further work

The work reported has demonstrated that altering the die geometry can, in some instances, have a profound effect on the quality of compact that can be produced from a given material. The nature of such effects depend not only on the material being examined but also the compression conditions employed.

The interpretation of the effects of shape on the properties of Emcompress compacts produced on the single punch machine have been based on the existing knowledge of the single ended compression process. The effects seen on the rotary machine are arguably far more important as the majority of pharmaceutical tablets are produced on such machines.

However, the effects are more difficult to explain as the movement of powders and transmission of forces during double ended compression has not been investigated. If the reasons for the tendency of the Avicel powder mixes to cap and the tensile strength differences between square and circular compacts are to be properly explained an improved understanding of the double ended compaction process is required.

Ideally an examination of the density distributions within compacts along the lines of the work of Train (1956), Macleod (1974) or Charlton and Newton (1985), but using compression speeds and compact sizes akin to those used in pharmaceutical production, should be performed. The problem in performing such studies is the development of a technique to measure density distributions within such small samples. The compact sizes in the aforementioned studies have largely been dictated by the low resolution of the methods used to determine density. Studies performed on single ended compaction, because of the poor resolution and the need to average values, have probably underestimated the density variations within compacts but have, nevertheless, contributed greatly to the understanding of the process. While it would be desirable to perform studies on appropriately sized compacts, the application of previously used techniques involving larger than normal tablet diameters would provide valuable information on the structure of compacts produced by double ended compaction. Compact manufacture for such studies should not be a problem due to advances in the technology of hydraulic presses, as evidenced by the development of compaction simulators.

The effects of shape have been attributed to the effects of die wall friction.

The tooling selected for this study had very sharp corners, with radii of curvature of 0.5mm in order to accentuate any effects. Such tooling would not be used in a pharmaceutical product because such sharp points would be unacceptable to a patient and could lead to swallowing difficulties. In practise shaped tablets all have rounded edges. An investigation into the relationship between the radius of curvature of the corners and the magnitude of any shape effects could be of value.

Flat faced tooling has been used in this study to isolate the effects of die wall geometry. Shaped pharmaceutical tablets are generally produced using a combination of a shaped die and contoured punches. Studies have shown that altering the punch tip geometry will affect the degree of lateral movement within a die during compression which will influence the stresses at the die wall. The ultimate aim must be to understand the interaction between the die wall geometry and punch tip geometry on the final structure of a compact.

CHAPTER 8

REFERENCES

Addinall, E. and Hackett, P. (1964) Civil Eng. Pub. Works Rev. **59**: 1250 - 1253

Akazawa, T. (1953) R.I.L.E.M. Bulletin No. 16: 11 - 23

Anon. (1989) Pharm. J. **281**: 88

Appl, F.J. (1972) J. Strain Anal. **7**: 178 -185

Armstrong, N.A., Abourida, N.M.A.H. and Gough, A.M. (1983) J. Pharm. Pharmacol. **35**: 320 - 321

Armstrong, N.A. and James, K.C. (1990) Understanding Experimental Design and Interpretation in Pharmaceutics, Ellis Horwood Ltd, Chichester

Armstrong, N.A. and Palfrey, L.P. (1987) J. Pharm. Pharmacol. **39**: 497 - 501

Aulton, M.E. and Tebby, H.G. (1975) J. Pharm. Pharmacol. **27**: Suppl. 4P

Aulton, M.E., Tebby, H.G. and White, P.J.P. (1974) J. Pharm. Pharmacol. **26**: Suppl. 59P - 60P

Awaji, H. and Sato, S. (1979) J. Eng. Mat. Tech. **101**: 139 - 147

Barcellos, F.L.L.B. and Carneiro, A. (1953) R.I.L.E.M. Bulletin No. 13: 97 -123

Berenbaum, R. and Brodie, I. (1959) Brit. J. Appl. Phys. **10**: 281 - 287

Brisbane, J.J. (1963) J. Appl. Mech. Trans. A.S.M.E. **85**: 306 -309

Carless, J.E. and Leigh, S. (1974) J. Pharm. Pharmacol. **26**: 289 - 297

Chapman, G.P. (1968) Concrete: 77 - 85

Charlton, B. and Newton, J.M. (1984) J.Pharm. Pharmacol. **36**: 645 - 651

Charlton, B. and Newton, J.M. (1985) Powder Tech. **41**: 123 - 134

Chatrath, M., Staniforth, J.N., Winiecki Newman, A. and Brittain, H.G. (1990) J. Pharm. Pharmacol. **42**: Suppl. 80P

Chemist and Druggist Directory (1992), Benn Business Information Services Ltd, Tonbridge

Church, M.S. (1983) PhD Thesis, University of Nottingham

Church, M.S. and Kennerley, J.W. (1982) J. Pharm. Pharmacol. **34**: Suppl. 50P

Church, M.S. and Kennerley, J.W. (1984) J. Pharm. Pharmacol. **36**: Suppl. 43P

Coombe, E.C. (1977) Notes on Dental Materials, 3rd Edition, Churchill Livingston, Edinburgh

Cooper, A.R. and Eaton, L.E. (1962) J. Am. Ceram. Soc. **45**: 97 - 101

David, S.T. and Augsburger, L.L. (1974) J. Pharm. Sci. **63**: 933 - 936

David, S.T. and Augsburger, L.L. (1977) J. Pharm. Sci. **66**: 155 - 159

Davies, J.P and Bose, D.K. (1968) A.C.I. Journal **8**: 662 - 669

Den Hartog, J.P. (1952) Advanced strength of materials. Mcgraw-Hill, New York

Draper, A. and Smith, H. (1966) Applied Regression Analysis, John Wiley and Sons, New York

Earnshaw, R. and Smith, D.C. (1966) Australian Dental Journal **11**: 415 - 422

Endicott, C.J., Lowenthall, W. and Gross, H.M. (1961) J. Pharm. Sci. **50**: 343 - 346

Esezebo, S. and Pilpel, N. (1976) J. Pharm. Pharmacol. **28**: 8 - 16

Fell, J.T. and Newton, J.M. (1970) J. Pharm. Sci. **59**: 688 - 691

Frocht, M.M. (1948) Photoelasticity, Volume 2. John Wiley and Sons Inc. New York

Gold, G., Duvall, R.N. and Palermo, B.T. (1980) J. Pharm. Sci. **69**: 384 - 386

Goodhart, F.W., Mayorga, G., Mills, M.N. and Ninger, F.C. (1968) J. Pharm. Sci. **57**: 1770 - 1775

Goodier, T.N. (1932) Trans A.S.M.E. **54**: 173 - 183

Handbook of Pharmaceutical Excipients (1986), The Pharmaceutical Society of Great Britain, London.

Hardman, J.S. and Lilley, B.A. (1973) Proc. R. Soc. Lond. A. **333**: 183 - 199

Hardy, C. (1939) Metal Prog. **35**: 171 - 172

Hausner, H.H. (1967) Int. J. Powd. Metall. **3**: 7

Heckel, R.W. (1961) Trans. Metall. Soc., A.I.M.E. **221**: 671 - 675

Hiestand, E.N. and Peot, C.B. (1974) J. Pharm. Sci. **63**: 605 - 612

Hiestand, E.N. and Smith, D.P. (1984) Powder Technol. **38**: 145 - 149

Hiestand, E.N., Wells, J.E., Peot, C.B. and Ochs, J.F. (1977) J. Pharm. Sci. **66**: 510 - 519

Higuchi, T., Elowe, L.N. and Busse, L.W. (1954) J. Am. Pharm. Assoc. (Sci. Ed.) **43**: 685 - 689

Hogan, J.E., (1989) Drug Dev. Ind. Pharm. **15**: 975 - 999

Hölzer, A.W and Sjøgren, J. (1978) Acta. Pharm. Suec. **15**: 59 - 66

Hunter, B.M. (1985) Postgraduate School on Production Processes in

Tablet Manufacture, School of Pharmacy, University of London

Jarosz, P.J. and Parrott, E.L.(1982) Drug Dev. Ind. Pharm. **8**: 445 -453

Jarosz, P.J. and Parrott, E.L. (1982) J. Pharm. Sci. **71**: 607 - 614

Jetzer, W., Leuenberger, H. and Sucker, H. (1983) Pharm. Technol. **7**: 33 - 39

Jordan, D.W. and Evans, I. (1962) Brit. J. Appl. Phys. **13**: 75 - 79

Kamm, R., Steinberg, M.A. and Wulff, J. (1949) Trans. A.I.M. (Met). E. **180**: 694 - 706

Kawakita, K. and Lüdde, K.H. (1970) Powder Technol. **4**: 61 - 68

Kennerley, J.W., Newton, J.M. and Stanley, P. (1977) J. Pharm. Pharmacol. **29**: Suppl. 39P

Kerridge, J.C. and Newton, J.M. (1986) J. Pharm. Pharmacol. **38**: Suppl. 79P

Knoechel, E.L., Sperry, C.C., Ross, H.E. and Lintner, C.J. (1967) J. Pharm. Sci. **56**: 109 - 115

Krycer, I., Pope, D.G. and Hersey, J.A. (1982) J. Pharm. Pharmacol. **34**: 802 - 804

Lamberson, R.L. and Raynor, G.E. (1976) Manuf. Chem. Aerosol News, June: 55 - 61

Lawrence, P. (1970) J. Mat. Sci. **5**: 633 - 638

Leonard, G.S., Tovey, G.D. and Aulton, M.E. (1989) Drug Dev. Ind. Pharm. **15**: 343 - 359

Leuenberger, H. (1982) Int. J. Pharm. **12**: 41 - 55

Leuenberger, H. and Rohera, B.D. (1986) Pharm. Res. **3**: 12 - 22

Luangtana-Anan, M. and Fell, J.T. (1990) Int. J. Pharm. **60**: 197 - 202

Macleod, H.M. (1974) PhD Thesis, University of Bradford

Mann, S.C., Bowen, D.B., Hunter, B.M., Roberts, R.J., Rowe, R.C. and Tracy, R.H.T. (1981) J. Pharm. Pharmacol. **35**: Suppl. 45P

Malamataris, S., Bin Baie, S. and Pilpel, N. (1984) J. Pharm. Pharmacol. **36**: 616 - 617

Marshall, K. (1963) J. Pharm. Pharmacol. **15**: 413 - 421

Mashadi, A.B. and Newton, J.M. (1987) J. Pharm. Pharmacol. **39**: 961 - 965

Mashadi, A.B. and Newton, J.M. (1988) J. Pharm. Pharmacol. **40**: 120P

Mechtersheimer, B. and Sucker, H. (1986) Pharm. Technol. (3): 38 - 50

Milosovich, G. (1963) Drug Cosmet. Ind. (5): 557 - 558, 656, 662 - 663

Mitchell, N.B. (1961) Materials Research and Standards **1**: 780 - 788

Moschos, A.E. and Rees, J.E. (1986) J. Pharm. Pharmacol. **38**: Suppl. 32P

Newton, J.M. and Grant, D.J.W. (1974) Powder Technol. **9**: 295 - 297

Newton, J.M., Ingham, S. and Onabajo, O.O. (1986) Acta. Pharm. Technol. **32**: (2) 61 - 62

Newton, J.M., Rowley, G. and Fell, J.T. (1972) J. Pharm. Pharmacol. **24**: 503 - 504

Newton, J.M. and Stanley, P. (1980) J. Pharm. Pharmacol. **32**: 852 - 854

Newton, J.M., Stanley, P. and Tan, C.S. (1977) J. Pharm. Pharmacol. **29**: Suppl. 40P

Nillson, S. (1961) R.I.L.E.M. Bulletin No. 11: 63 - 65

Nyström, C., Wulf, A., Malmquist, K. (1977) Acta. Pharma. Suec. **14**: 317 -320

Nyström, C., Malmquist, K., Mazur, J., Alex, W. and Hölzer. A.W. (1978) Acta. Pharm. Suec. **15**: 226 - 232

Oates, R.J. and Mitchell, A.G. (1989) J. Pharm. Pharmacol. **41**: 517 - 523

Peltier, R. (1954) R.I.L.E.M. Bulletin No. 19: 33 - 74

Phillips, H.B. and Mantei, C.L. (1969) Expl. Mech. **9**: 137 - 139

Phillips, R.W. (1982) Skinner's Science of Dental Materials, 8th Edition, W.B. Saunders Co., Philadelphia

Physicians Desk Reference (1991) 45th Edition, Medical Economics Data, New Jersey

Pitt, K.G., Newton, J.M., Richardson, R. and Stanley, P. (1989) J. Pharm. Pharmacol. **41**: 289 - 292

Pitt, K.G., Newton, J.M. and Stanley, P. (1989) J. Phys. D: Appl. Phys. **22**: 1114 - 1127

Rees, J.E., Hersey, J.A. and Cole, E.T. (1970) J. Pharm. Pharmacol. **22**: Suppl. 64S - 69S

Rees, J.E., Hersey, J.A. and Cole, E.T. (1972) J. Pharm. Sci. **61**: 1313 -1315

Rees, J.E. and Rue, P.J. (1978) Drug Dev. Ind. Pharm. **4**: 131 - 156

Rees, J.E., Rue, P.J. and Richardson, S.C. (1977) J. Pharm. Pharmacol. **66**: Suppl. 38P

Ridgway, K., Aulton, M.E. and Rosser, M.H. (1970) J. Pharm. Pharmacol. **22**: Suppl. 70S - 78S

Ridgway, K., Deer, J.J., Finlay, P.L. and Lazarou, C. (1972) J. Pharm. Pharmacol. **24**: 203 - 210

Ridgway Watt, P. and Rue, P.J. (1980) J. Pharm. Pharmacol. **32**: Suppl. 22P

Ritter, A. and Sucker, H.B. (1980) Pharm. Tech. Int. July: 25 - 33

Roberts, R.J. and Rowe, R.C. (1985) J. Pharm. Pharmacol. **37**: 377 - 384

Roberts, R.J. and Rowe, R.C. (1986) J. Pharm. Pharmacol. **38**: 526 - 528

Rubenstein, M.H. and Moody, G. (1985) Expo-Congr. Int. Technol. Pharm. 3rd, 5, 7 - 11

Rudnick, A., Hunter, A.R. and Holden, F.C. (1963) Materials Res. and Standards **3**: 283 - 289

Rue, P.J., Barkworth, P.M.R., Ridgway Watt, P., Rough, P., Sharland, D.C., Seager, H. and Fisher, H. (1979) Int. J. Pharm. Tech. and Prod. Mfr. **1**: 2 - 5

Rue, P.J., Seager, H., Burt, I., Ryder, J., Murray, S. and Beal, N. (1979) J. Pharm. Pharmacol. **31**: Suppl. 23P

Rue, P.J. and Rees, J.E. (1978) J. Pharm. Pharmacol. **30**: 642 - 643

Ryshkewitch, E. (1953) J. Am. Ceram. Soc. **36**: 65 - 68

Salpekar, A.M. and Augsburger, L.L. (1974) J. Pharm. Sci. **63**: 289 - 292

Seelig, R.P. and Wulff, J. (1946) Trans A.I.M. (Met). E. **166**: 492 - 505

Sheikh-Salem, M. and Fell, J.T. (1981) J. Pharm. Pharmacol. **33**: 491 - 494

Shotton, E. and Ganderton, D. (1960) J. Pharm. Pharmcol. **12**: Suppl. 87T - 92T

Shotton, E. and Ganderton, D. (1961) J. Pharm. Pharmacol. **13**: Suppl. 144T - 151T

Shotton, E. and Lewis, C.S. (1964) J. Pharm. Pharmacol. **16**: Suppl.

111T - 120T

Sixsmith, D. and McCluskey, D. (1981) J. Pharm. Pharmacol. **33**: 79 - 81

Snedecor, G.W. and Cochran, W.G. (1980) Statistical Methods, 7th Edition, Iowa State University Press, Iowa

Stanley, P. and Newton, J.M. (1978) J. of Powder and Bulk Solids Tech. **1**: 13 - 19

Stanley, P. and Newton, J.M. (1980) J. Pharm. Pharmacol. **32**: 852 - 854

Sundara, K.T. and Chandrashekhara, K. (1962) Brit. J. Appl. Phys. **13**: 501 - 507

Tovey, G.D. (1987) Pharm. J. **239**: 363 - 364

Train, D. (1956) J. Pharm. Pharmacol. **8**: 745 -761

Train, D. (1957) Trans. Instn. Chem. Engrs. **35**: 258 - 262

Weibull, W. (1951) J. Appl. Mech. **18**: 293

Wetherill, G.B. (1981) Intermediate Statistical Methods, 1st Edition, Chapman and Hall, London

Williams, J.J. and Stiel, D.M. (1984) Pharm. Technol. (3): 26 - 38

Wray, P. (1969) Drug Cosmet. Ind. (9): 58 - 68, 158 - 160

Wright, P.J.F. (1955) Magazine of Concrete Research **7**: 87 - 96

York, P. (1979) J. Pharm. Pharmacol. **31**: 244 - 246

Zein, E.E. (1989) Proc. 8th. Parmaceutical Technology Conference : 73 - 89

Appendix 1

Worked example of backwards elimination regression

The contour plots illustrated in Chapter 6 were generated from regression equations that had been calculated using a backwards elimination regression procedure. The procedure is demonstrated in this appendix using the results of the diametral compression test on circular compacts prepared on the rotary tablet machine (Table 6.5)

The first step in the procedure is to generate a regression equation, by the least squares method, containing all 9 variables. This provides the following equation;

$$Y = 1.678 - 0.0988X_1 - 0.0869X_2 - 0.648X_3 - 0.000273X_1X_2 + 0.0440X_1X_3 + 0.193X_2X_3 + 0.00191X_1^2 - 0.00903X_2^2 - 0.585X_3^2$$

The Analysis of Variance (ANOVA) of the regression is calculated;

Table A1

Analysis of Variance Table for regression equation containing 9 independent variables

Source	Sum of squares	Degrees of freedom	Mean Square	F - value
Total	1.142314			
Regression	1.018778	9	0.113198	62.7558
Residual	0.122657	68	0.001804	

Multiple R^2 value = 0.892541

Standar deviation of the regression = 0.042471

The overall F-value for the equation is 62.76 which is statistically significant, exceeding F(9, 68, 0.99) = 2.68.

To assess whether the individual variables are contributing significantly to the regression equation it is necessary to compare the ANOVA results in Table A1 with ANOVA results from regression equations containing 8 variables. It is necessary, therefore, to perform least square regressions to generate 9 equations each containing 8 independent variables. The contribution of each variable can then be measured by comparing the sum of squares due to regression.

To illustrate this, consider the contribution of Avicel (X_1) to the equation. The least squares regression performed using all the independent variables except Avicel yields the following ANOVA table:

Table A2

Analysis of Variance table for regression equation containing all independent variables except Avicel

Source	Sum of squares	Degrees of freedom	Mean square	F-value
Total	1.142314			
Regression	0.826275	8	0.103284	22.61266
Residual	0.315161	69	0.004568	

The contribution of Avicel to the regression sum of squares is obtained by subtracting the regression sum of squares in Table A2 (0.826275) from the regression sum of squares in Table A1 (1.018778). The F-value of the

contribution is calculated by dividing the mean square of the contribution (0.000879) by the residual mean square of the complete regression (0.001804). The t-value is the square root of the F-value.

Table A3

Contribution of Avicel to the regression sum of squares

Source	Sum of squares	Degrees of freedom	Mean square	F-value	t-value
Total	1.142314				
Complete regression equation	1.018778	9	0.113197	62.76	
Regression equation omitting Avicel	1.017899	8	0.127237	70.54	
Contribution of Avicel	0.000879	1	0.000879	0.487	0.698
Residual	0.122657	68	0.001804		

This process is repeated for the other 8 variables, the results of which are summarised in Table A4.

The significance level is the probability of observing a t-value as large or larger than the one observed under the null hypothesis that the coefficient is zero. The highest significance level is compared to a predetermined significance level. For this experiment the predetermined level was 0.1. If the highest significance level exceeds the predetermined level the variable producing that level is eliminated and a new regression computed. Examination of Table A4 reveals that the variable X_1X_2 has a significance

level of 0.4875. A new regression is therefore computed with 8 variables but omitting X_1X_2. The contributions of the remaining variables are assessed by comparing the regression sum of squares of equations containing 7 variables with that of the equation containing all variables except X_1X_2 (Table A5).

Examination of the significance levels listed in Table A5 reveals that the values for all the variables used in the regression are below 0.1 . Thus the backward elimination selection procedure is terminated and yields the following equation;

$$Y = 1.684 - 0.0982X_1 - 0.0912X_2 - 0.659X_3 + 0.0438X_1X_3 + 0.191X_2X_3 + 0.00188X_1^2 - 0.00880X_2^2 - 0.567X_3^2.$$

Significance of the contribution of independent variables

to the regression equation

Variable name	Fitted coefficient	t-value	Significance level
Avicel (X_1)	-0.0988	10.33	0.0001
Primojel (X_2)	-0.0869	6.08	0.0001
Magnesium Stearate (X_3)	-0.648	4.49	0.0001
X_1X_2	-0.000273	0.70	0.49
X_1X_3	0.0440	8.58	0.0001
X_2X_3	0.193	11.48	0.0001
X_1^2	0.00191	7.59	0.0001
X_2^2	-0.00903	5.63	0.0001
X_3^2	-0.585	4.31	0.0001

Table A5

Significance of the contribution of independent variables

to the regression equation

Variable name	Fitted coefficient	t-value	Significance level
Avicel (X_1)	-0.0982	10.35	0.0001
Primojel (X_2)	-0.0912	7.09	0.0001
Magnesium Stearate (X_3)	-0.659	4.62	0.0001
X_1X_3	0.0438	8.59	0.0001
X_2X_3	0.191	11.72	0.0001
X_1^2	0.00188	7.65	0.0001
X_2^2	-0.00880	5.62	0.0001
X_3^2	-0.567	4.27	0.0001